NASA TECHNICAL NOTE

NASA TN D-6018

NASA TN D-6018

AERODYNAMICS OF A MODEL OF THE HL-10 FLIGHT-TEST VEHICLE AT MACH 0.35 TO 1.80

by Charles L. Ladson and Acquilla S. Hill

Langley Research Center
Hampton, Va. 23365

NATIONAL AERONAUTICS AND SPACE ADMINISTRATION • WASHINGTON, D. C. • FEBRUARY 1971

1. Report No.	2. Government Accession No.	3. Recipient's Catalog No.
NASA TN D-6018		

4. Title and Subtitle

AERODYNAMICS OF A MODEL OF THE HL-10 FLIGHT-TEST VEHICLE AT MACH 0.35 TO 1.80

5. Report Date: February 1971

6. Performing Organization Code

7. Author(s)

Charles L. Ladson and Acquilla S. Hill

8. Performing Organization Report No.: L-7265

10. Work Unit No.: 124-64-02-07

9. Performing Organization Name and Address

NASA Langley Research Center
Hampton, Va. 23365

11. Contract or Grant No.

13. Type of Report and Period Covered: Technical Note

12. Sponsoring Agency Name and Address

National Aeronautics and Space Administration
Washington, D.C. 20546

14. Sponsoring Agency Code

15. Supplementary Notes

16. Abstract

A summary is presented of tests conducted at the Langley Research Center to determine the aerodynamic characteristics of a model of the HL-10 lifting-body flight vehicle at speeds from low subsonic through a Mach number of 1.80. Data throughout this speed range are given for the trimmed longitudinal, directional and lateral stability, and lateral control characteristics. The subsonic and transonic data were taken from NASA TM X-2119 and NASA TM X-1918. Detailed results at Mach 1.50 and 1.80 are also presented.

17. Key Words (Suggested by Author(s))

Lifting-body entry vehicle
HL-10
Supersonic aerodynamics
Mach number effects

18. Distribution Statement

Unclassified – Unlimited

19. Security Classif. (of this report)	20. Security Classif. (of this page)	21. No. of Pages	22. Price*
Unclassified	Unclassified	130	$3.00

*For sale by the National Technical Information Service, Springfield, Virginia 22151

AERODYNAMICS OF A MODEL OF THE HL-10 FLIGHT-TEST VEHICLE AT MACH 0.35 TO 1.80

By Charles L. Ladson and Acquilla S. Hill
Langley Research Center

SUMMARY

The results of wind-tunnel tests of the HL-10 lifting-body configuration are summarized and presented together with detailed results of tests at Mach 1.50 and 1.80. (This vehicle is currently being flown at the Flight Research Center.) The summary of the trimmed aerodynamic characteristics throughout the Mach number range from 0.22 to 1.80 shows a maximum subsonic trimmed lift-drag ratio of about 4 at a Reynolds number of about 18×10^6. The data indicate the vehicle to be stable and controllable over the Mach number and angle-of-attack ranges of the investigation. Adverse yawing moment due to aileron deflection is noted at low angles of attack at the higher supersonic speeds. Adverse roll due to rudder deflection is also noted at the higher supersonic speeds as would be expected from a center-fin rudder mounted above the vehicle center of gravity. However, these adverse effects are not of sufficient magnitude to present control problems.

INTRODUCTION

Extensive wind-tunnel tests at the Langley Research Center have resulted in the development of a lifting body designated HL-10 and led to the construction of the one-man flight-test vehicle which made its first flight in December 1966. In numerous glide and powered flights at the Flight Research Center, the vehicle has been flown to a Mach number in excess of 1.80 and at altitudes above 90 300 feet (27.5 km). Reference 1, covering the first 14 flights, indicates satisfactory longitudinal handling qualities with the stability-augmentation system on but in the first flight noted a reduction in the roll-control effectiveness at a particular combination of angles of attack and sideslip at a Mach number of about 0.6. Subsequent wind-tunnel tests indicated that this loss of roll control was associated with flow separation occurring in the region of the leading edge of the tip fins and extending over the inner surface of the fins and the vehicle upper surface and elevons. Wind-tunnel tests established that the loss of roll control could be eliminated by increasing the camber of the inner surface (designated modification I) or by an extended, cambered leading edge attached to the fin (modification II). As a result of these tests, the vehicle was altered by using the second modification and returned to flight status in March 1968.

This paper presents the detailed results of the wind-tunnel tests at Mach numbers of 1.50 and 1.80 as well as a summary of the data for the trimmed conditions throughout the complete Mach number range of the investigation; thus, the wind-tunnel results of the flight configuration are made available in one reference. The data for the subsonic and transonic summary figures were obtained from references 2 and 3.

SYMBOLS

b	span of body without tip fins
C_D	drag coefficient, $\frac{\text{Drag force}}{qS}$
C_L	lift coefficient, $\frac{\text{Lift force}}{qS}$
C_l	rolling-moment coefficient, $\frac{\text{Rolling moment}}{qSb}$
C_{l_β}	effective dihedral parameter, $\frac{\Delta C_l}{\Delta\beta}$ (from pitch test at $\beta = 0^\circ$ and 3°), per degree
C_m	pitching-moment coefficient, $\frac{\text{Pitching moment}}{qSl}$
C_n	yawing-moment coefficient, $\frac{\text{Yawing moment}}{qSb}$
C_{n_β}	directional-stability parameter, $\frac{\Delta C_n}{\Delta\beta}$ (from pitch test at $\beta = 0^\circ$ and 3°), per degree
C_Y	side-force coefficient, $\frac{\text{Side force}}{qS}$
C_{Y_β}	side-force parameter, $\frac{\Delta C_Y}{\Delta\beta}$ (from pitch test at $\beta = 0^\circ$ and 3°), per degree
L/D	lift-drag ratio
l	body length
M	free-stream Mach number
q	free-stream dynamic pressure
R	Reynolds number based on model length, l

S	reference area
x,y,z	distances along longitudinal, lateral, and vertical axes, respectively
x_{cp}	longitudinal location of center of pressure
α	angle of attack measured relative to reference line of model, deg
β	angle of sideslip, deg
δ_a	roll-control deflection (equal to right-elevon deflection angle minus left-elevon deflection angle), deg
δ_e	elevon deflection angle measured in plane perpendicular to hinge line, positive when trailing edge is down, deg
δ_{ef}	elevon-flap deflection angle, angle between elevon flap and body upper surface in region of elevon, positive when trailing edge is above body surface at $\delta_e = 0^o$
δ_{if}	deflection angle of inner flap on tip fin, angle between flap and tip-fin inner surface measured normal to hinge line, positive when trailing edge moves toward body center line, deg
δ_{of}	deflection angle of outer flap on tip fin, angle between flap and tip-fin outer surface measured normal to hinge line, positive when trailing edge moves toward body center line, deg
δ_r	rudder deflection angle measured in plane perpendicular to hinge line, positive when trailing edge is left, deg
ψ	rudder included angle, positive for converging trailing edge, deg

MODELS AND DESIGNATIONS

A planform and a side-view drawing of the vehicle are shown in figure 1(a). Details of the tip-fin planform, tip-fin flaps, and elevon flaps are shown in figure 1(b), and the pitot boom, which was on the model for all tests (except those at low speed and high Reynolds number), is shown in figure 1(c). Vertical cross sections of both the basic and

modified tip fins are presented in figures 2(a) and 2(b), respectively, and a photograph of the model is shown in figure 3. A photograph of the flight vehicle (fig. 4) shows details of the rudder and outer tip-fin flaps as well as the modified tip fin.

The basic tip-fin planform has been designated I_4 and the center fin designated E_2 as in previously published data on this vehicle. In reference 4 (and other papers using the I_4 fin planform), the tip-fin cross sections show that the inner surface was curved. During design and construction of the flight vehicle, it was decided to alter this curved surface to a plane surface (see fig. 2(a)), and data were obtained to establish the aerodynamics of this fin section. The results obtained at Mach 1.50 and 1.80 on this fin section are presented herein. Since the vehicle incorporates two-position tip-fin and elevon flaps and a split rudder for improvements in maximum subsonic trimmed lift-drag ratio and transonic longitudinal stability, the following table is presented to define the combination of flap deflection angles used for these speed regimes:

Flap position	δ_{ef}, deg	δ_{if}, deg	δ_{of}, deg	ψ, deg
Subsonic	-8	0	40	6
Transonic	20	30	0	-6

The same model was used for the tests at Mach 1.50 and 1.80 as was used for the tests throughout the Mach number range presented herein. It was machined from aluminum and was 16 inches (40.64 cm) in length. The moment center for all tests is located at 53 percent of the body length behind the nose and at 1.25 percent of the body length below the reference center line. The reference areas and lengths are as follows:

S . . . . . 0.634 ft^2 (0.0589 m^2)
b . . . . . 10.30 in. (26.16 cm)
l . . . . . 16.00 in. (40.64 cm)

APPARATUS, TESTS, AND PROCEDURE

The supersonic tests were conducted in the low Mach number test section of the Langley Unitary Plan wind tunnel. A brief description of this facility is presented in reference 5. For the tests at both Mach 1.50 and 1.80, the stagnation temperature was 150° F (339° K) and the dynamic pressure was about 380 psf (18.2 kN/m^2). The Reynolds number was about 2.1×10^6 based on the model length. Description of the facilities and the test conditions for data obtained at the other speeds are given in the reference reports (refs. 2 and 3) from which the data were taken.

The aerodynamic forces and moments were measured on a six-component electrical strain-gage balance housed within the model. The balance was rigidly mounted to the tunnel support system. Angles of attack and sideslip were corrected for deflection

of the balance and sting support under aerodynamic load. The data have also been corrected for tunnel flow angularity. The drag data presented are gross measurements as obtained during the tests and no adjustments have been made to relate drag coefficient levels to free-stream conditions at the model base.

All longitudinal performance data are referred to the stability-axis system, whereas the directional and lateral stability and control data are referred to the body-axis system. The directional and lateral stability derivatives presented were obtained from tests at two sideslip angles, but some data are presented as a function of sideslip to give an indication of the linearity of the data. At Mach 1.50 and angles of attack above about 30°, schlieren flow photographs have indicated that a reflection of the bow shock wave from the tunnel wall strikes the aft end of the model; thus, data at these higher angles of attack should be regarded as qualitative.

PRESENTATION OF RESULTS

The basic data obtained at Mach 1.50 and 1.80 are presented as well as a summary of data over the Mach number range. An index to the figures follows:

Basic Data Plots

β, deg	Control variable	Mach number	Tip fin	Figure
	Plots of C_L, C_D, L/D, and C_m against α			
0	δ_e	1.50	Basic	5
0	δ_e	1.80	Basic	6
0, 3	δ_e	1.50	Modification II	7
0, 3	δ_e	1.80	Modification II	8
0	δ_a, δ_e	1.50	Modification II	9
	δ_a, δ_e	1.80	Modification II	10
0	δ_r, δ_e	1.50	Modification II	11
0	δ_r, δ_e	1.80	Modification II	12
	Plots of C_l, C_n, and C_Y against β			
-4 to 6	δ_a, δ_e	1.50	Modification II	13
-4 to 6	δ_a, δ_e	1.80	Modification II	14
-4 to 6	δ_r, δ_e	1.50	Modification II	15
-4 to 6	δ_r, δ_e	1.80	Modification II	16
	Plots of C_{l_β}, C_{n_β}, and C_{Y_β} against α			
Between 0 and 3	δ_e	1.50	Basic	17
	δ_e	1.80	Basic	18
	δ_e	1.50	Modification II	19
	δ_e	1.80	Modification II	20
	δ_a, δ_e	1.50	Modification II	21
	δ_a, δ_e	1.80	Modification II	22
	δ_r, δ_e	1.50	Modification II	23
↓	δ_r, δ_e	1.80	Modification II	24
	Plots of C_l, C_n, and C_Y against α			
0	δ_a, δ_e	1.50	Modification II	25
3	δ_a, δ_e	1.50	Modification II	26
0	δ_a, δ_e	1.80	Modification II	27
3	δ_a, δ_e	1.80	Modification II	28
0	δ_r, δ_e	1.50	Modification II	29
3	δ_r, δ_e	1.50	Modification II	30
0	δ_r, δ_e	1.80	Modification II	31
3	δ_r, δ_e	1.80	Modification II	32

Summary Plots

Mach number	Tip fin	Flap position	Figure
Plot of C_L, L/D, and δ_e against α_{trim}			
1.50, 1.80	Basic Modification II	Transonic	33
Plot of C_{l_β}, C_{n_β}, and C_{Y_β} against α_{trim}			
1.50, 1.80	Basic Modification II	Transonic	34
Plots of C_L, L/D, and δ_e against α_{trim}			
0.22 to 0.70 0.60 to 1.80	Modification II Modification II	Subsonic Transonic	35 36
Plots of x_{cp}/l against α_{trim}			
0.22 to 0.70 0.60 to 1.80	Modification II Modification II	Subsonic Transonic	37 38
Plots of C_{l_β}, C_{n_β}, and C_{Y_β} against α_{trim}			
0.35 to 0.70 0.60 to 1.80	Modification II Modification II	Subsonic Transonic	39 40
Plots of ΔC_l, ΔC_n, and ΔC_Y against α_{trim}			
0.35 to 0.70 0.60 to 1.80 1.50, 1.80	Modification II Modification II Modification II	Subsonic Transonic Transonic	41 42 43

DISCUSSION

Comparisons of the trimmed longitudinal aerodynamic characteristics and directional and lateral stability characteristics of the model having basic tip fin with those of the model having modification II tip fins show that the addition of the cambered leading edge to the tip fin has no significant effect on these parameters at the supersonic Mach numbers. (See figs. 33 and 34.)

The trimmed longitudinal data for the vehicle with modification II tip fins and flaps in the subsonic position are summarized in figure 35 for Mach numbers from 0.22 to 0.70. The results shown indicate the increase in maximum trimmed subsonic lift-drag ratio with Reynolds number. The maximum subsonic L/D of about 4.0 was obtained with an elevon deflection angle of -15° at a Reynolds number of about 18×10^6. A rearward center-of-gravity shift will reduce the trim losses and increase the maximum lift-drag ratio. As the Mach number increases to 0.70, the maximum L/D decreases to about 3.3. Since the trimmed lift coefficient remains the same or increases slightly with Mach number for a given angle of attack, the decrease in lift-drag ratio must be attributed to an increase in drag. For the tests at Mach 0.22 in the Langley low-turbulence pressure tunnel, the model did not have the pitot boom installed.

The results of the longitudinal aerodynamic characteristics for the vehicle with the flaps in the transonic position are shown in figure 36. The maximum trimmed lift-drag ratio decreases from about 2.50 at Mach 0.60 to 1.30 at Mach 1.80. The lift-drag ratio L/D decreases from about 3.30 to 2.50 because of changing the flaps from the subsonic to the transonic position at Mach 0.60 and 0.70. With the flaps in the transonic position,

positive elevon deflection angles are required for trim at low angles of attack, mainly because of the upward deflection of the elevon flap. At $\delta_e = 0^o$, the vehicle trims at an angle of attack of about 22^o at Mach 0.60, and for this setting, the trim angle of attack decreases to about 16^o at Mach 1.00. At the lower Mach numbers, only positive elevon deflection angles were used since this range covered the angle-of-attack range of interest; but, as the Mach number increases, negative elevon deflections were included to obtain the desired trim range.

Longitudinal center-of-pressure locations for the flaps in the subsonic and transonic positions are presented in figures 37 and 38, respectively. These data are presented to give an indication of the angle-of-attack range over which the vehicle can be trimmed and to show the effects of center-of-gravity shifts.

Directional and lateral stability derivatives for the vehicle with flaps in the subsonic position are shown in figure 39. The level of C_{n_β} remains about the same from Mach 0.35 to Mach 0.70 as does the level of C_{l_β} at low angles of attack. The lateral stability increases with angle of attack at low subsonic speeds but is essentially constant at Mach numbers of 0.60 and 0.70. With the flaps in the transonic position, a rapid loss in C_{n_β} is observed with increasing angle of attack at transonic Mach numbers, and at Mach 0.95, this parameter becomes negative at angles of attack above 27^o. (See fig. 40.) This decrease in C_{n_β} with increasing angle of attack diminishes at supersonic Mach numbers, becomes zero, or even increases under some conditions. The lateral-stability parameter C_{l_β} is essentially constant throughout the angle-of-attack range for all Mach numbers.

Lateral control data for the vehicle with flaps in the subsonic position are presented in figure 41. For the lower speeds, the control effectiveness appears to be about linear with aileron deflection, but at Mach 0.70, large nonlinearities are noted. The control effectiveness remains about constant with angle of attack, and favorable yaw due to aileron deflection is noted. Data for the vehicle with flaps in the transonic position are presented in figure 42. At Mach numbers of 1.20 and below, the lateral-control effectiveness decreases with increasing angle of attack except for the $\delta_a = 10^o$ case at Mach 0.95 where it increases slightly. For the supersonic Mach numbers of 1.50 and 1.80, however, the control effectiveness increases with angle of attack up to about 15^o but decreases at the higher angles. At the two higher Mach numbers, the control effectiveness is near zero at angles of attack near 0^o and at the highest angle of attack. For all Mach numbers where data are available for two aileron deflection angles, the control effectiveness is about linear with the deflection angle. Favorable yawing moments due to aileron control are generally noted up to Mach 1.20; at the higher speeds, adverse yaw exists at angles of attack up to about 20^o. This adverse yaw does not present a problem on the flight

vehicle, since the dynamic lateral control is a function not only of Cn_{δ_a} but also of Cn_β, Cl_β, and Cl_{δ_a}. For the HL-10 vehicle, the combination of these parameters is such that a favorable control system exists throughout the angle-of-attack range.

Yaw-control data are available for the vehicle with the modification II tip fins at the two higher supersonic Mach numbers only, and the results are shown in figure 43. The yaw control tends to decrease with increasing angle of attack and is nonlinear with control deflection angle. Adverse rolling moment due to rudder deflection exists at both Mach numbers for all angles of attack. This condition is typical of a center rudder located well above the vehicle reference axis. For other Mach numbers, the yaw-control data was assumed to be unaffected by the modification of the tip-fin leading edge and previously published data are being used in simulator studies as well as for other purposes.

CONCLUDING REMARKS

A summary of the trimmed aerodynamic characteristics of a model of the HL-10 lifting-body flight vehicle at speeds from low subsonic through supersonic shows a maximum subsonic trimmed lift-drag ratio of about 4.0 at a Reynolds number of about 18×10^6. The configuration was stable and controllable over the Mach number and angle-of-attack ranges of the investigation. Adverse yawing moment due to aileron deflection is noted at low angles of attack at the higher supersonic speeds. Adverse roll due to rudder deflection is also noted at the higher supersonic speeds as would be expected from a center fin mounted well above the vehicle center of gravity. However, these adverse effects are not of sufficient magnitude to present control problems.

Langley Research Center,
National Aeronautics and Space Administration,
Hampton, Va., August 27, 1970.

REFERENCES

1. Layton, Garrison P., Jr.: Interim Results of the Lifting-Body Flight-Test Program. NASA TM X-1827, 1969.

2. McKinney, Linwood W.; and Huffman, Jarrett K.: Subsonic Aerodynamic Characteristics of a Model of the HL-10 Flight Research Vehicle With Basic and Modified Tip Fins. NASA TM X-2119, 1970.

3. Harris, Charles D.: Transonic Aerodynamic Characteristics of a Manned Lifting Entry Vehicle With Modified Tip Fins. NASA TM X-1918, 1970.

4. Ladson, Charles L.: Effects of Various Canopies on the Aerodynamic Characteristics of a Manned Lifting Entry Vehicle at Mach 0.06 to 6.8. NASA TM X-1321, 1966.

5. Schaefer, William T., Jr.: Characteristics of Major Active Wind Tunnels at the Langley Research Center. NASA TM X-1130, 1965.

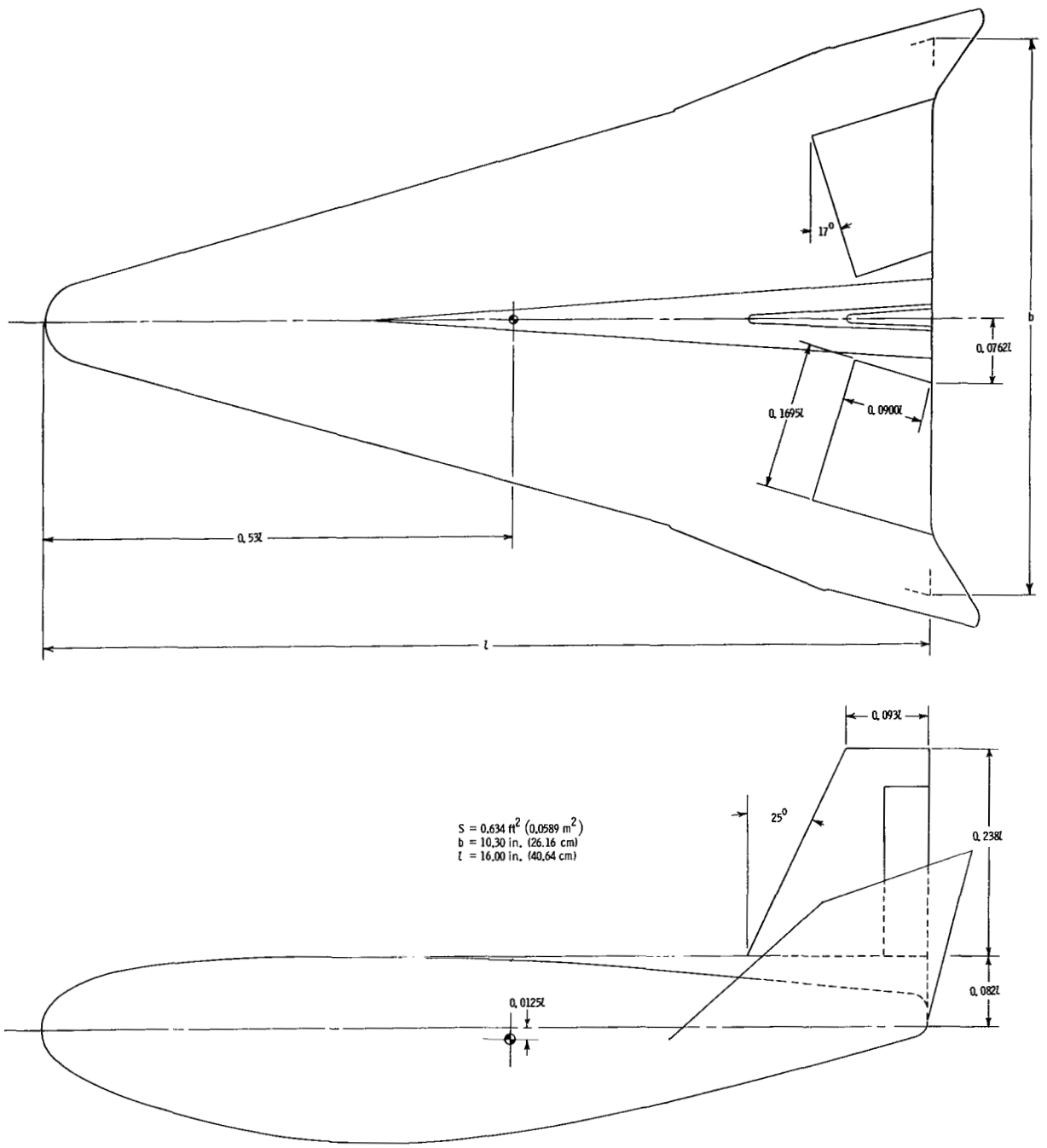

(a) Details of body.

Figure 1.- Details of model tested.

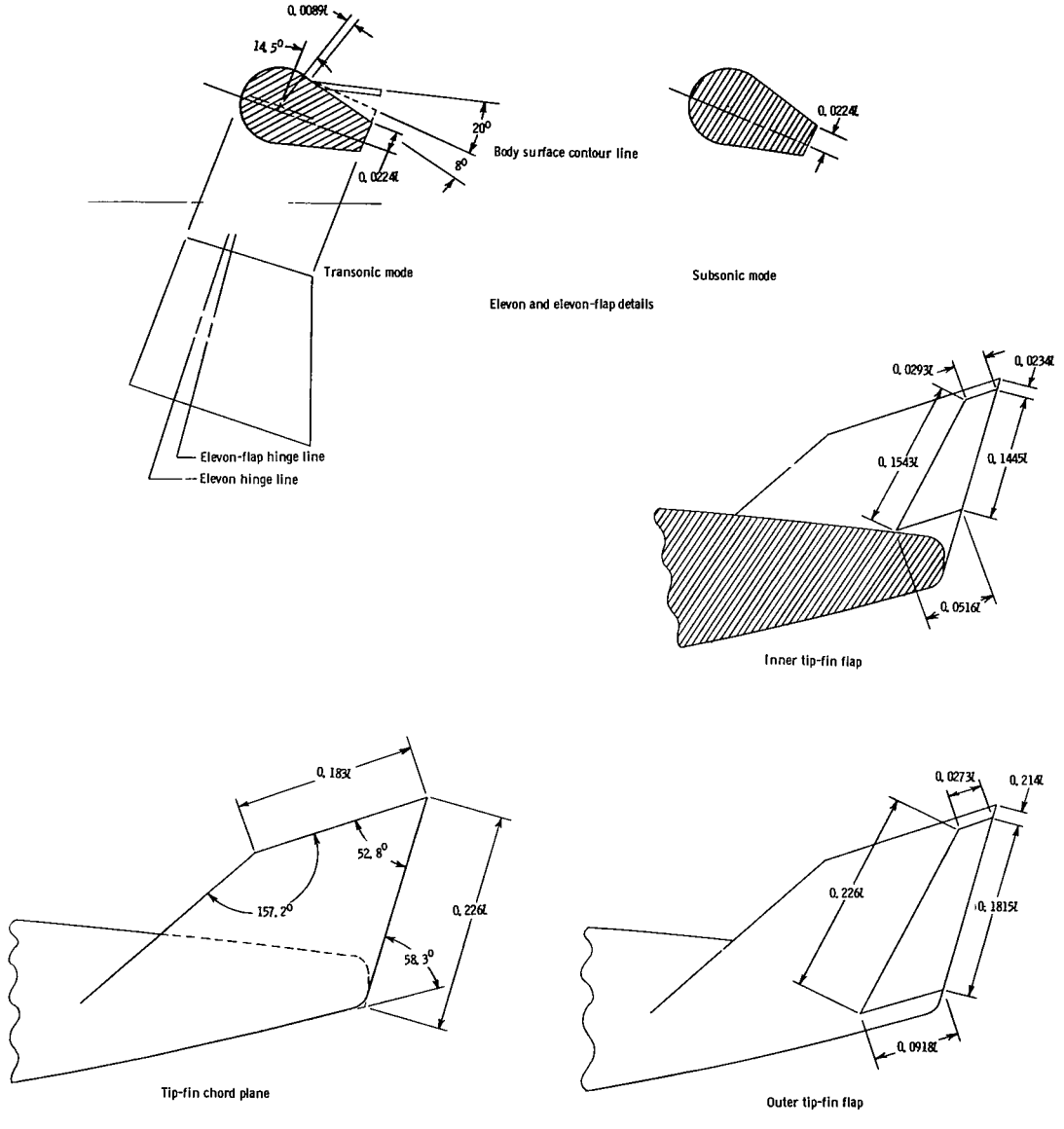

(b) Tip fin, tip-fin flap, and elevon-flap details.

Figure 1.- Continued.

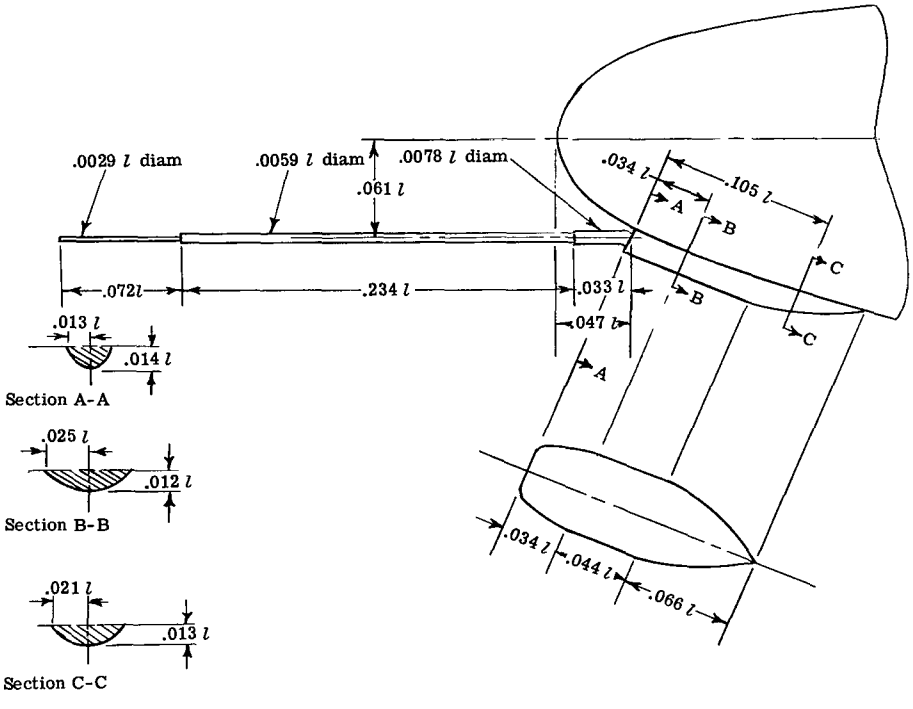

(c) Pitot boom.

Figure 1.- Concluded.

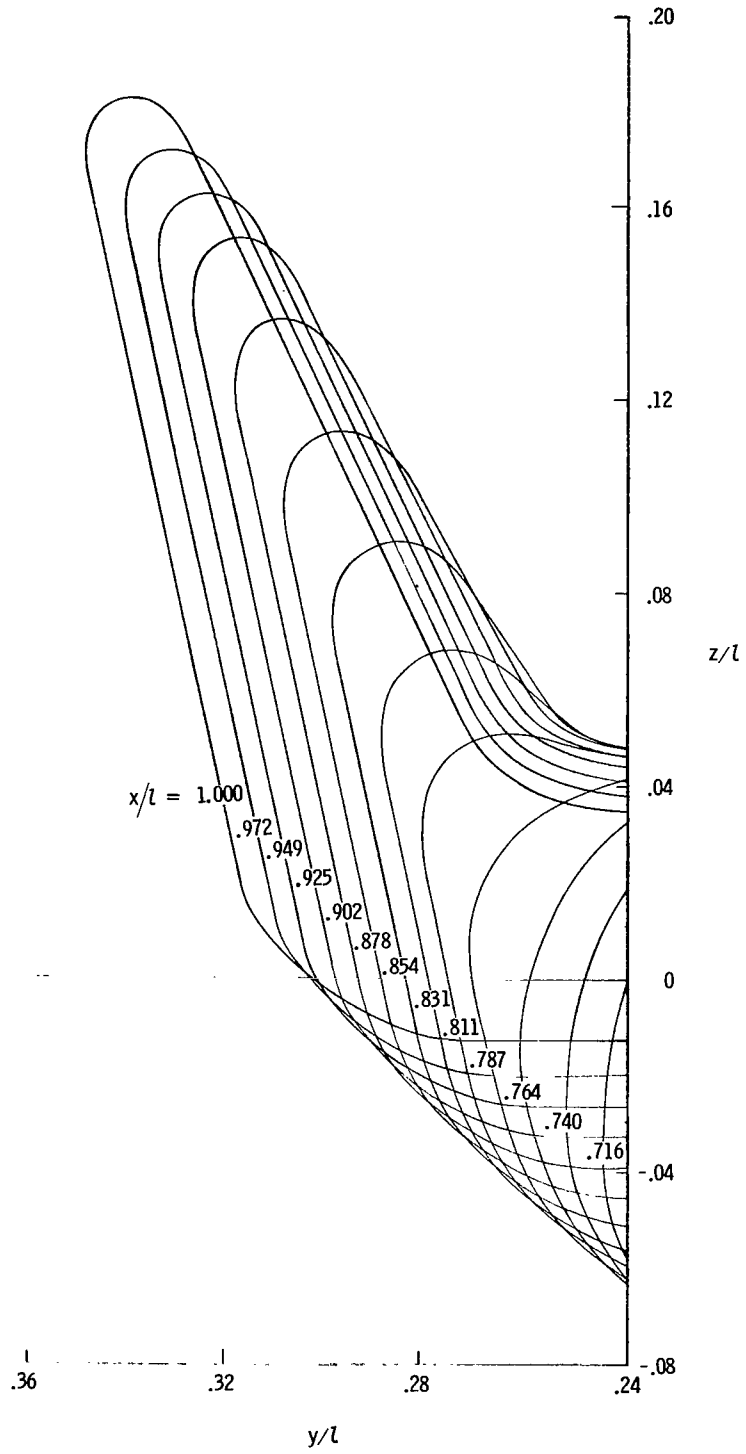

(a) Original tip fin.

Figure 2.- Tip-fin cross sections.

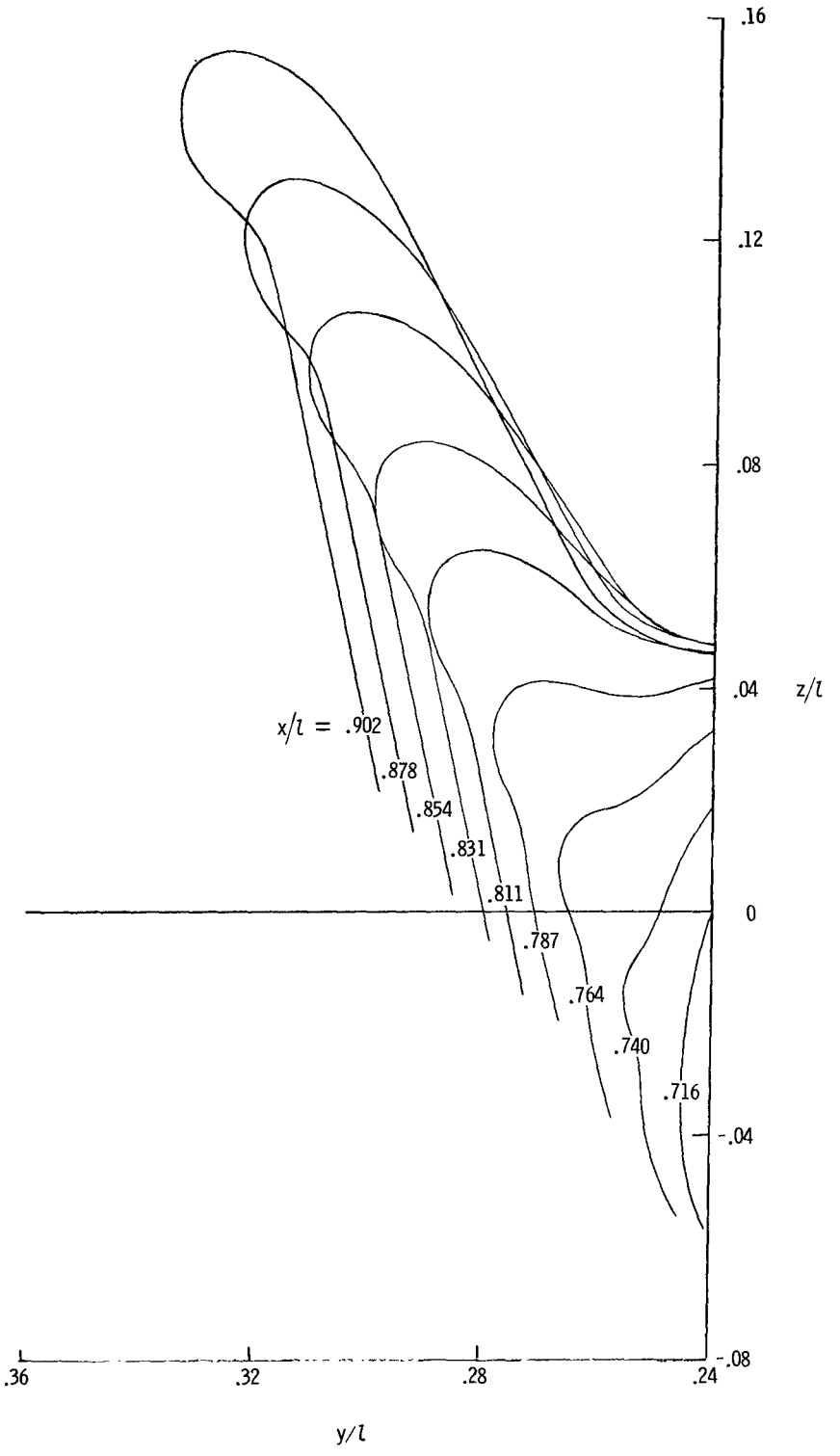

(b) Tip fin with modification II.

Figure 2.- Concluded.

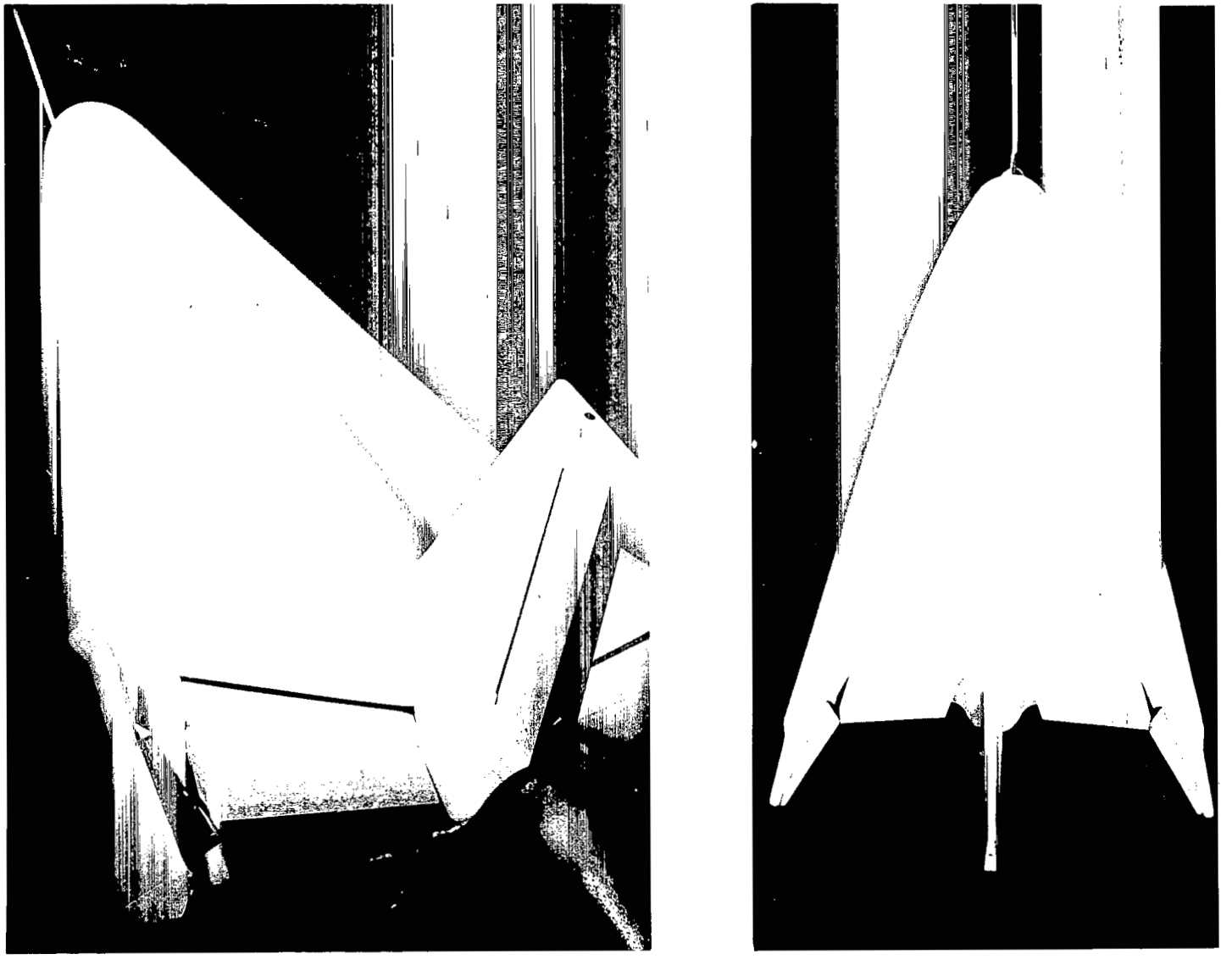

L-70-4761

Figure 3.- Photographs of model tested.

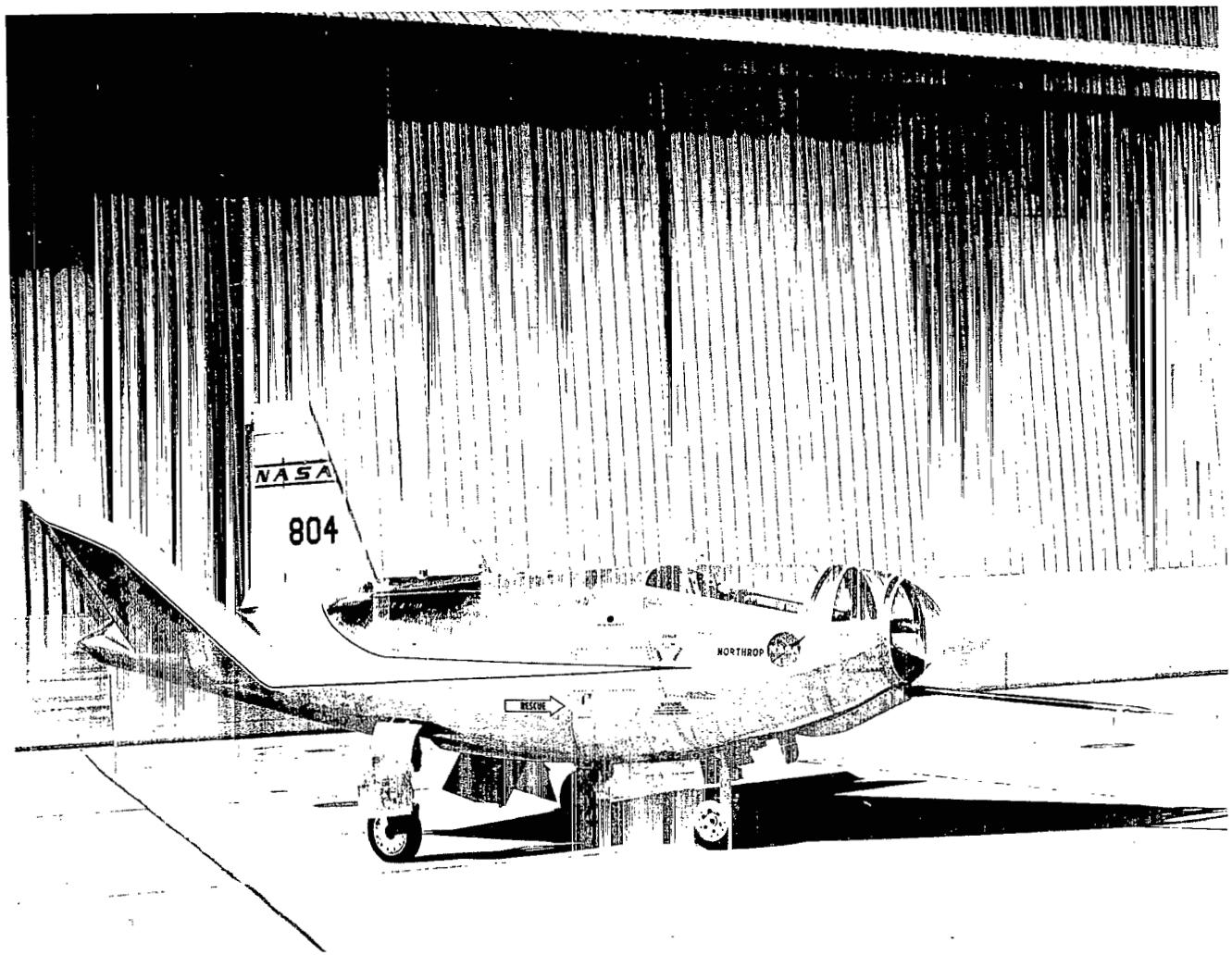

E-18261

Figure 4.- Photograph of HL-10 flight vehicle taken at Flight Research Center.

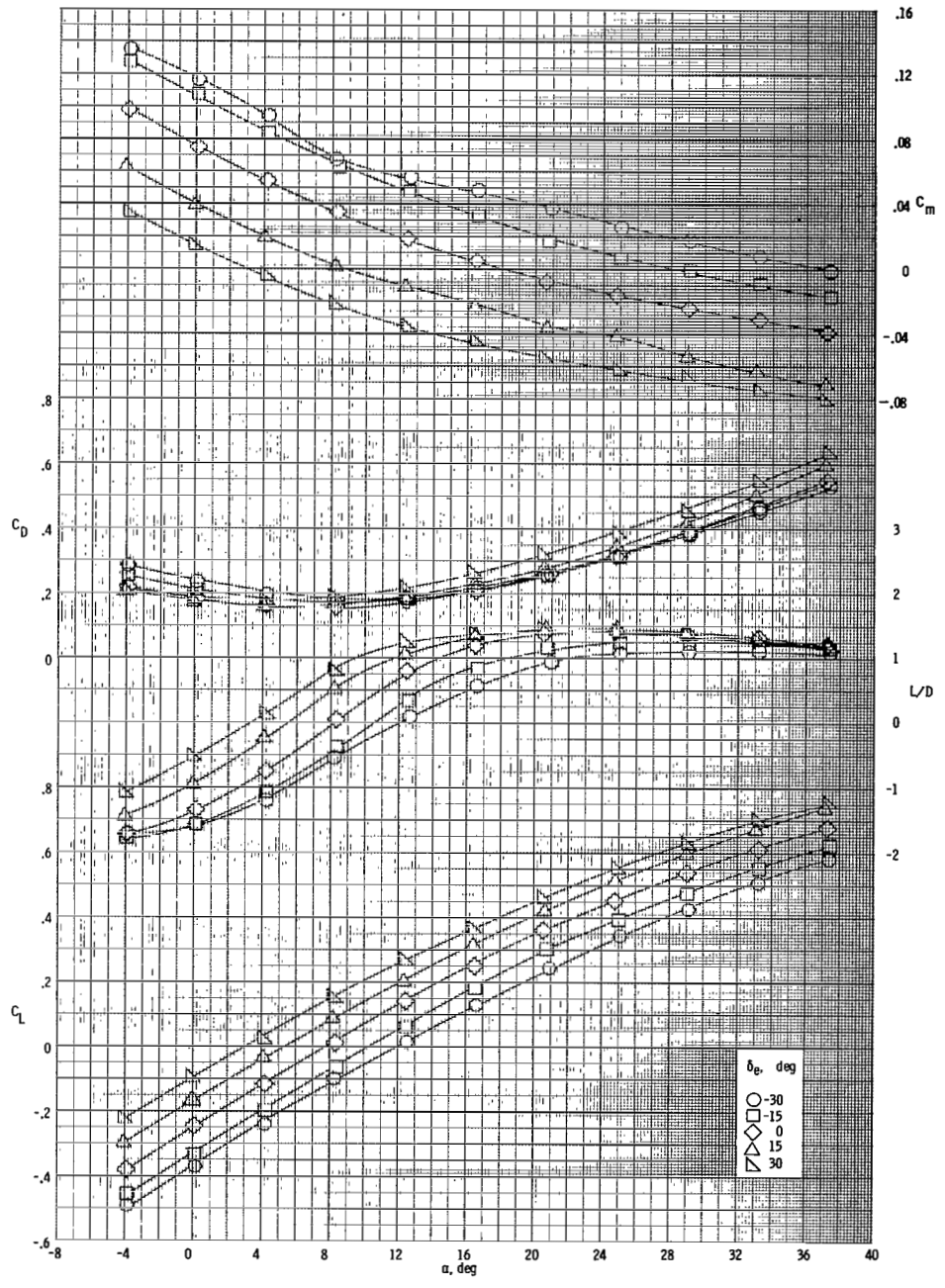

Figure 5.- Effects of elevon deflection on longitudinal aerodynamic characteristics of vehicle with basic tip fins. $\beta = 0^{\circ}$; M = 1.50.

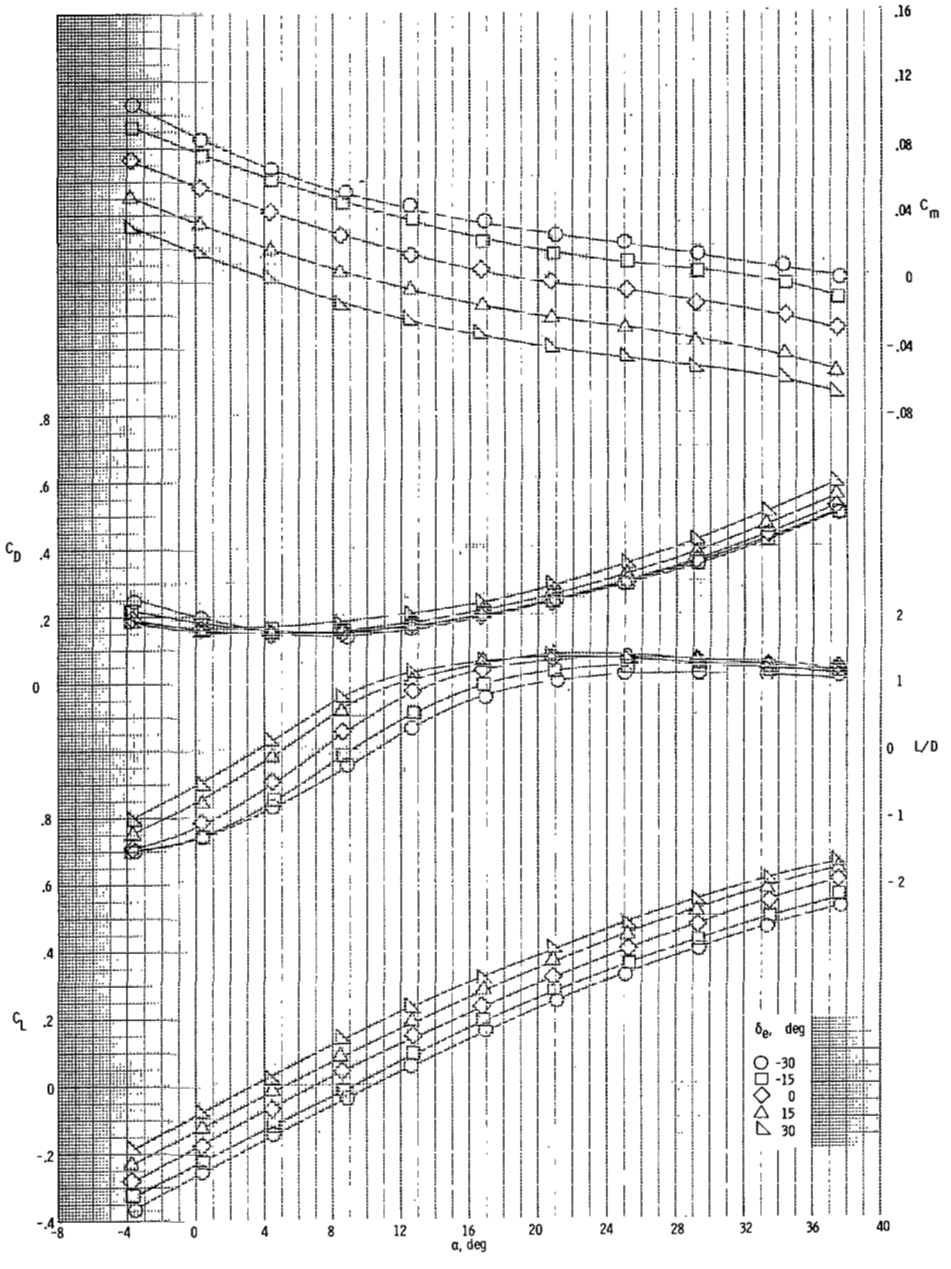

Figure 6.- Effects of elevon deflection on longitudinal aerodynamic characteristics of vehicle with basic tip fins. $\beta = 0^{\circ}$; $M = 1.80$.

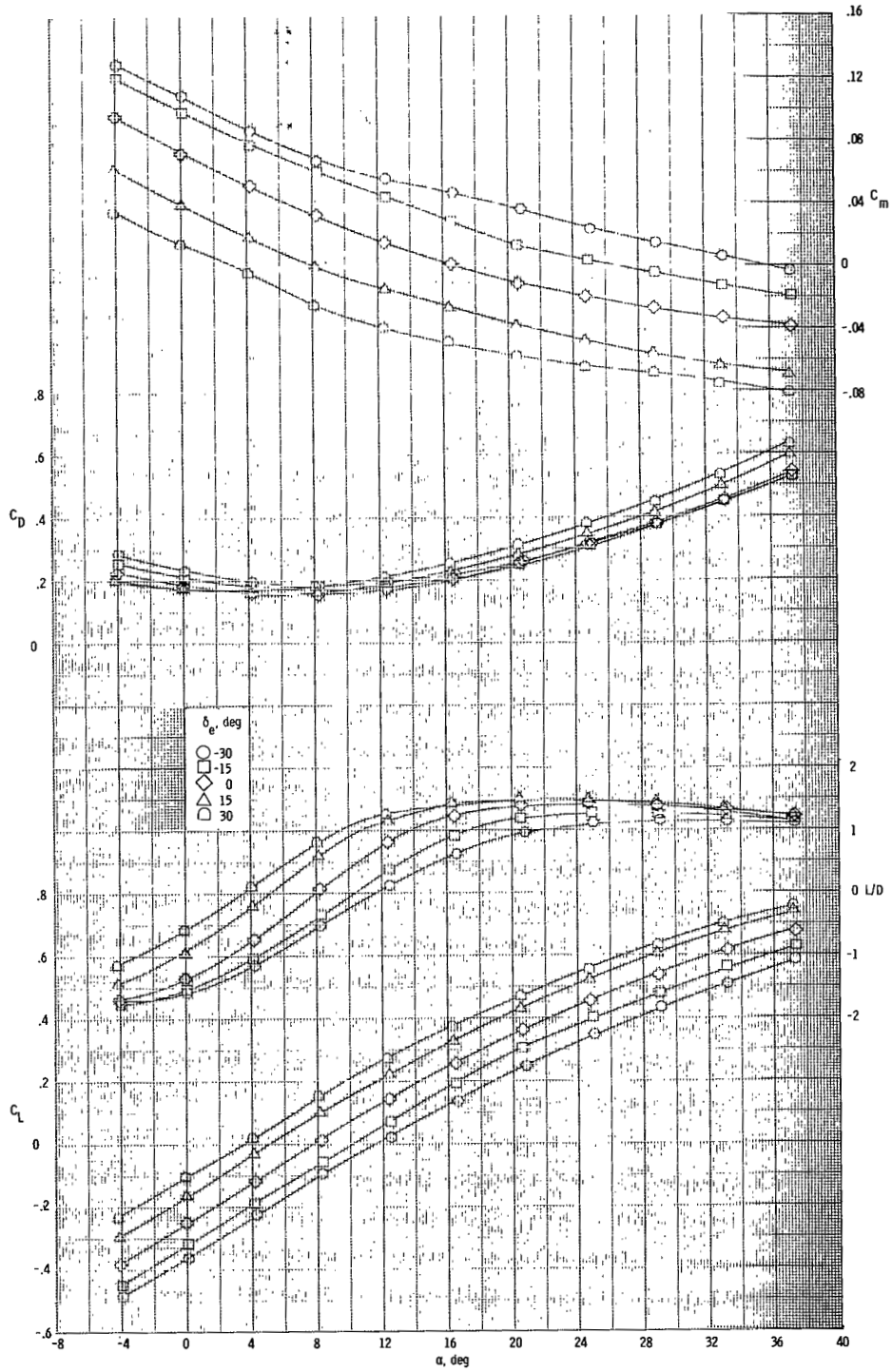

(a) $\beta = 0^{\circ}$.

Figure 7.- Effects of elevon deflection on longitudinal aerodynamic characteristics of vehicle with modification II tip fins. M = 1.5.

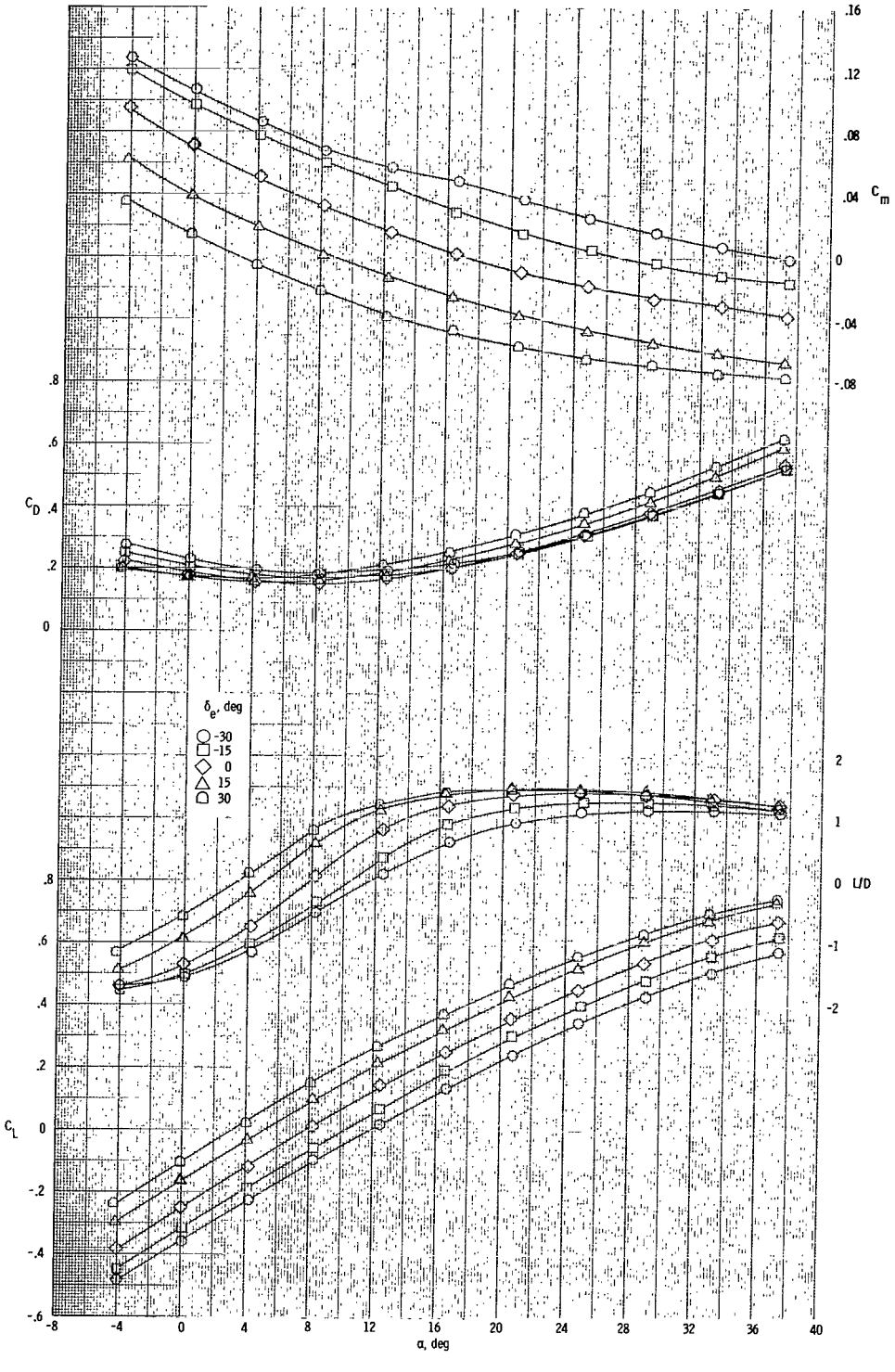

(b) $\beta = 3^{\circ}$.

Figure 7.- Concluded.

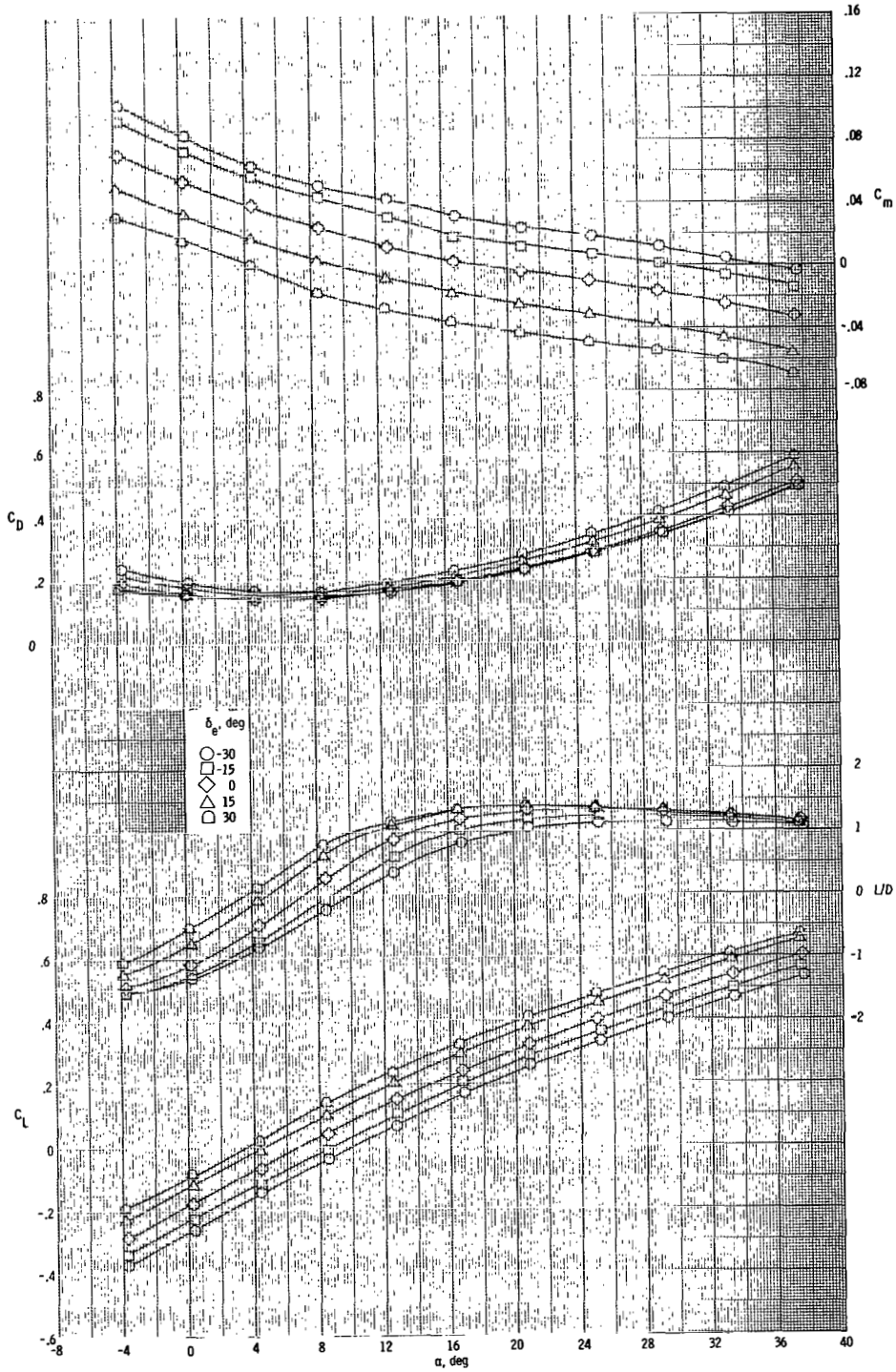

(a) $\beta = 0^{\circ}$.

Figure 8.- Effects of elevon deflection on longitudinal aerodynamic characteristics of vehicle with modification II tip fins. M = 1.8.

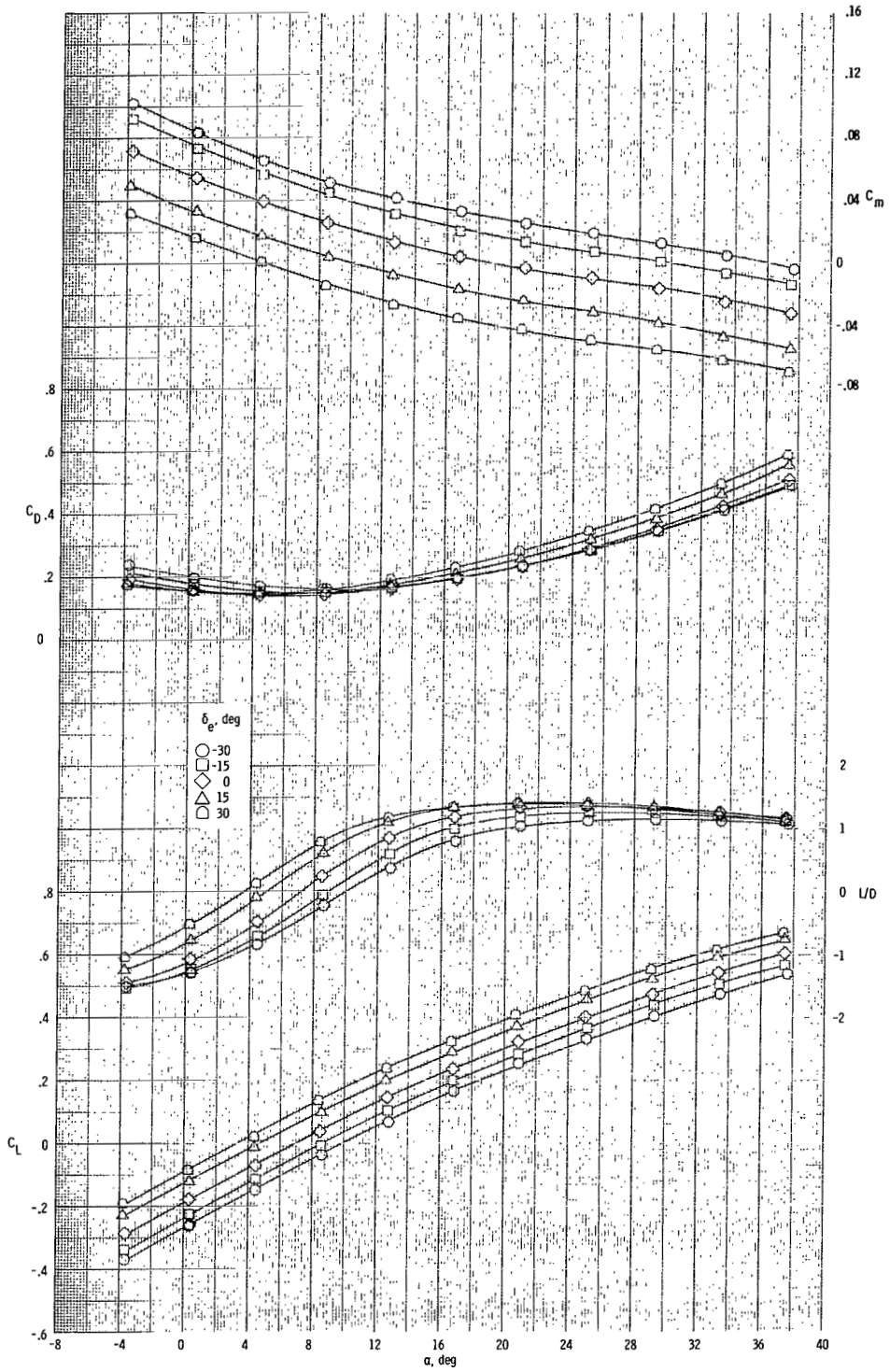

(b) $\beta = 3^{\circ}$.

Figure 8.- Concluded.

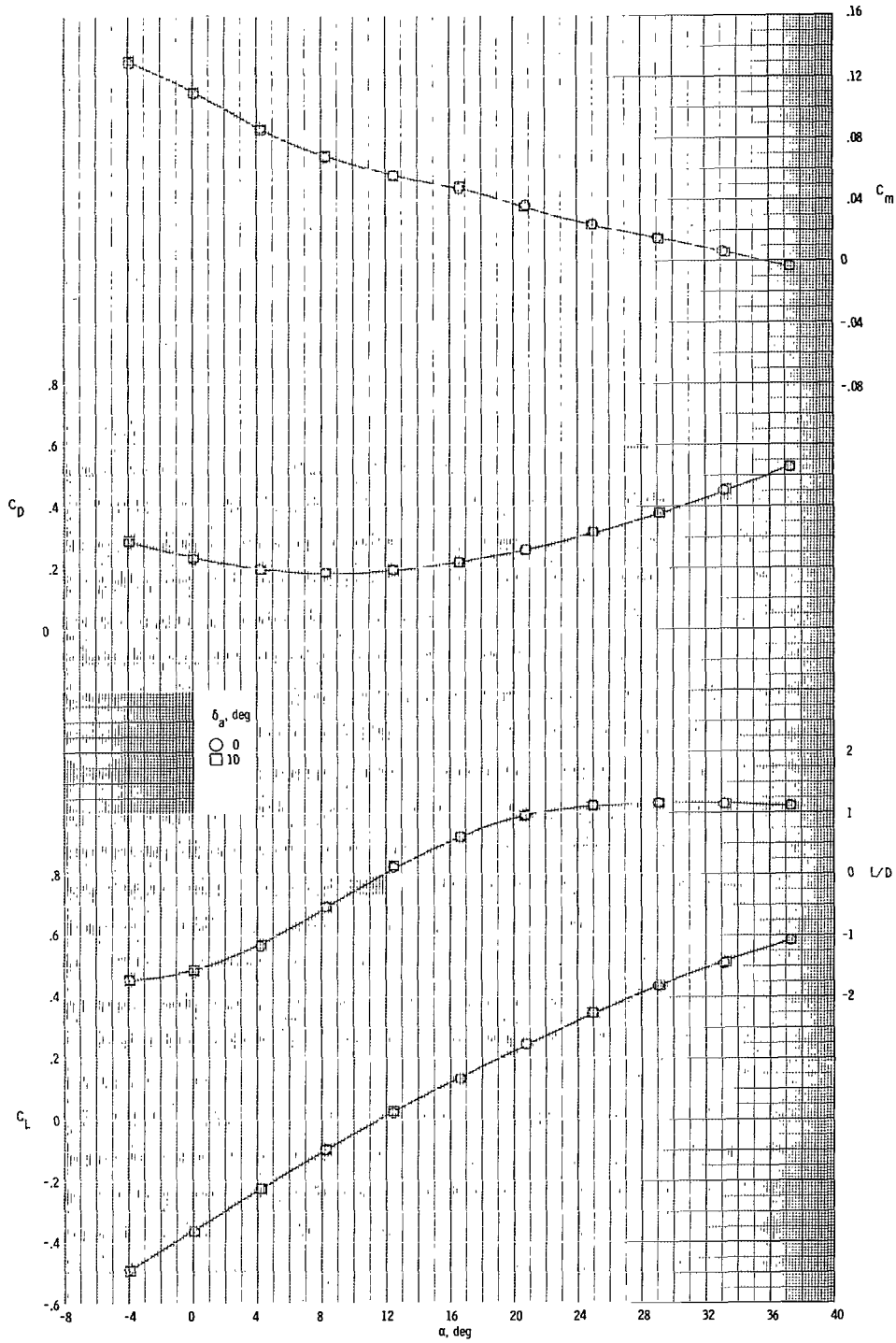

(a) $\delta_e = -30^\circ$.

Figure 9.- Effects of aileron deflection on longitudinal aerodynamic characteristics of vehicle with modification II tip fins for various elevon deflection angles. $\beta = 0^\circ$; M = 1.50.

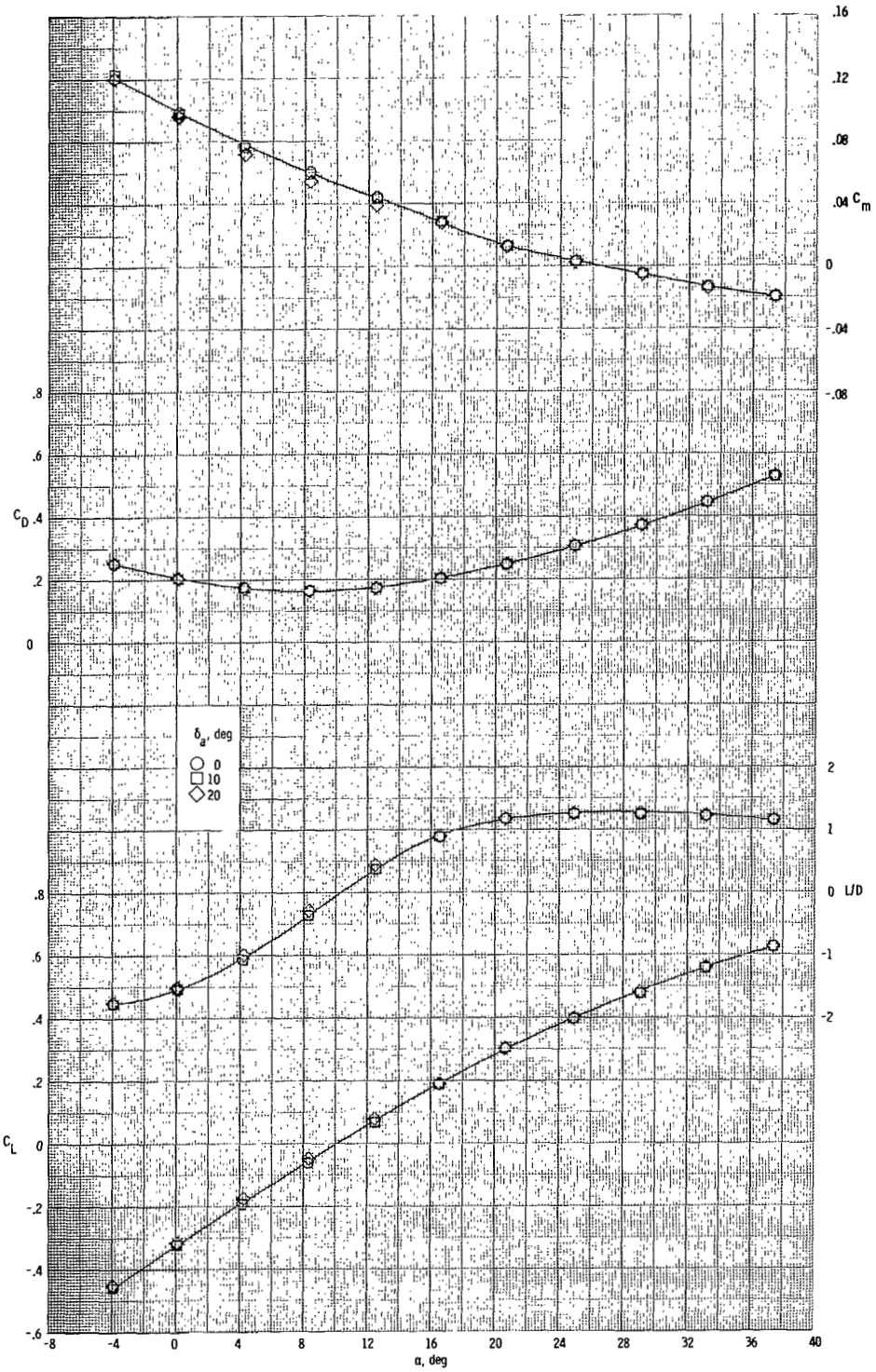

(b) $\delta_e = -15^\circ$.

Figure 9.- Continued.

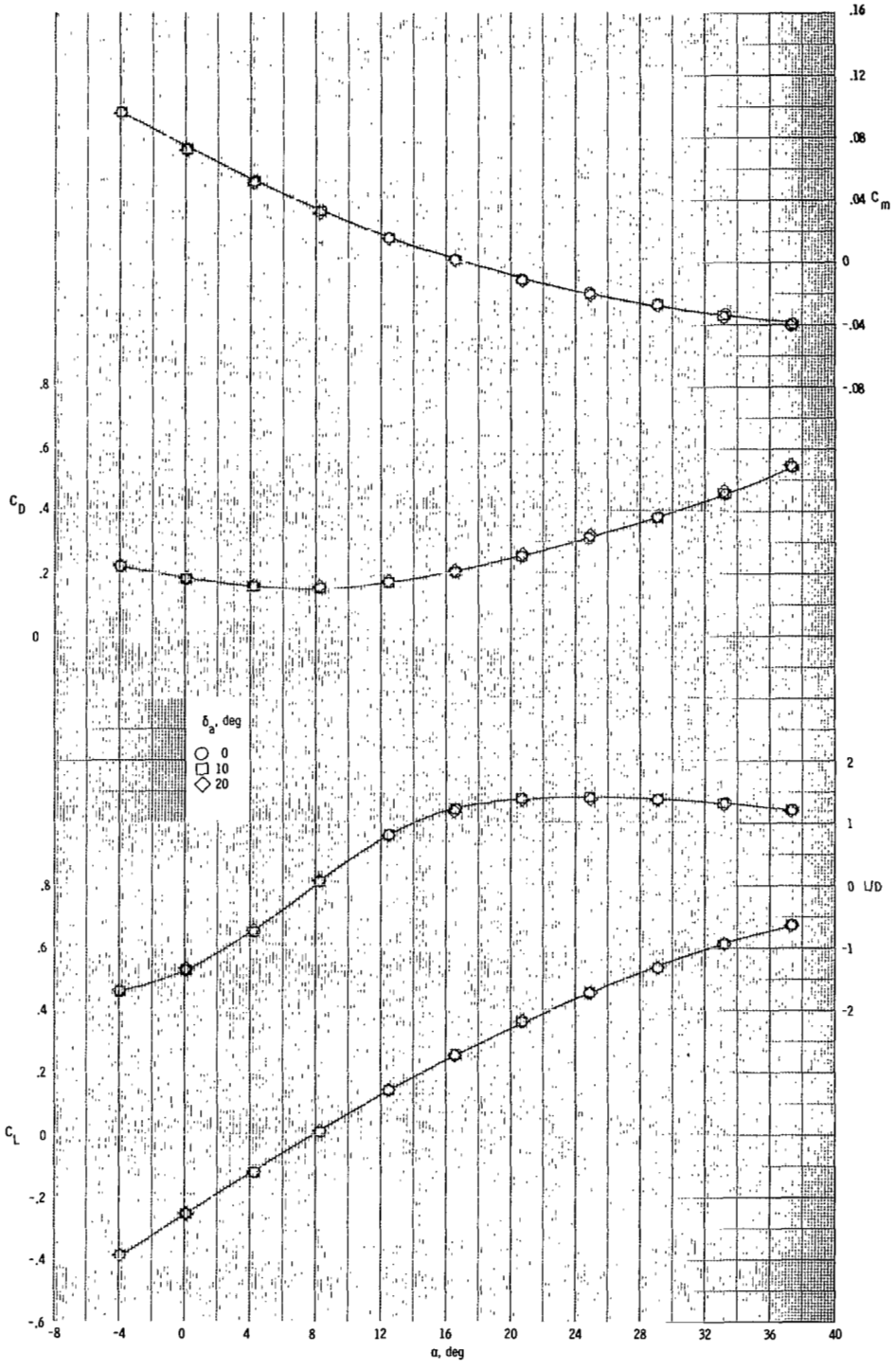

(c) $\delta_e = 0^\circ$.

Figure 9.- Continued.

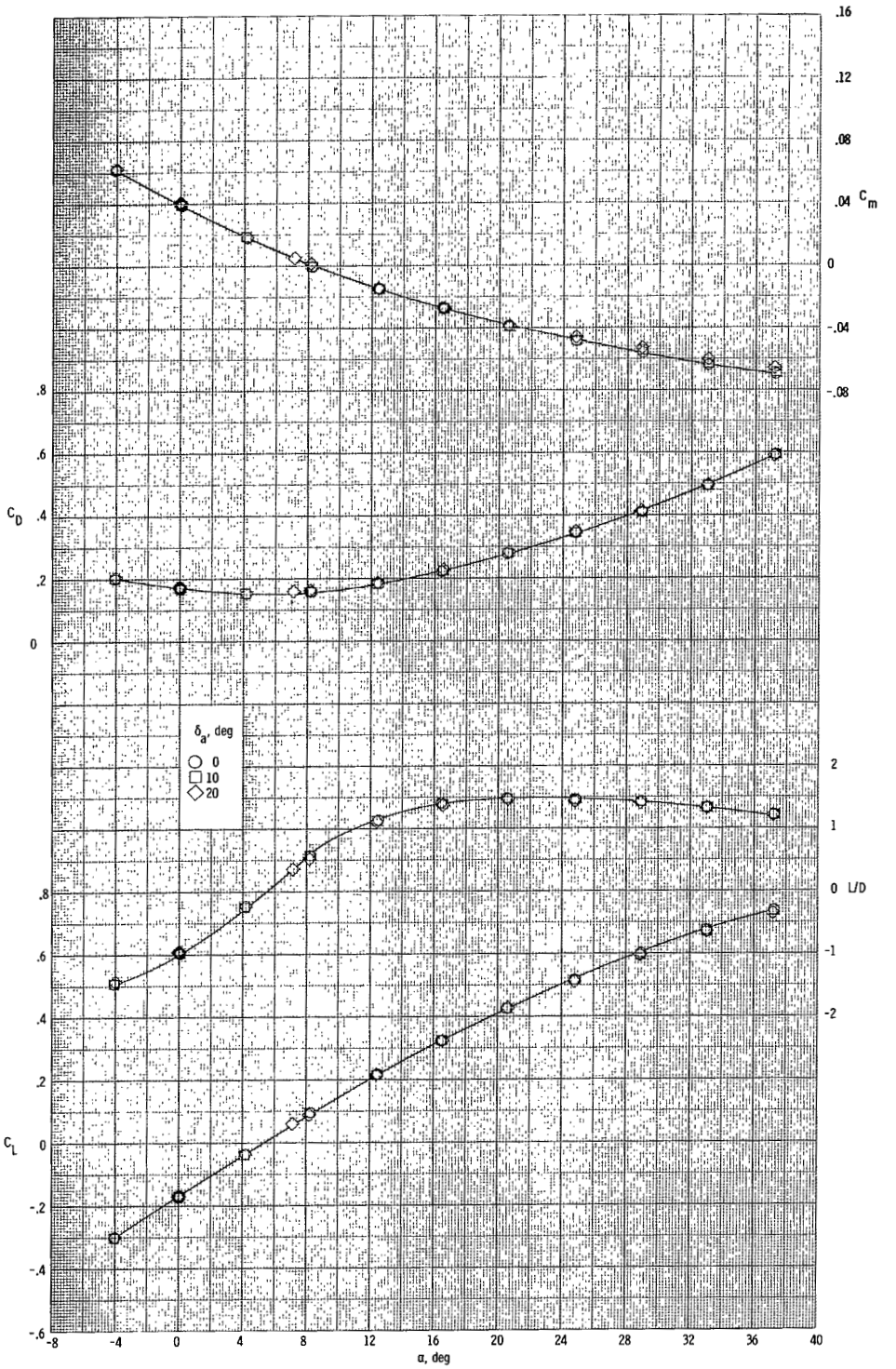

(d) $\delta_e = 15^\circ$.

Figure 9.- Continued.

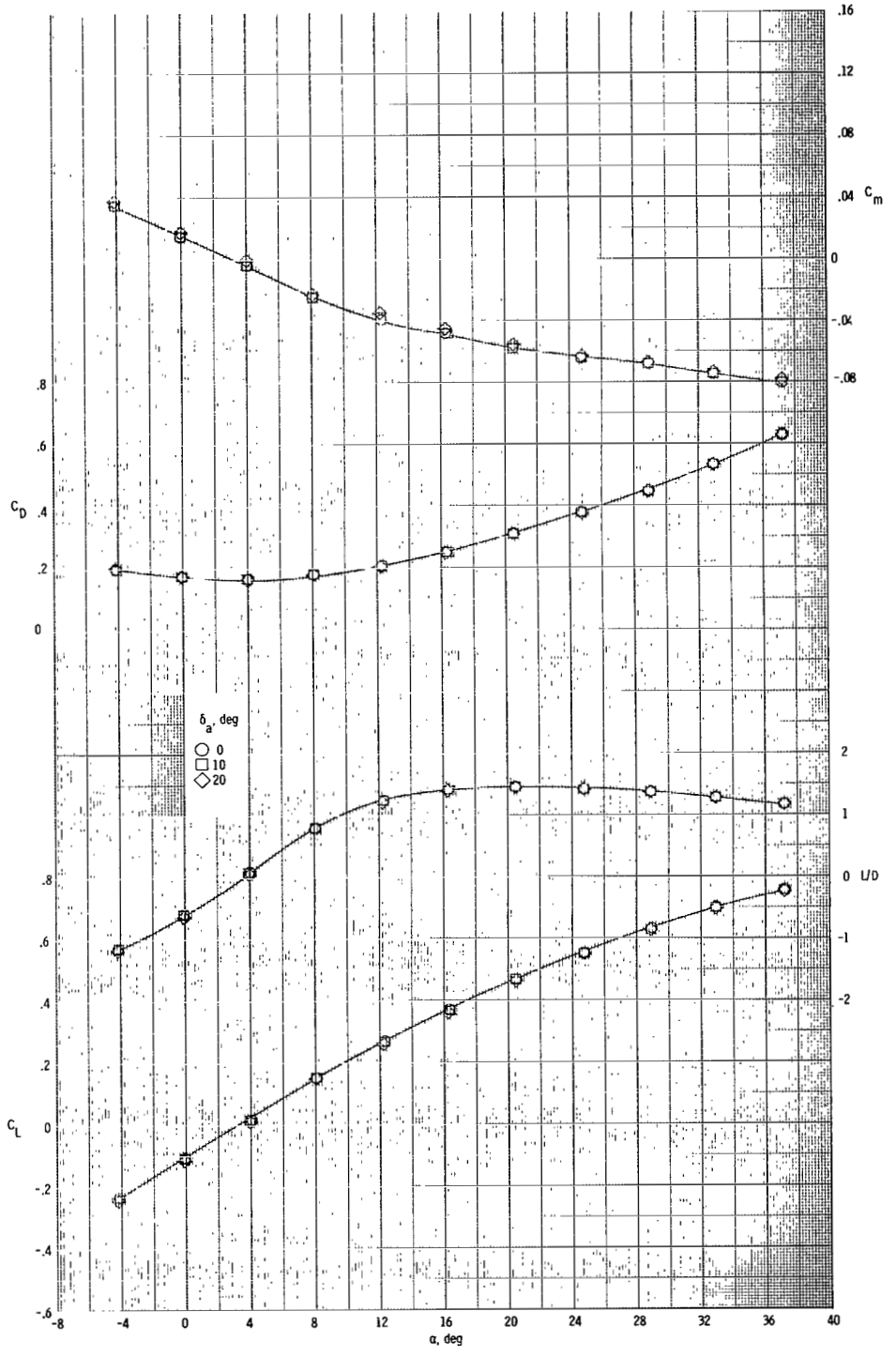

(e) $\delta_e = 30^\circ$.

Figure 9.- Concluded.

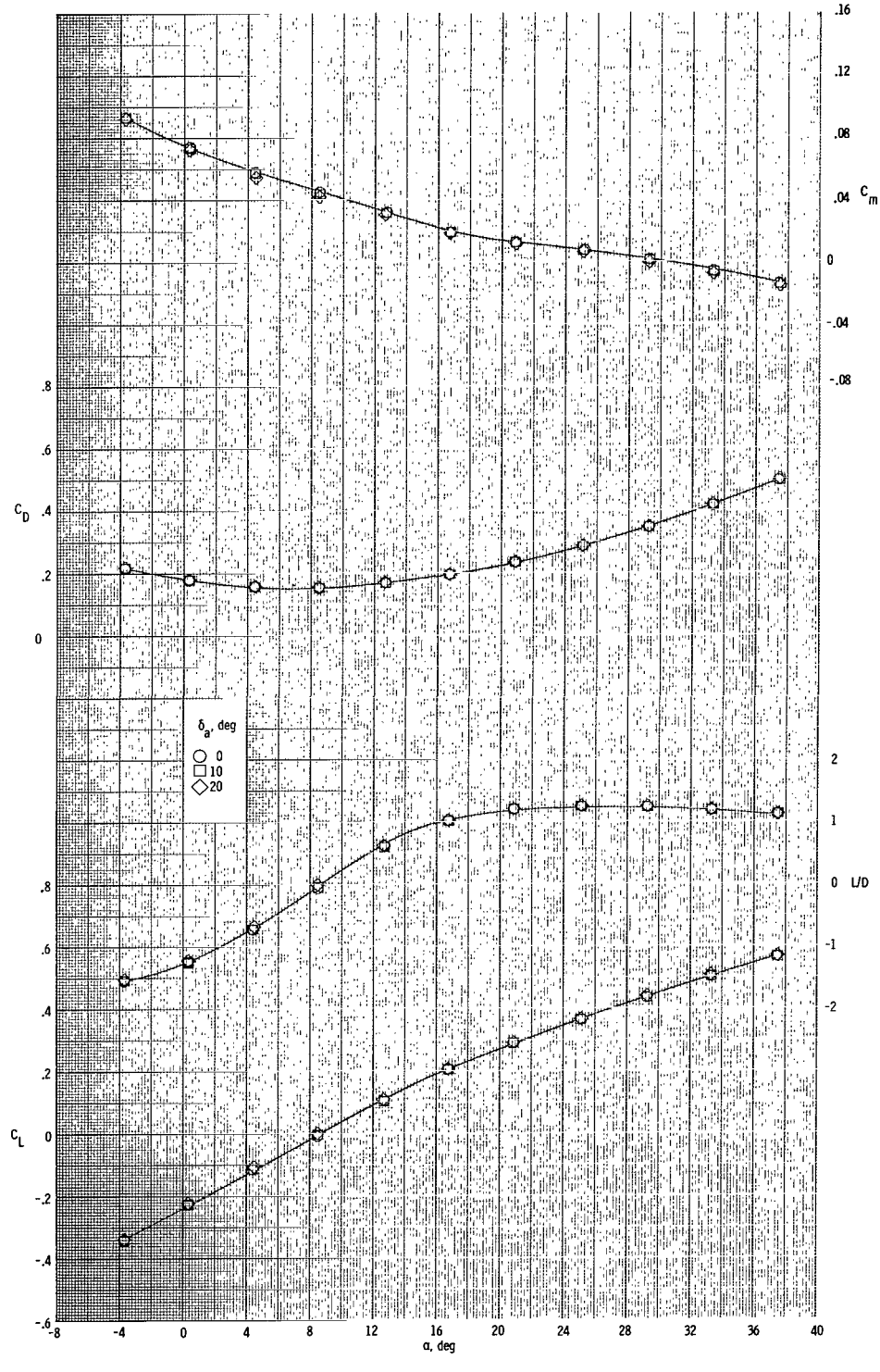

(a) $\delta_e = -15^\circ$.

Figure 10.- Effects of aileron deflection on longitudinal aerodynamic characteristics of vehicle with modification II tip fins for various elevon deflection angles. M = 1.80.

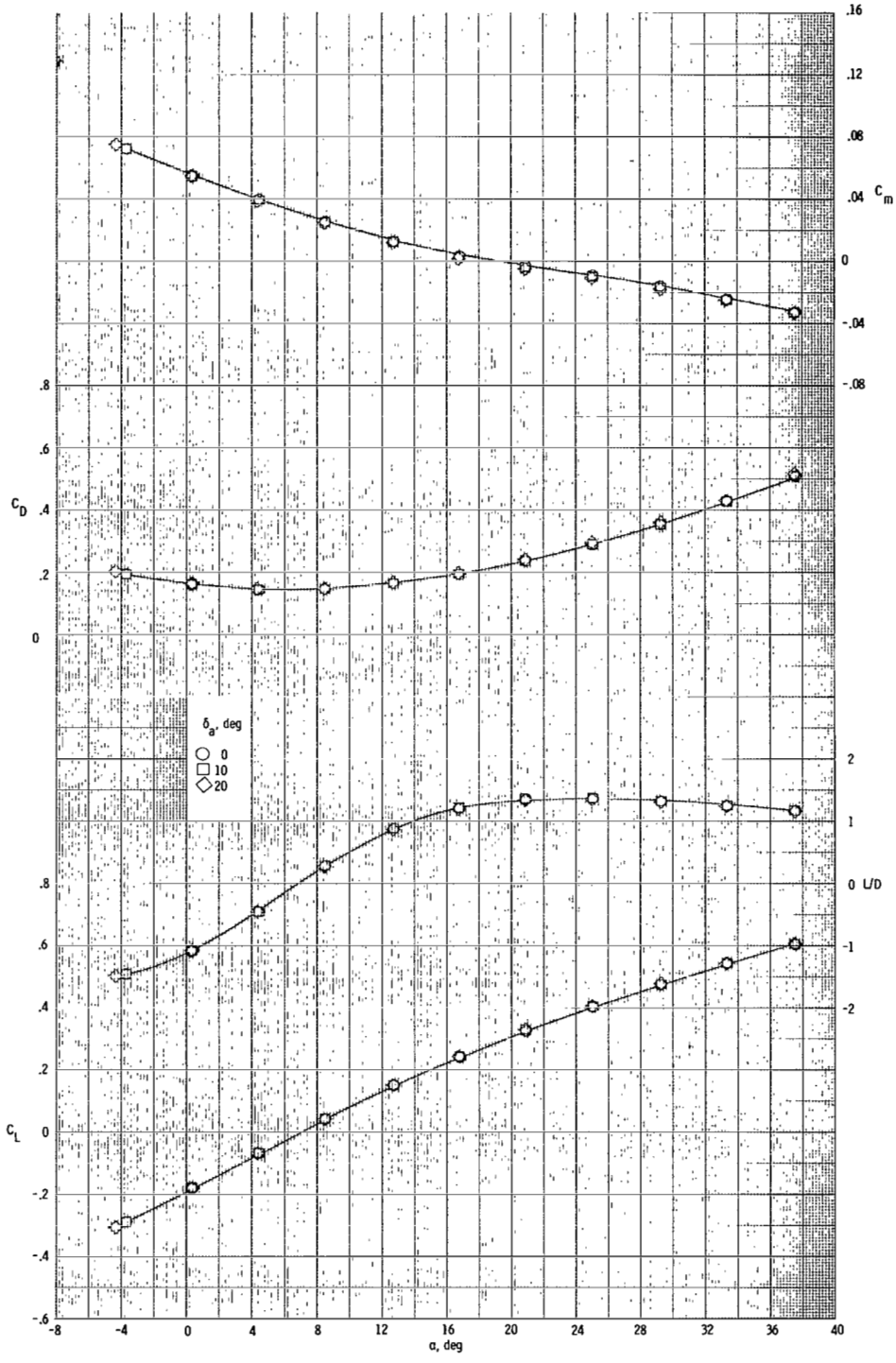

(b) $\delta_e = 0^o$.

Figure 10.- Continued.

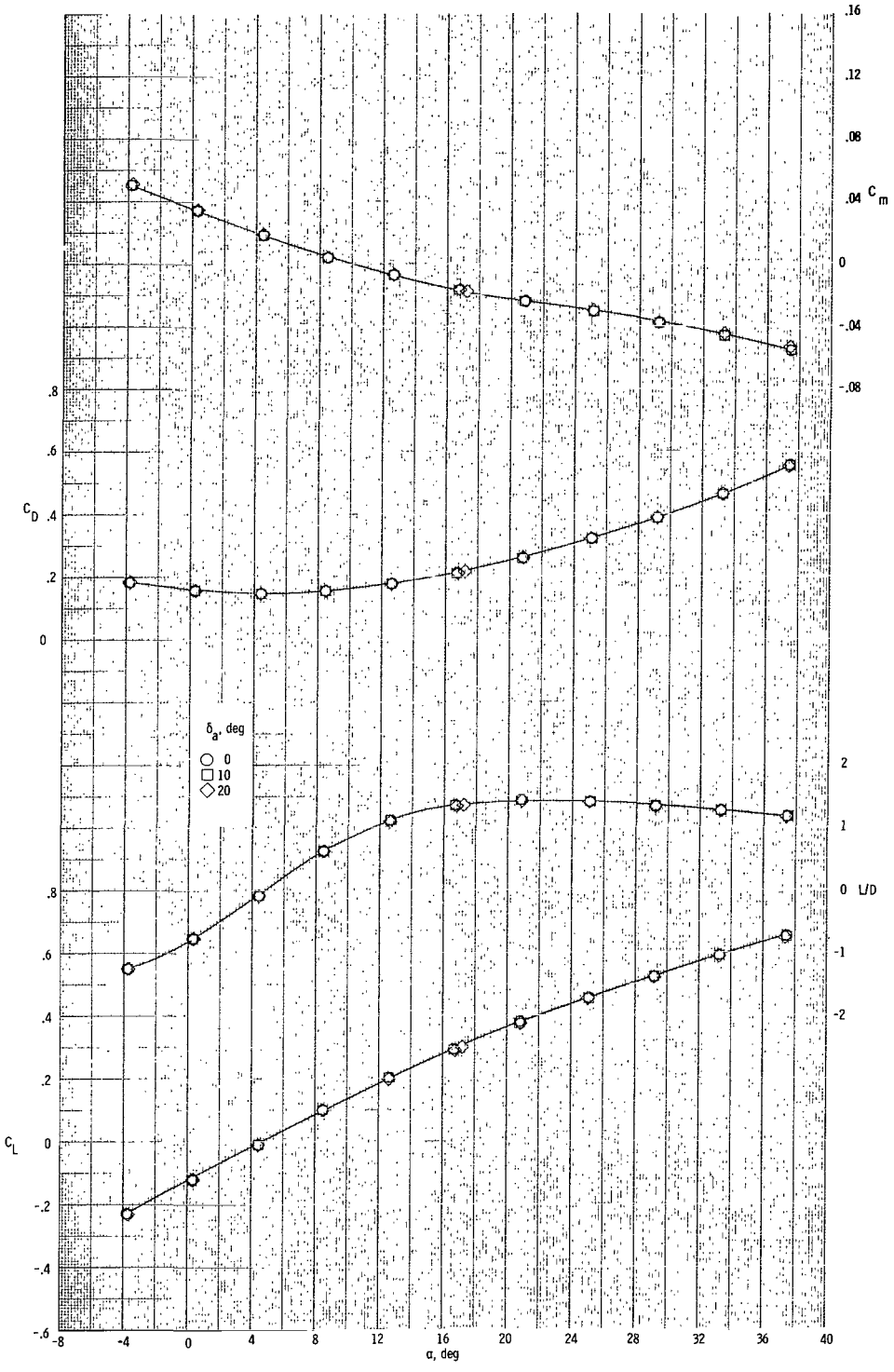

(c) $\delta_e = 15^\circ$.

Figure 10.- Continued.

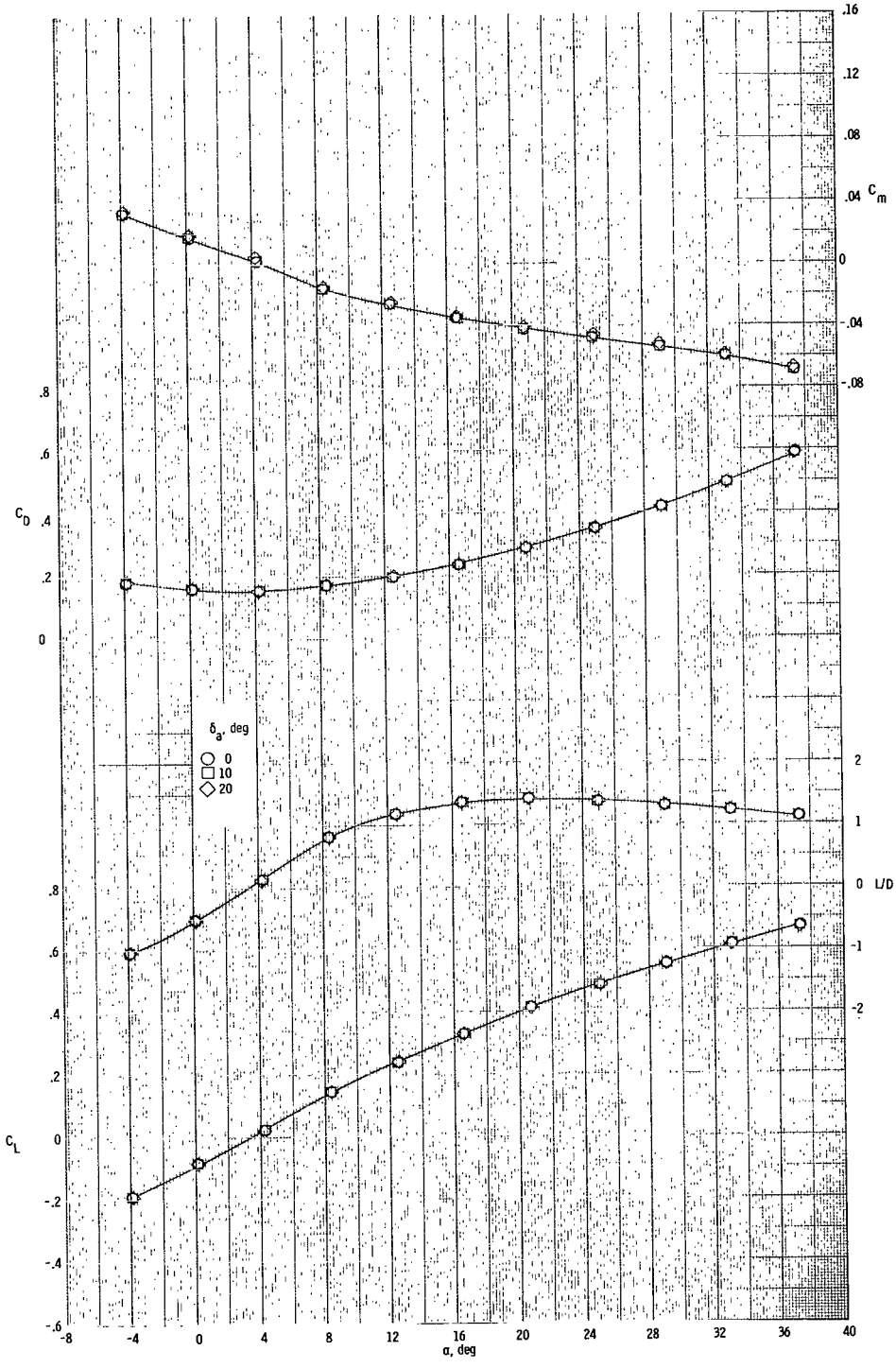

(d) $\delta_e = 30^\circ$.

Figure 10.- Concluded.

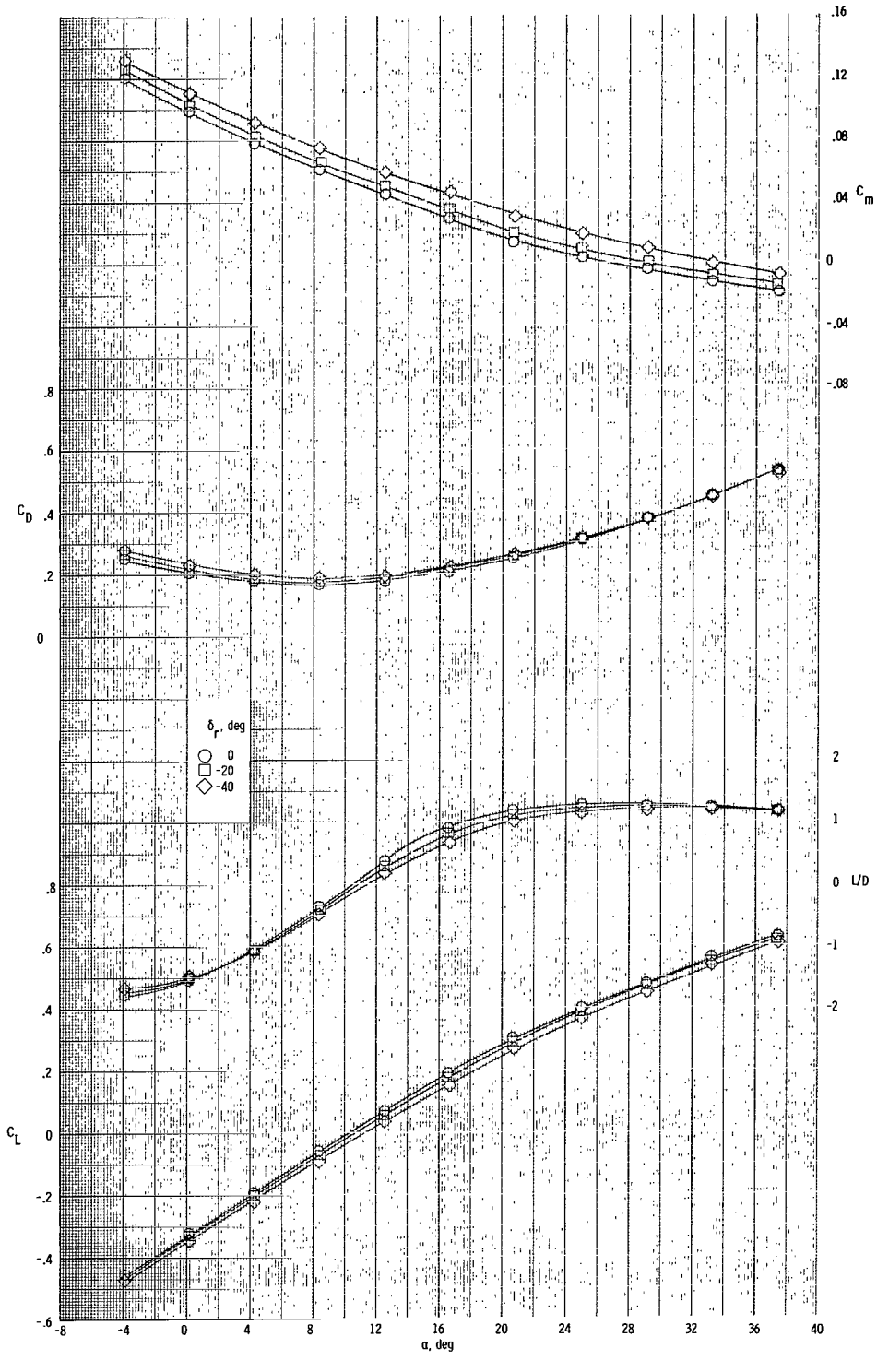

(a) $\delta_e = -15^\circ$.

Figure 11.- Effects of rudder deflection on longitudinal aerodynamic characteristics of vehicle with modification II tip fins for various elevon deflection angles. $\beta = 0^\circ$; $M = 1.50$.

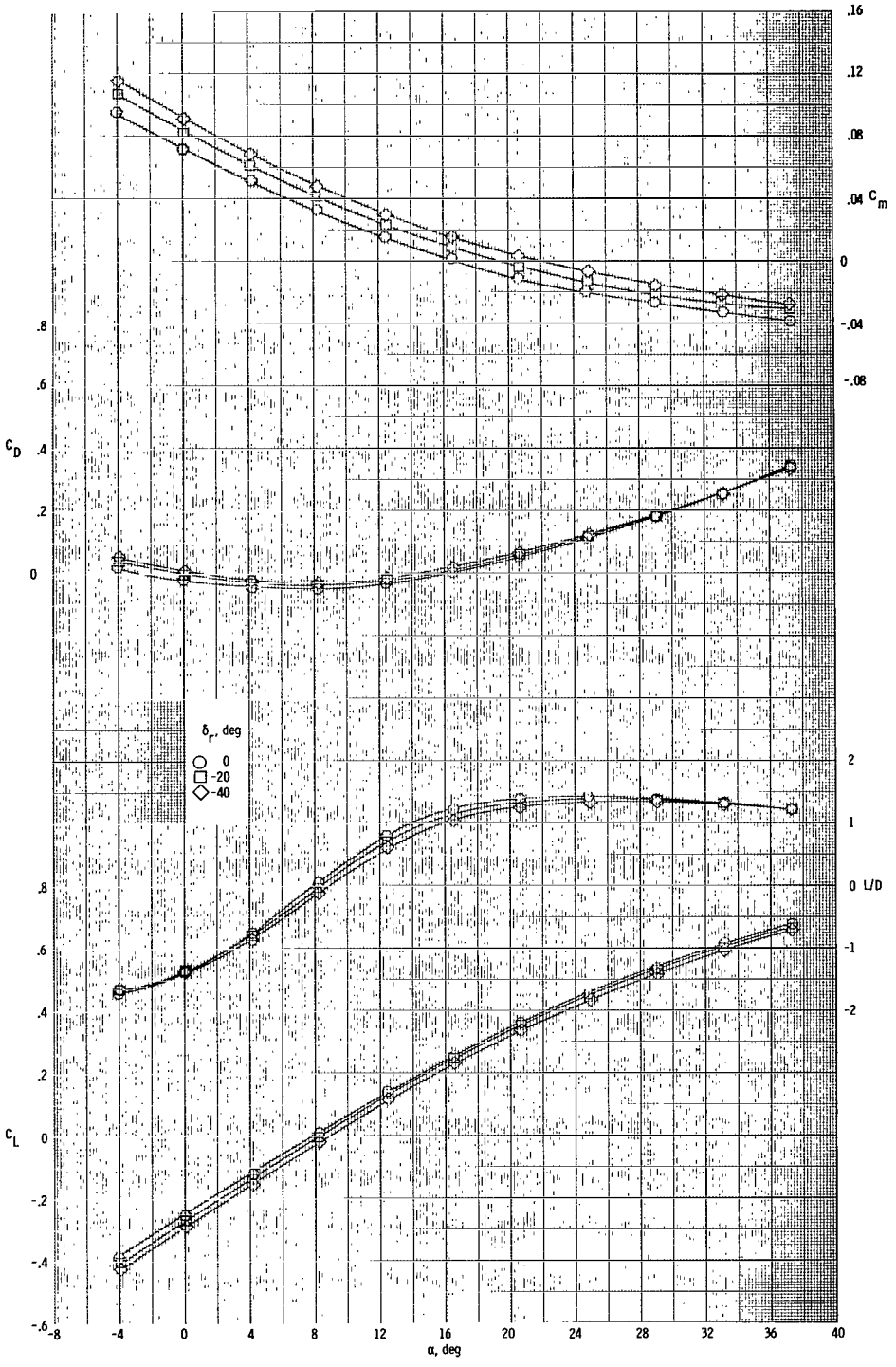

(b) $\delta_e = 0^o$.

Figure 11.- Continued.

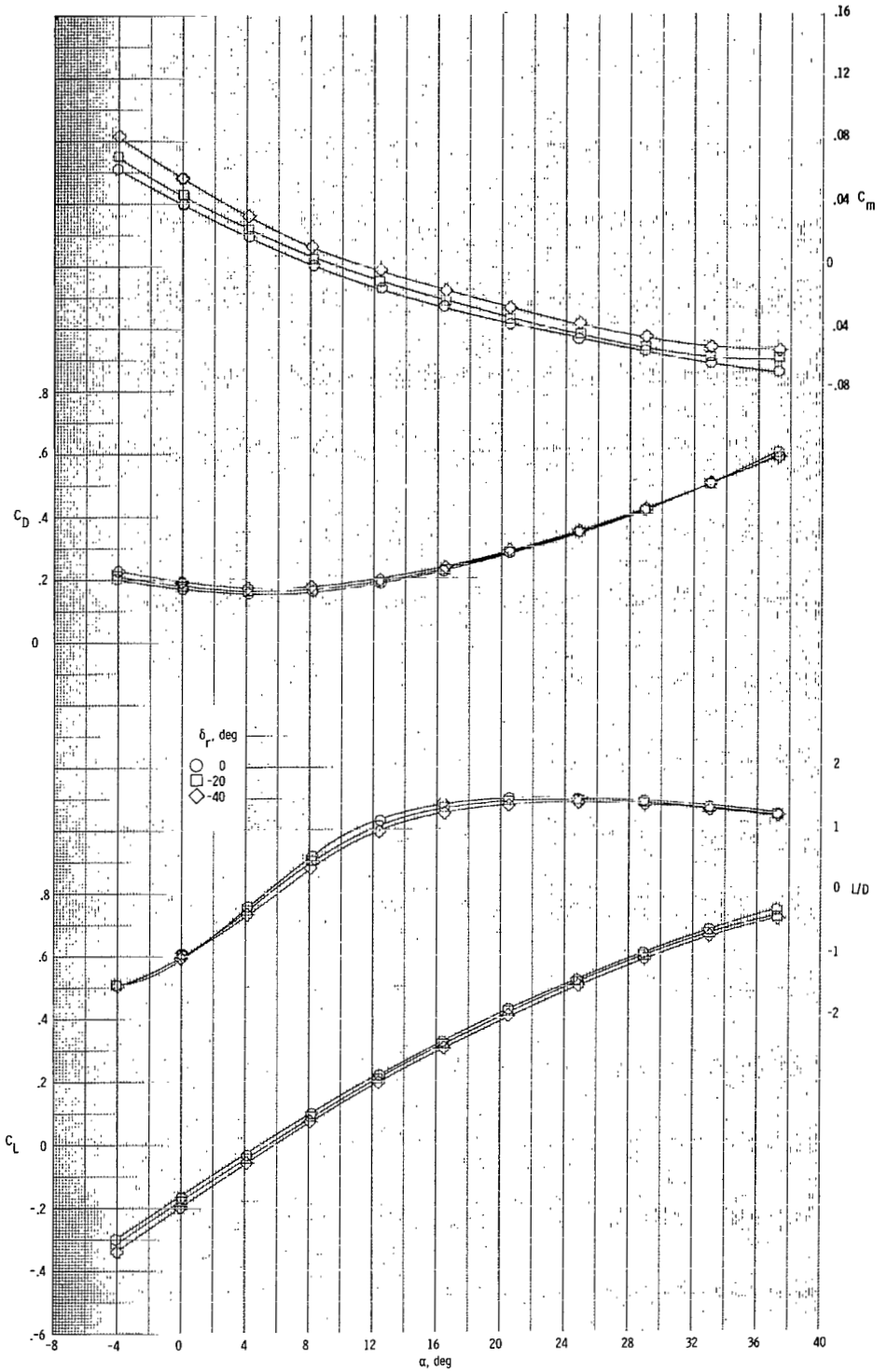

(c) $\delta_e = 15°$.

Figure 11.- Continued.

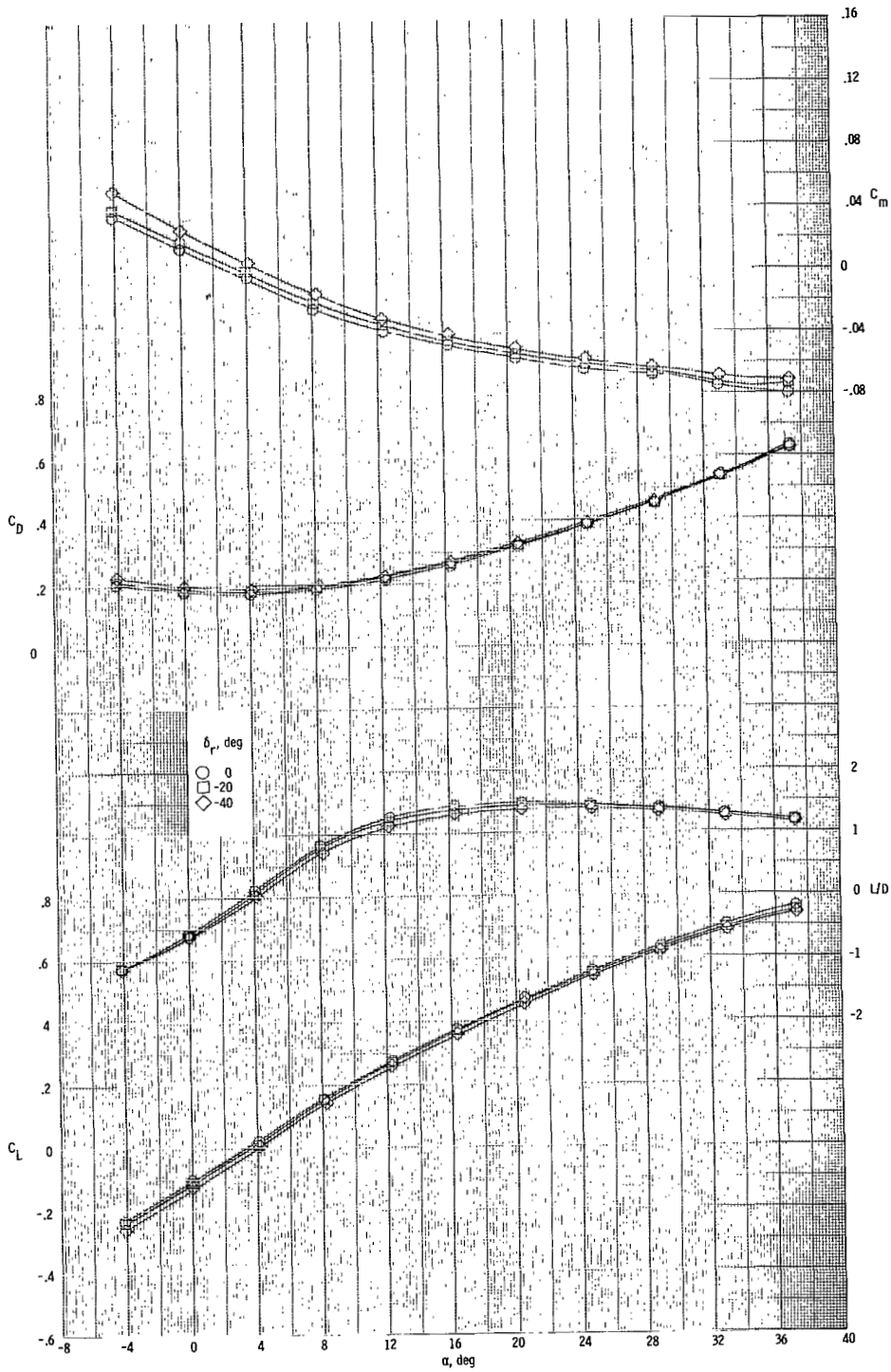

(d) $\delta_e = 30^\circ$.

Figure 11.- Concluded.

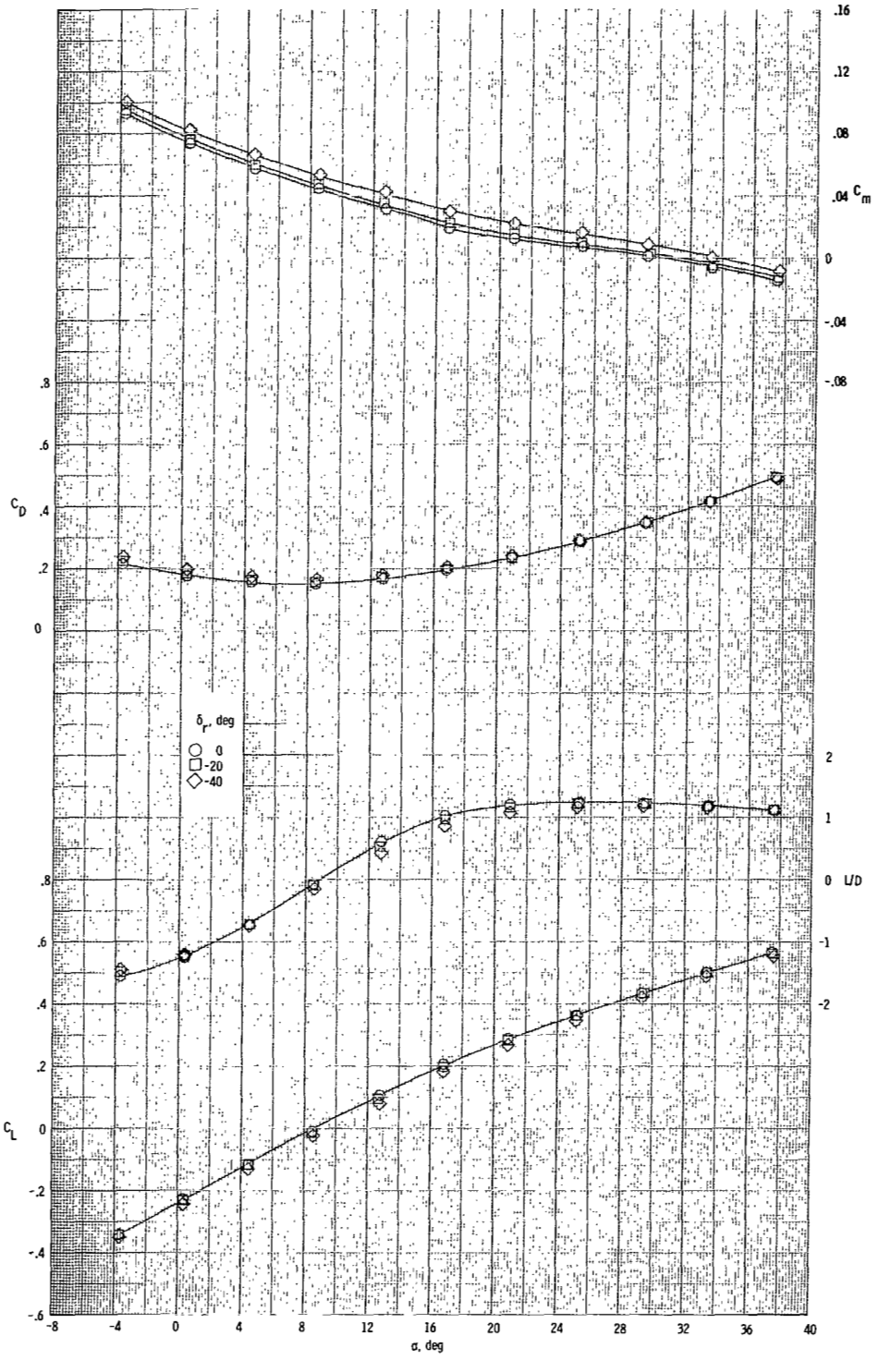

(a) $\delta_e = -15^\circ$.

Figure 12.- Effects of rudder deflection on longitudinal aerodynamic characteristics of vehicle with modification II tip fins for various elevon deflection angles. $\beta = 0^\circ$; M = 1.80.

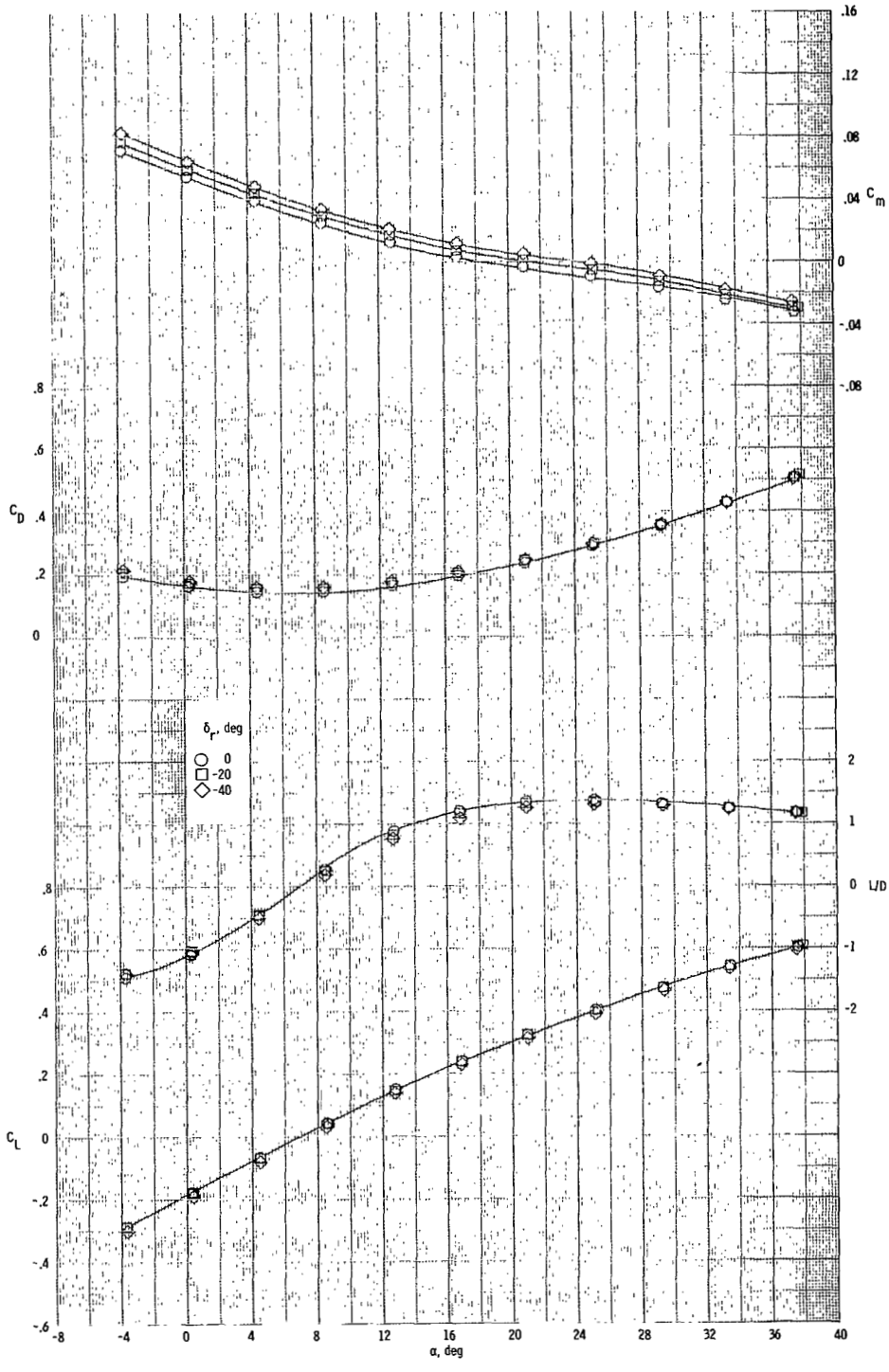

(b) $\delta_e = 0^o$.

Figure 12.- Continued.

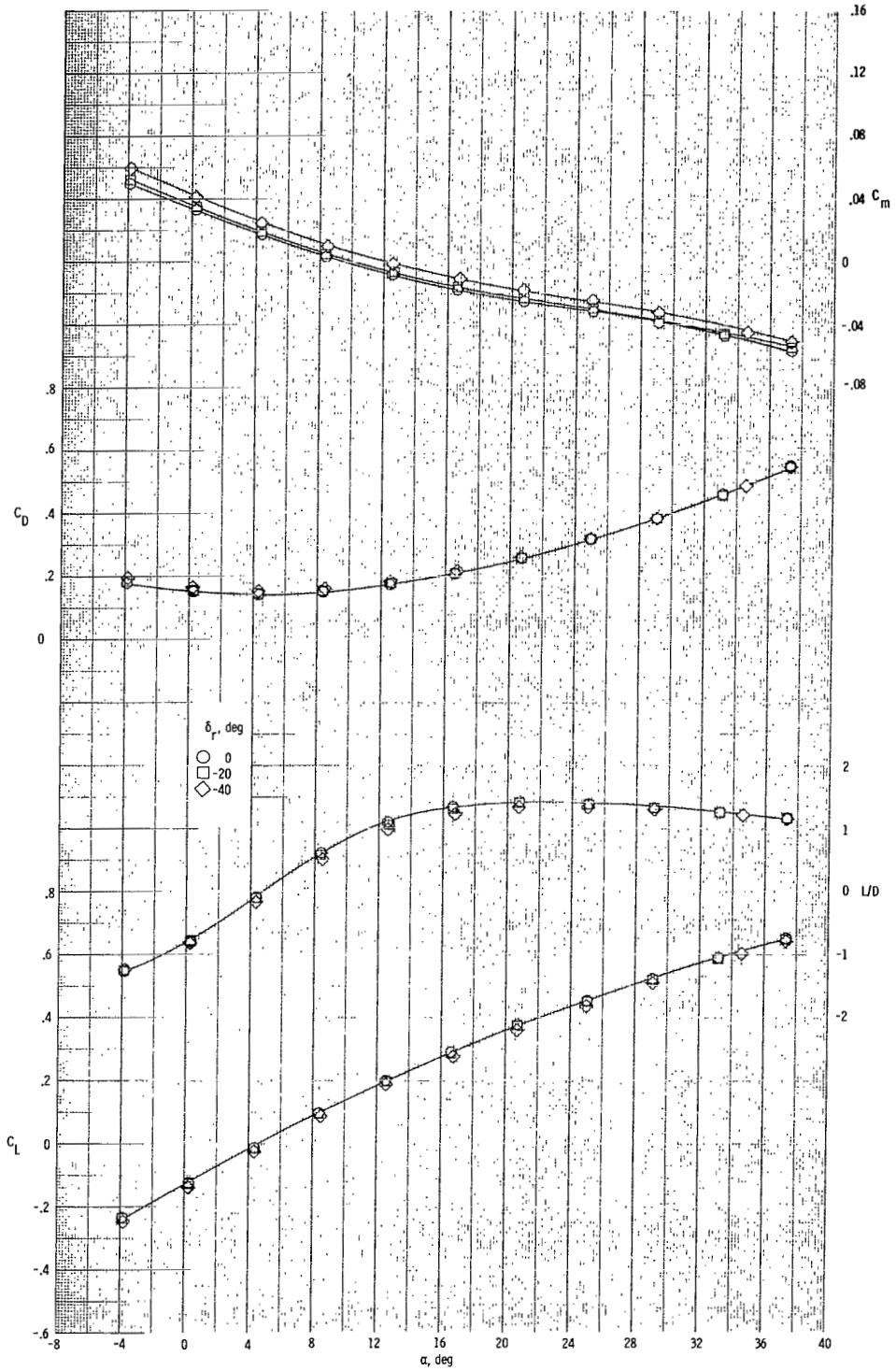

(c) $\delta_e = 15°$.

Figure 12.- Continued.

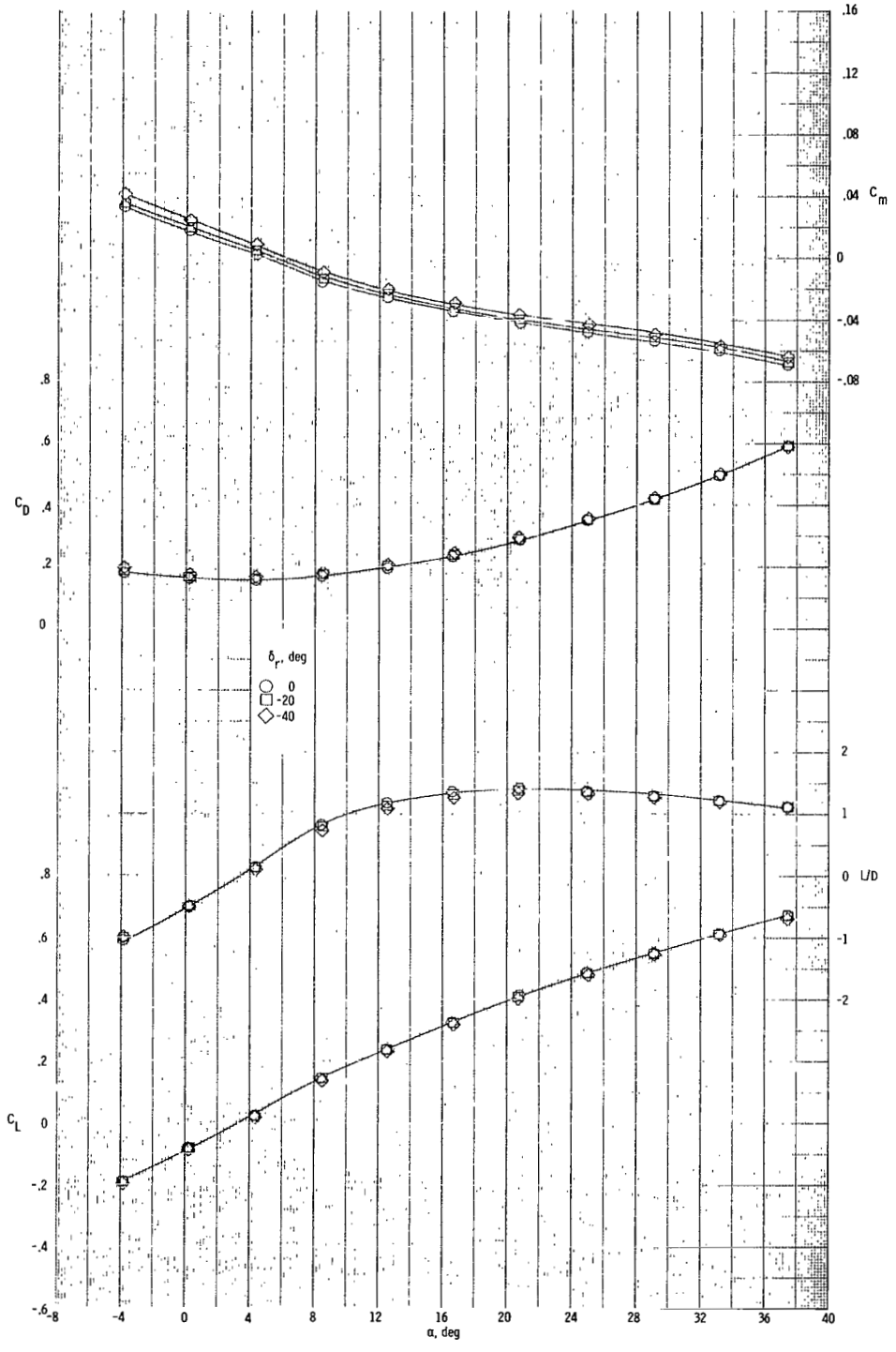

(d) $\delta_e = 30^\circ$.

Figure 12.- Concluded.

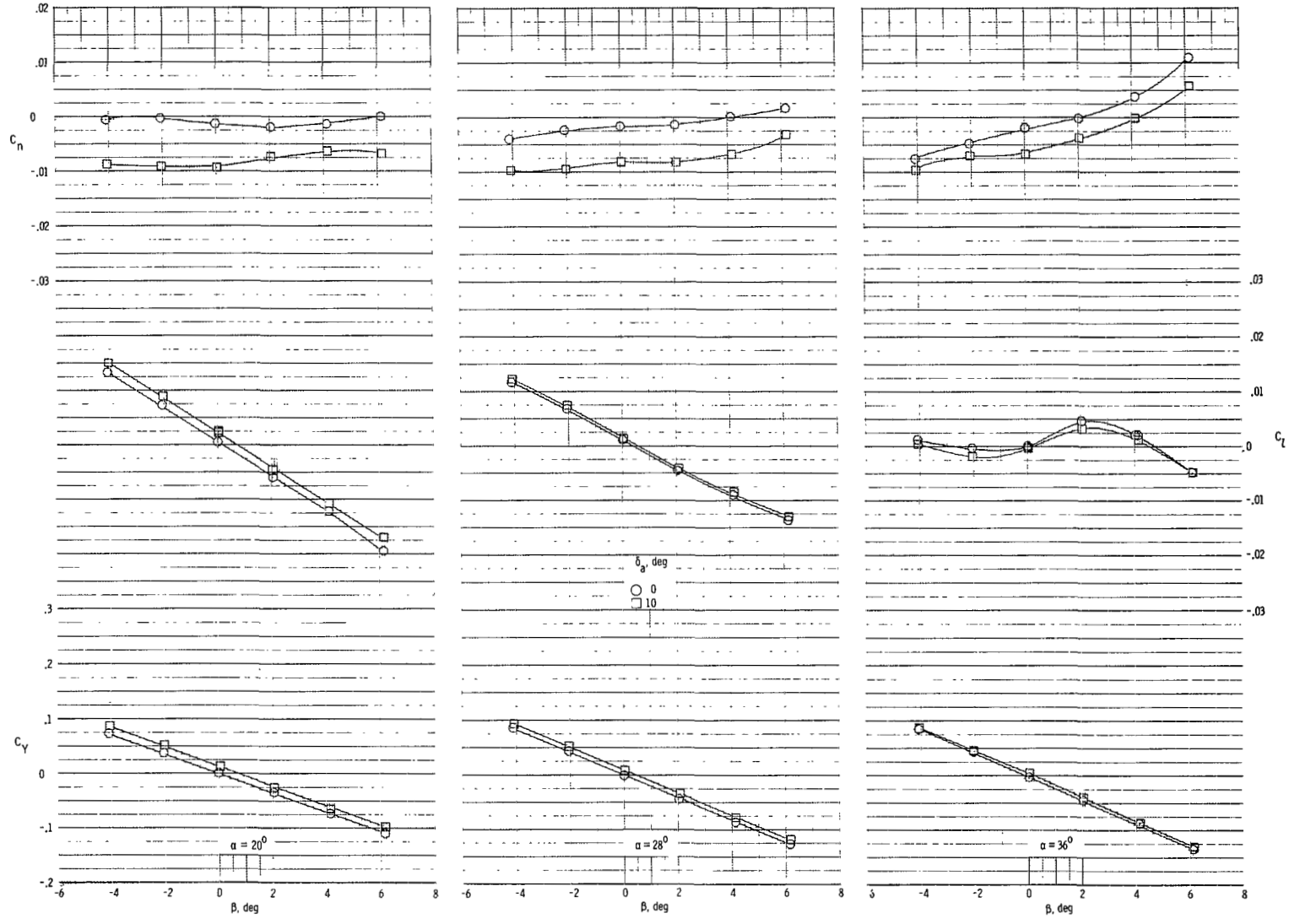

(a) $\delta_e = -30°$.

Figure 13.- Effects of aileron deflection on variation of lateral aerodynamic characteristics with sideslip angle for vehicle with modification II tip fins at selected angles of attack and several elevon deflection angles. M = 1.50.

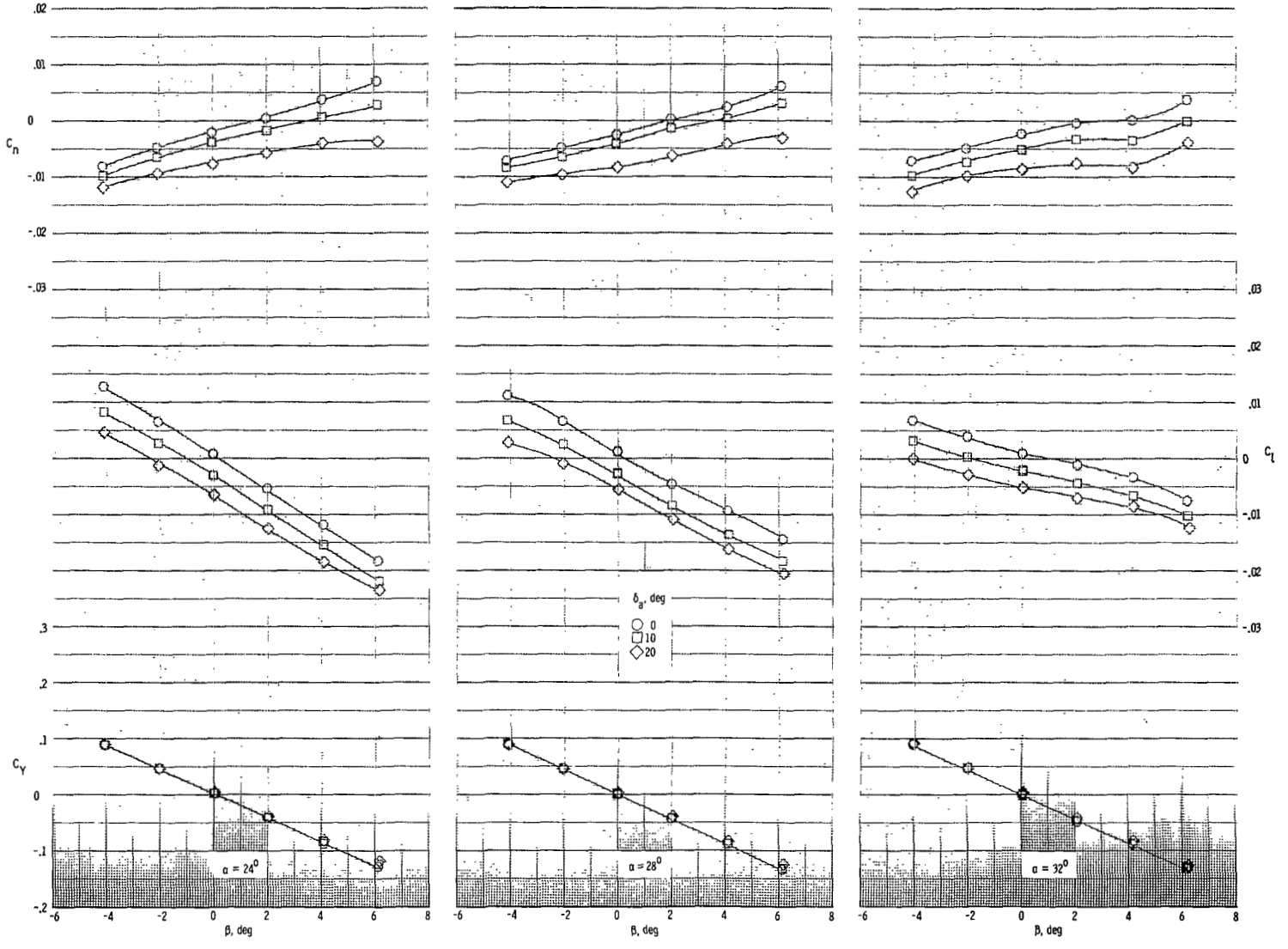

(b) $\delta_e = -15^\circ$.

Figure 13.- Continued.

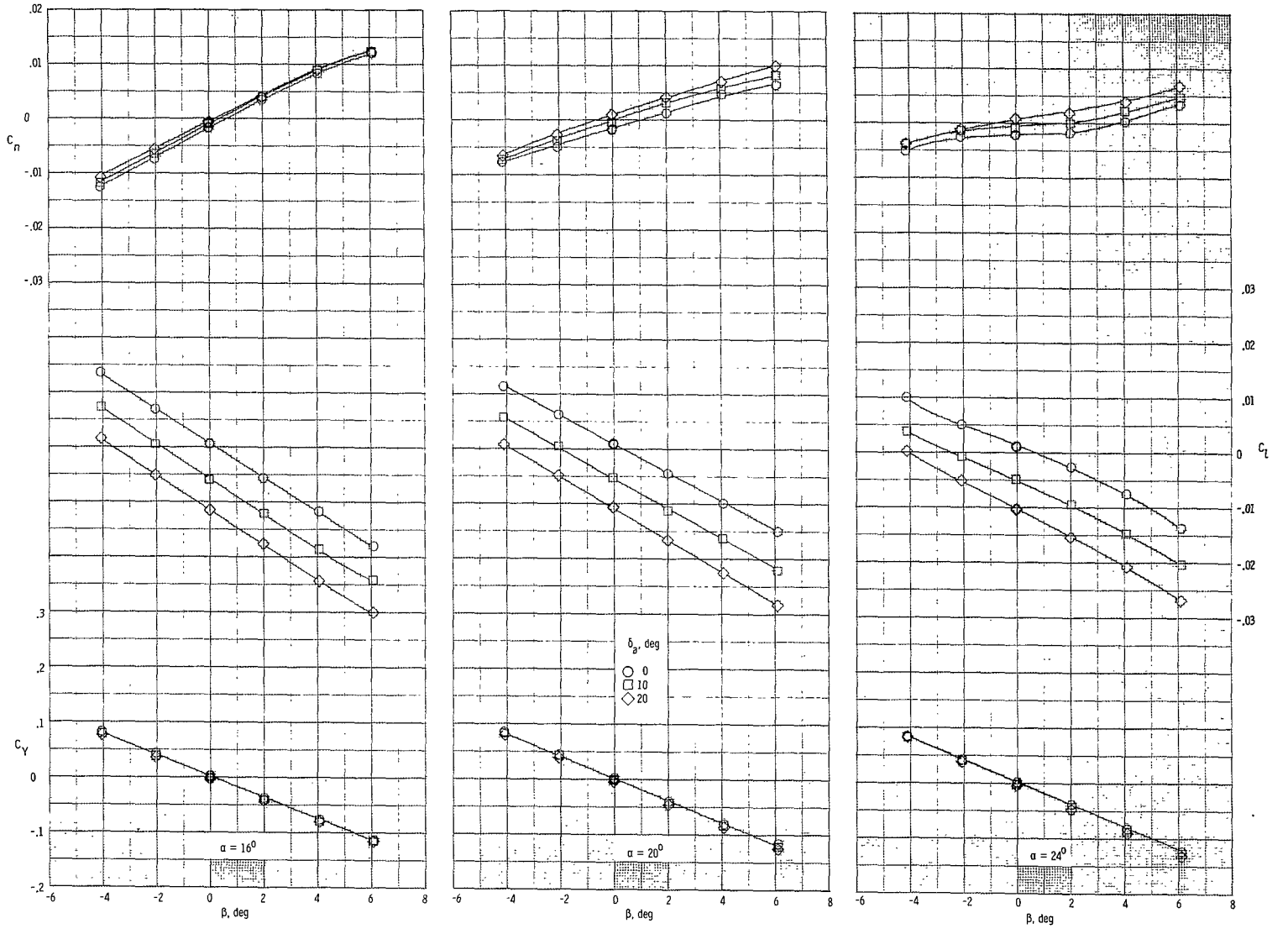

(c) $\delta_e = 0°$.

Figure 13.- Continued.

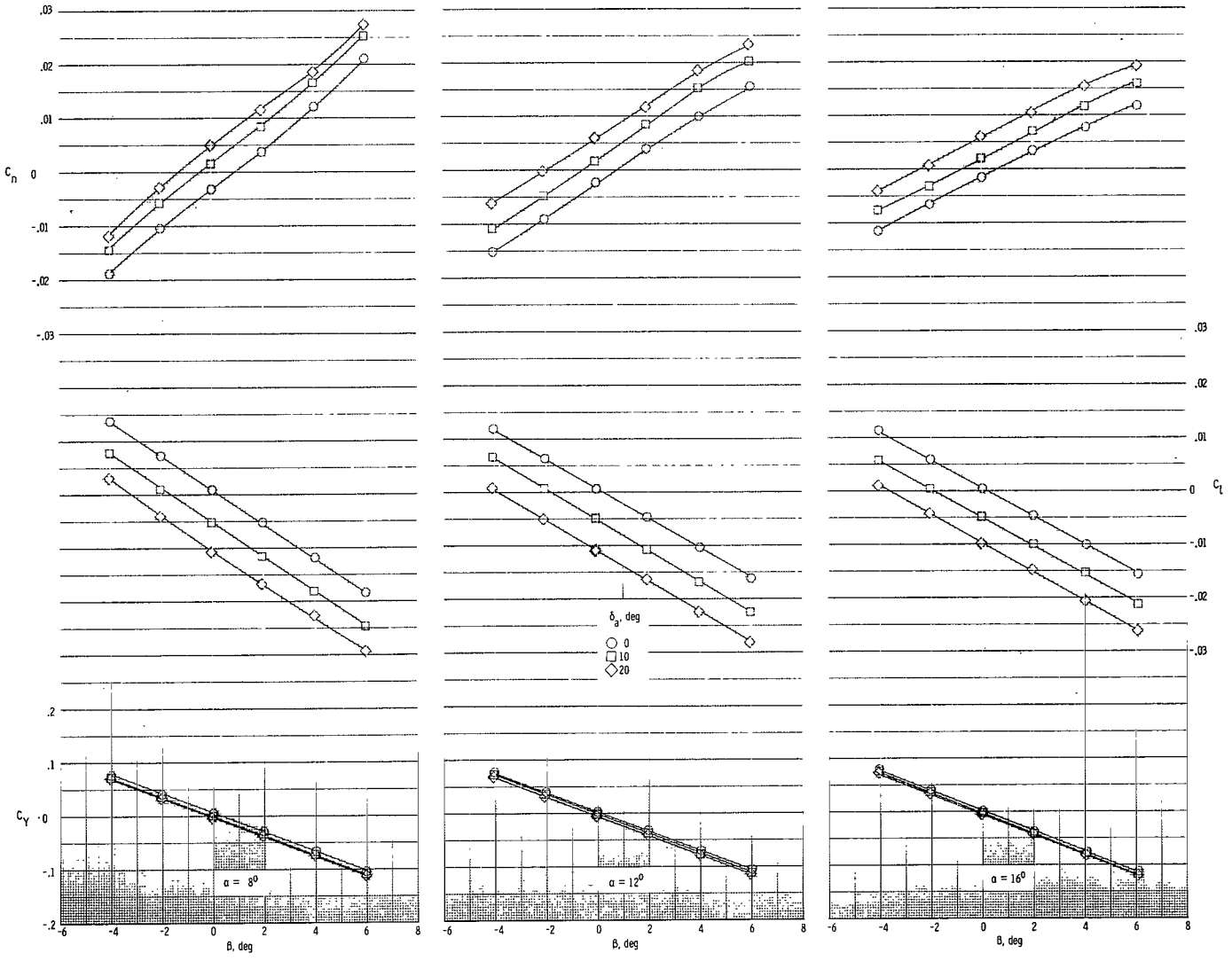

(d) $\delta_e = 15^\circ$.

Figure 13.- Continued.

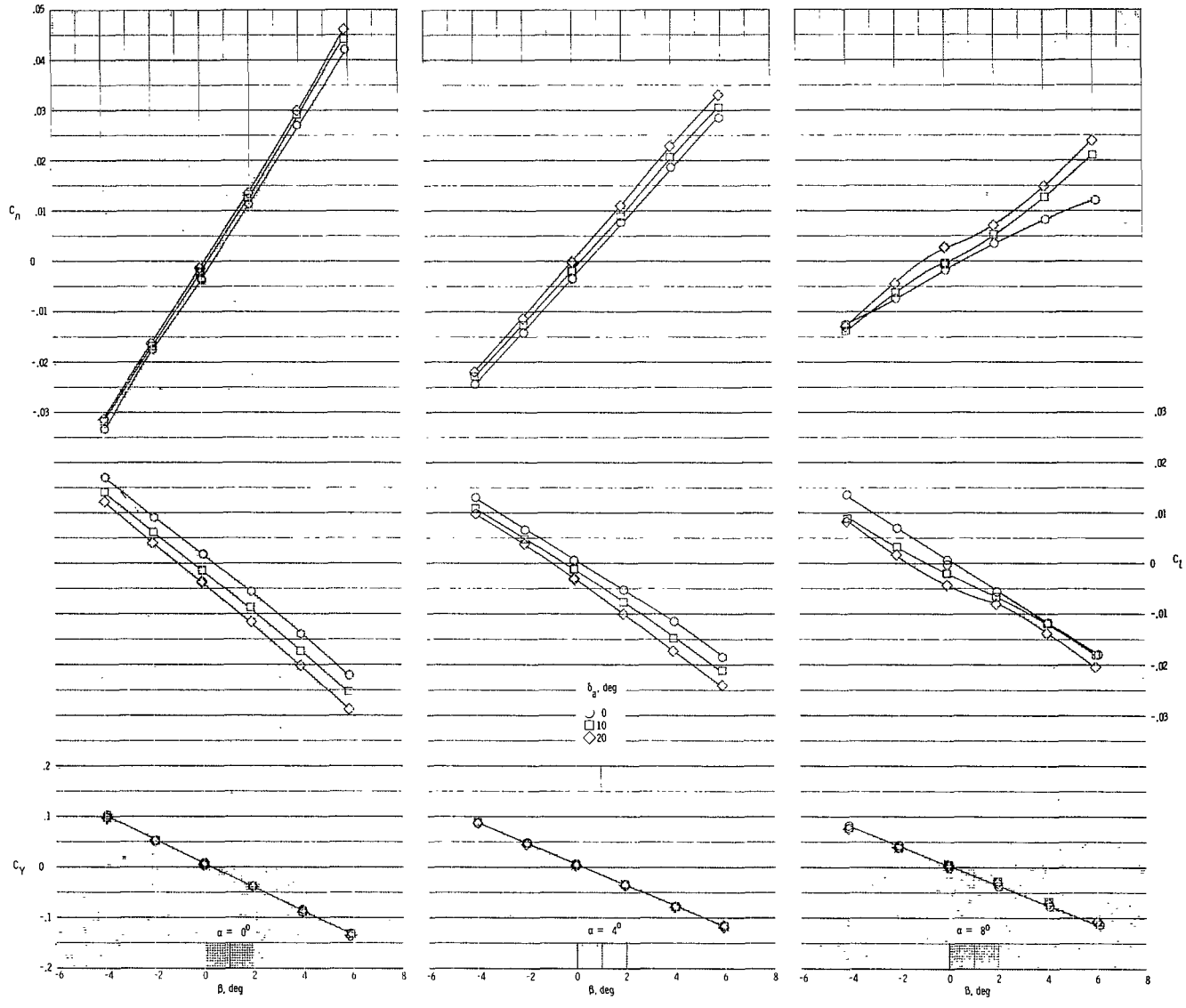

(e) $\delta_e = 30^\circ$.

Figure 13.- Concluded.

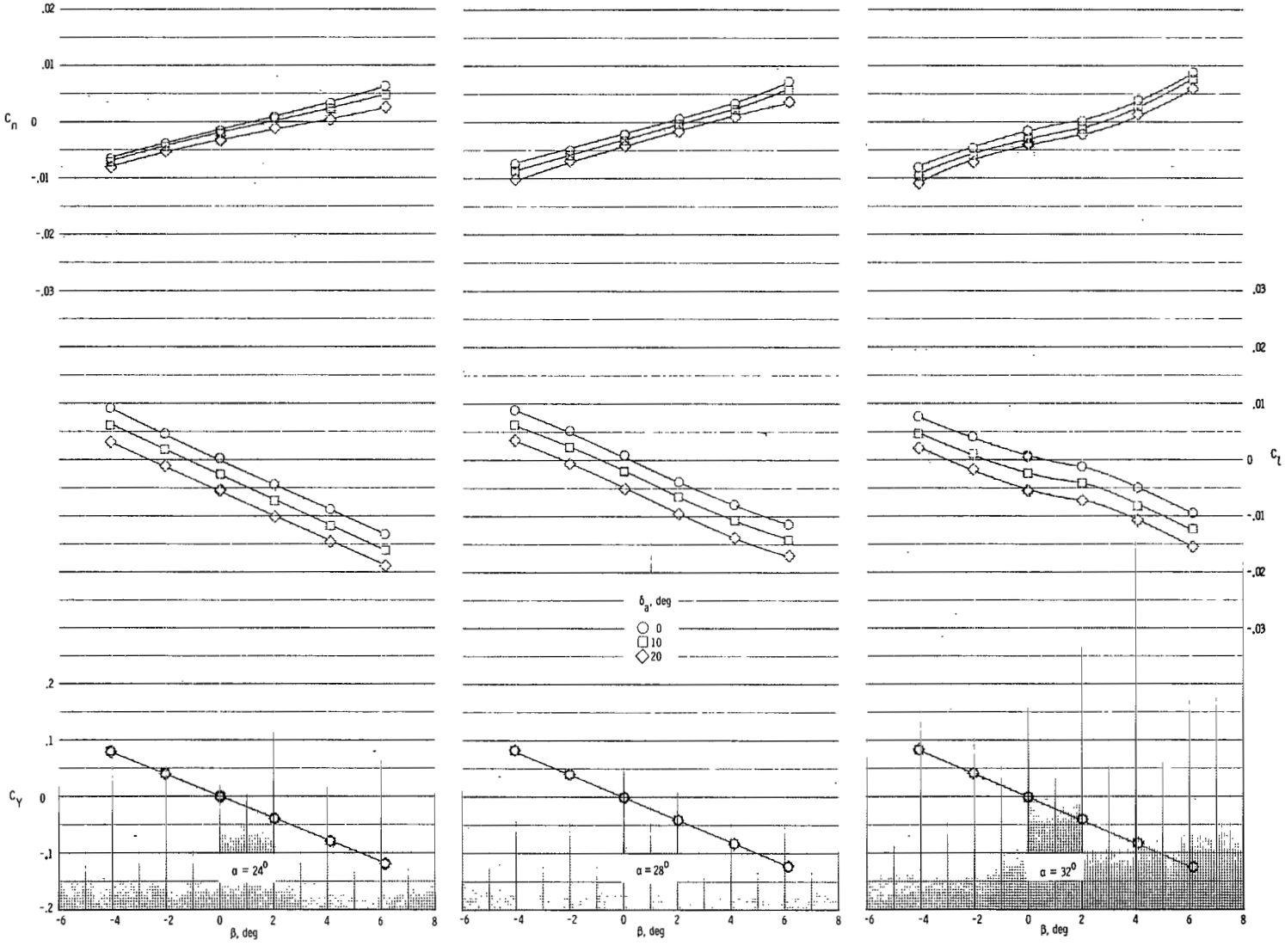

(a) $\delta_e = -15°$.

Figure 14.- Effects of aileron deflection on variation of lateral aerodynamic characteristics with sideslip angle for vehicle with modification II tip fins at selected angles of attack and several elevon deflection angles. M = 1.80.

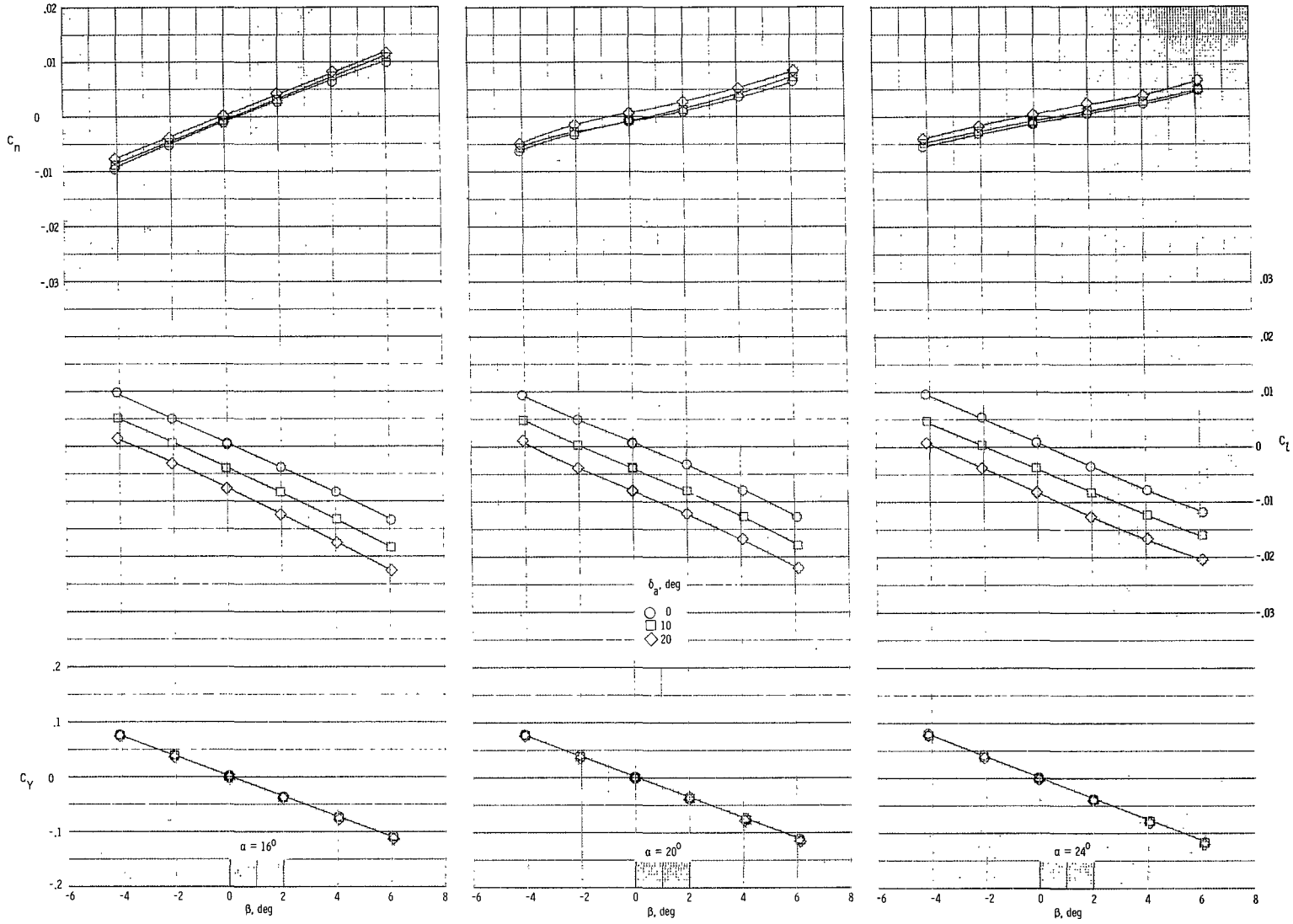

(b) $\delta_e = 0°$.

Figure 14.- Continued.

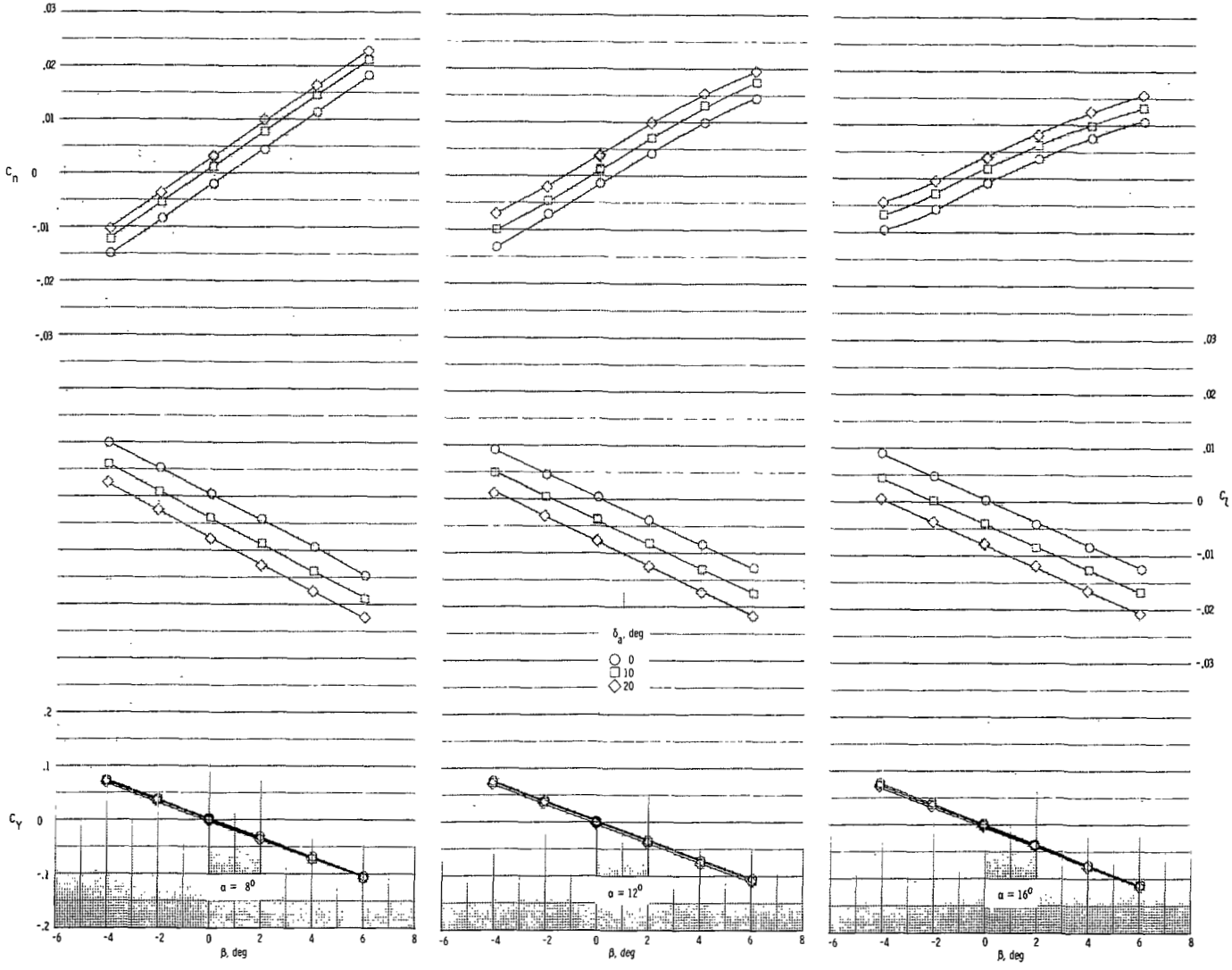

(c) $\delta_e = 15°$.

Figure 14.- Continued.

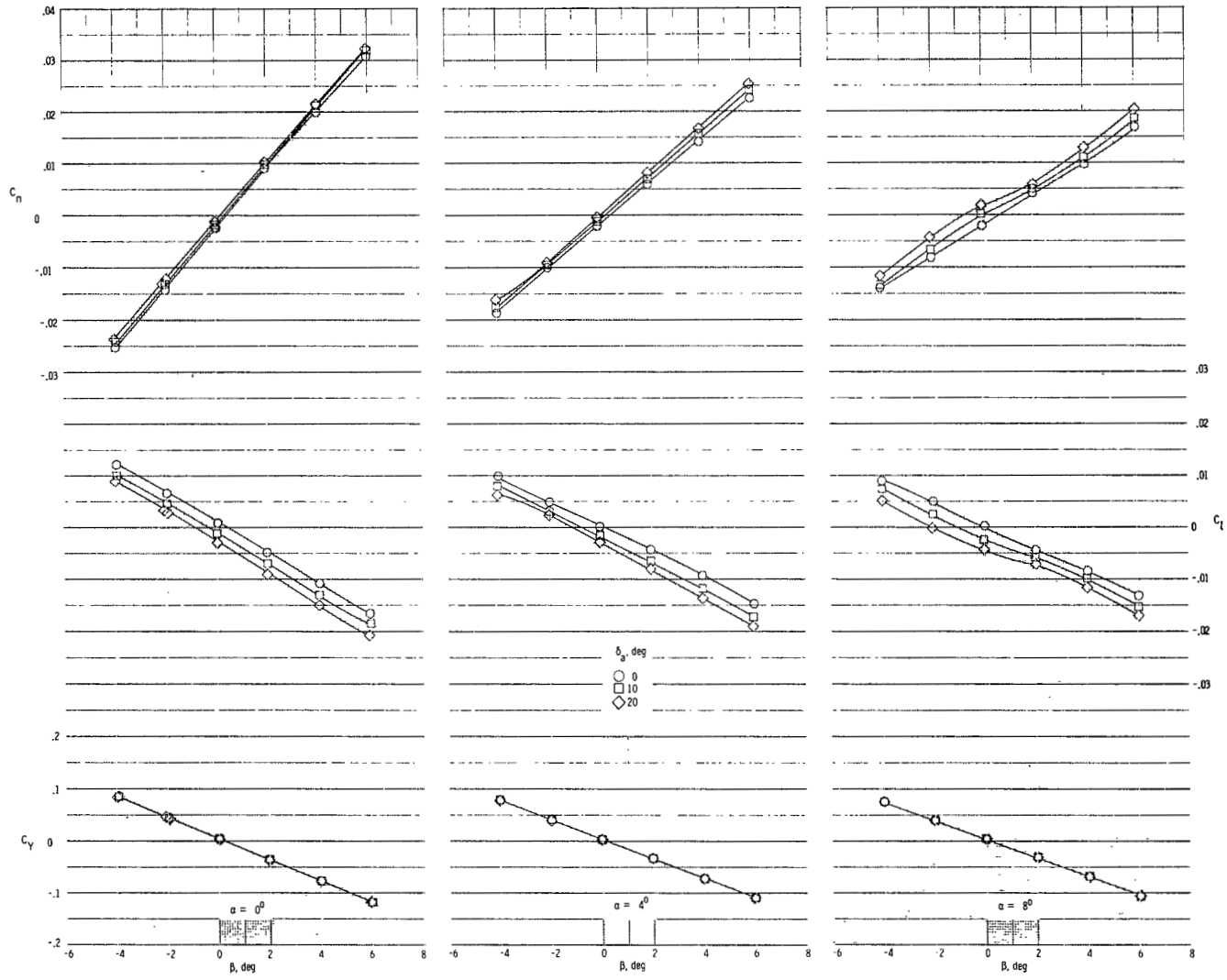

(d) $\delta_e = 30°$.

Figure 14.- Concluded.

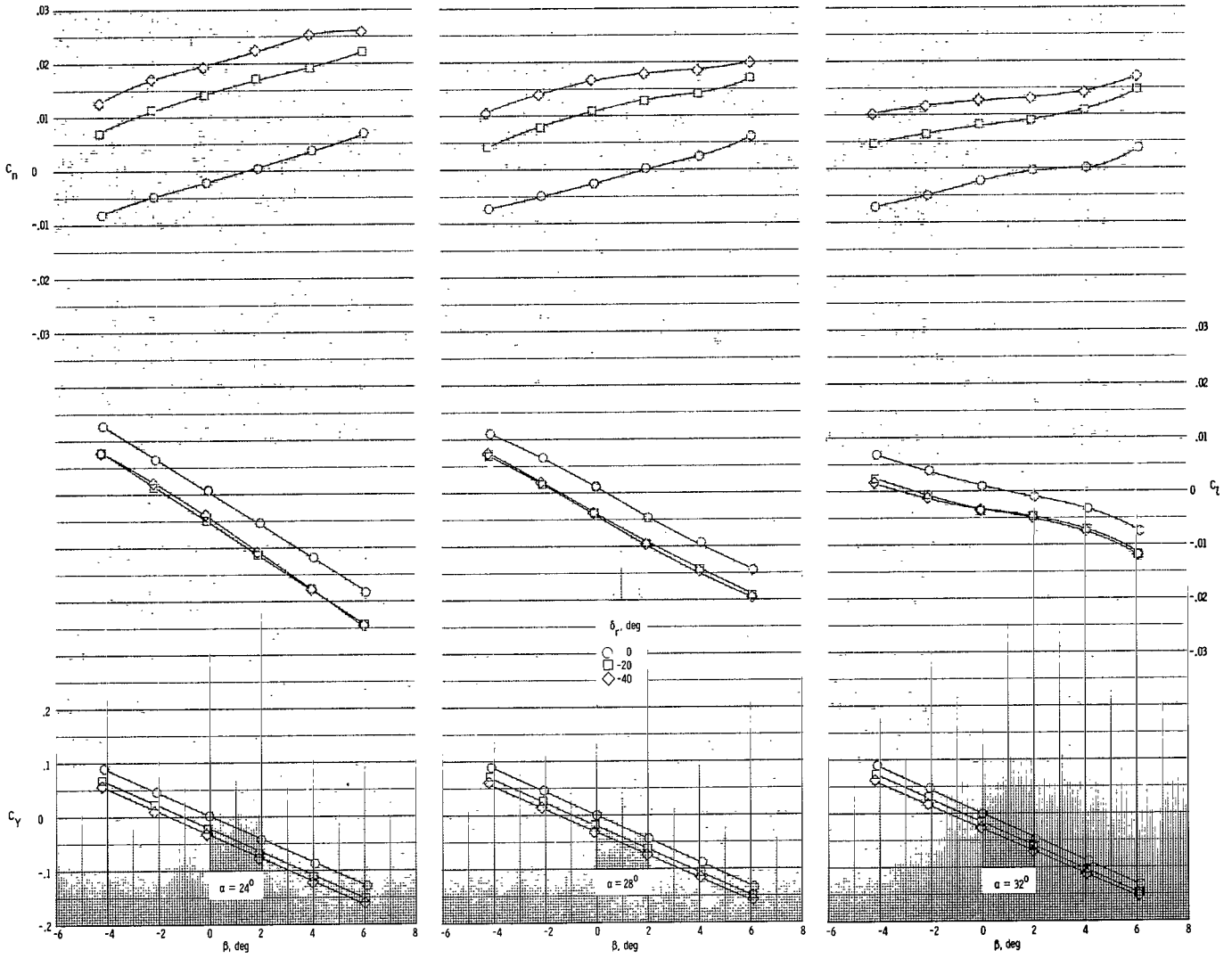

(a) $\delta_e = -15°$.

Figure 15.- Effects of rudder deflection on variation of lateral aerodynamic characteristics with sideslip angle for vehicle with modification II tip fins at selected angles of attack and several elevon deflection angles. M = 1.50.

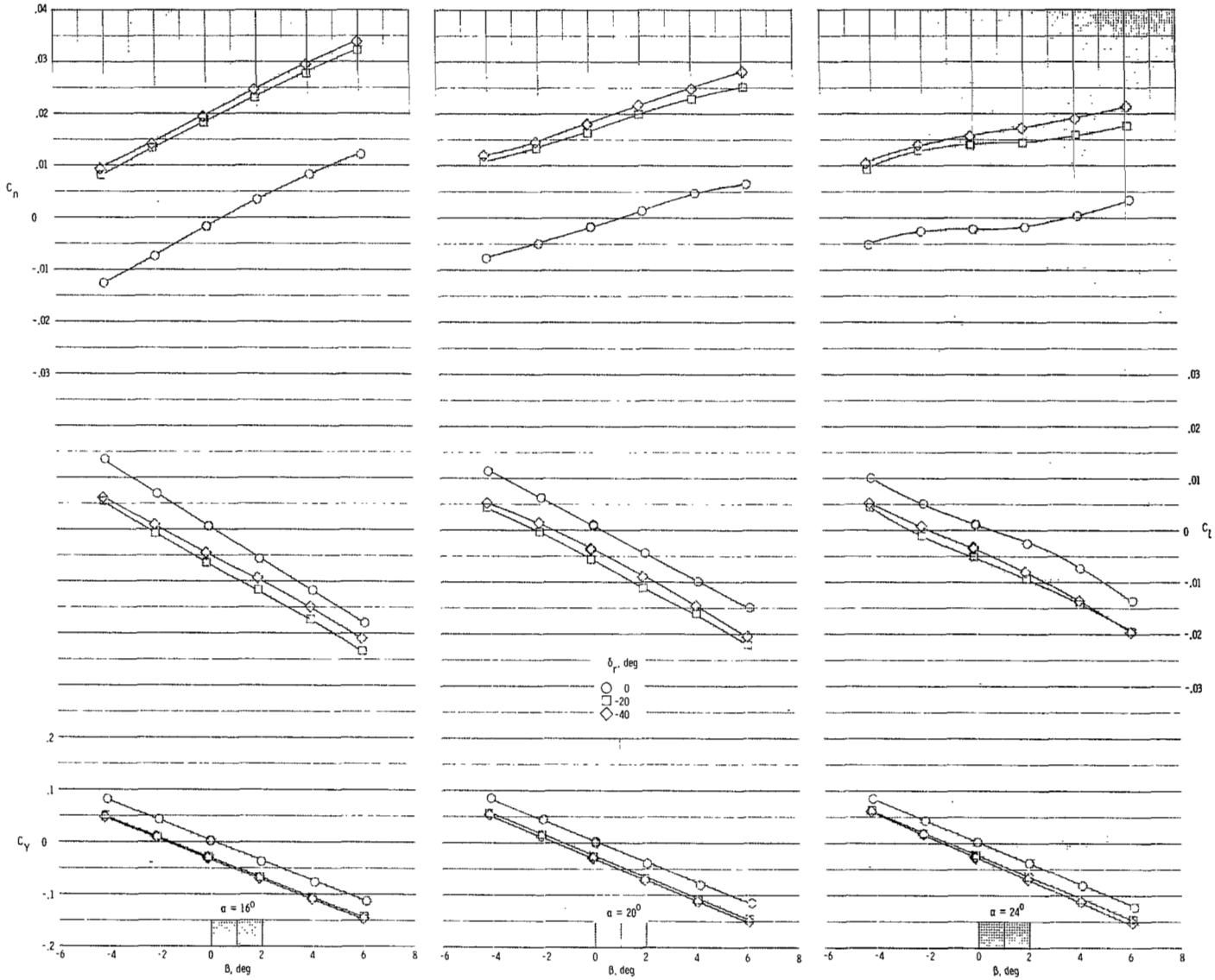

(b) $\delta_e = 0^\circ$.

Figure 15.- Continued.

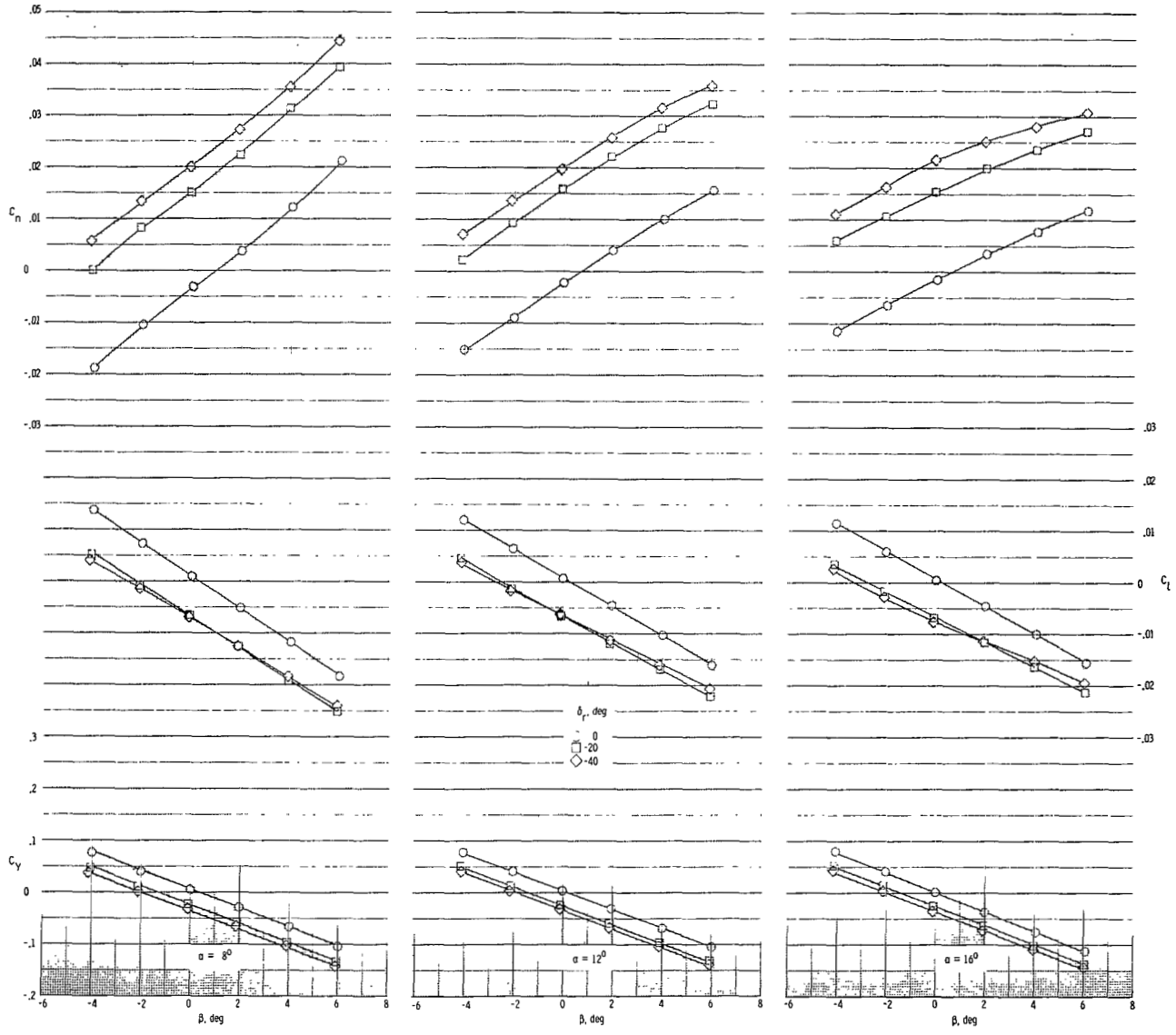

(c) $\delta_e = 15°$.

Figure 15.- Continued.

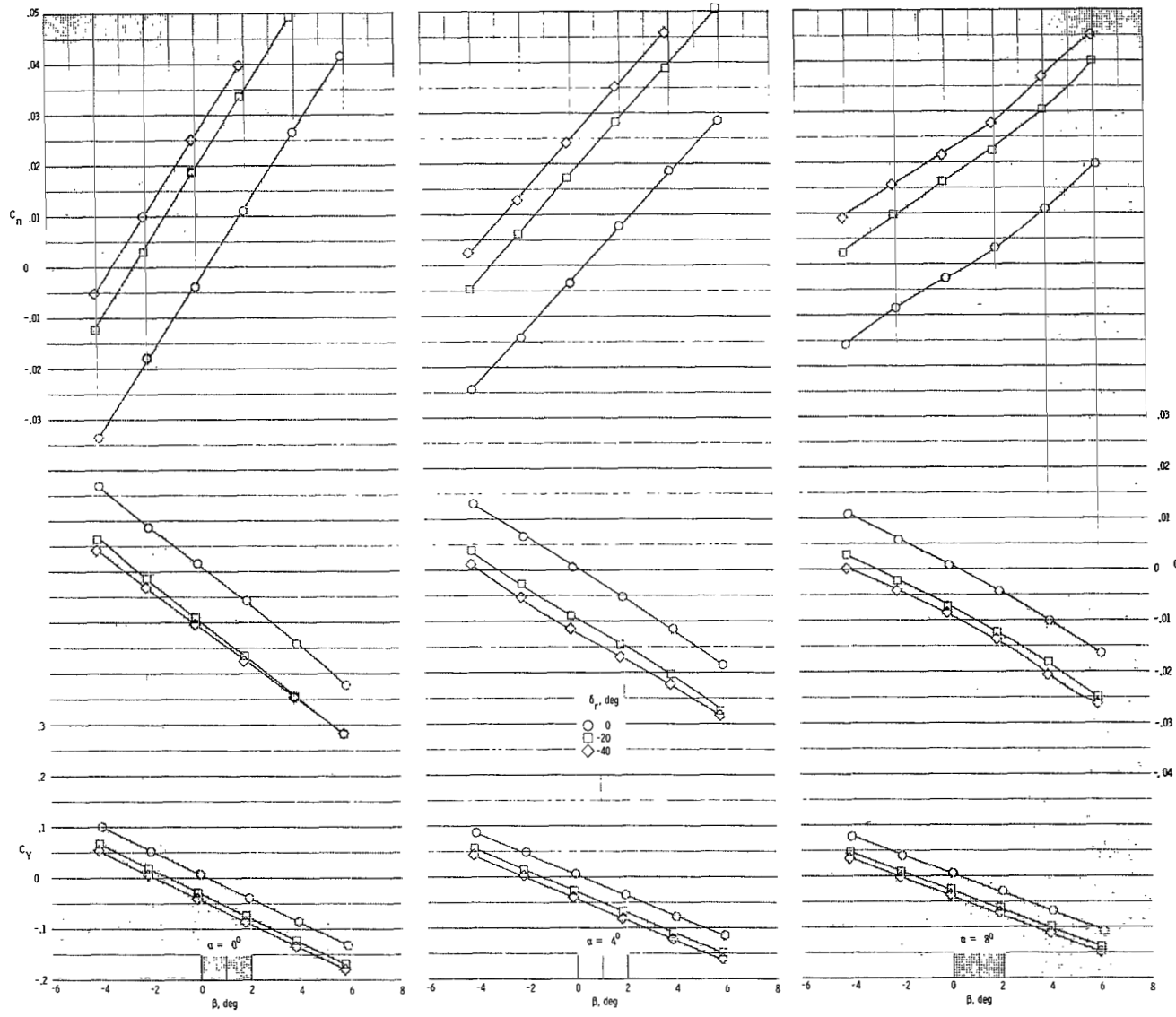

(d) $\delta_e = 30°$.

Figure 15.- Concluded.

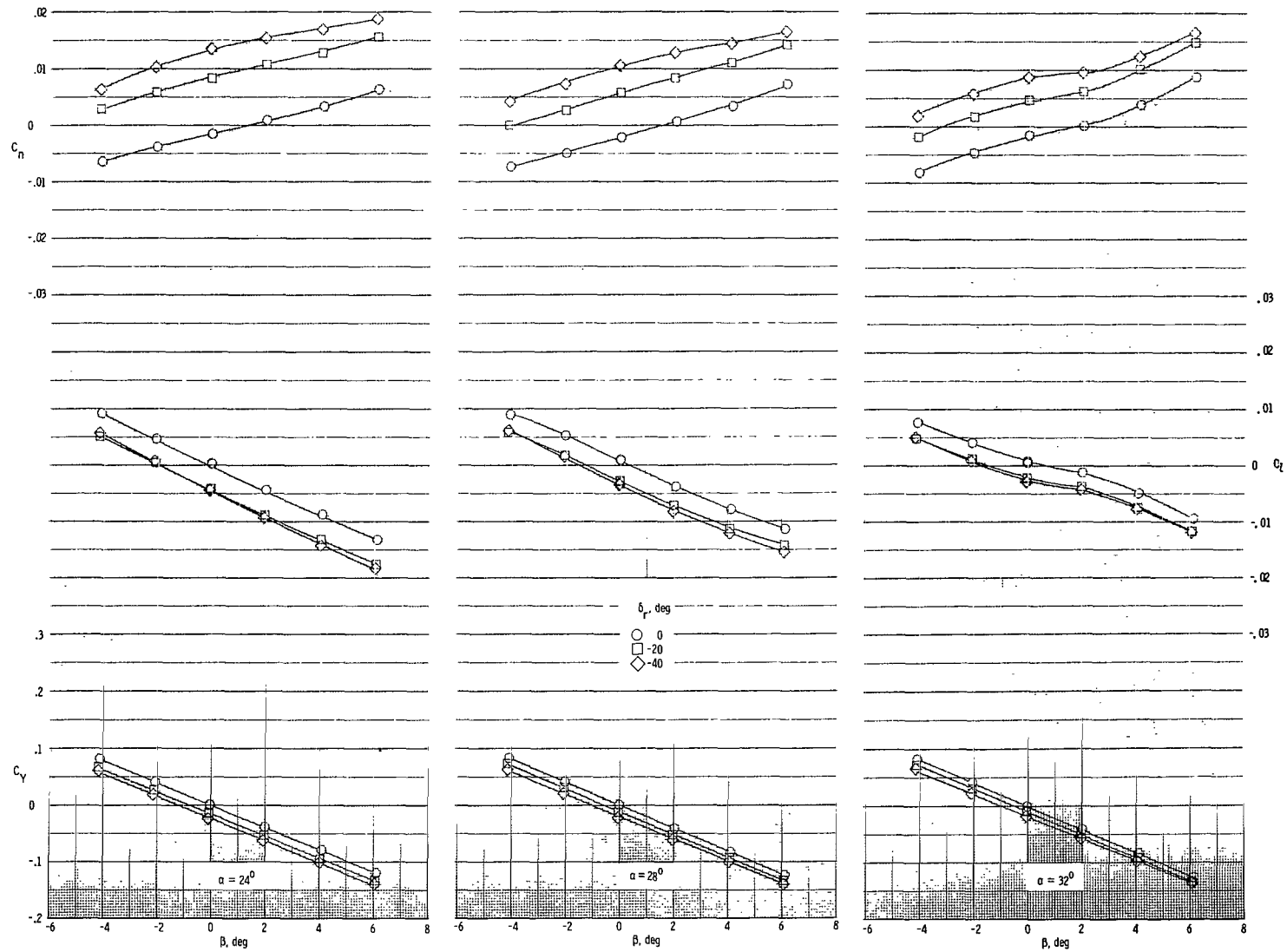

(a) $\delta_e = -15°$.

Figure 16.- Effects of rudder deflection on variation of lateral aerodynamic characteristics with sideslip angle for vehicle with modification II tip fins at selected angles of attack and several elevon deflection angles. M = 1.80.

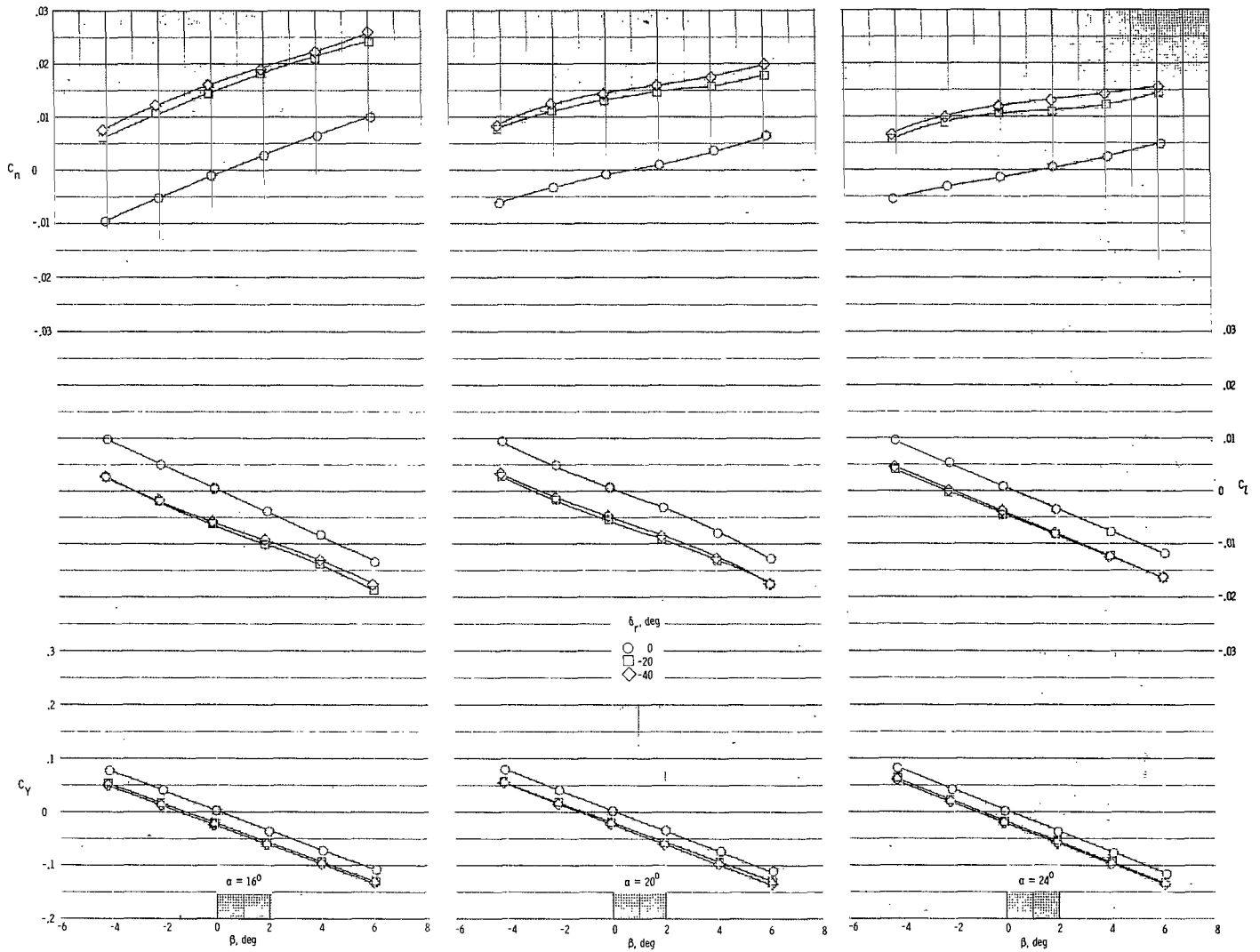

(b) $\delta_e = 0°$.

Figure 16.- Continued.

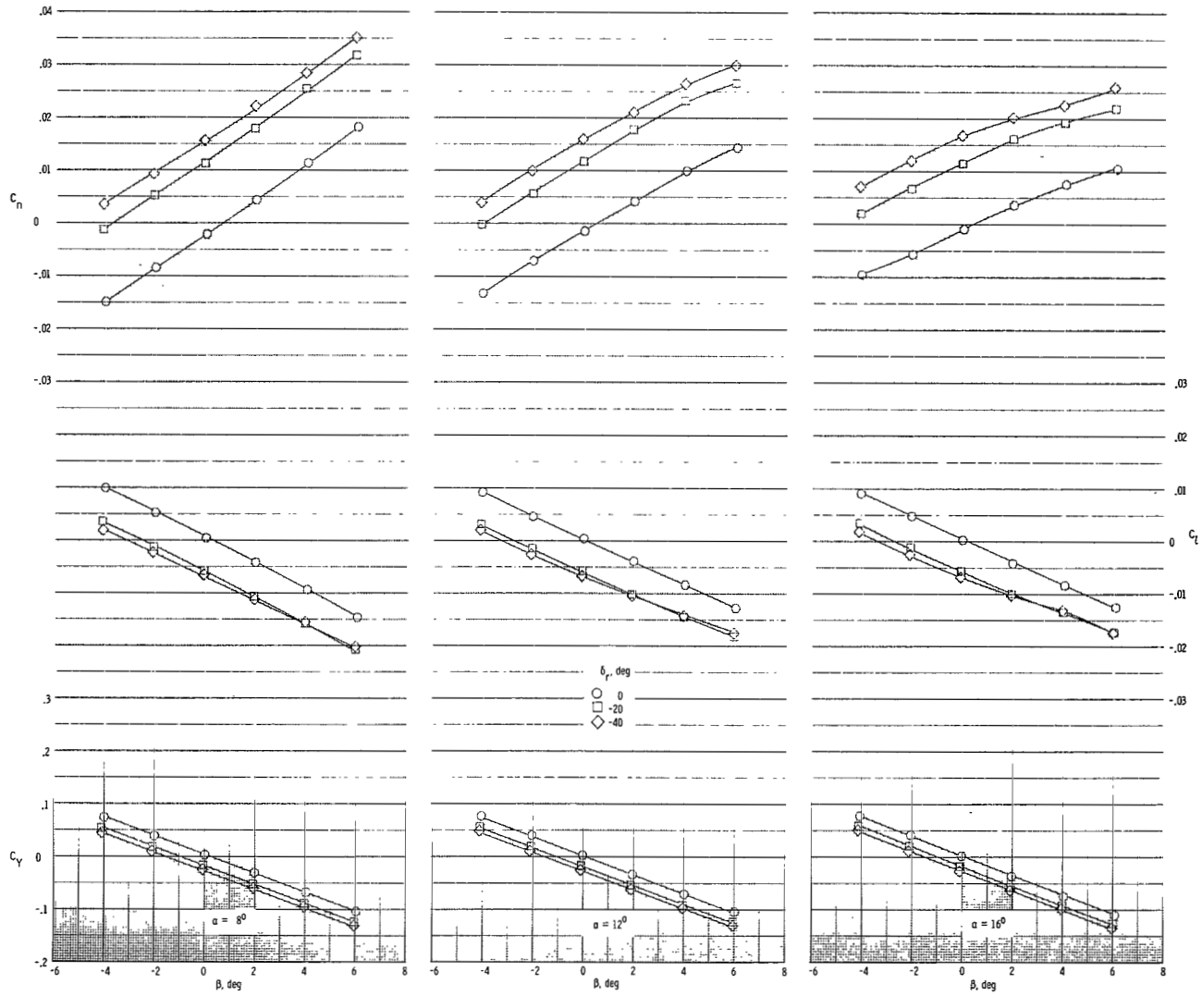

(c) $\delta_e = 15°$.

Figure 16.- Continued.

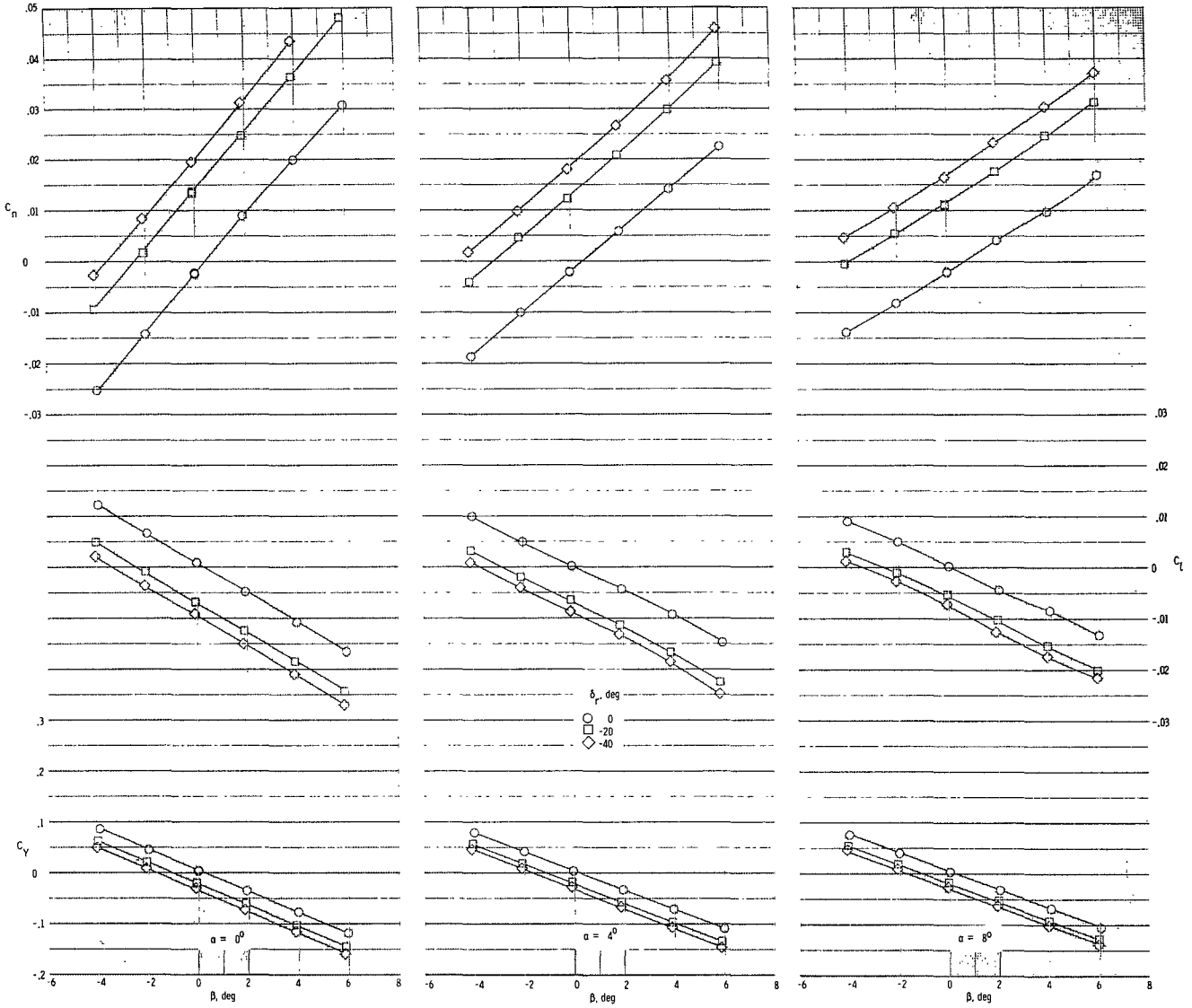

(d) $\delta_e = 30°$.

Figure 16.- Concluded.

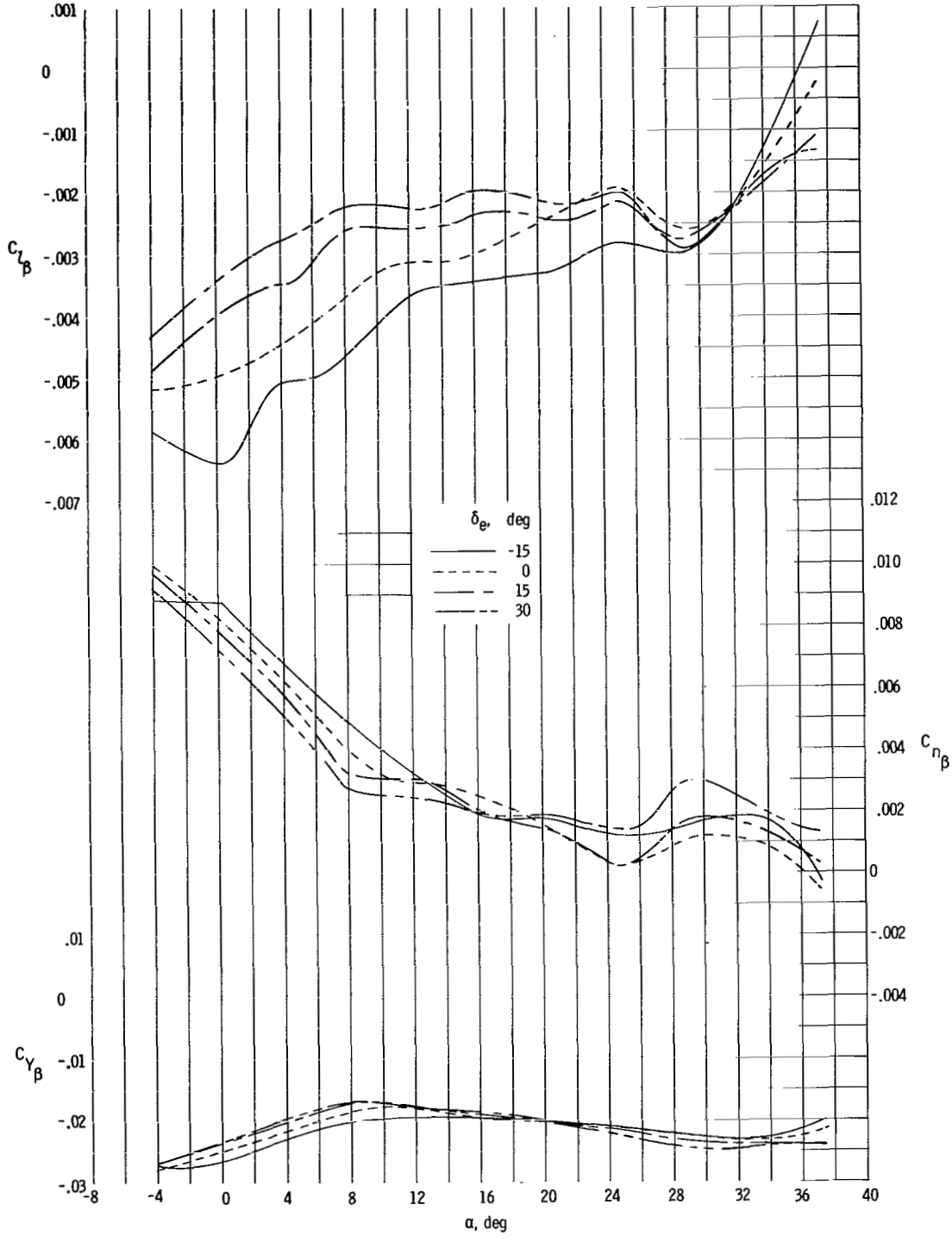

Figure 17.- Effects of elevon deflection on directional and lateral stability characteristics of vehicle with basic tip fins. M = 1.50.

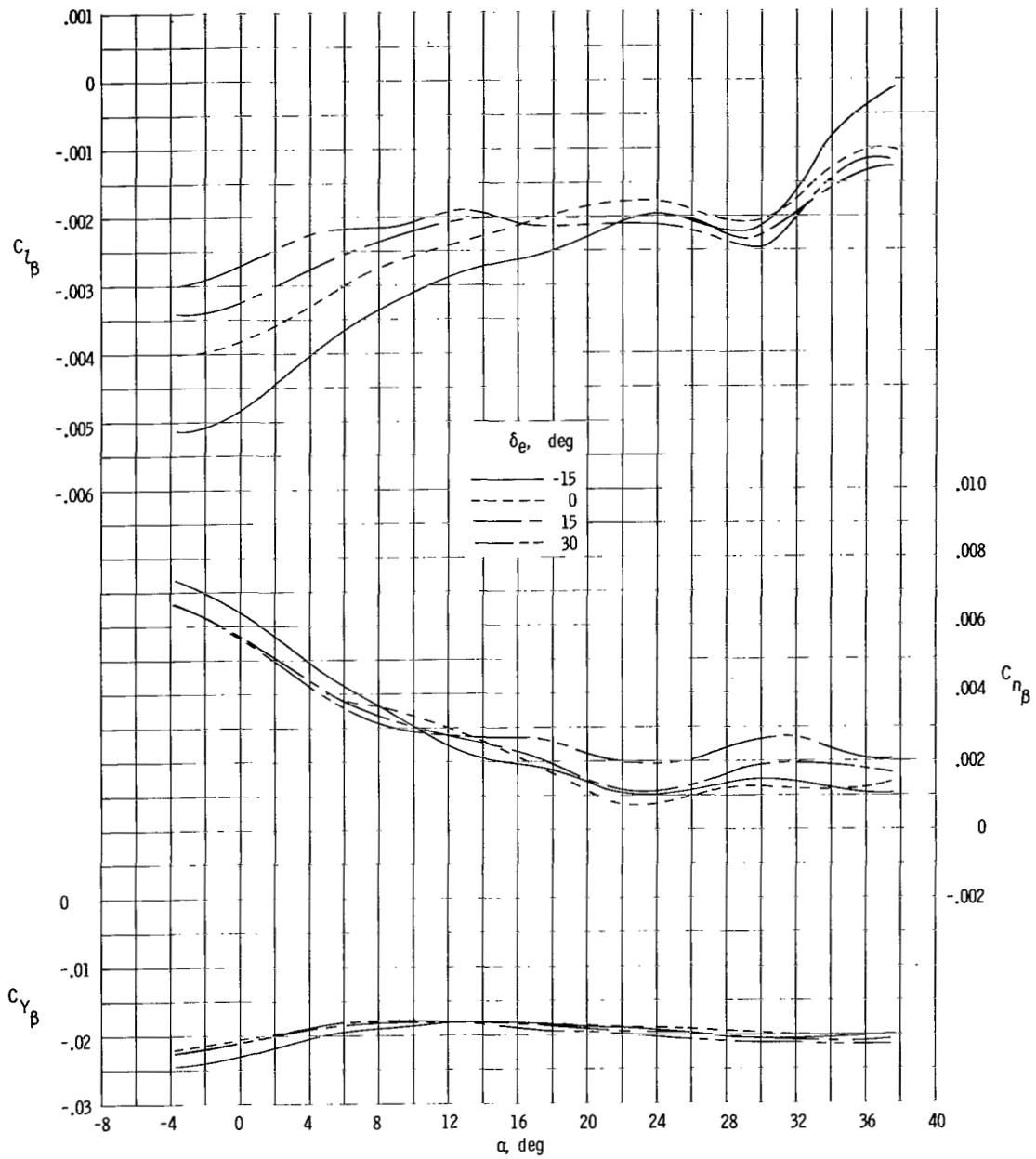

Figure 18.- Effects of elevon deflection on directional and lateral stability characteristics of vehicle with basic tip fins. M = 1.80.

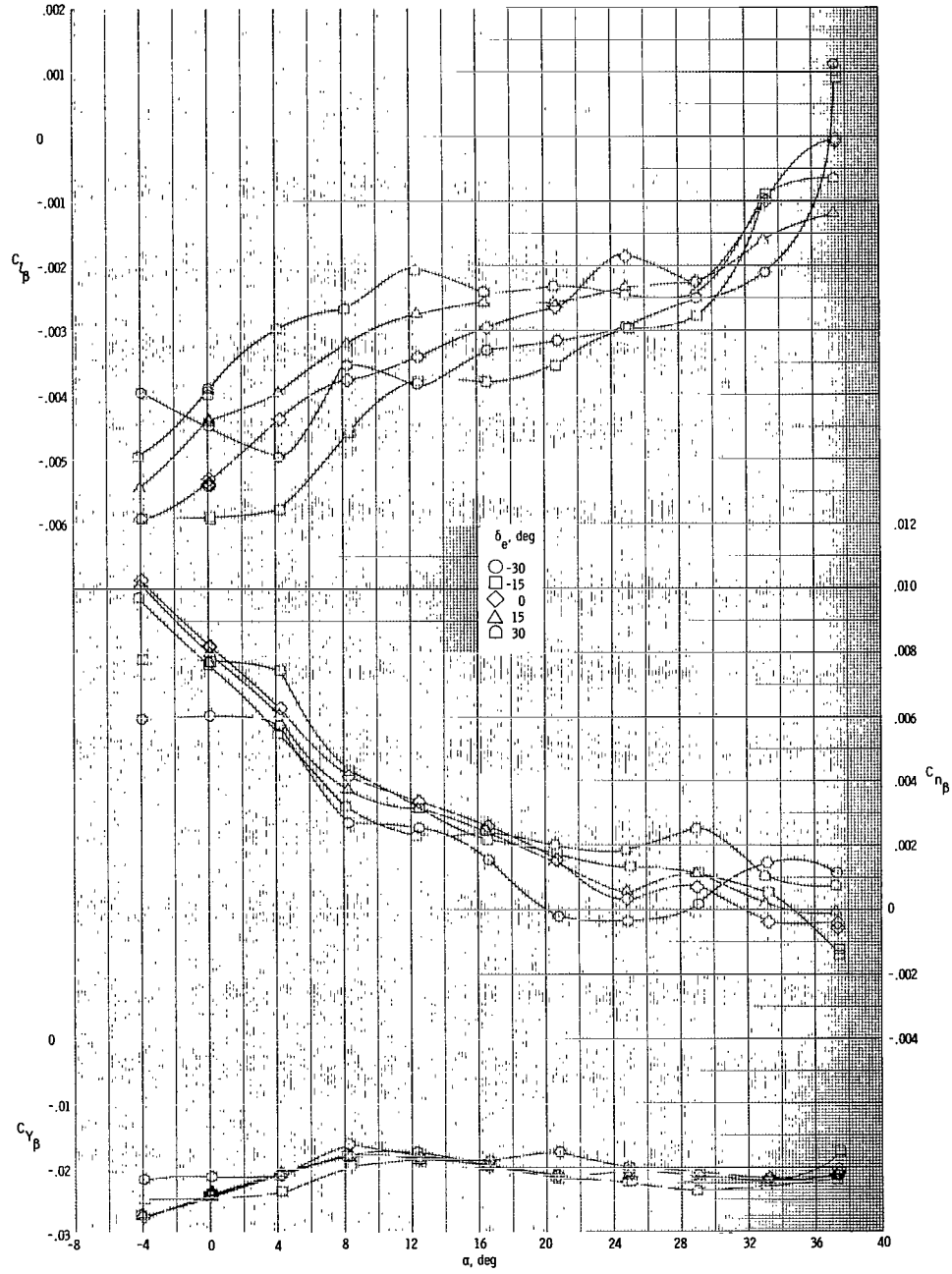

Figure 19.- Effects of elevon deflection on directional and lateral stability characteristics of vehicle with modification II tip fins. M = 1.50.

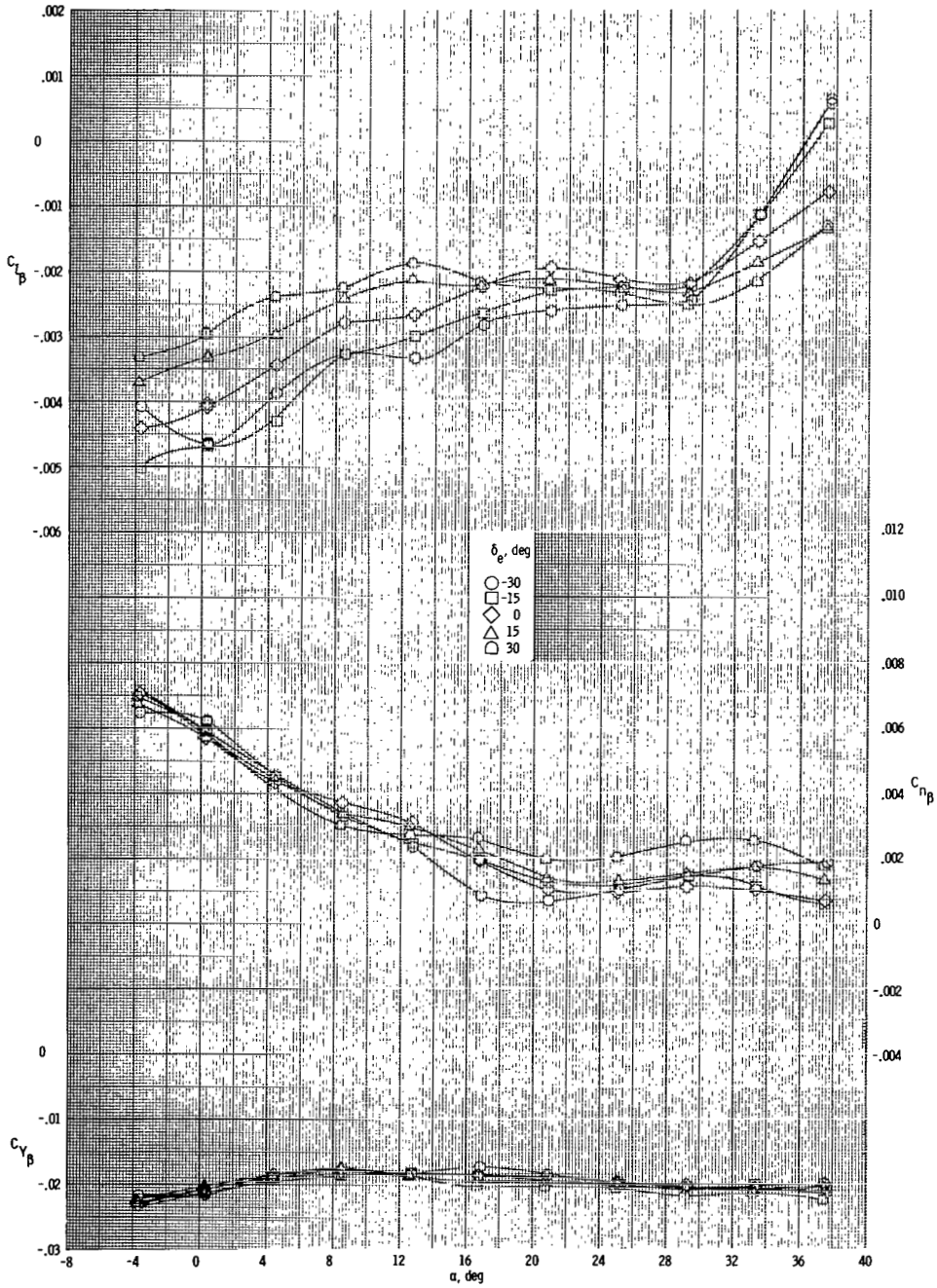

Figure 20.- Effects of elevon deflection on directional and lateral stability characteristics of vehicle with modification II tip fins. M = 1.80.

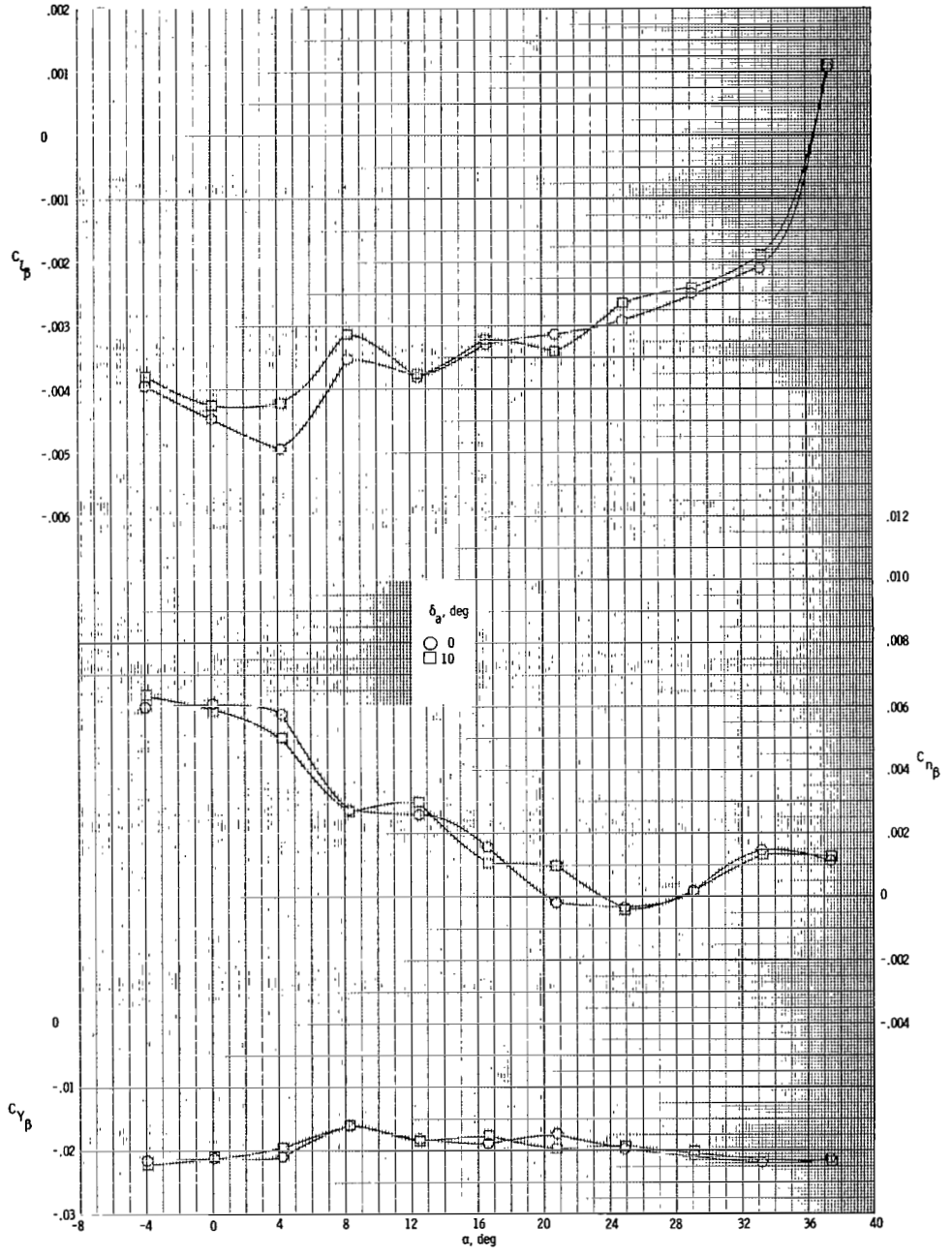

(a) $\delta_e = -30^\circ$.

Figure 21.- Effects of aileron deflection on directional and lateral stability characteristics of vehicle with modification II tip fins. M = 1.50.

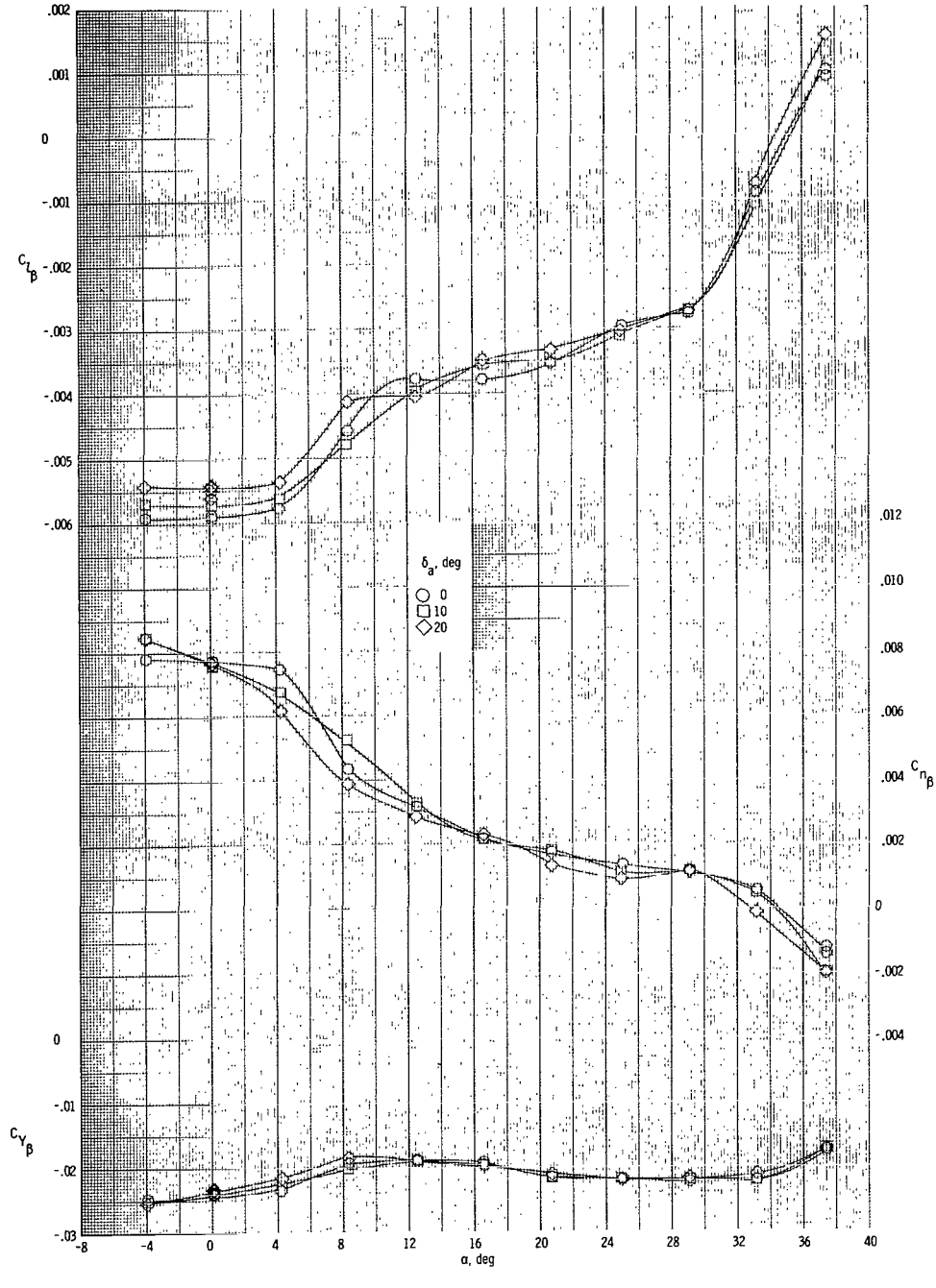

(b) $\delta_e = -15^o$.

Figure 21.- Continued.

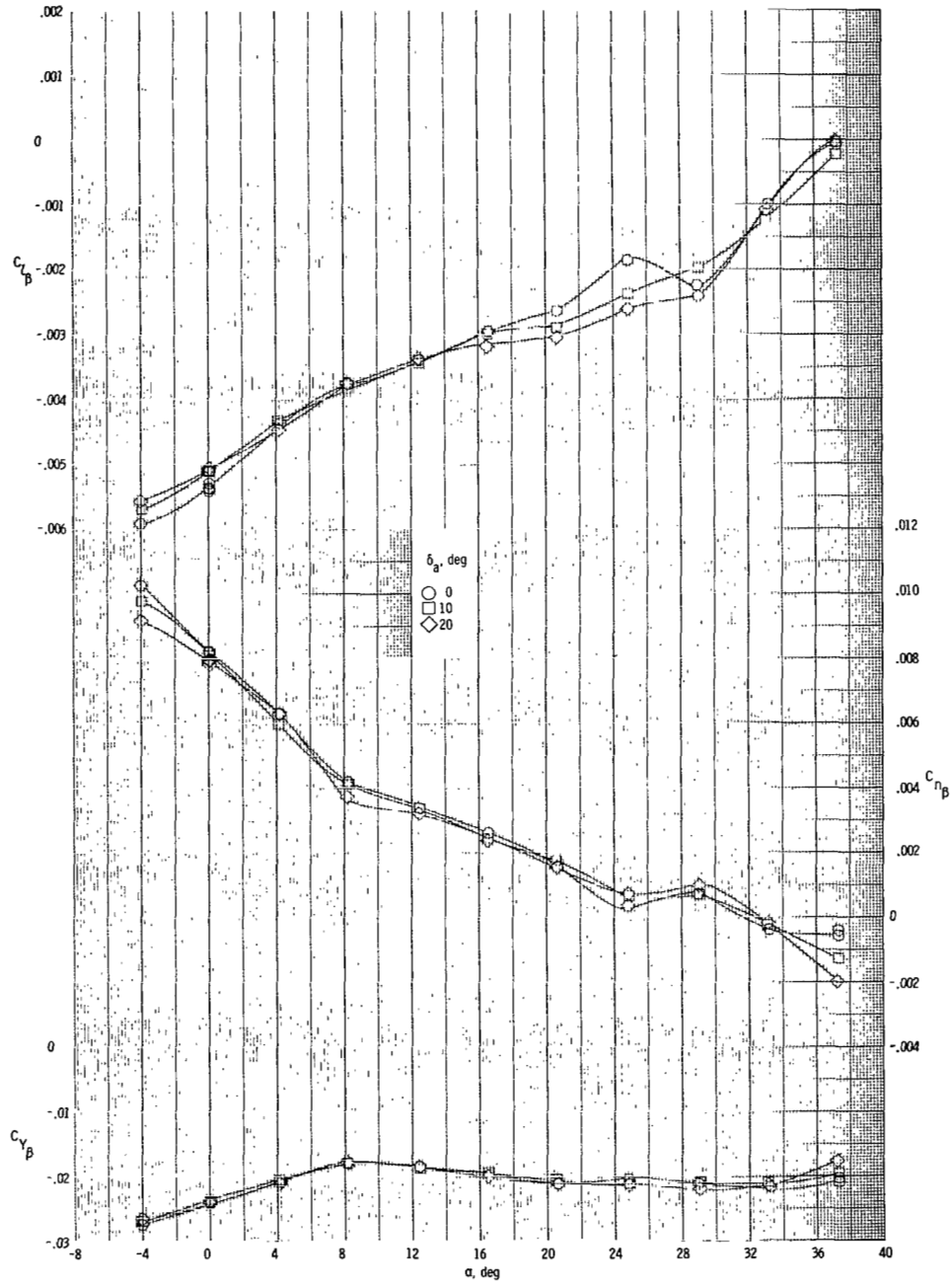

(c) $\delta_e = 0^\circ$.

Figure 21.- Continued.

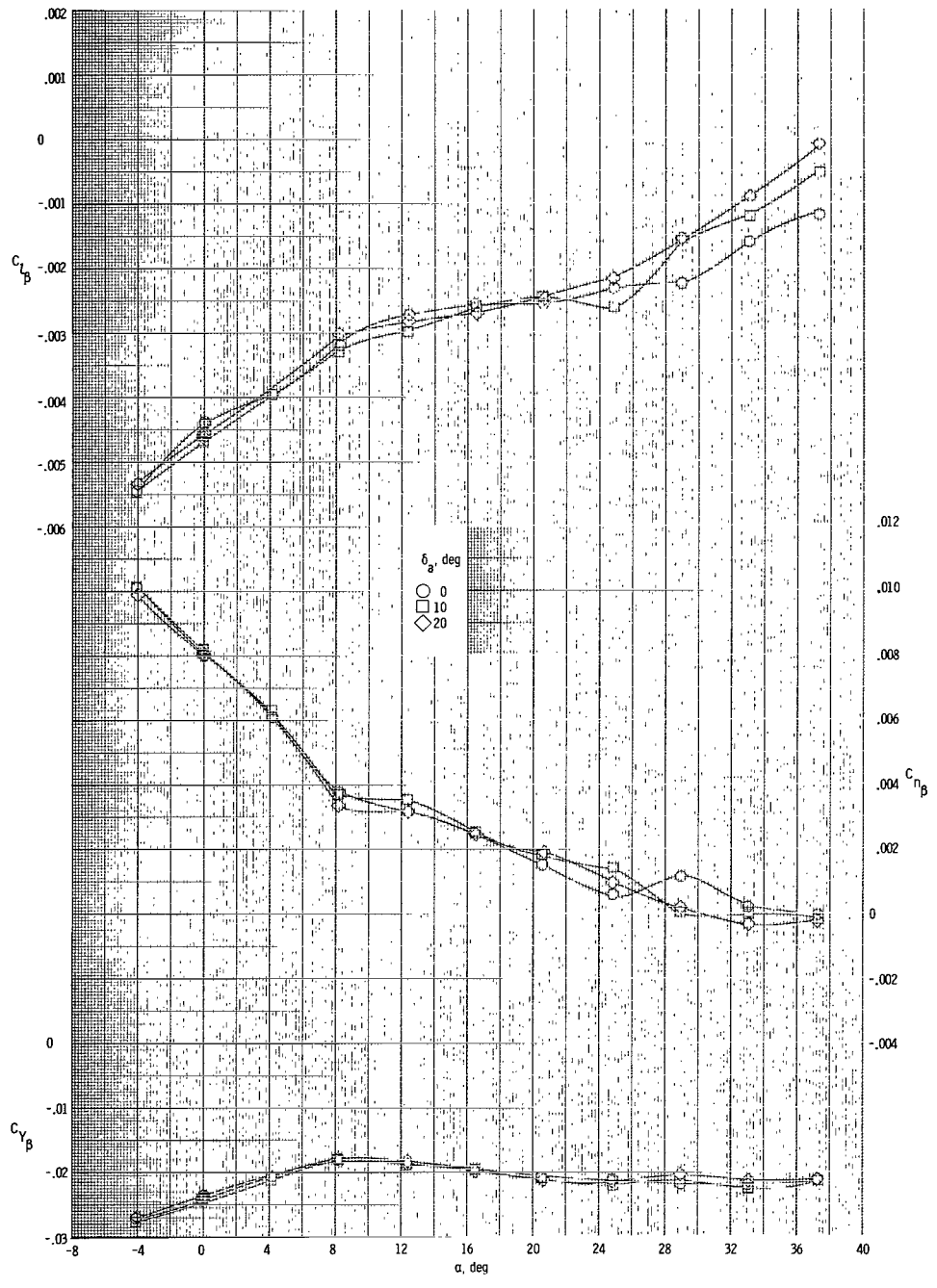

(d) $\delta_e = 15^\circ$.

Figure 21.- Continued.

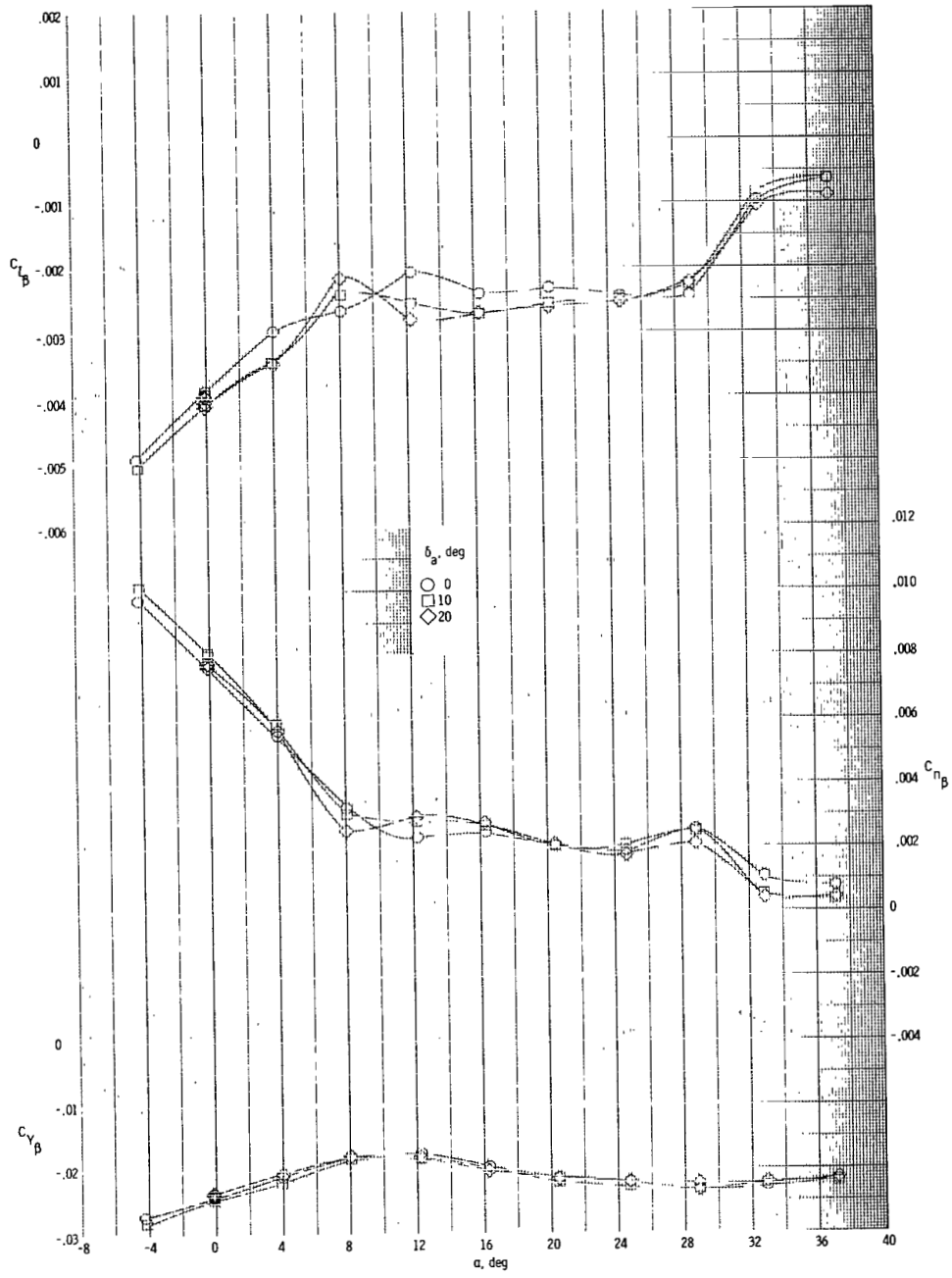

(e) $\delta_e = 30^\circ$.

Figure 21.- Concluded.

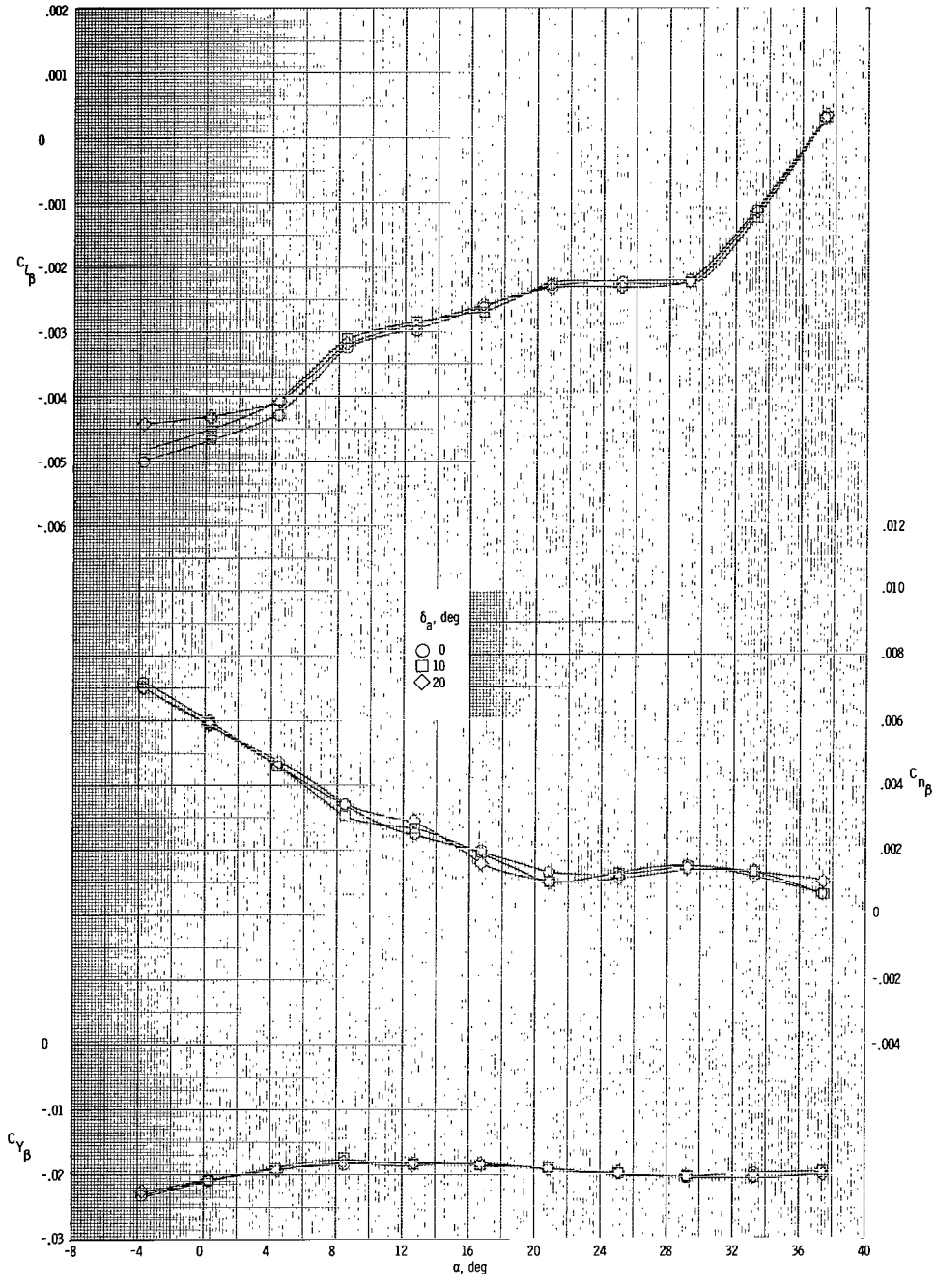

(a) $\delta_e = -15^\circ$.

Figure 22.- Effects of aileron deflection on directional and lateral stability characteristics of vehicle with modification II tip fins. M = 1.80.

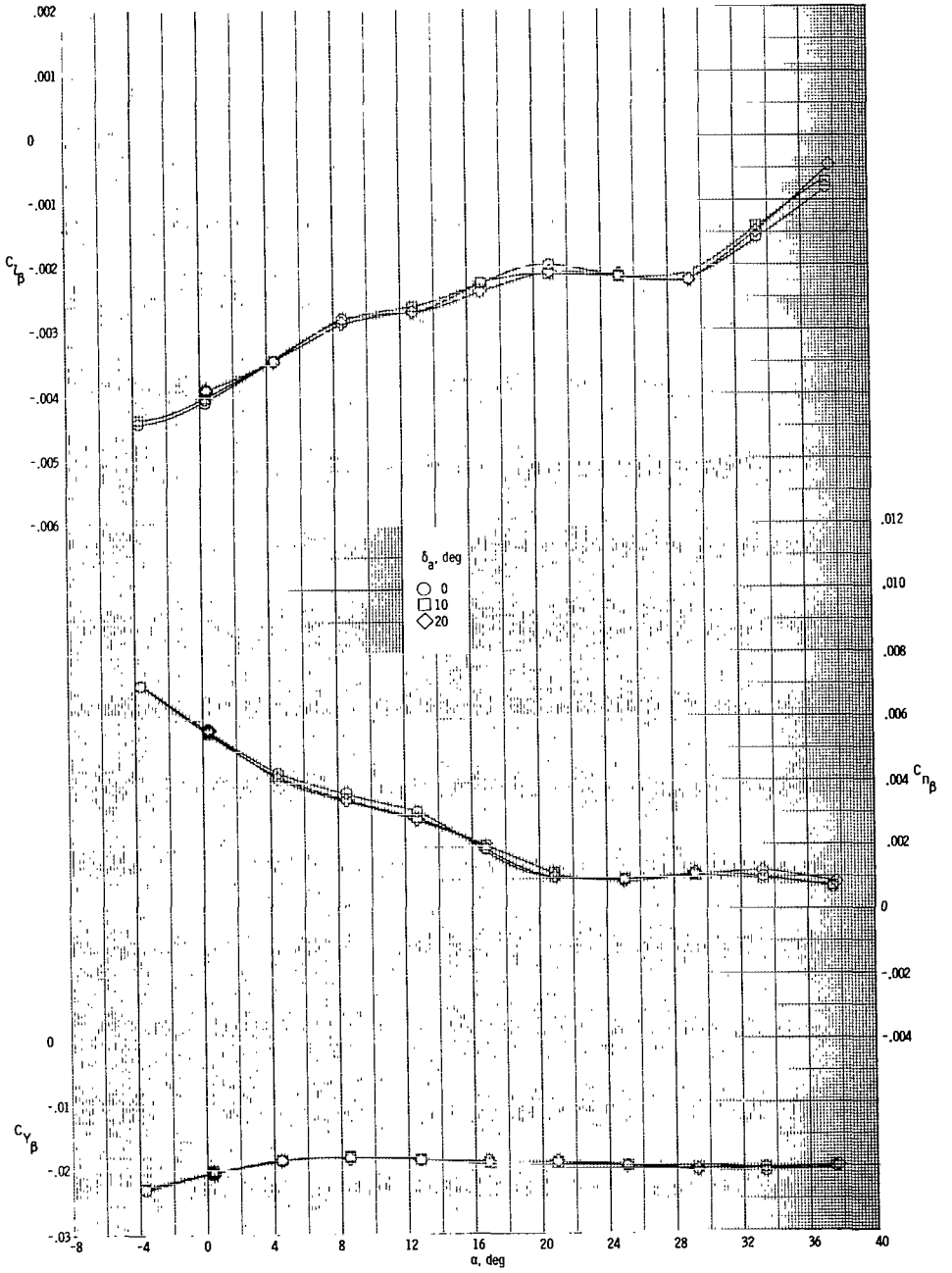

(b) $\delta_e = 0^\circ$.

Figure 22.- Continued.

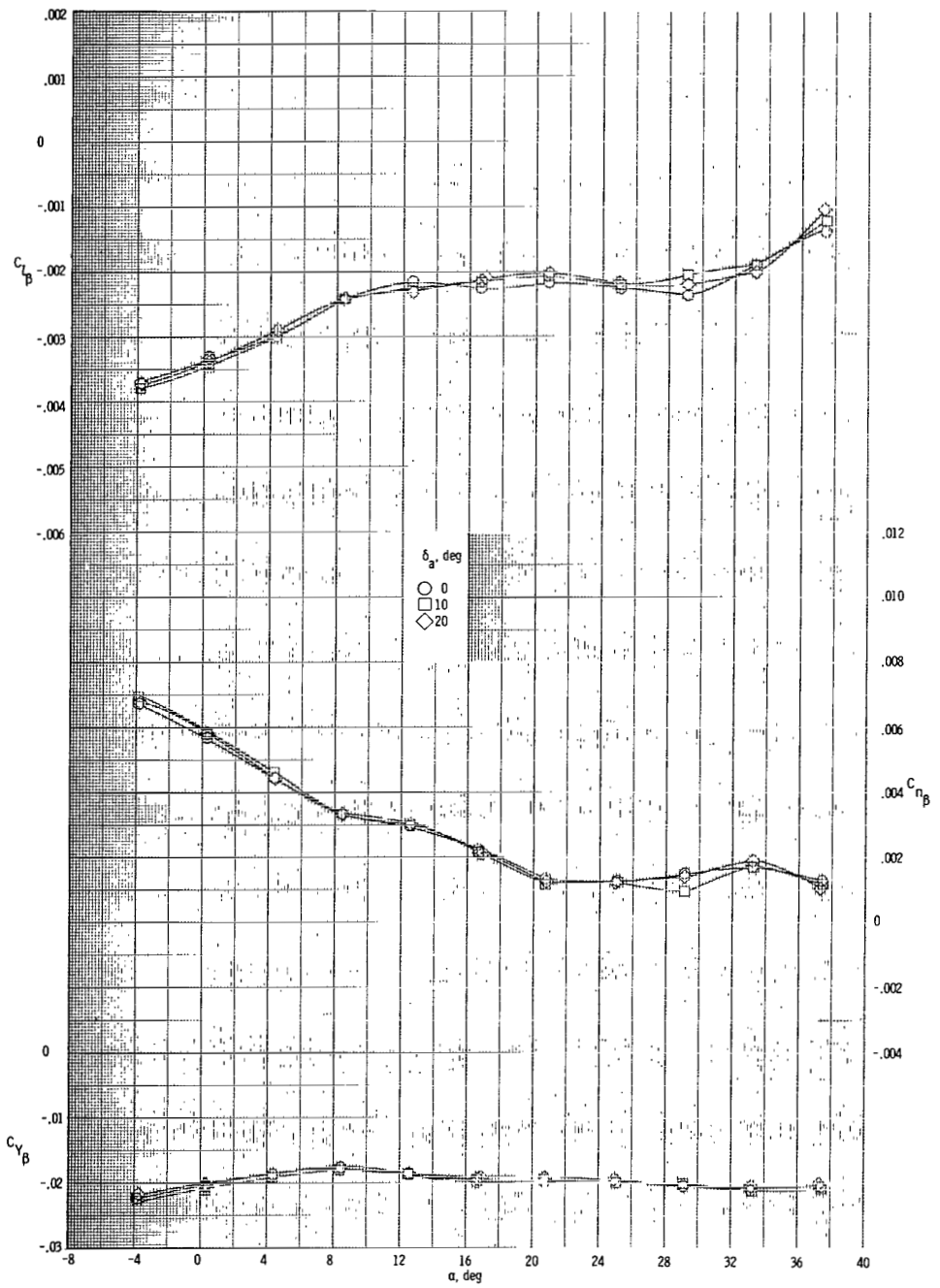

(c) $\delta_e = 15^\circ$.

Figure 22.- Continued.

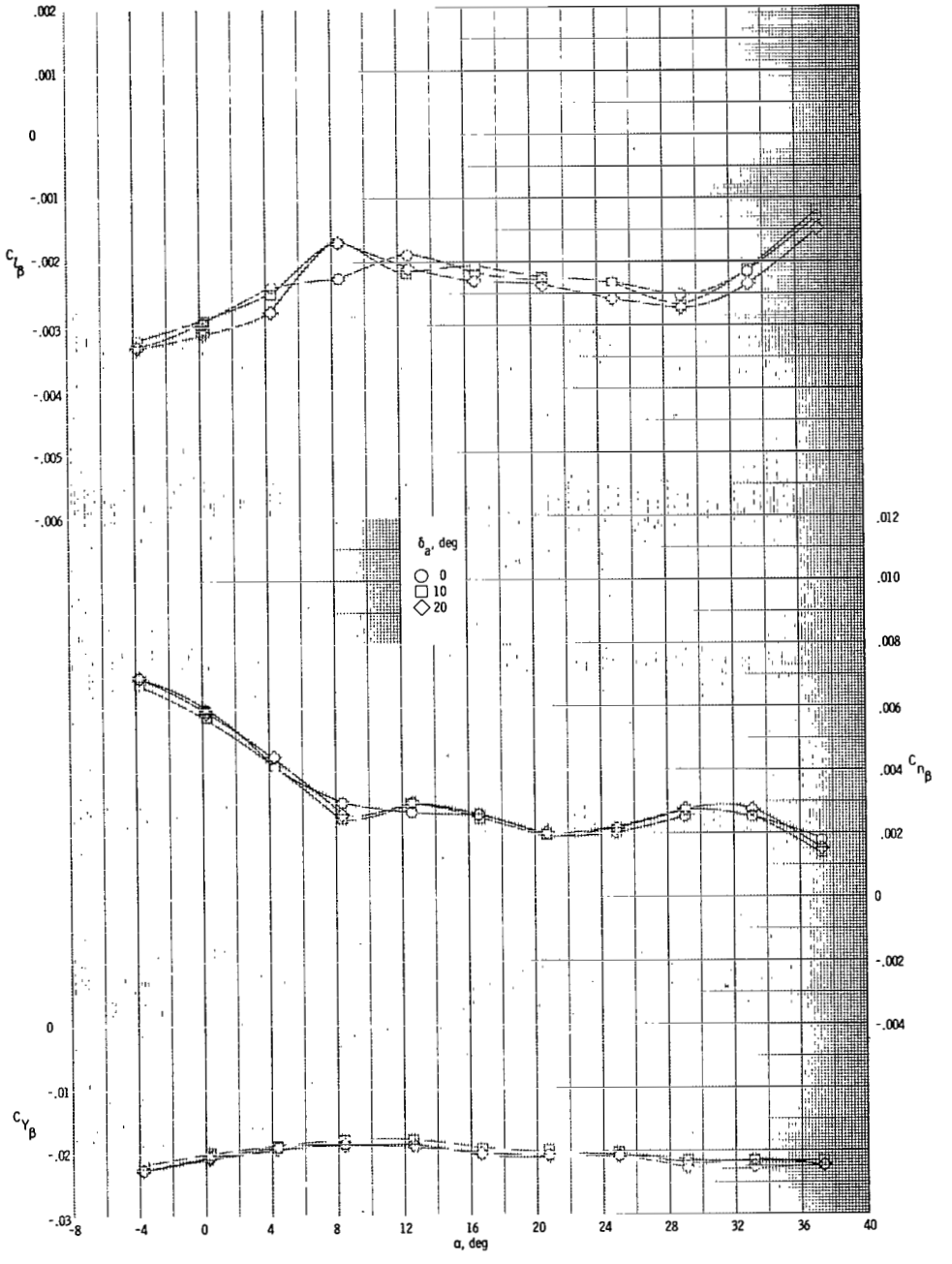

(d) $\delta_e = 30^\circ$.

Figure 22.- Concluded.

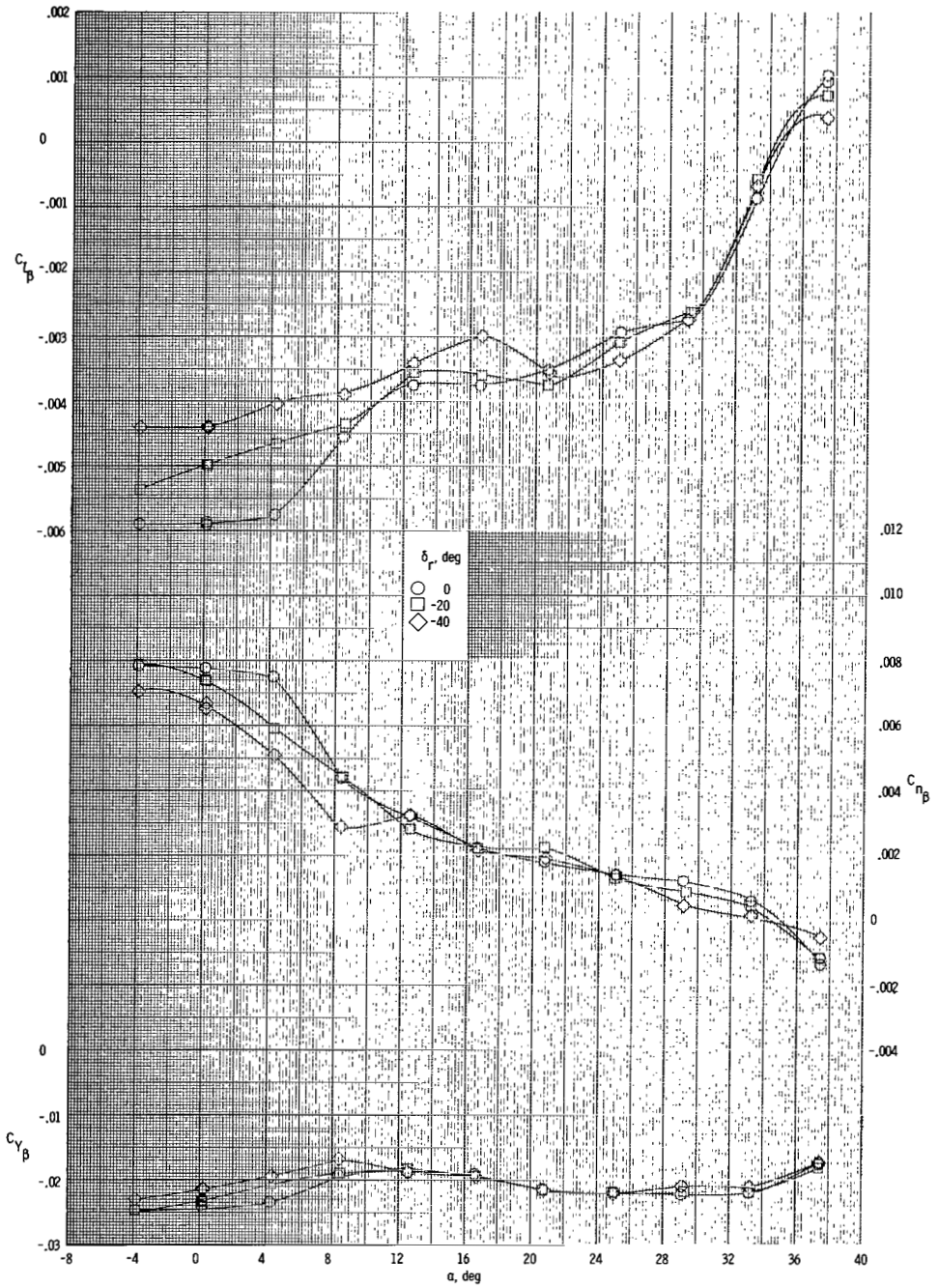

(a) $\delta_e = -15^\circ$.

Figure 23.- Effects of rudder deflection on directional and lateral stability characteristics of vehicle with modification II tip fins. M = 1.50.

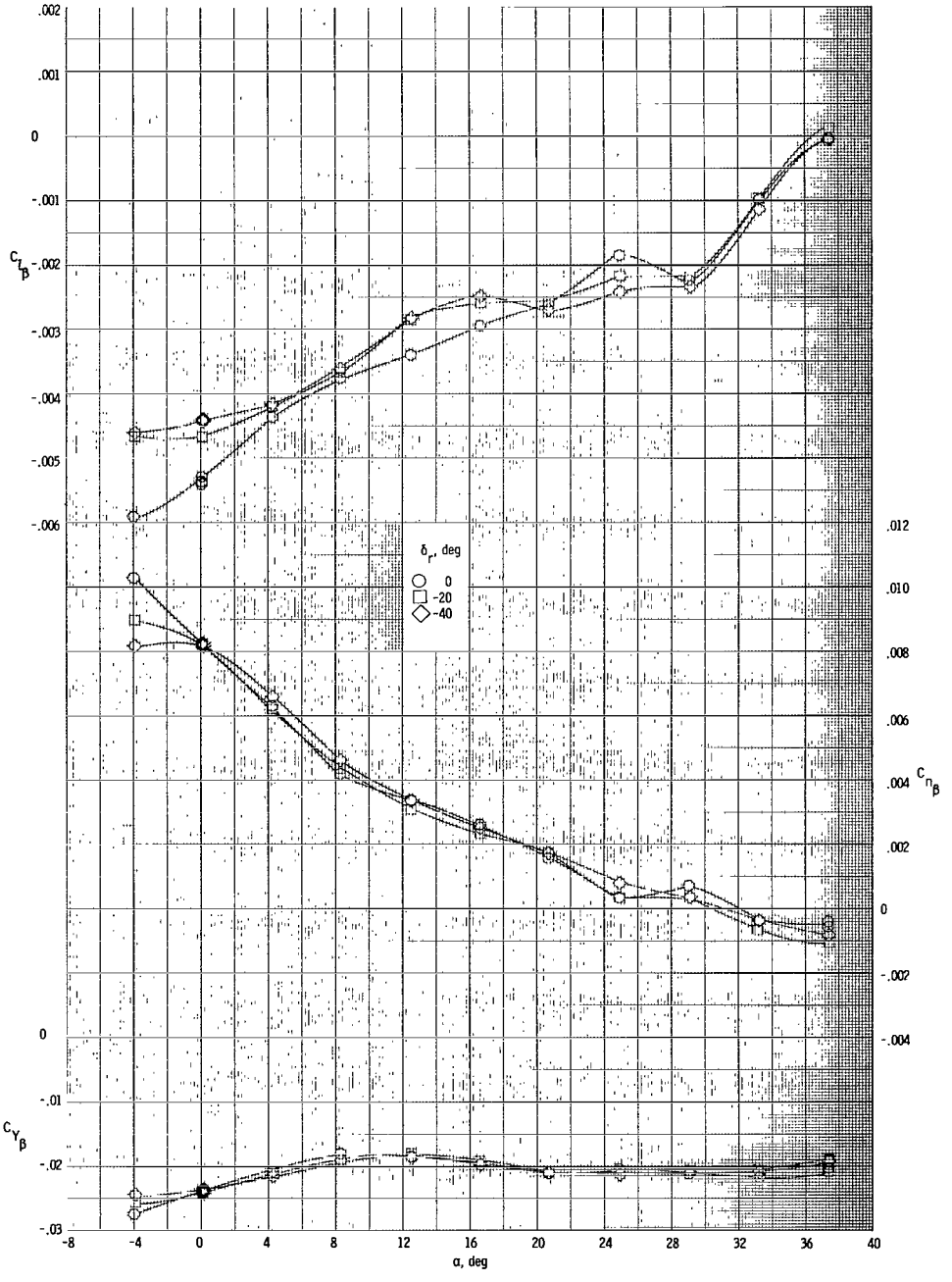

(b) $\delta_e = 0^\circ$.

Figure 23.- Continued.

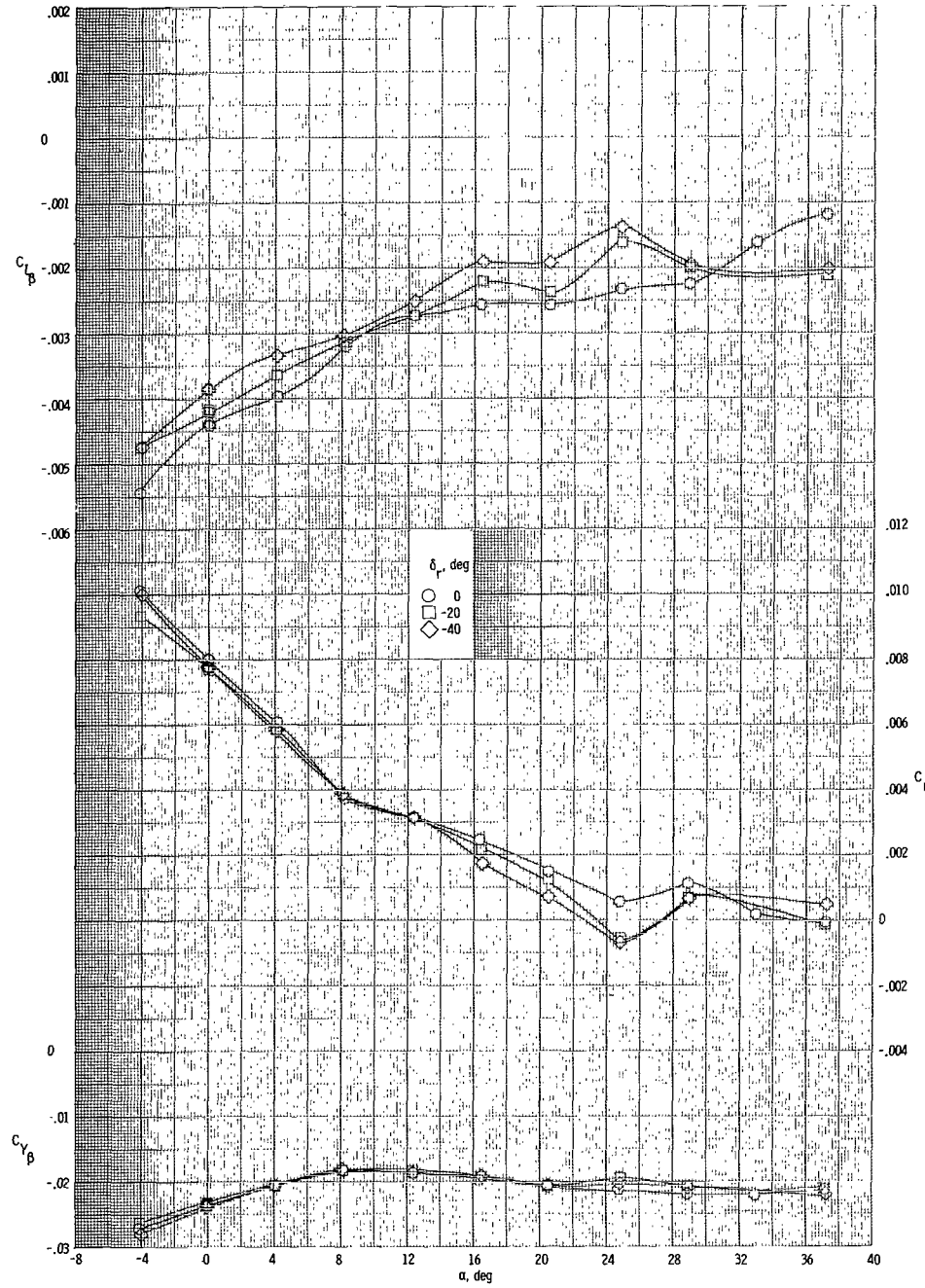

(c) $\delta_e = 15^\circ$.

Figure 23.- Continued.

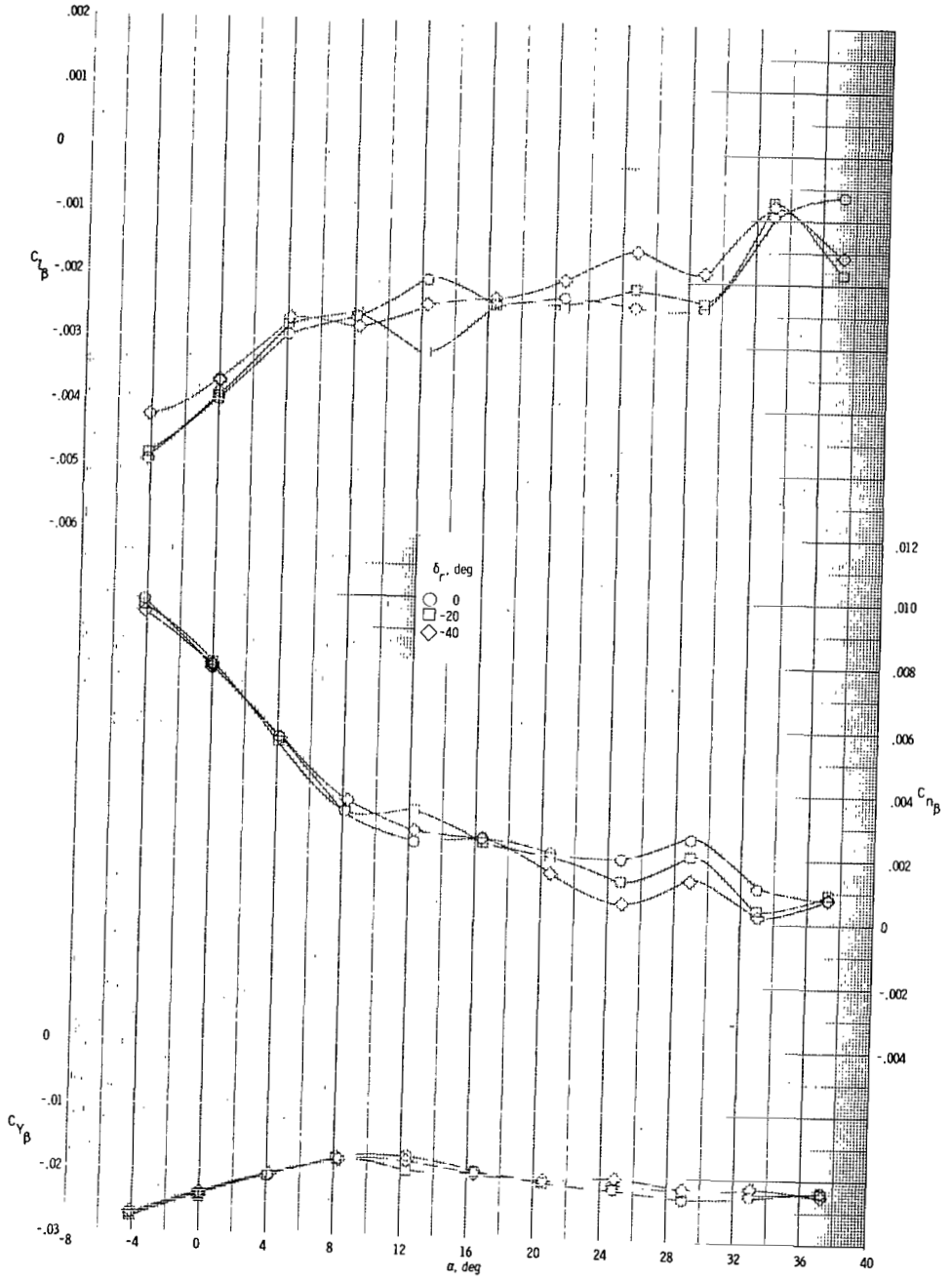

(d) $\delta_e = 30^\circ$.

Figure 23.- Concluded.

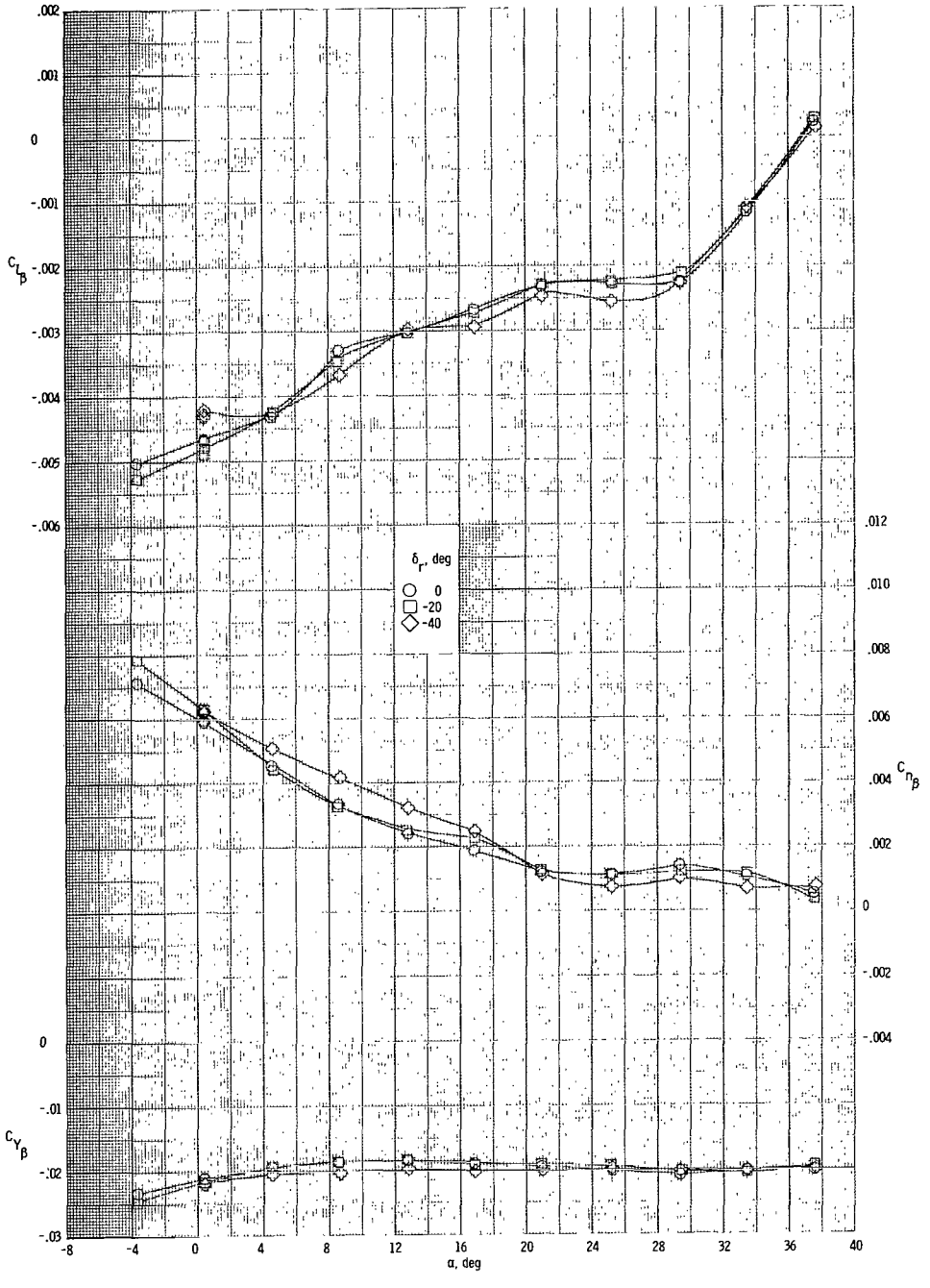

(a) $\delta_e = -15^\circ$.

Figure 24.- Effects of rudder deflection on directional and lateral stability characteristics of vehicle with modification II tip fins. M = 1.80.

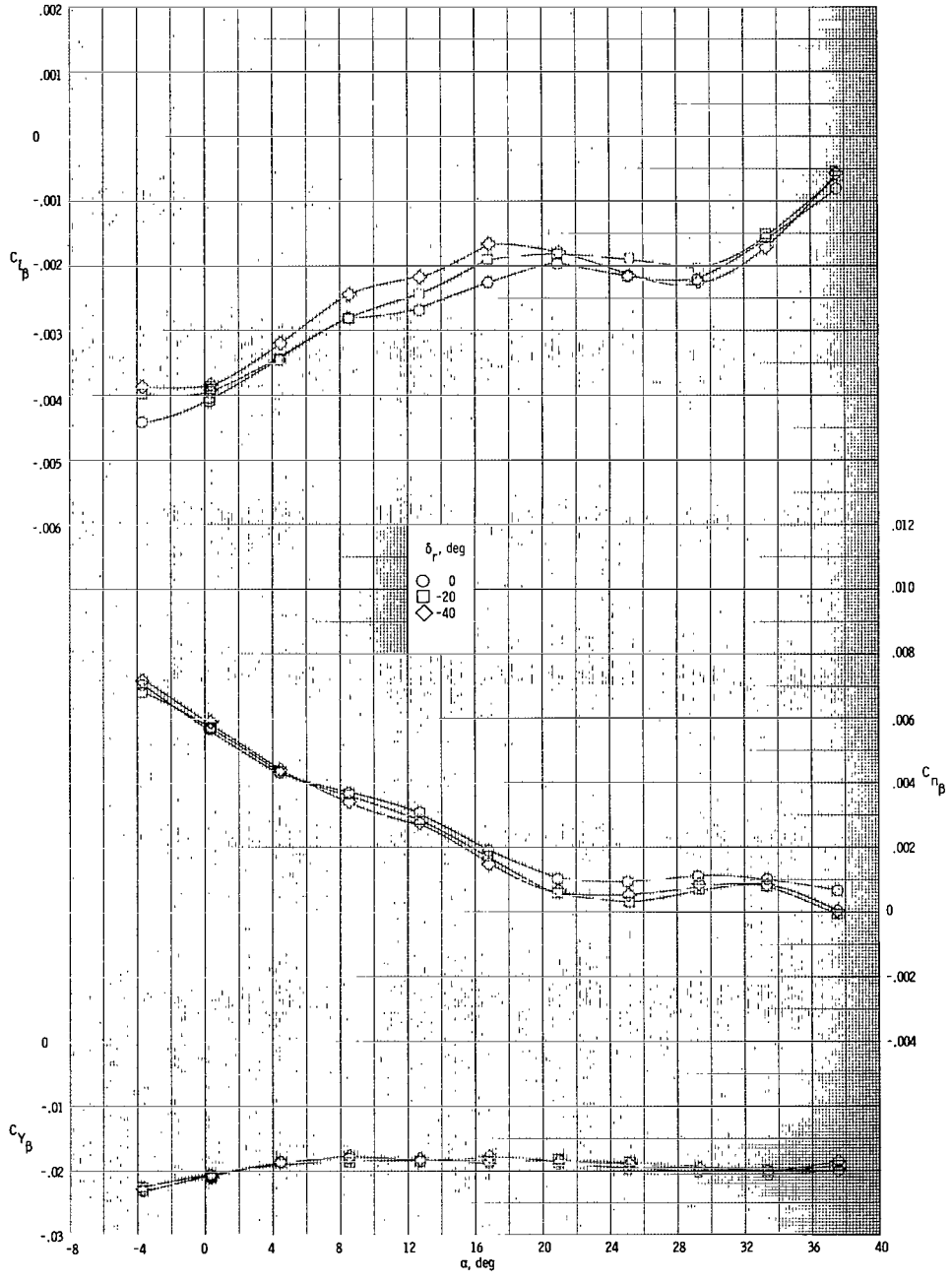

(b) $\delta_e = 0^\circ$.

Figure 24.- Continued.

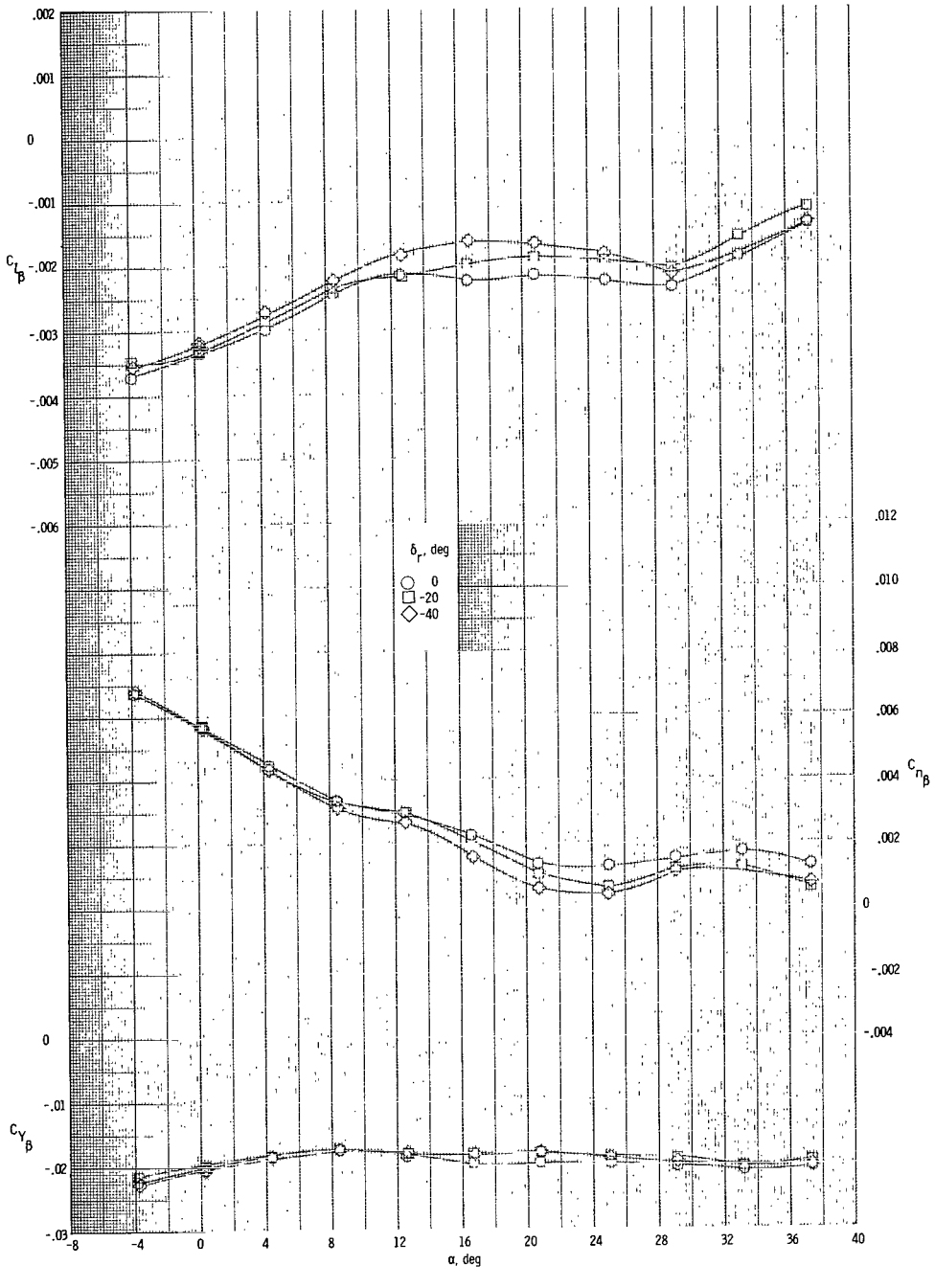

(c) $\delta_e = 15^\circ$.

Figure 24.- Continued.

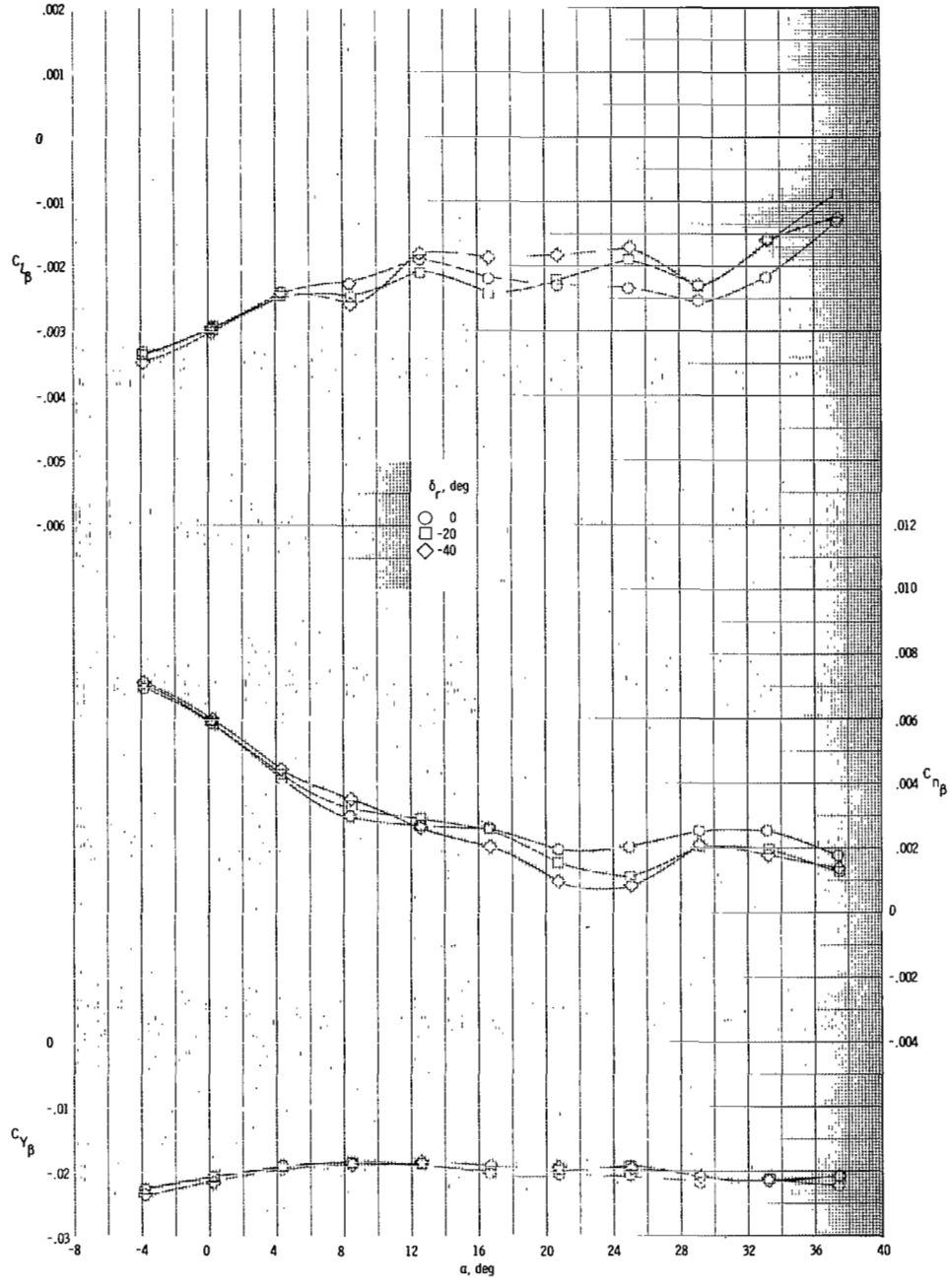

(d) $\delta_e = 30^\circ$.

Figure 24.- Concluded.

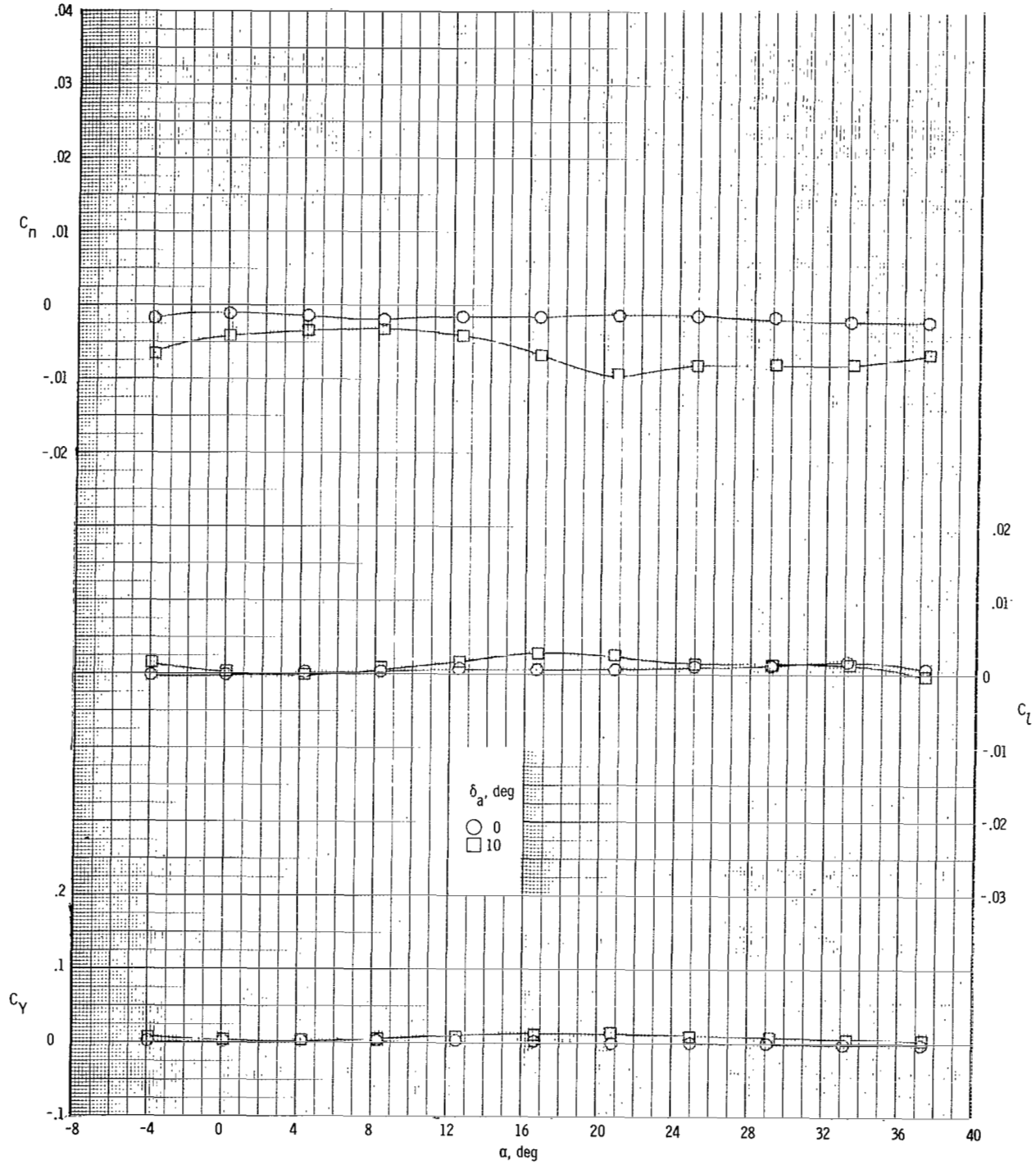

(a) $\delta_e = -30^\circ$.

Figure 25.- Effects of aileron deflection on lateral aerodynamic characteristics of vehicle with modification II tip fins for several elevon deflection angles. $\beta = 0^\circ$; M = 1.50.

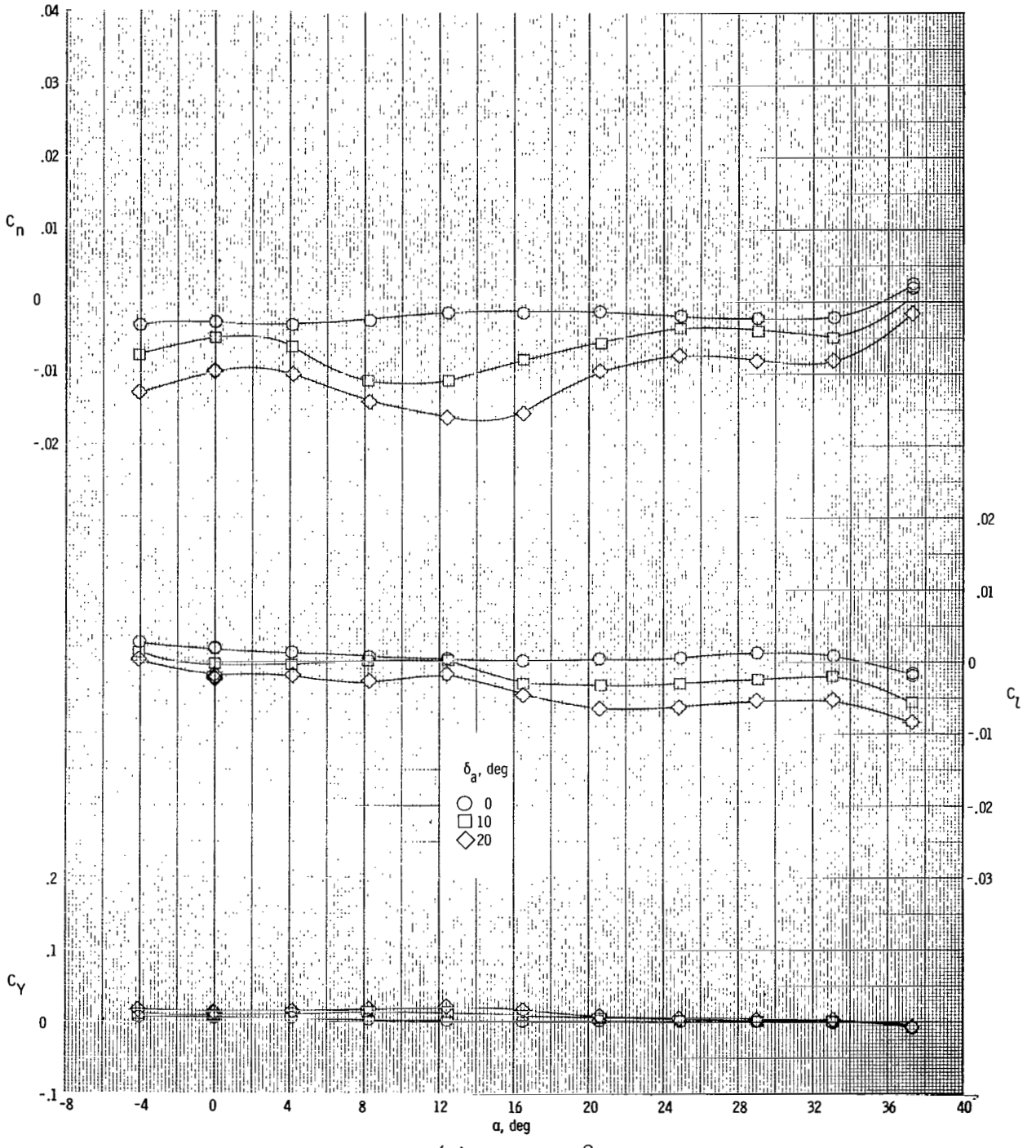

(b) $\delta_e = -15°$.

Figure 25.- Continued.

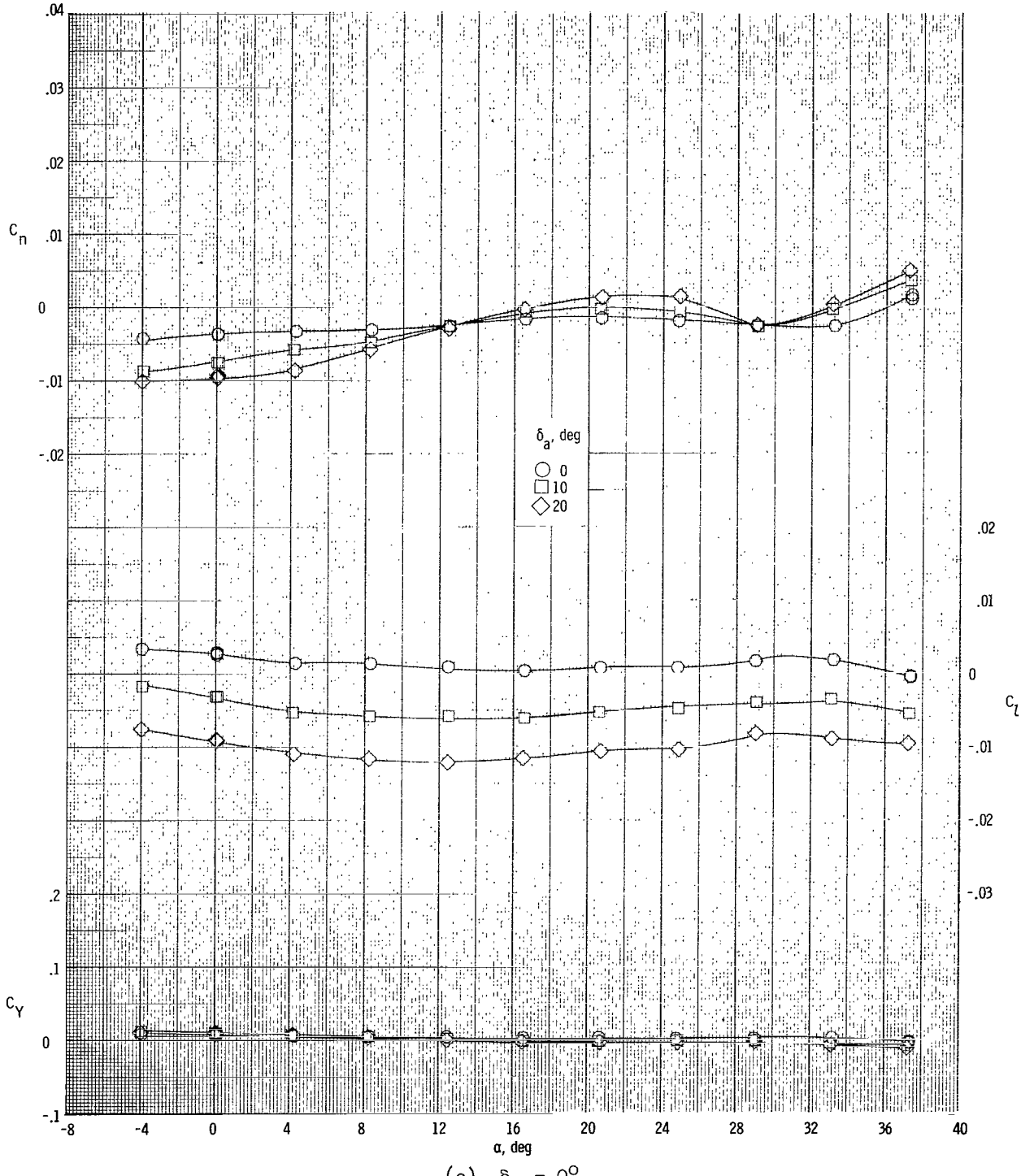

(c) $\delta_e = 0^o$.

Figure 25.- Continued.

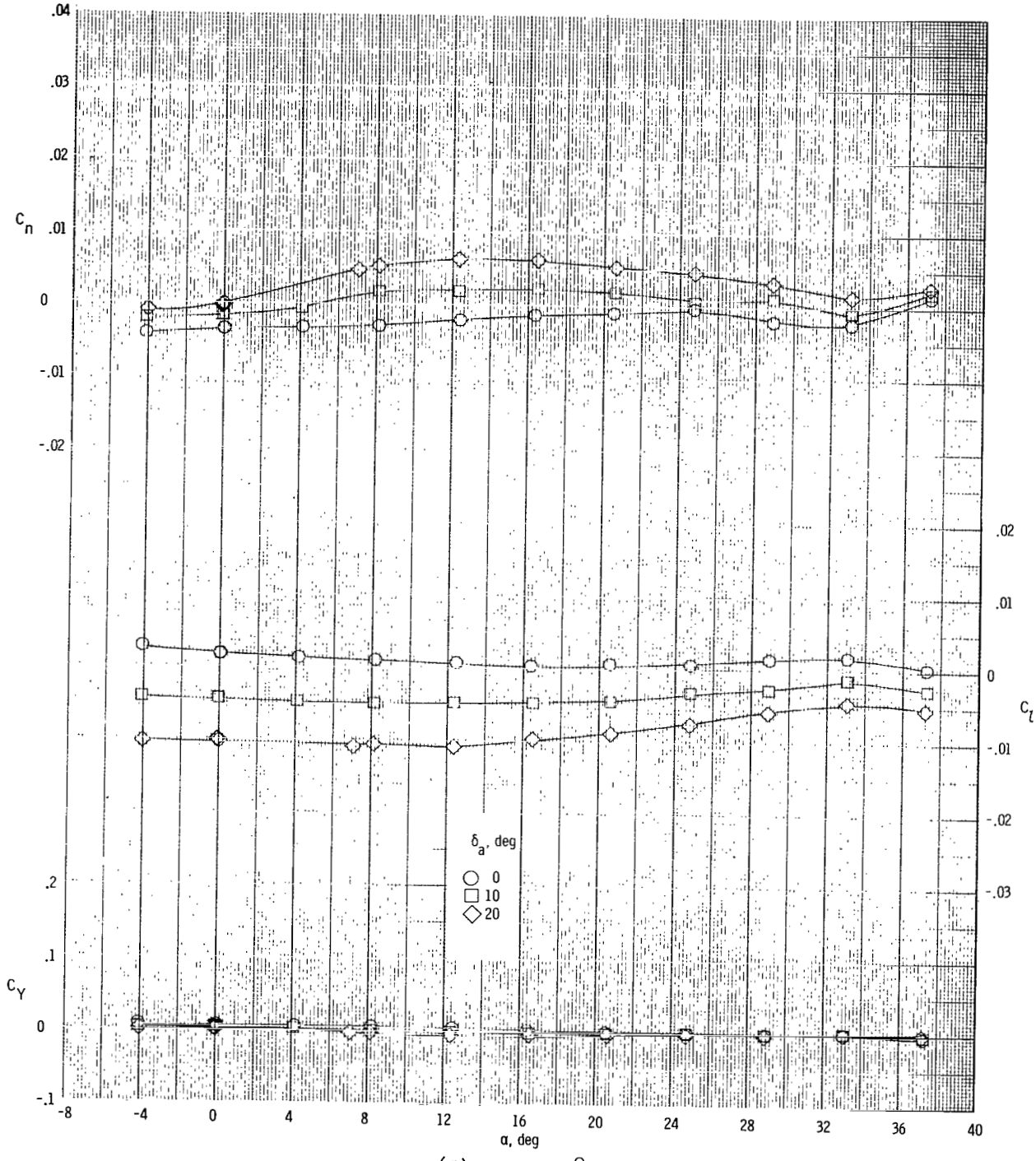

(d) $\delta_e = 15°$.

Figure 25.- Continued.

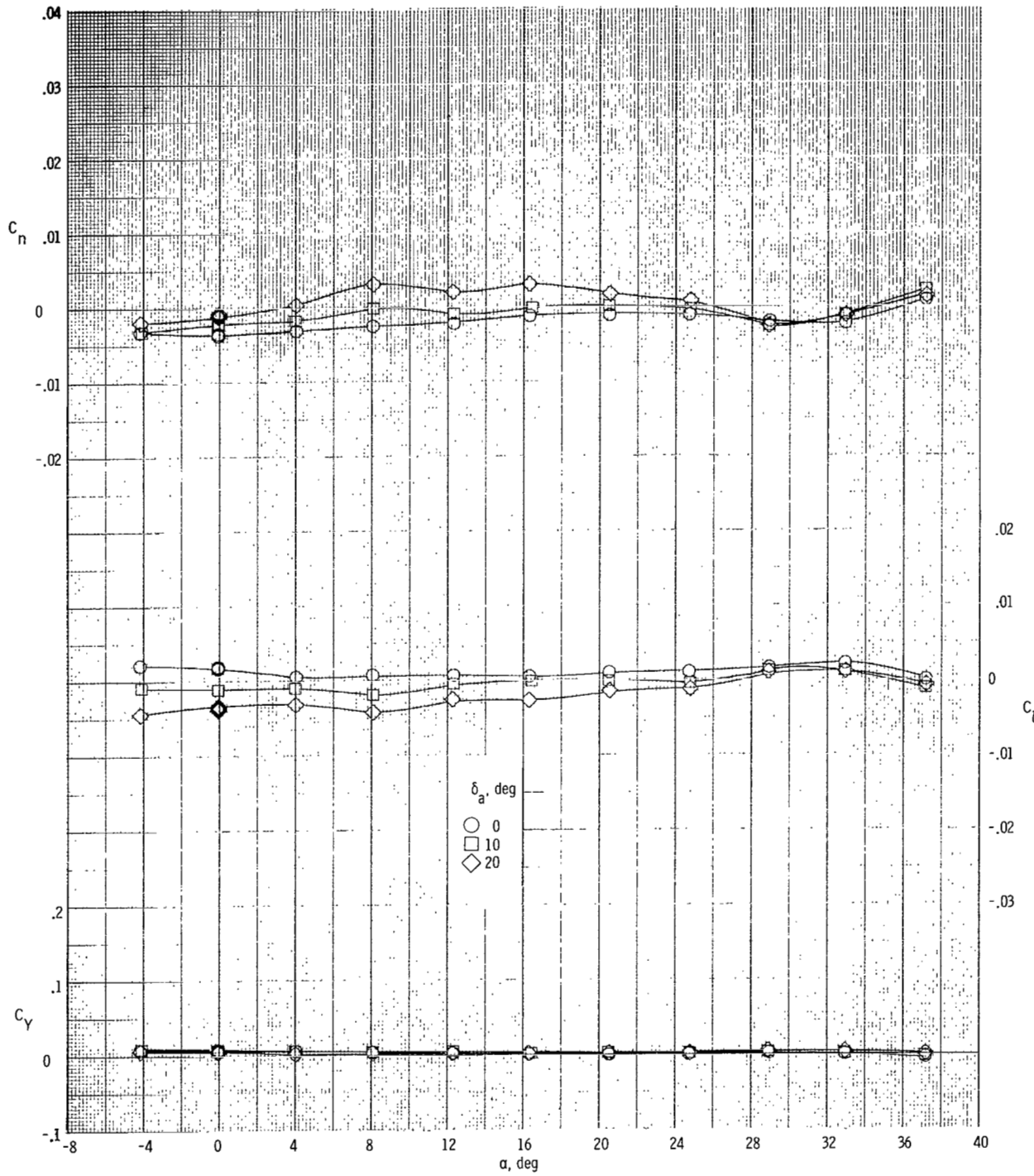

(e) $\delta_e = 30^\circ$.

Figure 25.- Concluded.

(a) $\delta_e = -30^\circ$.

Figure 26.- Effects of aileron deflection on lateral aerodynamic characteristics of vehicle with modification II tip fins for several elevon deflection angles. $\beta = 3^\circ$; M = 1.50.

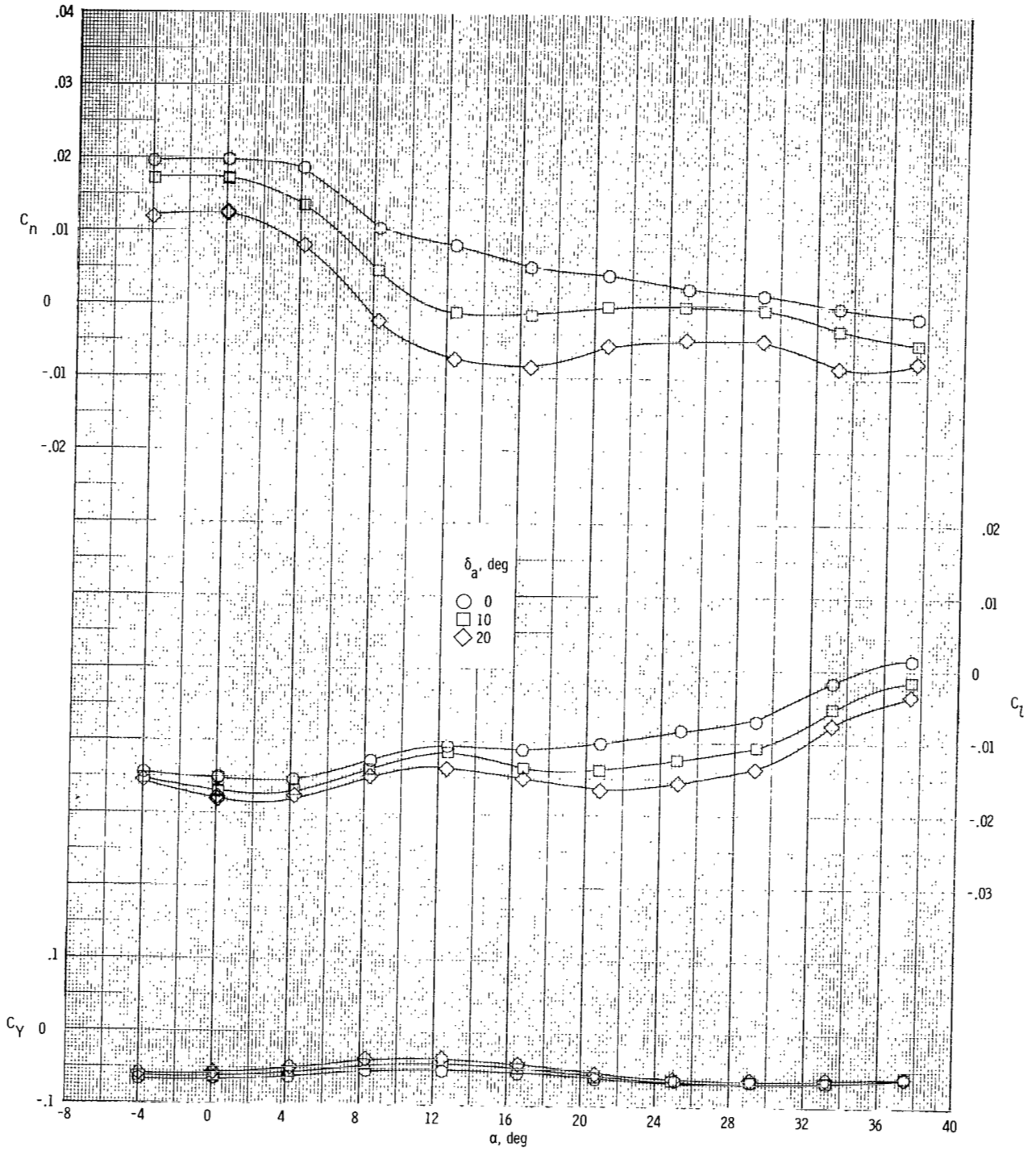

(b) $\delta_e = -15°$.

Figure 26.- Continued.

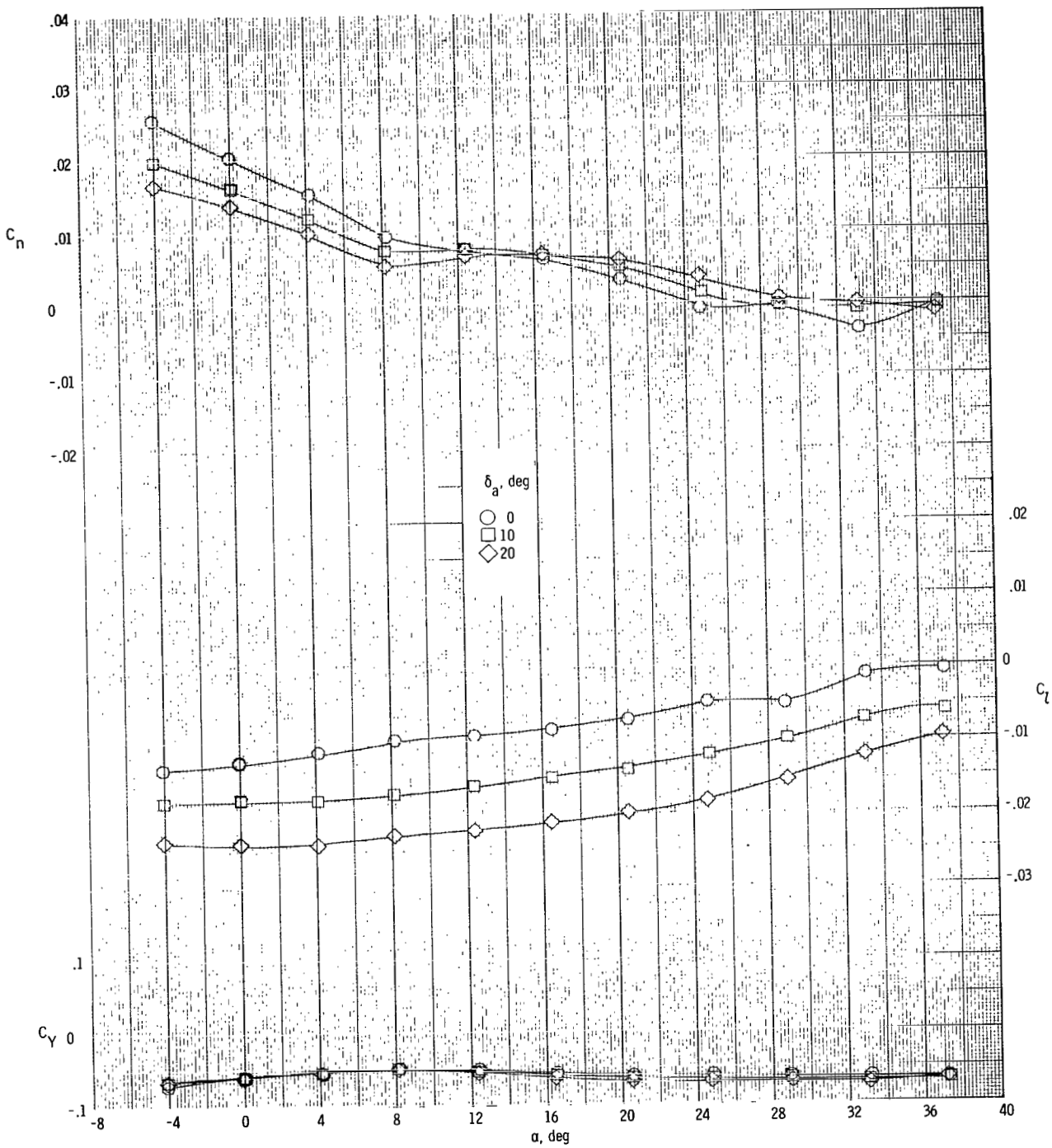

(c) $\delta_e = 0^o$.

Figure 26.- Continued.

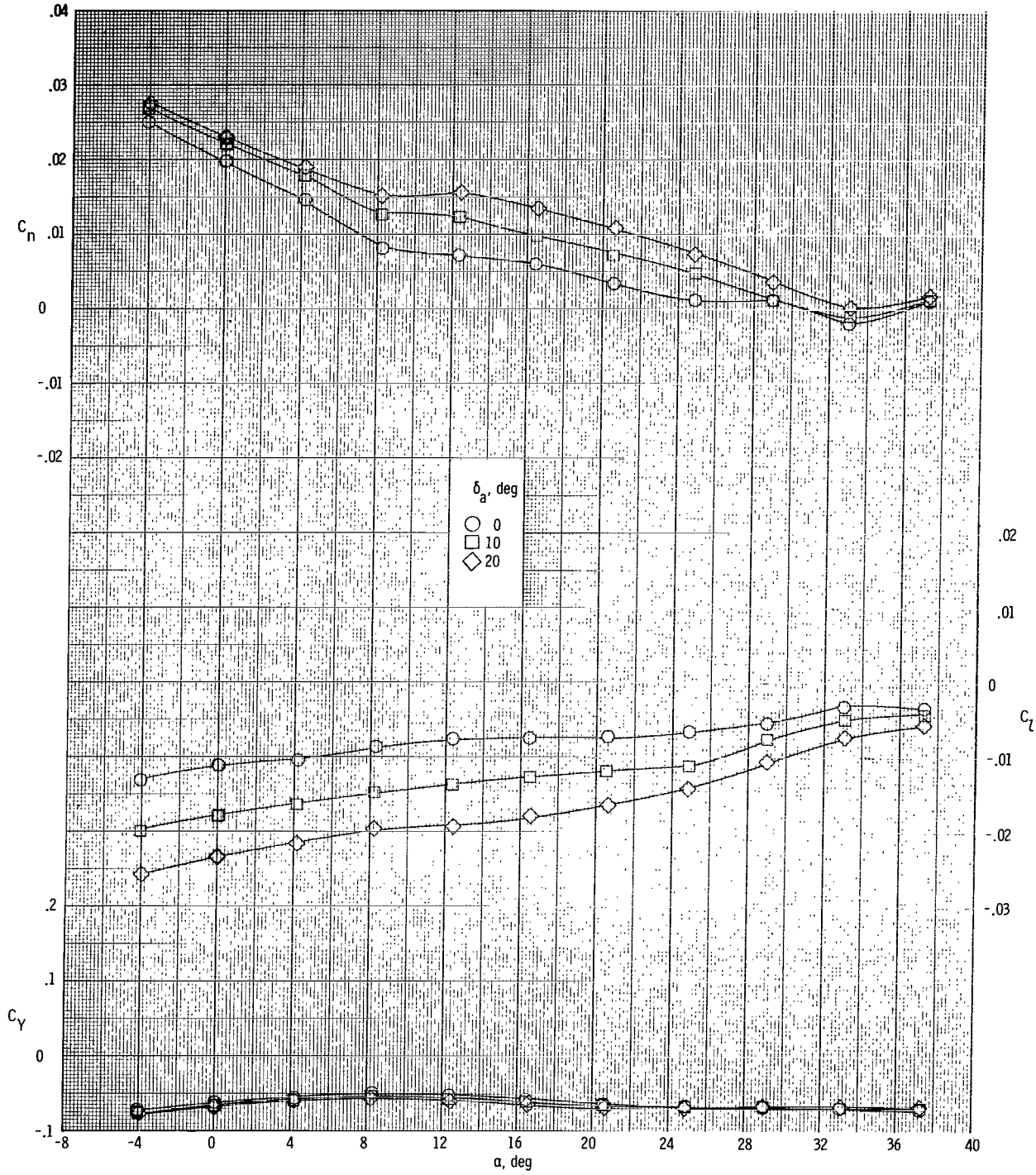

(d) $\delta_e = 15^\circ$.

Figure 26.- Continued.

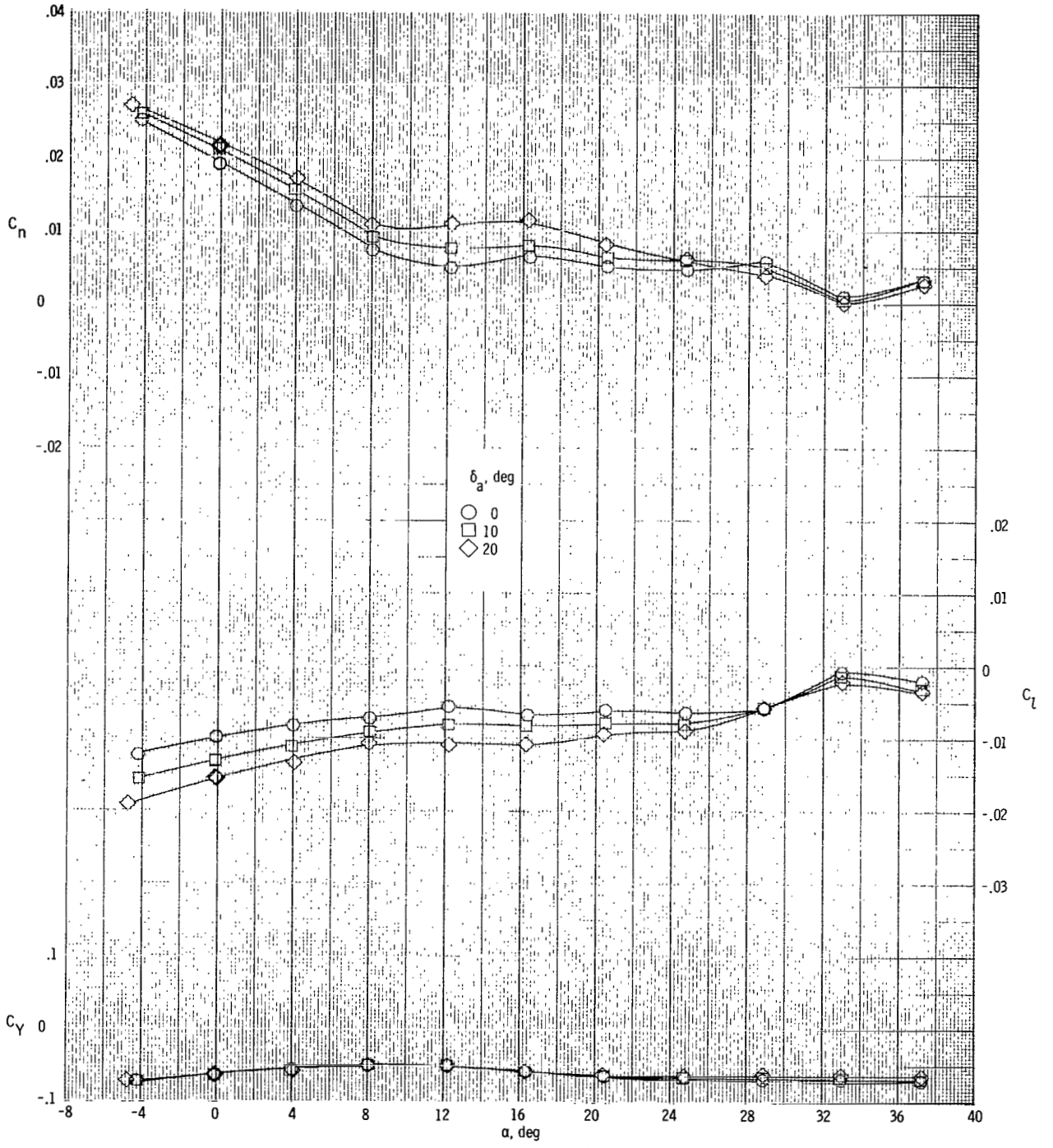

(e) $\delta_e = 30^\circ$.

Figure 26.- Concluded.

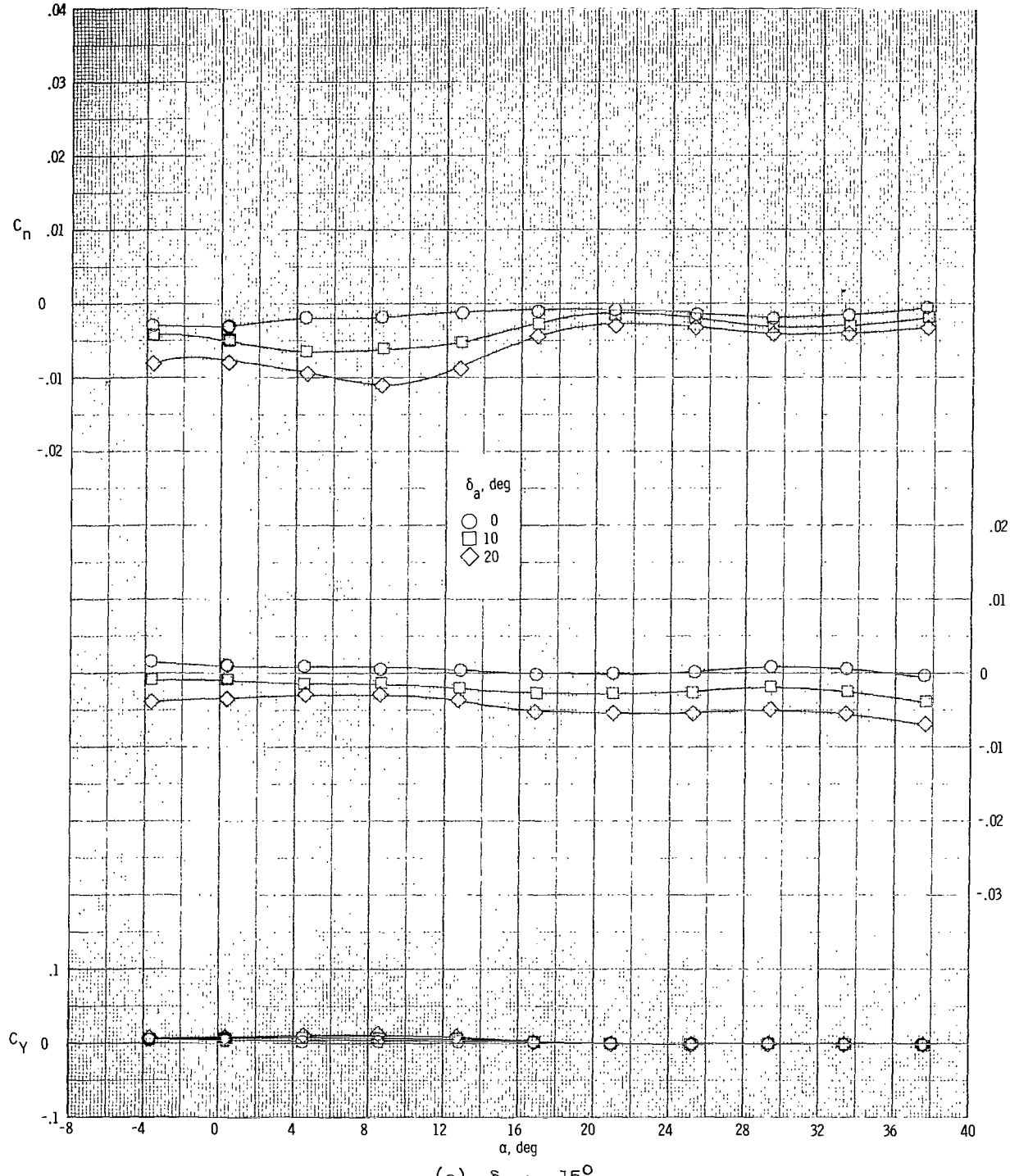

(a) $\delta_e = -15^\circ$.

Figure 27.- Effects of aileron deflection on lateral aerodynamic characteristics of vehicle with modification II tip fins for several elevon deflection angles. $\beta = 0^\circ$; $M = 1.80$.

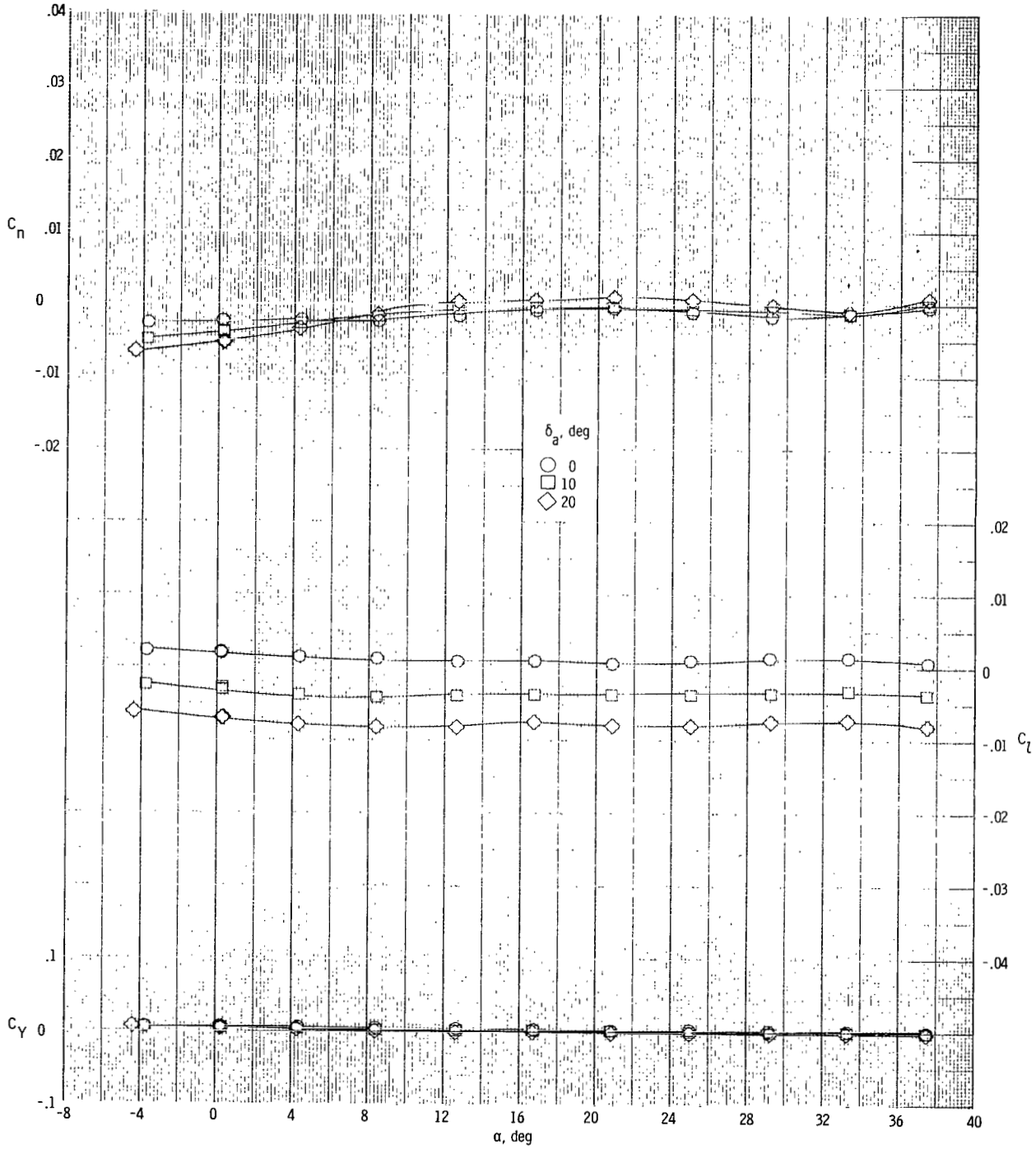

(b) $\delta_e = 0^o$.

Figure 27.- Continued.

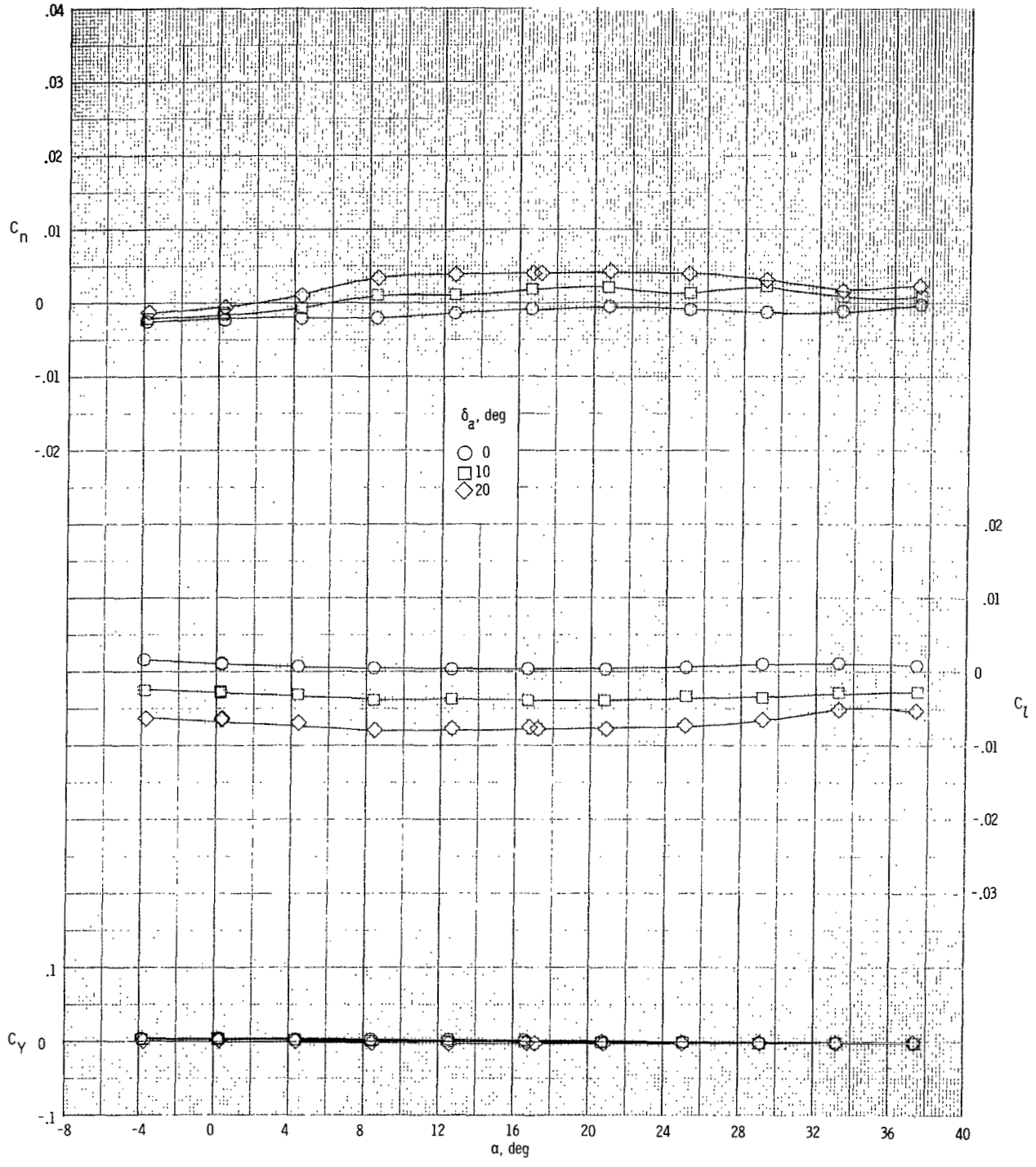

(c) $\delta_e = 15°$.

Figure 27.- Continued.

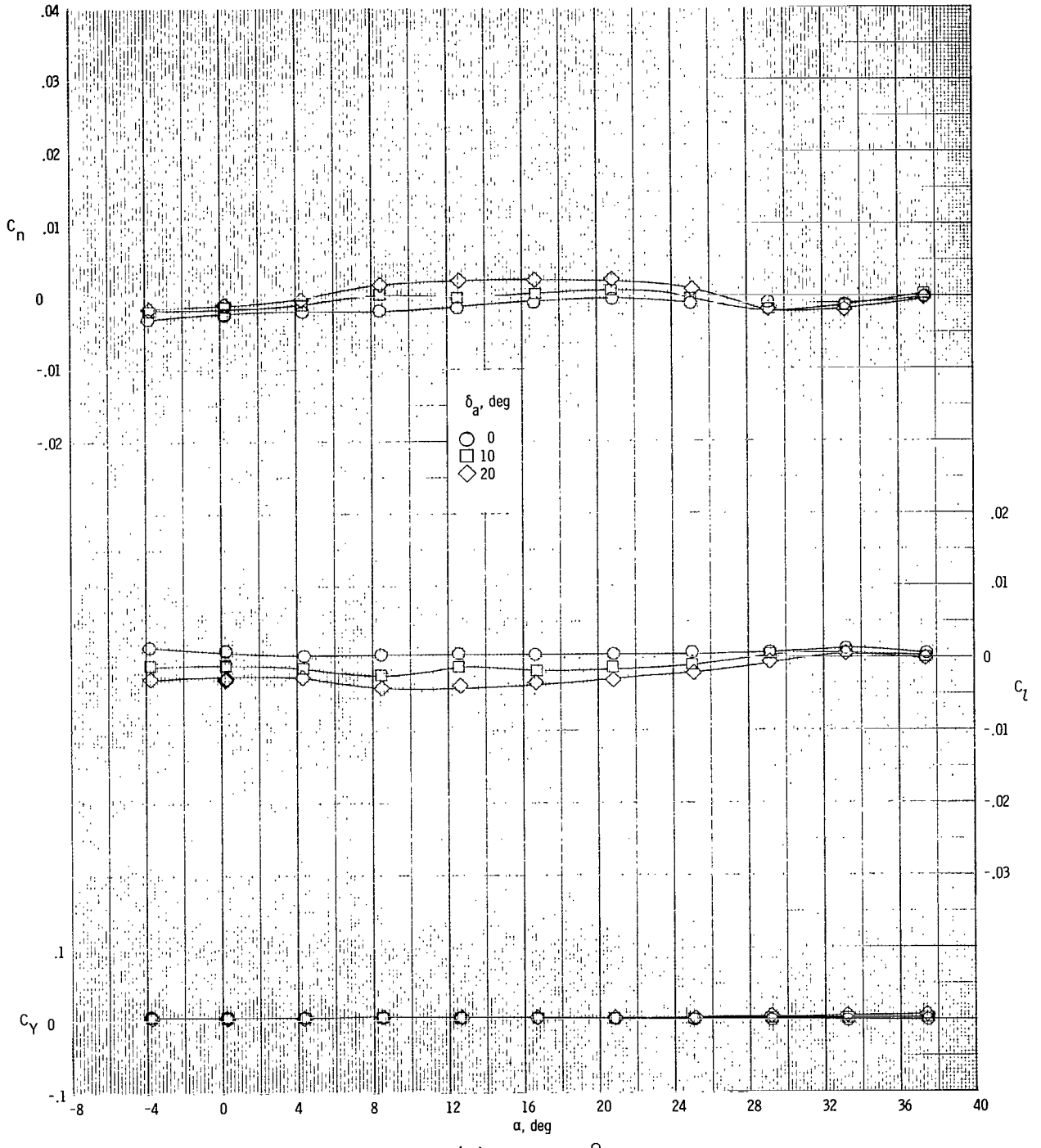

(d) $\delta_e = 30^\circ$.

Figure 27.- Concluded.

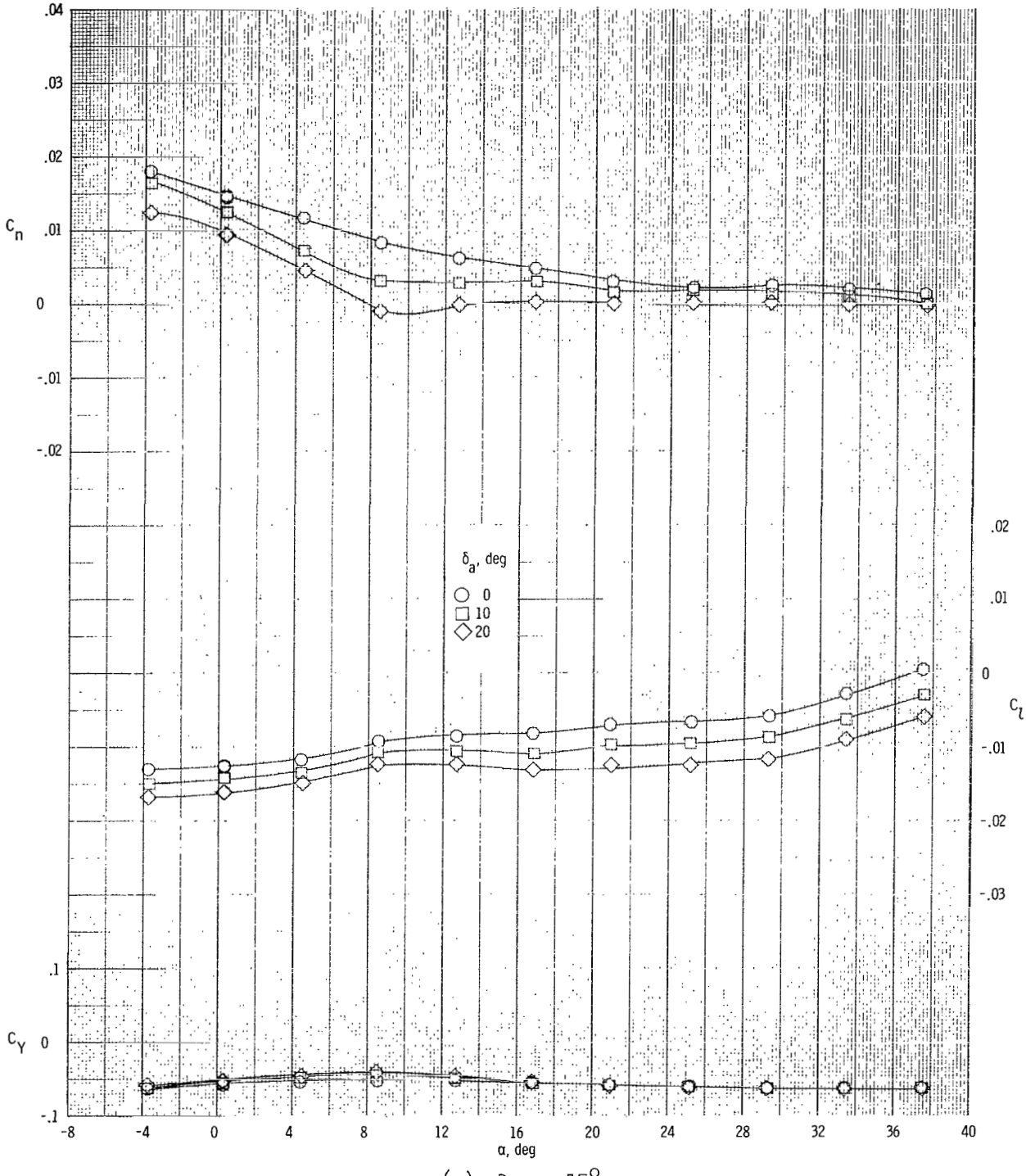

(a) $\delta_e = -15°$.

Figure 28.- Effects of aileron deflection on lateral aerodynamic characteristics of vehicle with modification II tip fins for several elevon deflection angles. $\beta = 3°$; $M = 1.80$.

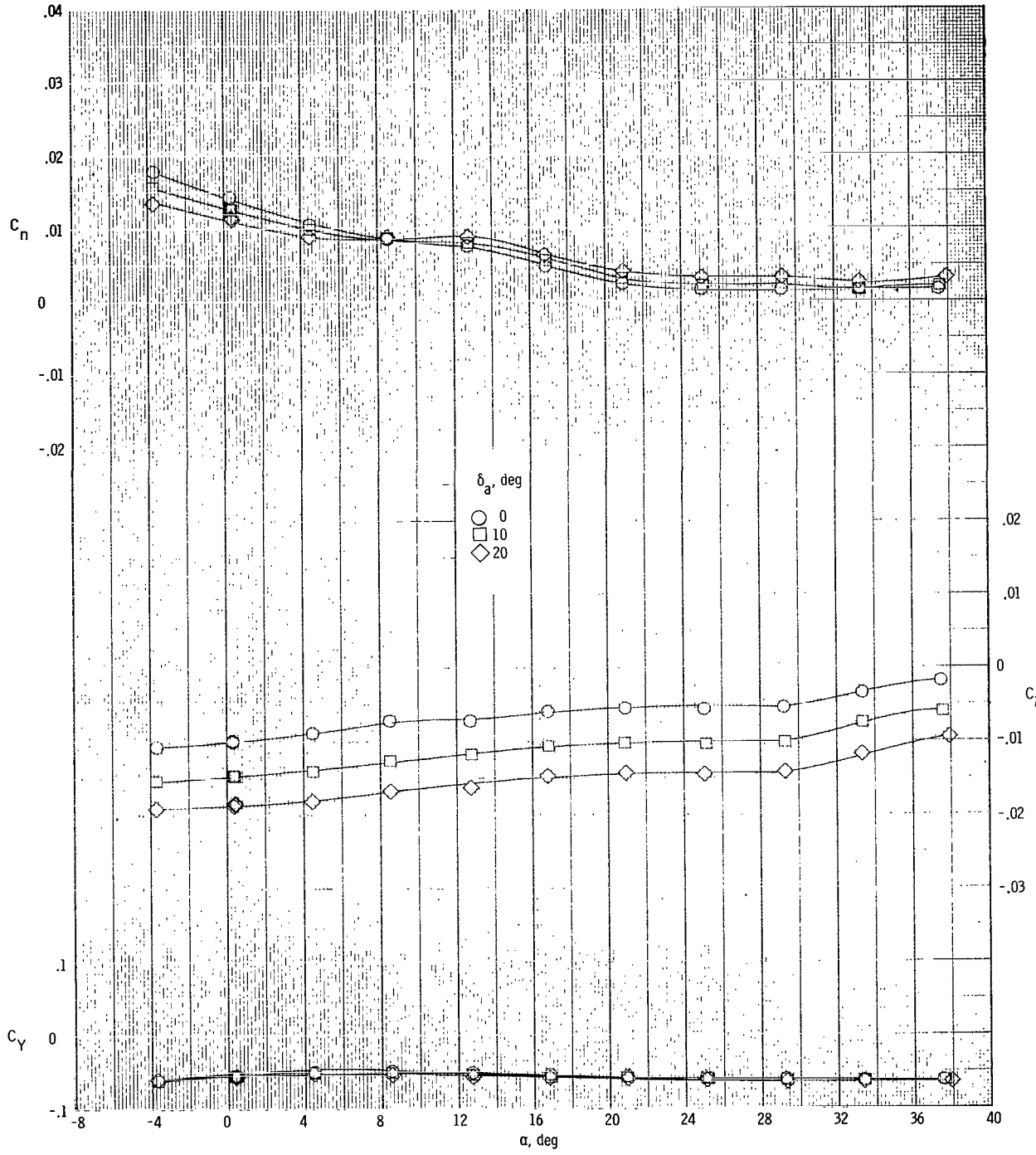

(b) $\delta_e = 0^o$.

Figure 28.- Continued.

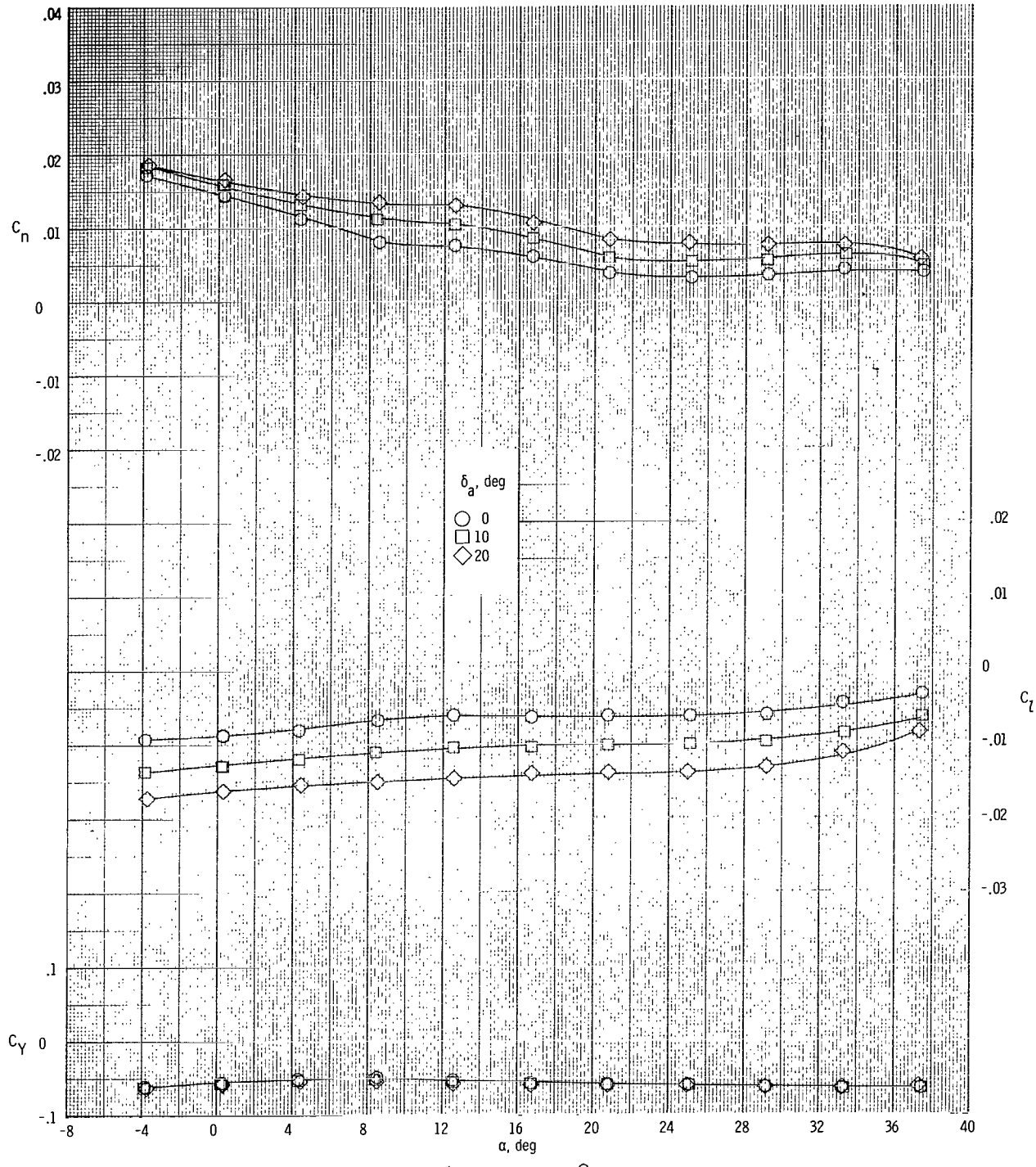

(c) $\delta_e = 15°$.

Figure 28.- Continued.

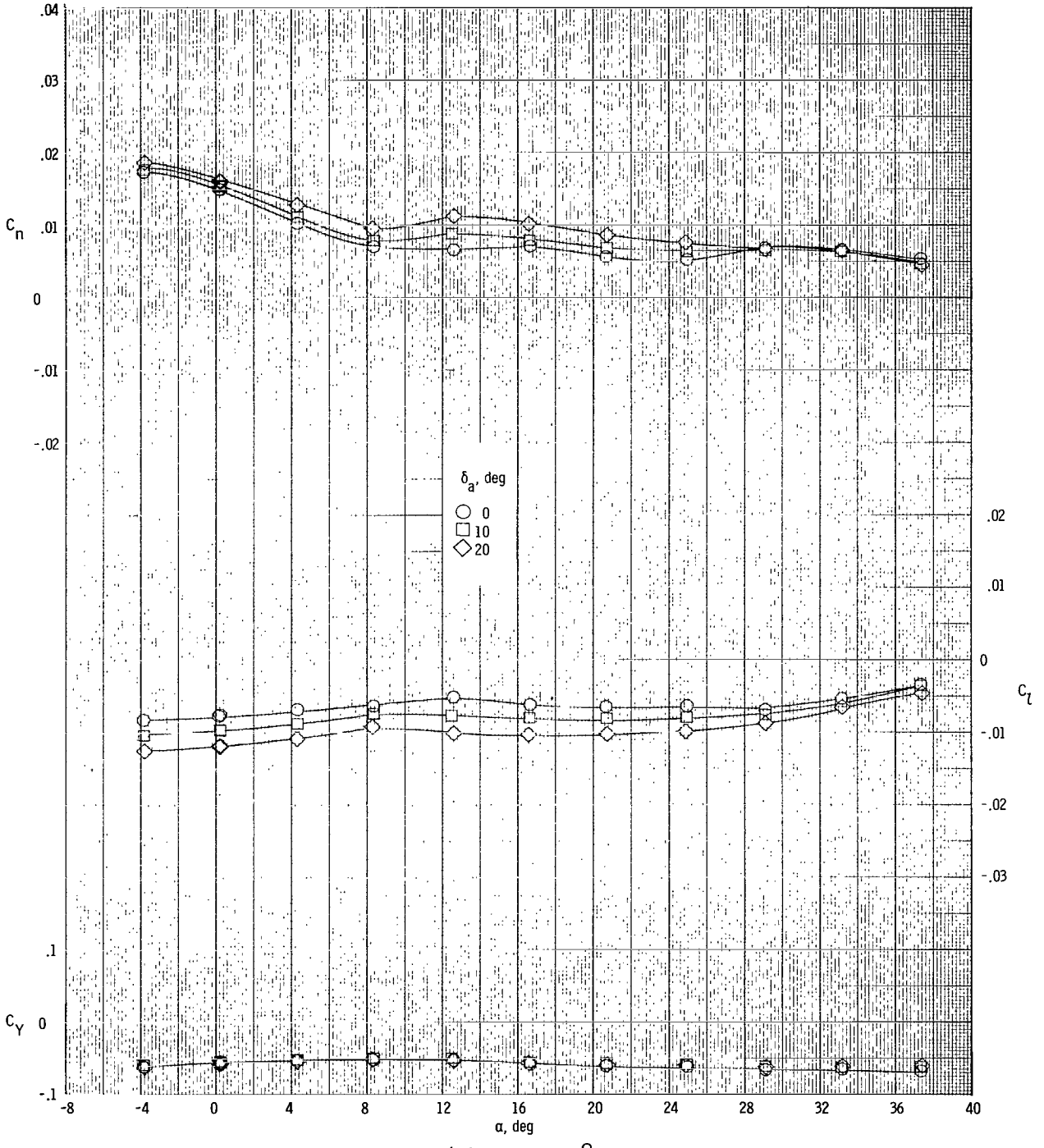

(d) $\delta_e = 30^\circ$.

Figure 28.- Concluded.

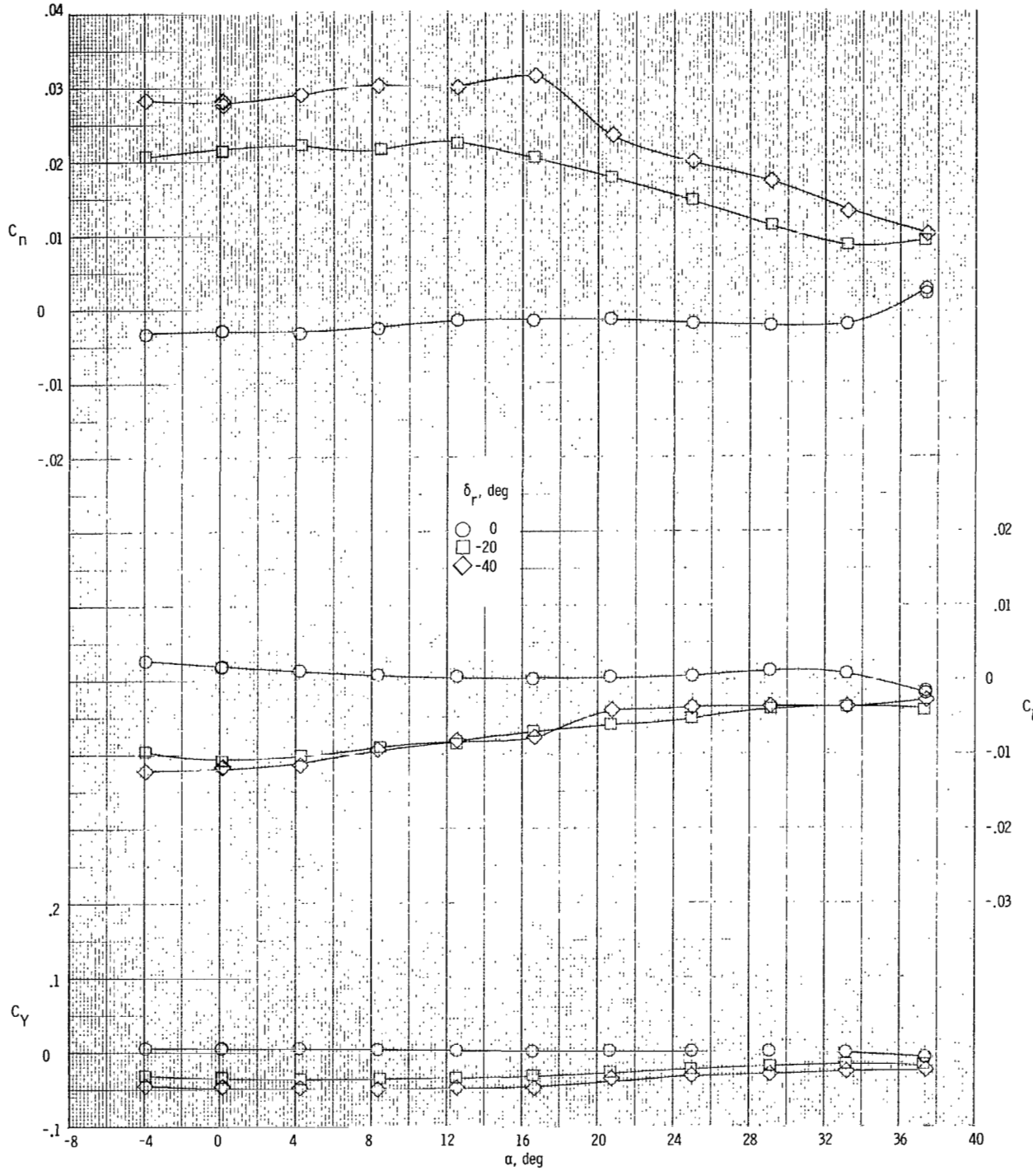

(a) $\delta_e = -15^\circ$.

Figure 29.- Effects of rudder deflection on directional aerodynamic characteristics of vehicle with modification II tip fins for several elevon deflection angles. $\beta = 0^\circ$; M = 1.50.

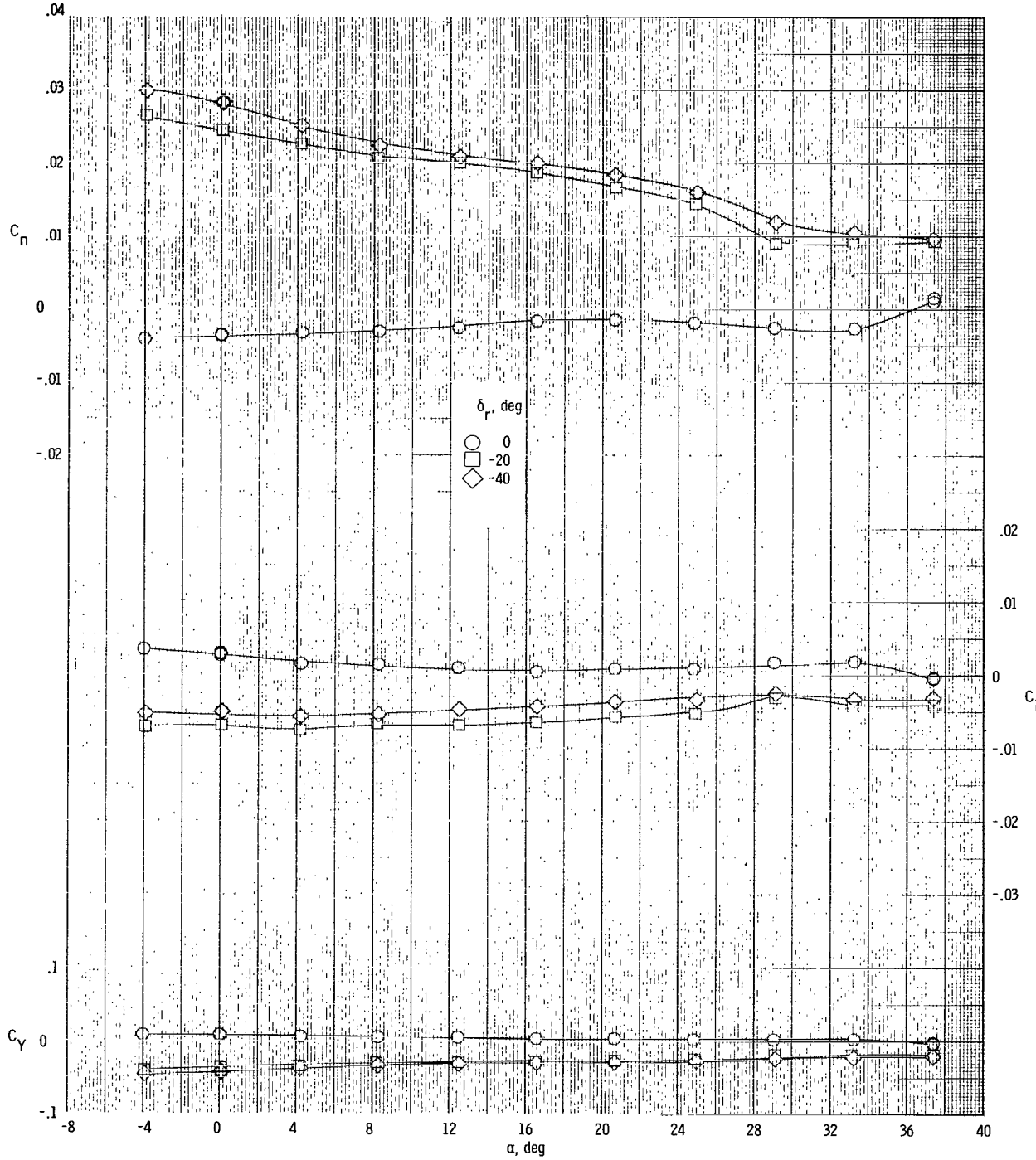

(b) $\delta_e = 0°$.

Figure 29.- Continued.

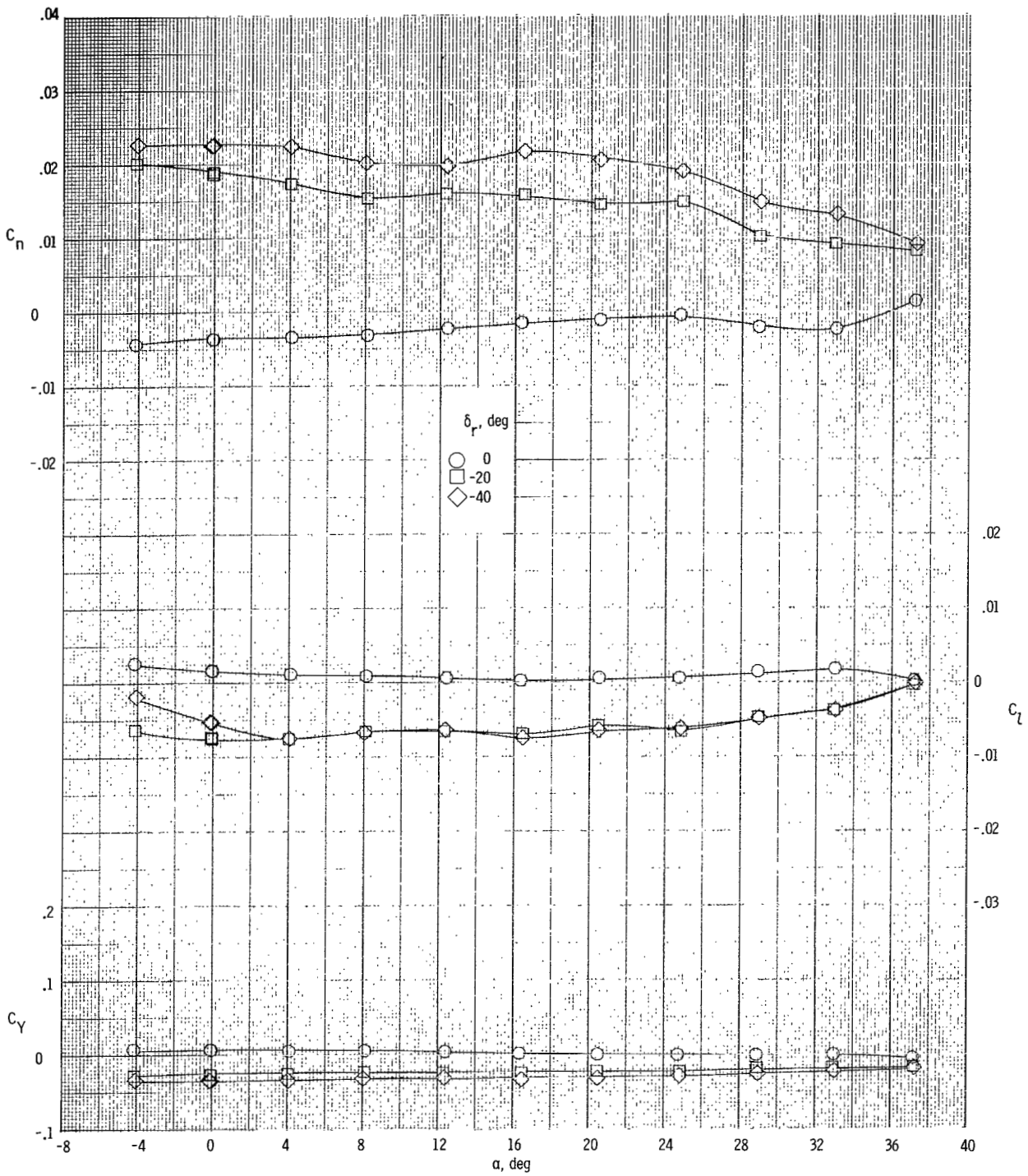

(c) $\delta_e = 15^\circ$.

Figure 29.- Continued.

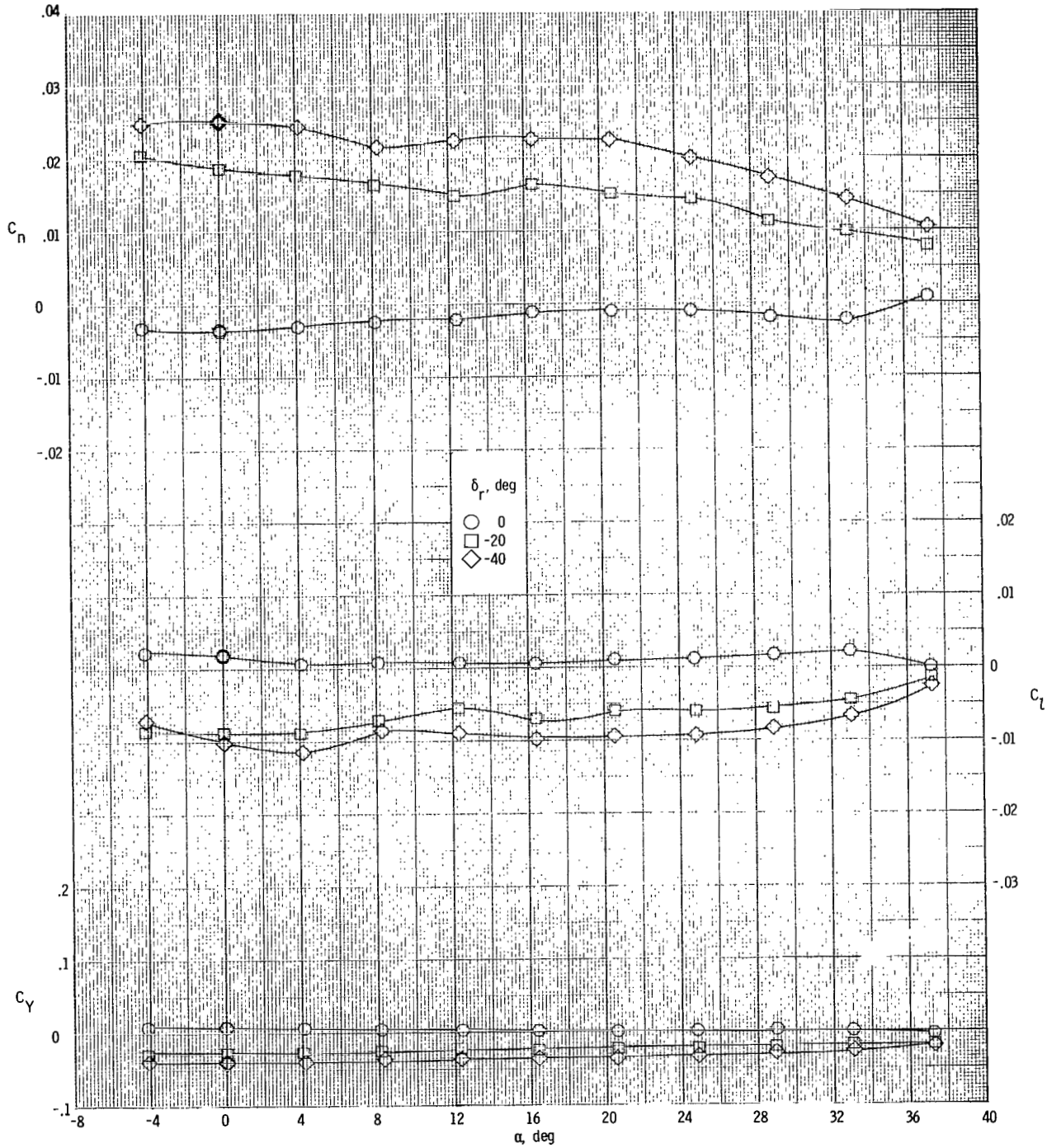

(d) $\delta_e = 30^\circ$.

Figure 29.- Concluded.

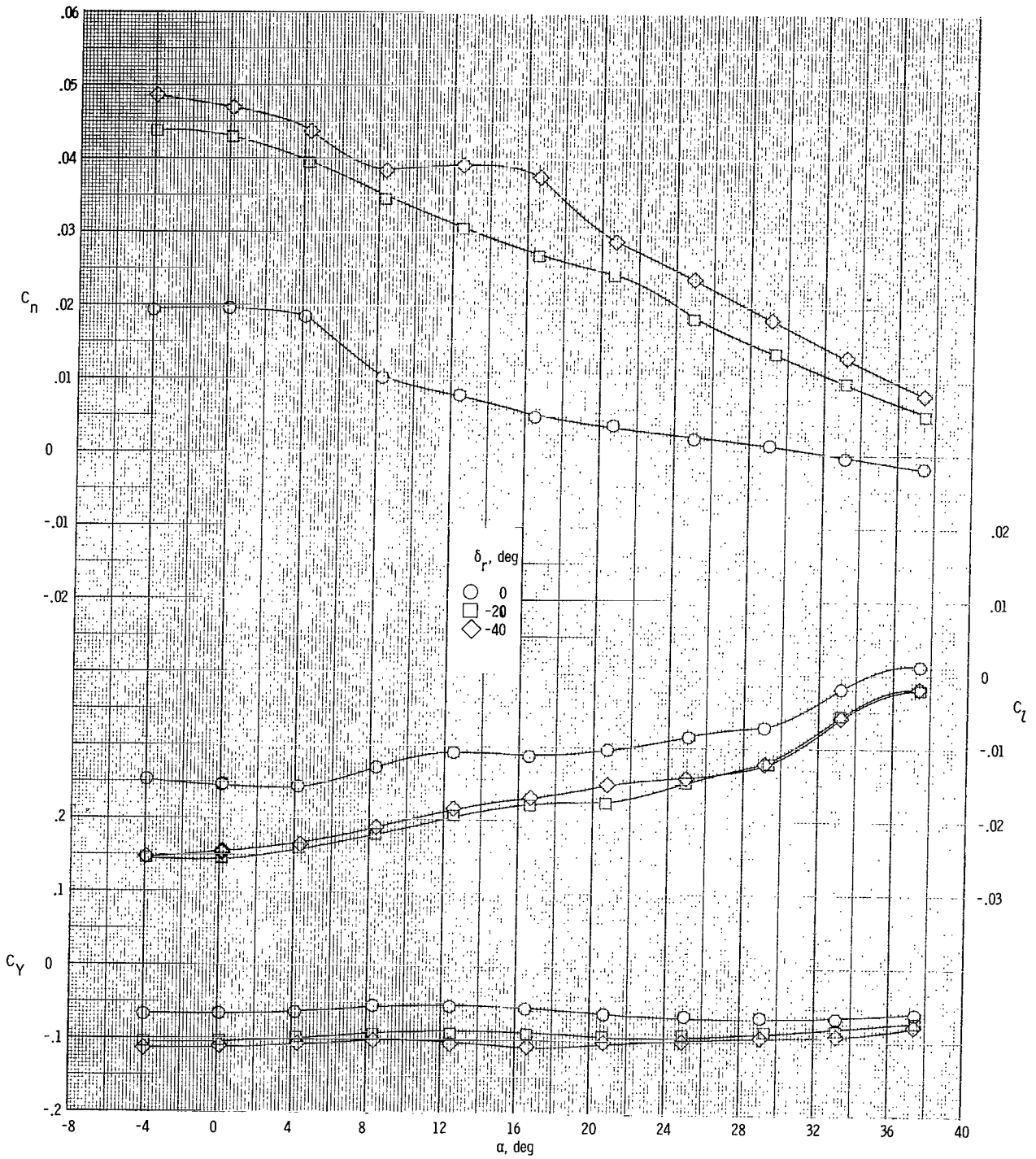

(a) $\delta_e = -15^\circ$.

Figure 30.- Effects of rudder deflection on directional aerodynamic characteristics of vehicle with modification II tip fins for several elevon deflection angles. $\beta = 3^\circ$; $M = 1.50$.

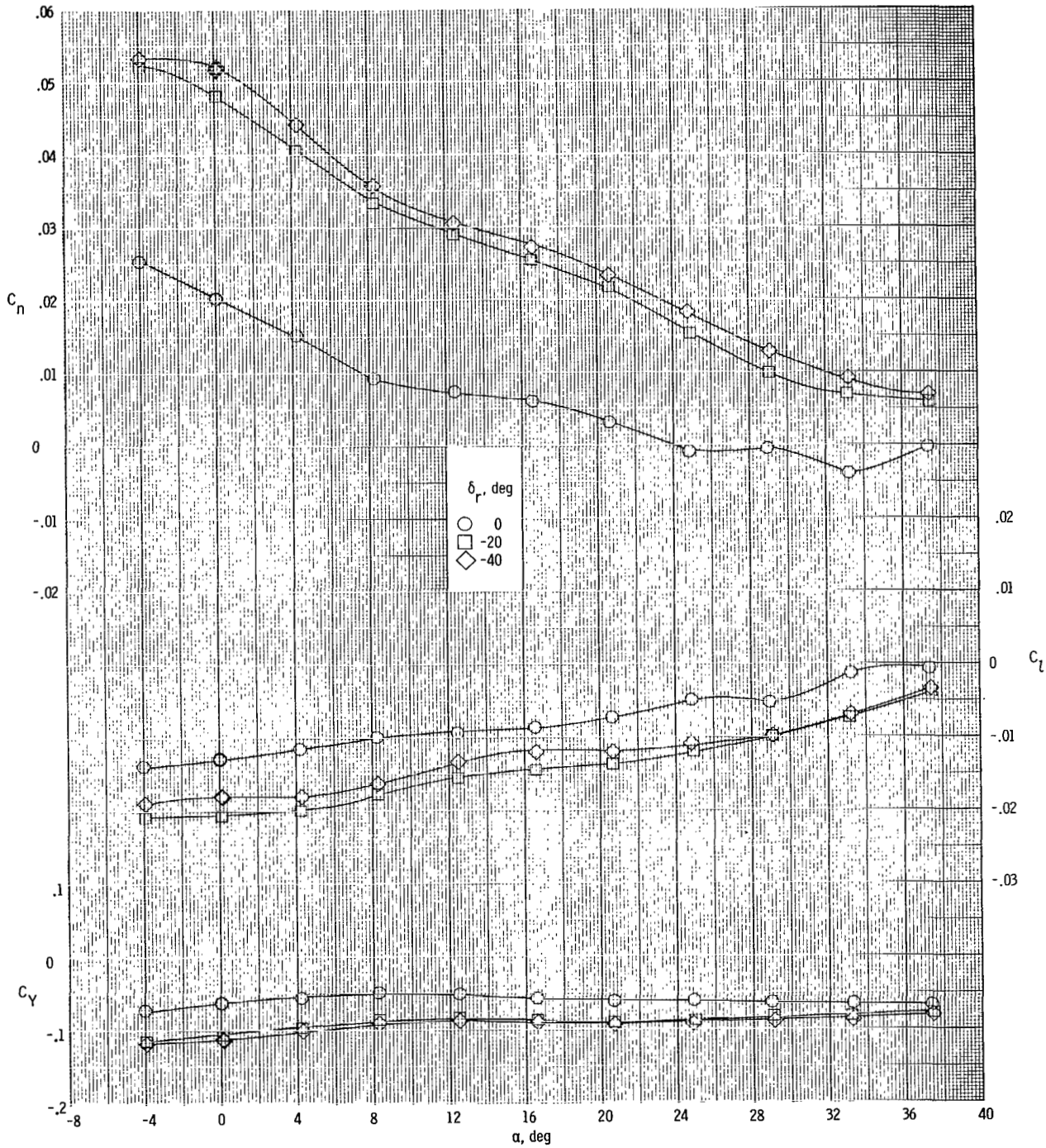

(b) $\delta_e = 0^\circ$.

Figure 30.- Continued.

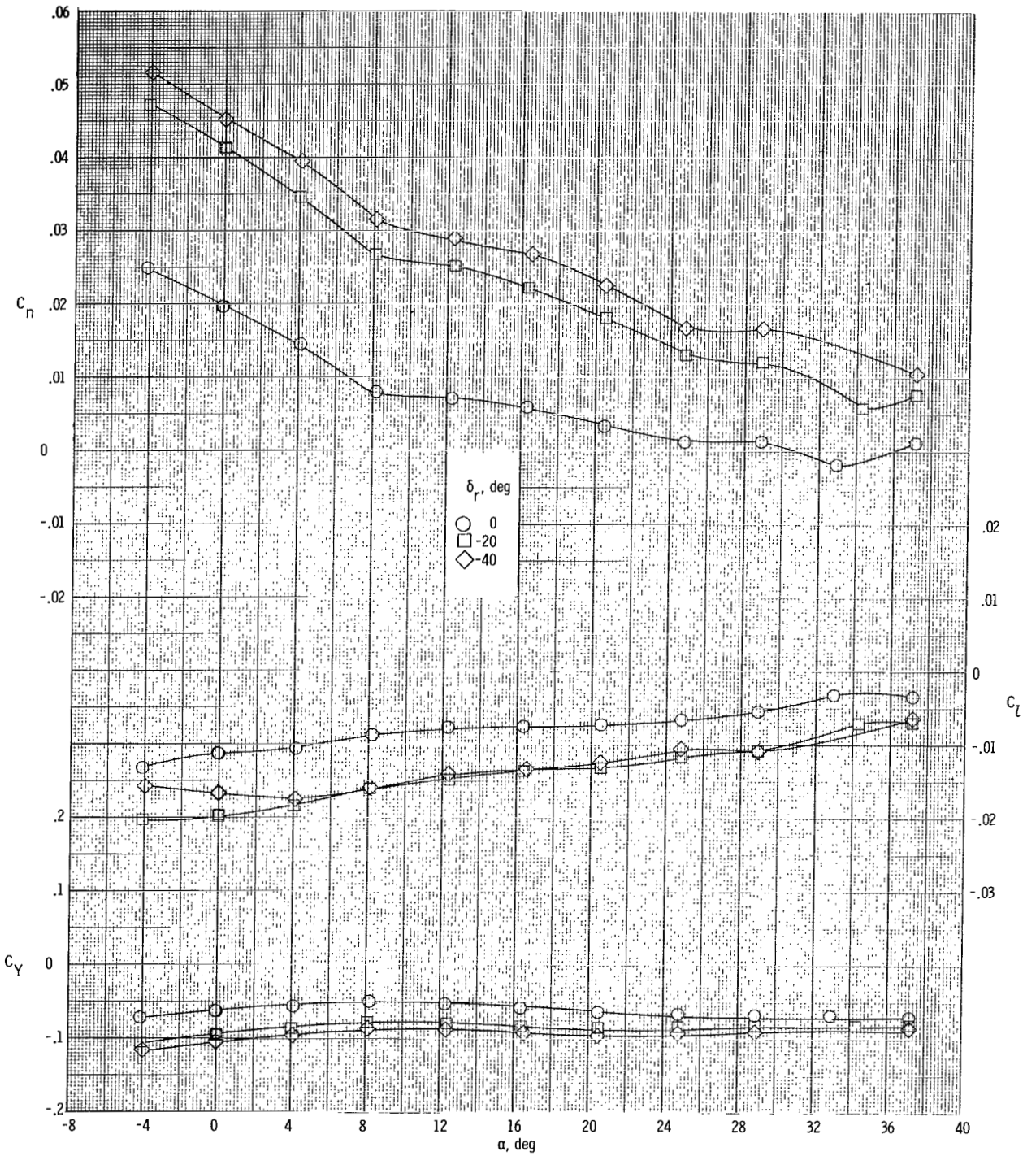

(c) $\delta_e = 15^\circ$.

Figure 30.- Continued.

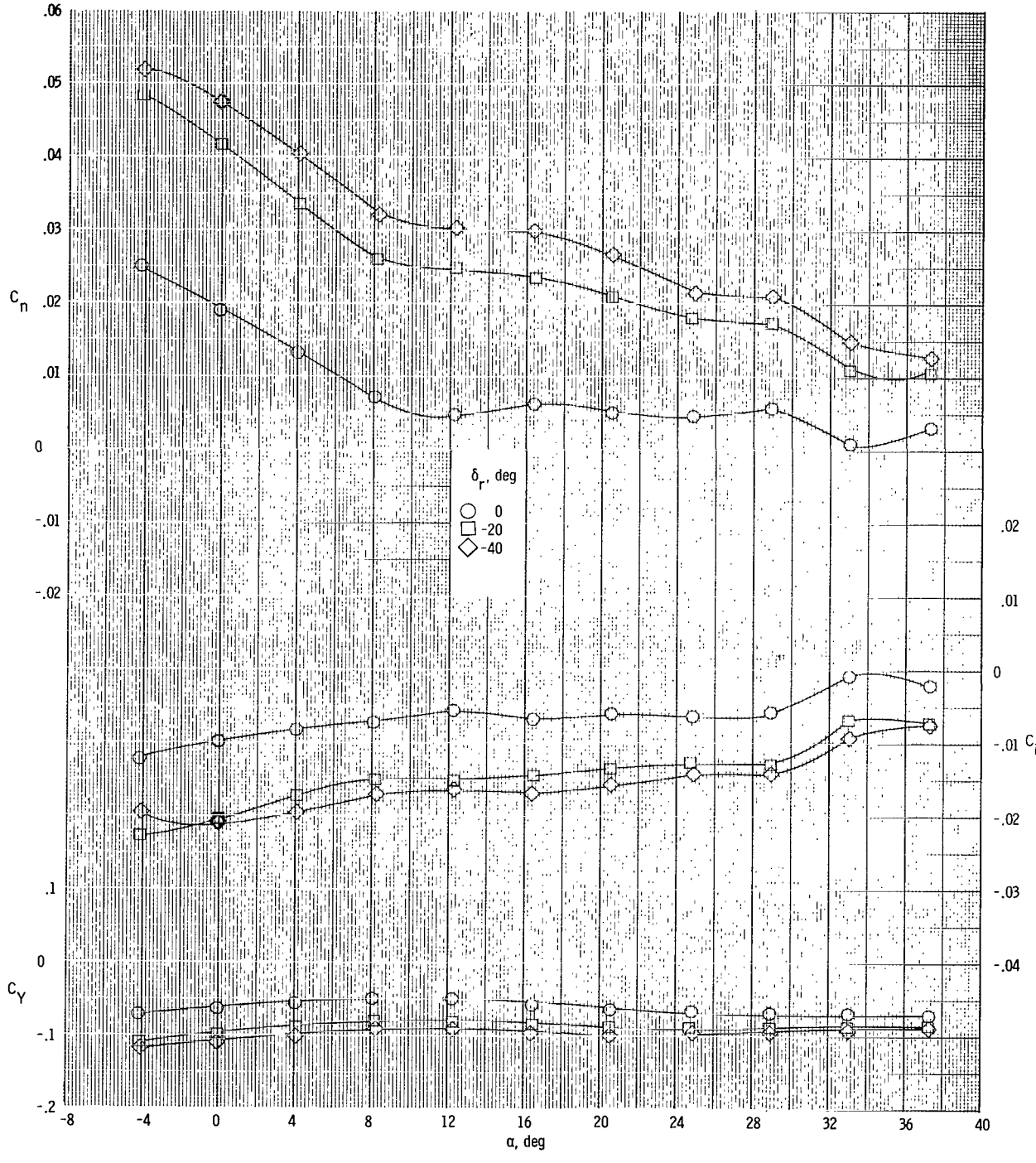

(d) $\delta_e = 30^\circ$.

Figure 30.- Concluded.

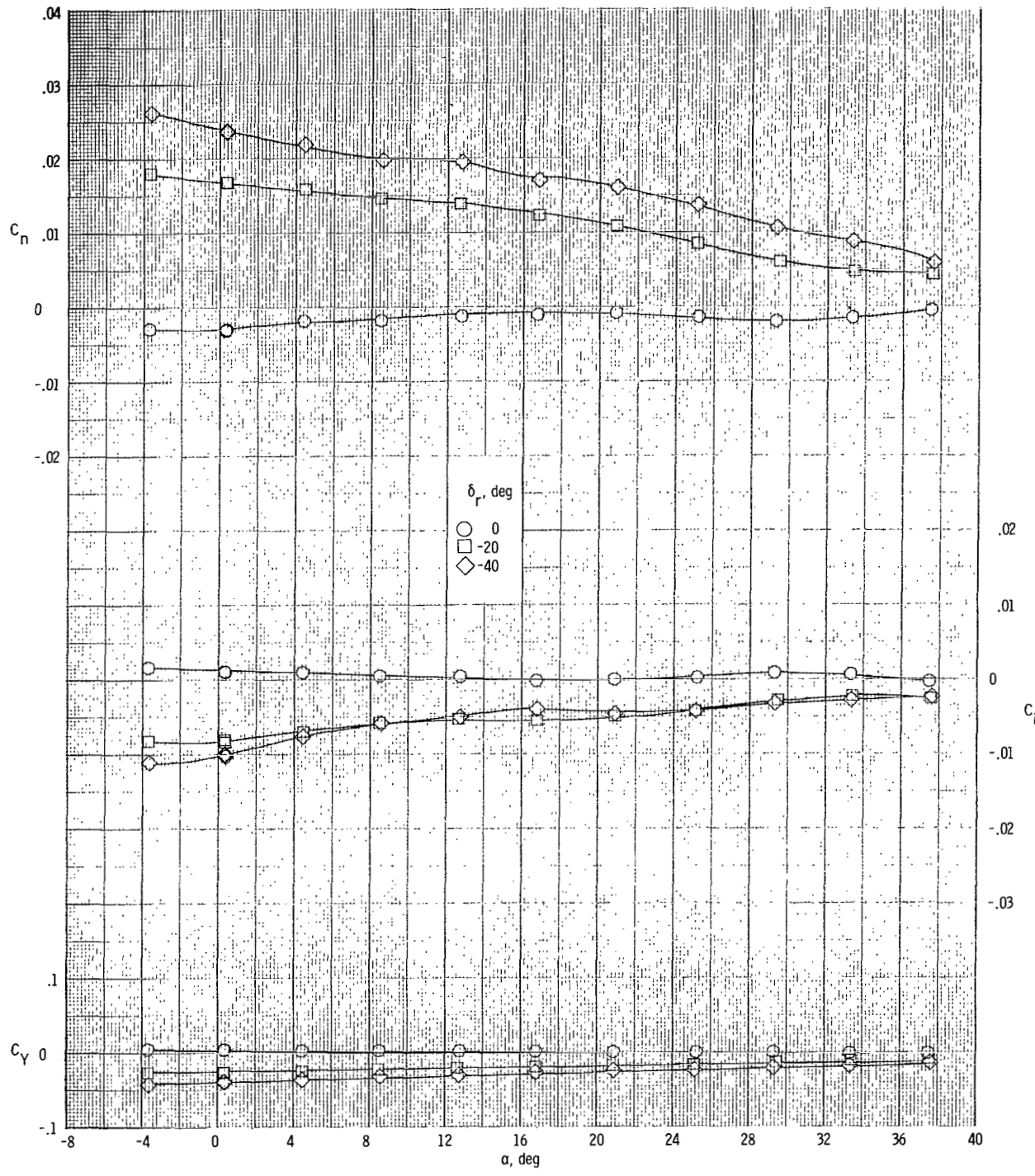

(a) $\delta_e = -15^\circ$.

Figure 31.- Effects of rudder deflection on directional aerodynamic characteristics of vehicle with modification II tip fins for several elevon deflection angles. $\beta = 0^\circ$; $M = 1.80$.

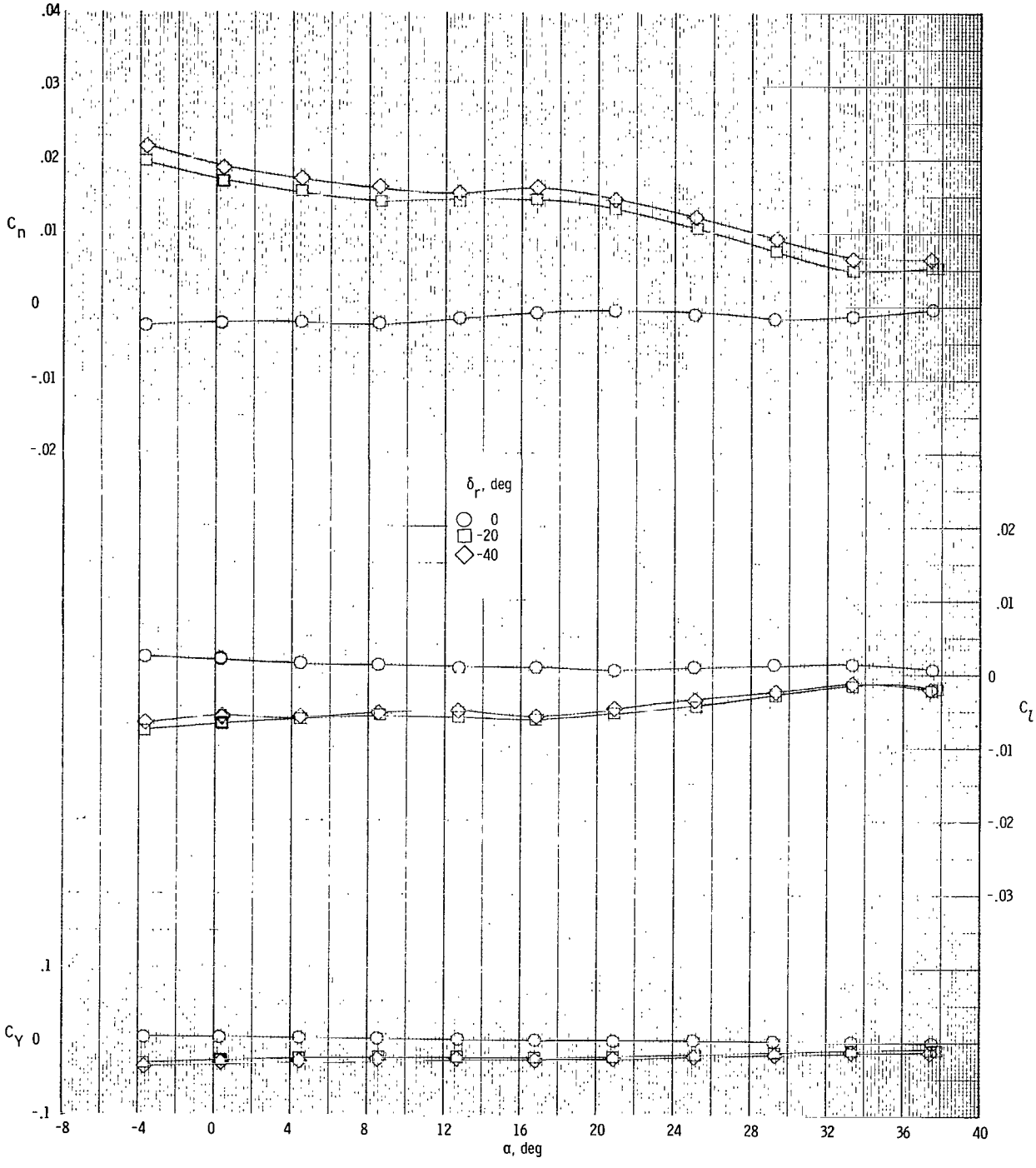

(b) $\delta_e = 0^\circ$.

Figure 31.- Continued.

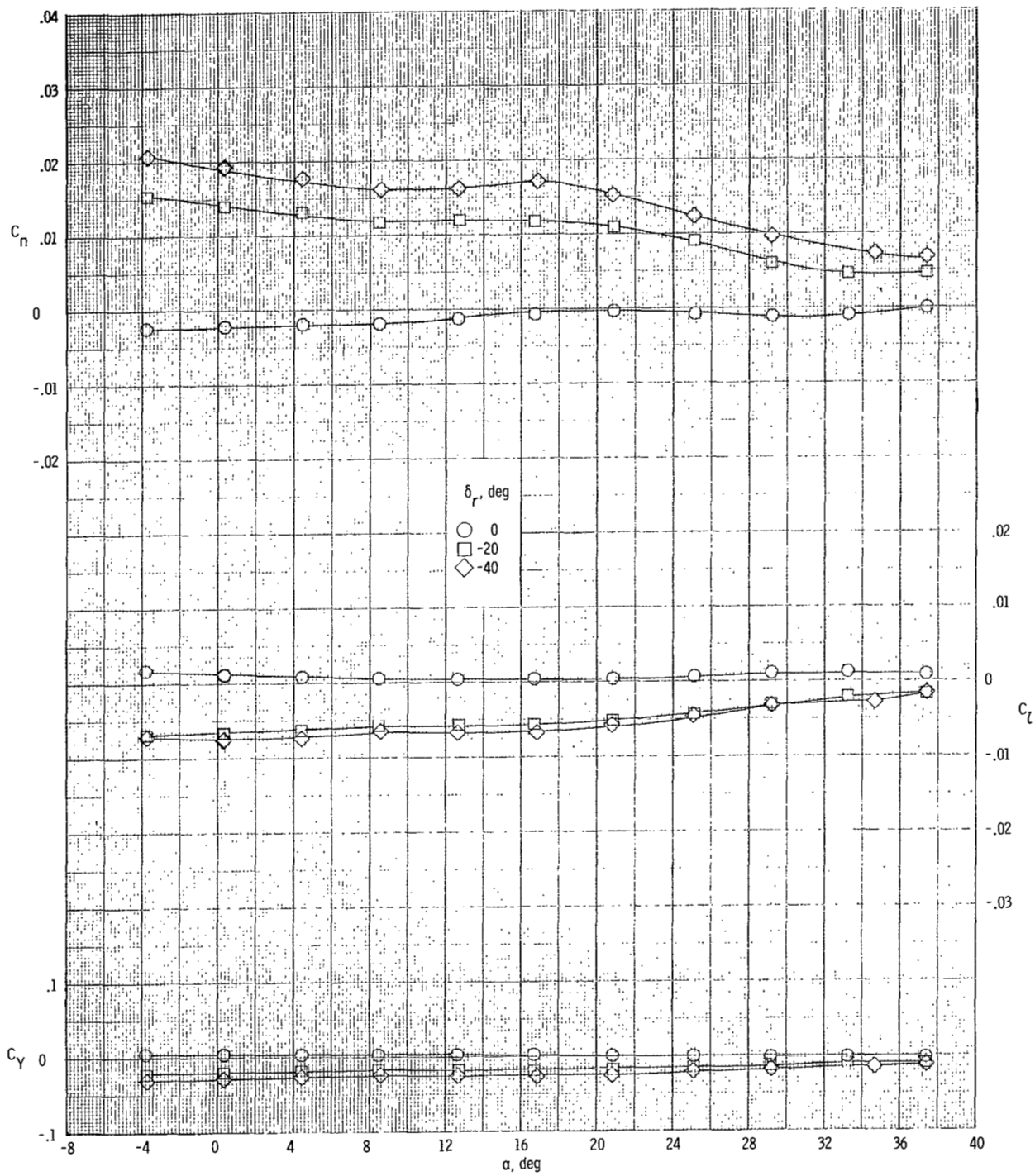

(c) $\delta_e = 15^\circ$.

Figure 31.- Continued.

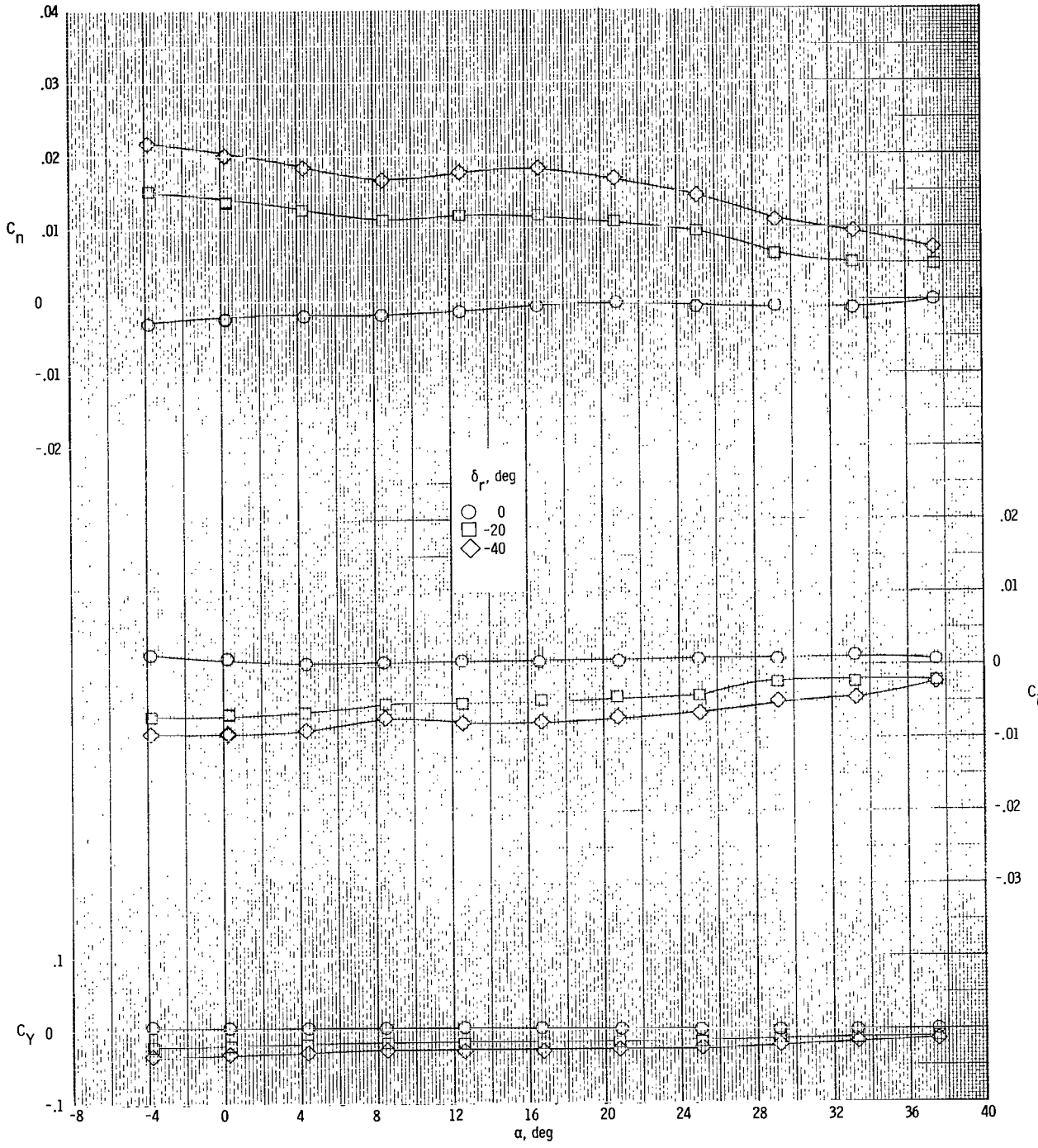

(d) $\delta_e = 30^\circ$.

Figure 31.- Concluded.

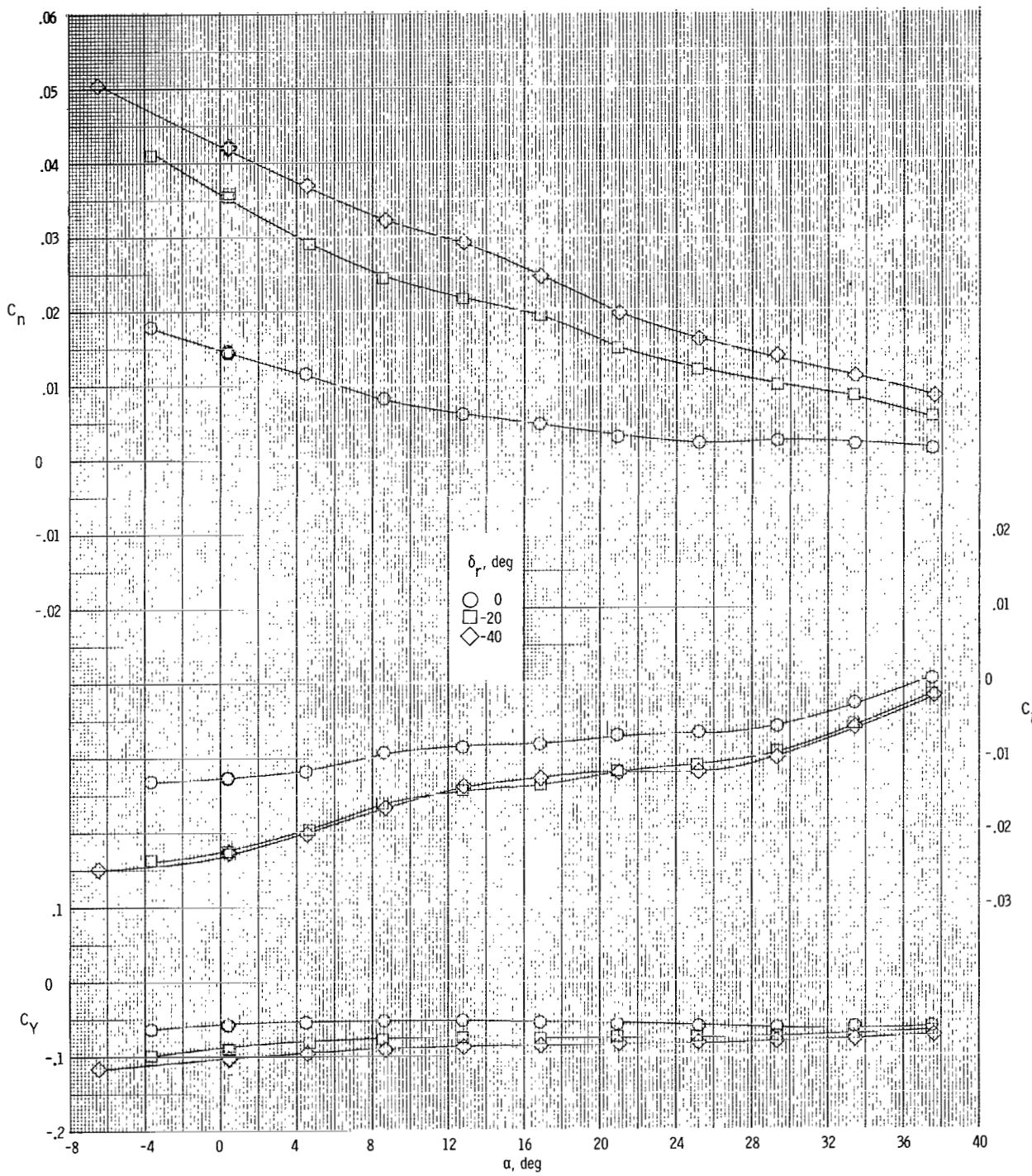

(a) $\delta_e = -15^\circ$.

Figure 32.- Effects of rudder deflection on directional aerodynamic characteristics of vehicle with modification II tip fins for several elevon deflection angles. $\beta = 3^\circ$; M = 1.80.

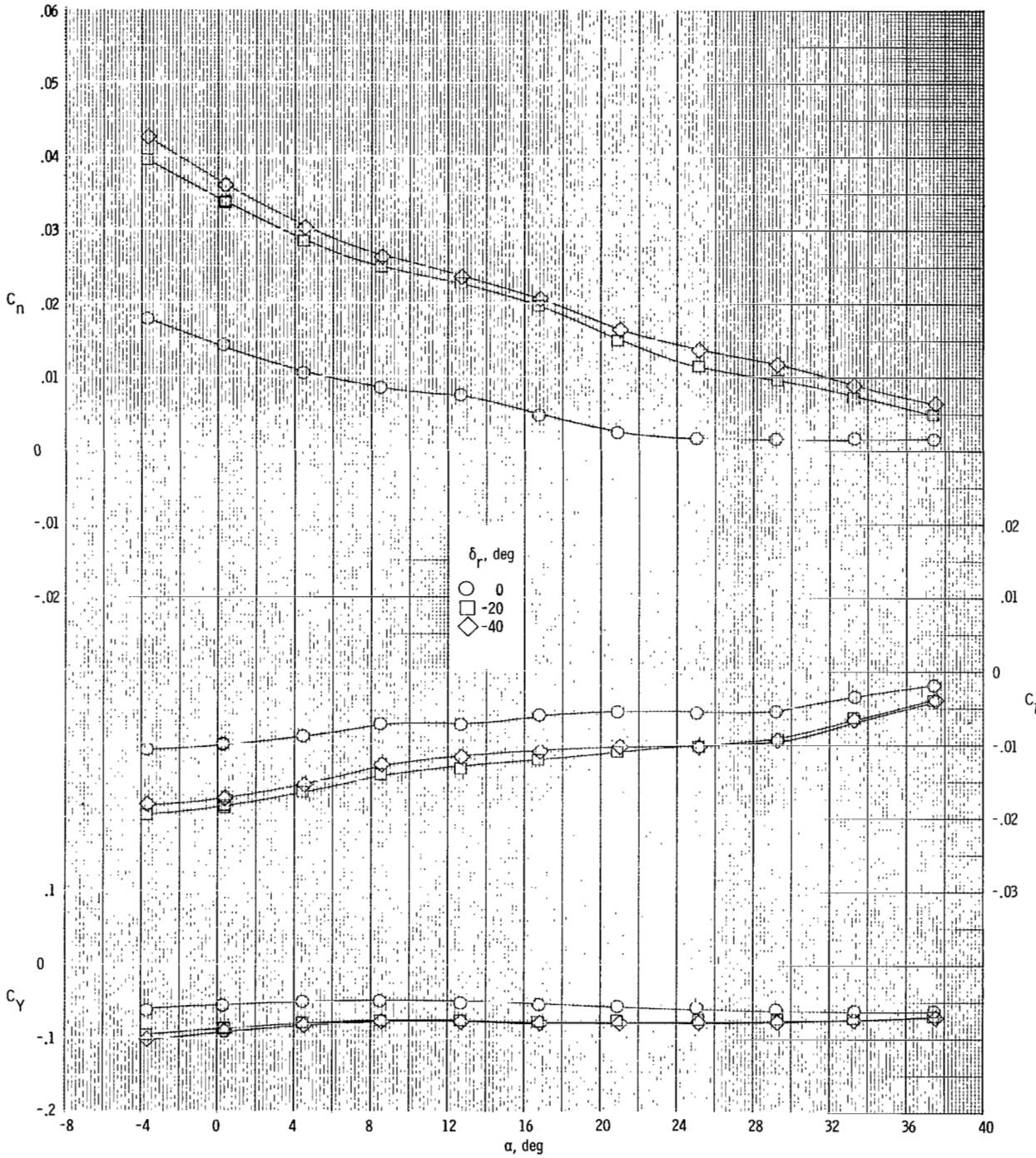

(b) $\delta_e = 0^\circ$.

Figure 32.- Continued.

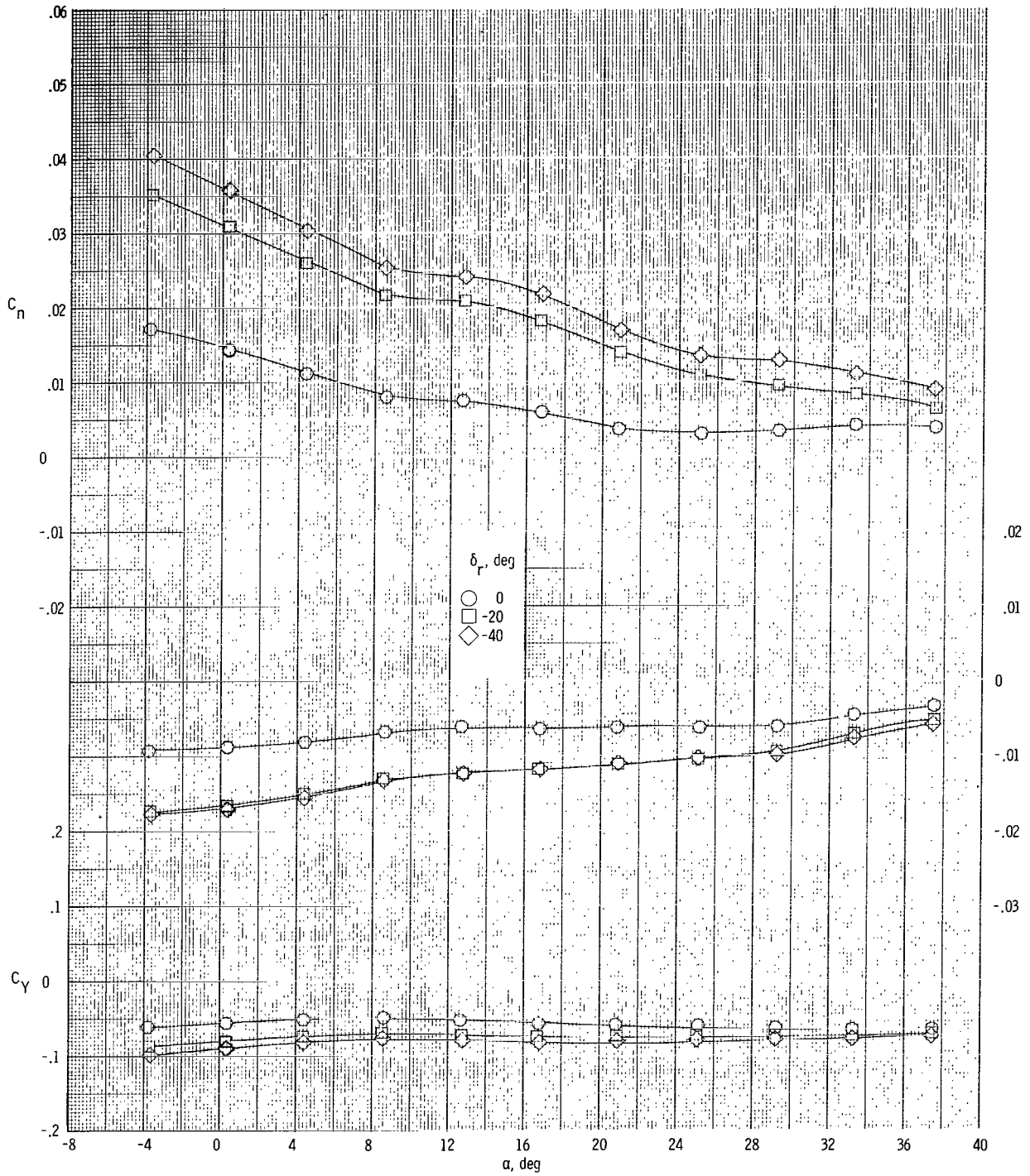

(c) $\delta_e = 15°$.

Figure 32.- Continued.

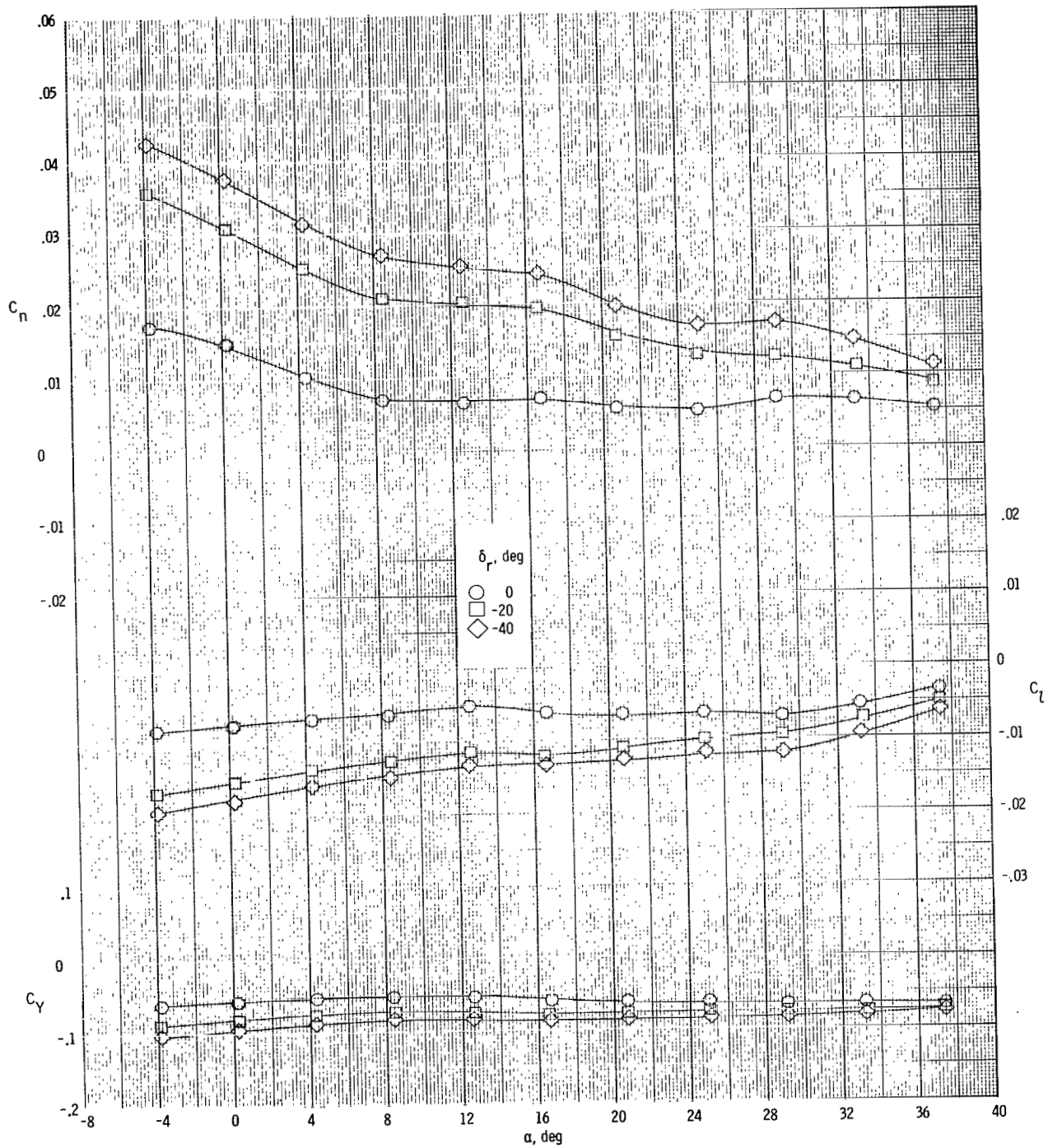

(d) $\delta_e = 30^\circ$.

Figure 32.- Concluded.

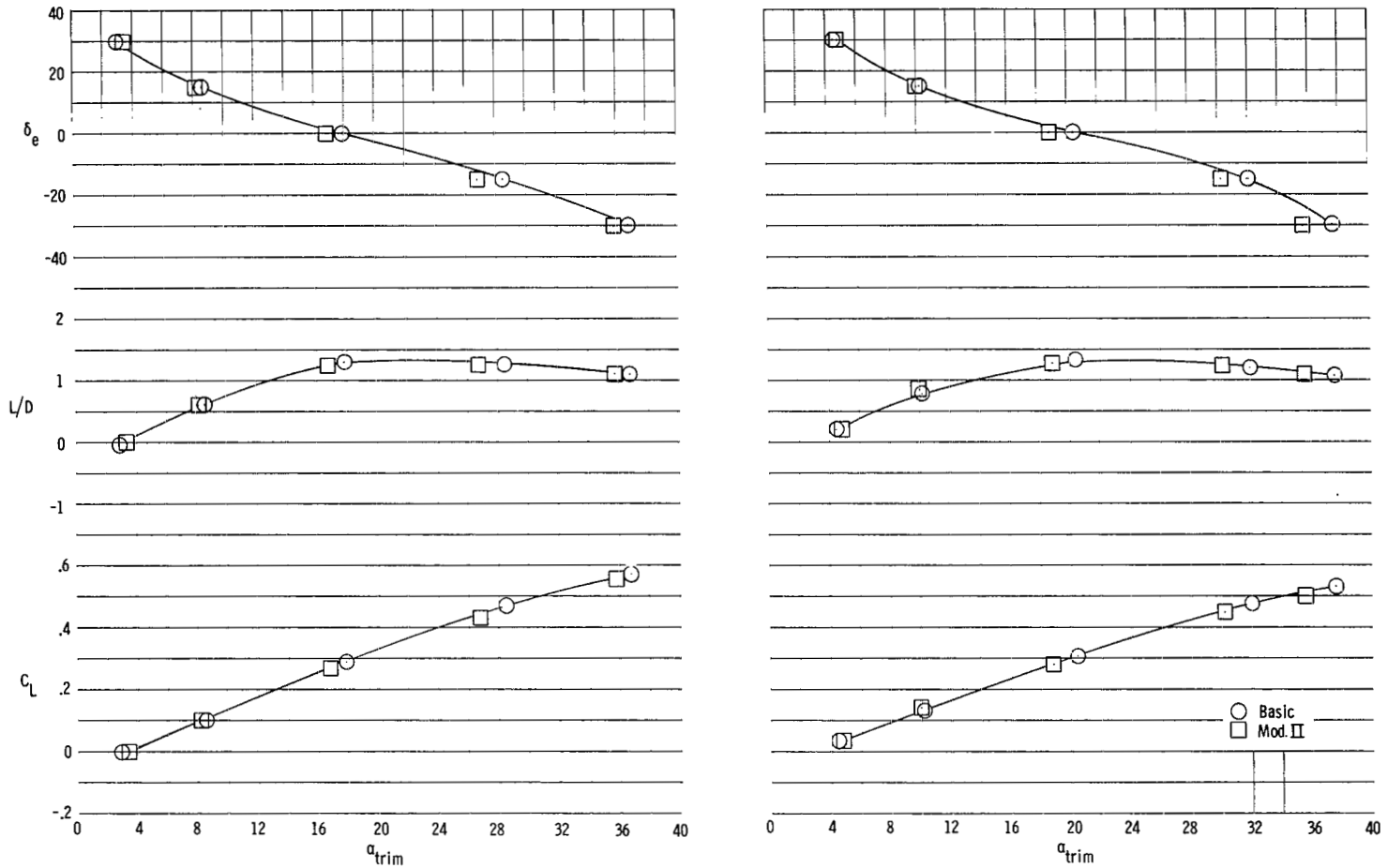

(a) M = 1.50.

(b) M = 1.80.

Figure 33.- Trimmed longitudinal aerodynamic characteristics of vehicle with both basic and modification II tip fins.

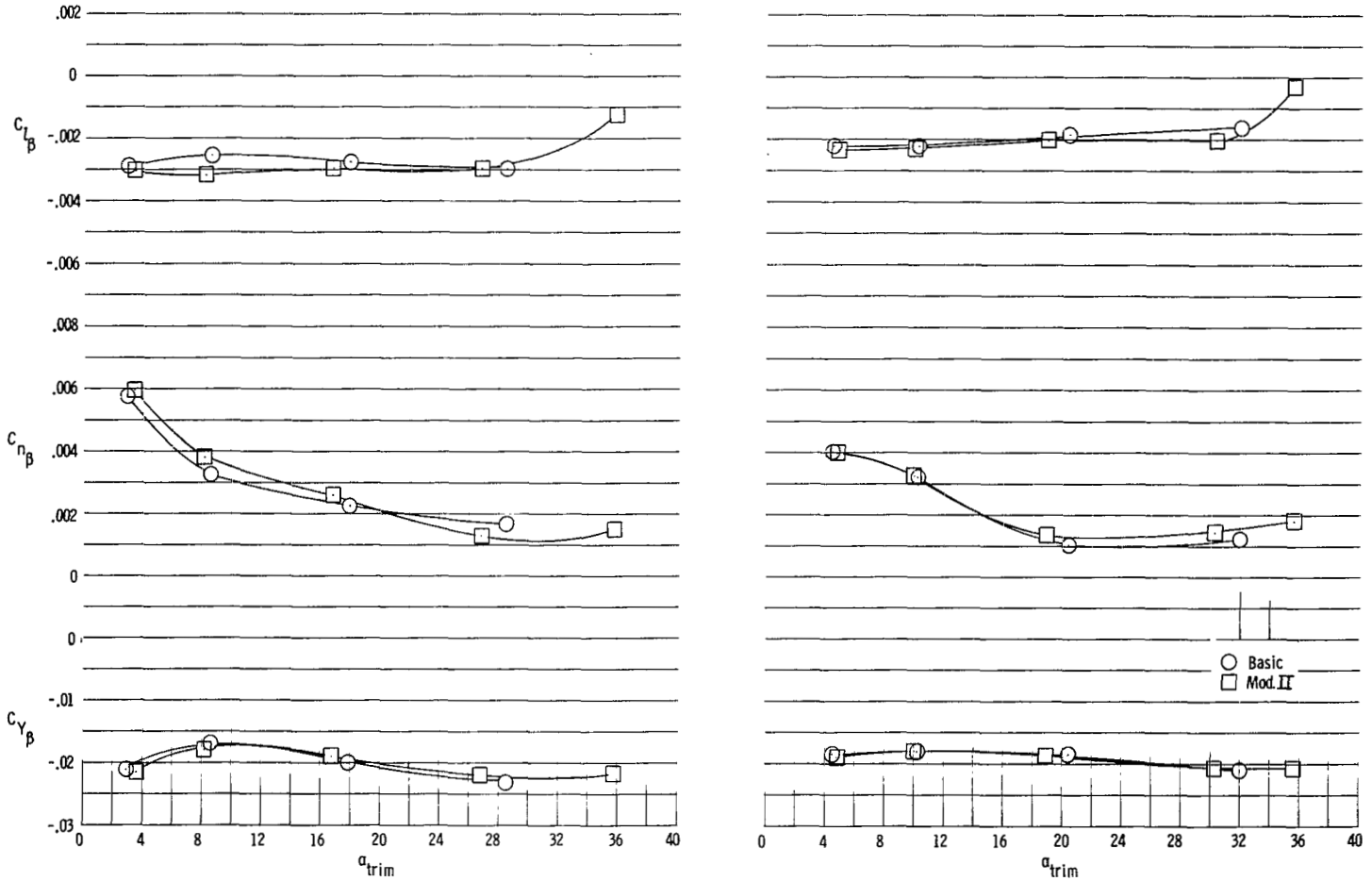

(a) M = 1.50.

(b) M = 1.80.

Figure 34.- Trimmed directional and lateral stability characteristics of vehicle with both basic and modification II tip fins.

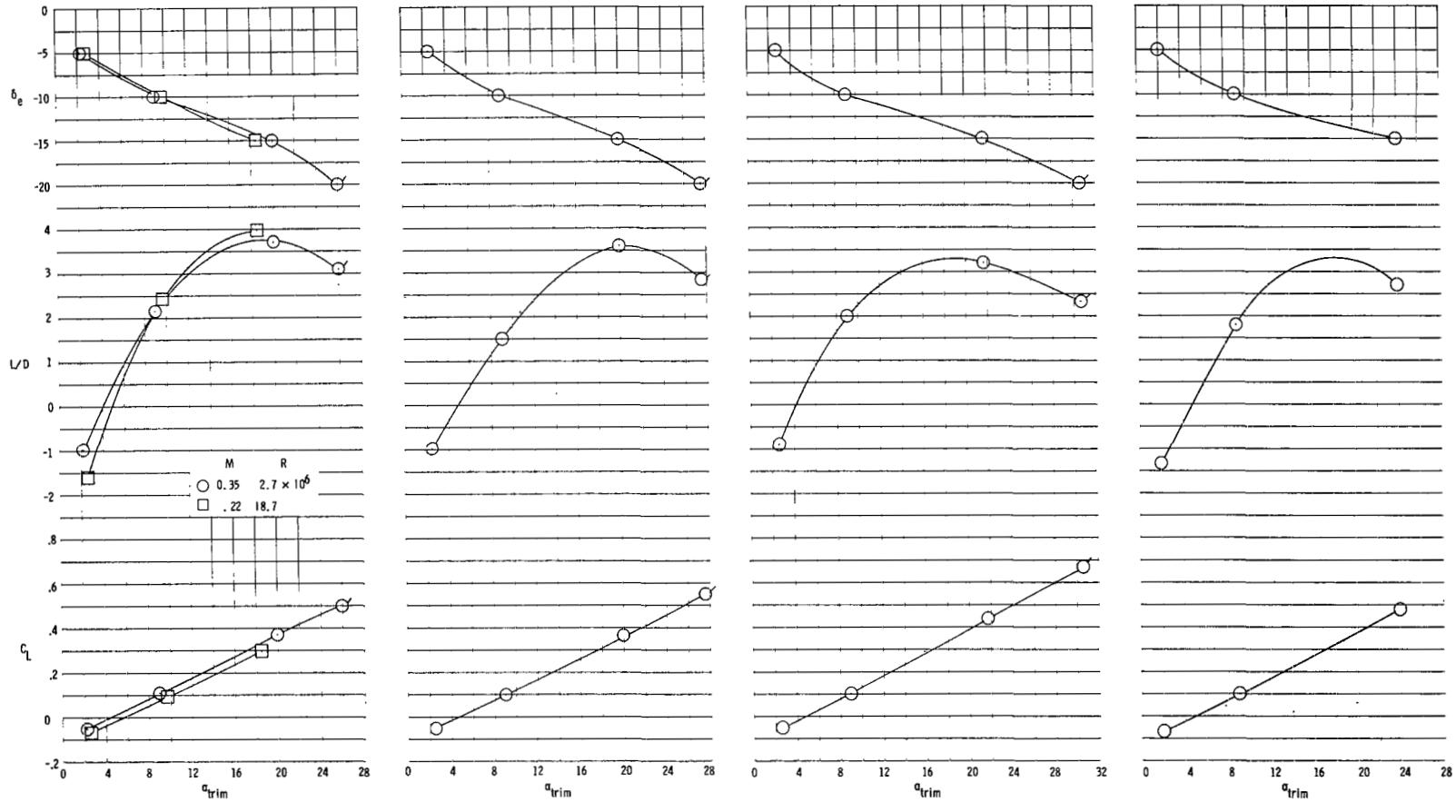

(a) Subsonic. (b) M = 0.50. (c) M = 0.60. (d) M = 0.70.

Figure 35.- Summary of trimmed longitudinal aerodynamic characteristics of vehicle with modification II tip fins at subsonic speeds. Flaps in subsonic position. Flagged symbols indicate extrapolated data.

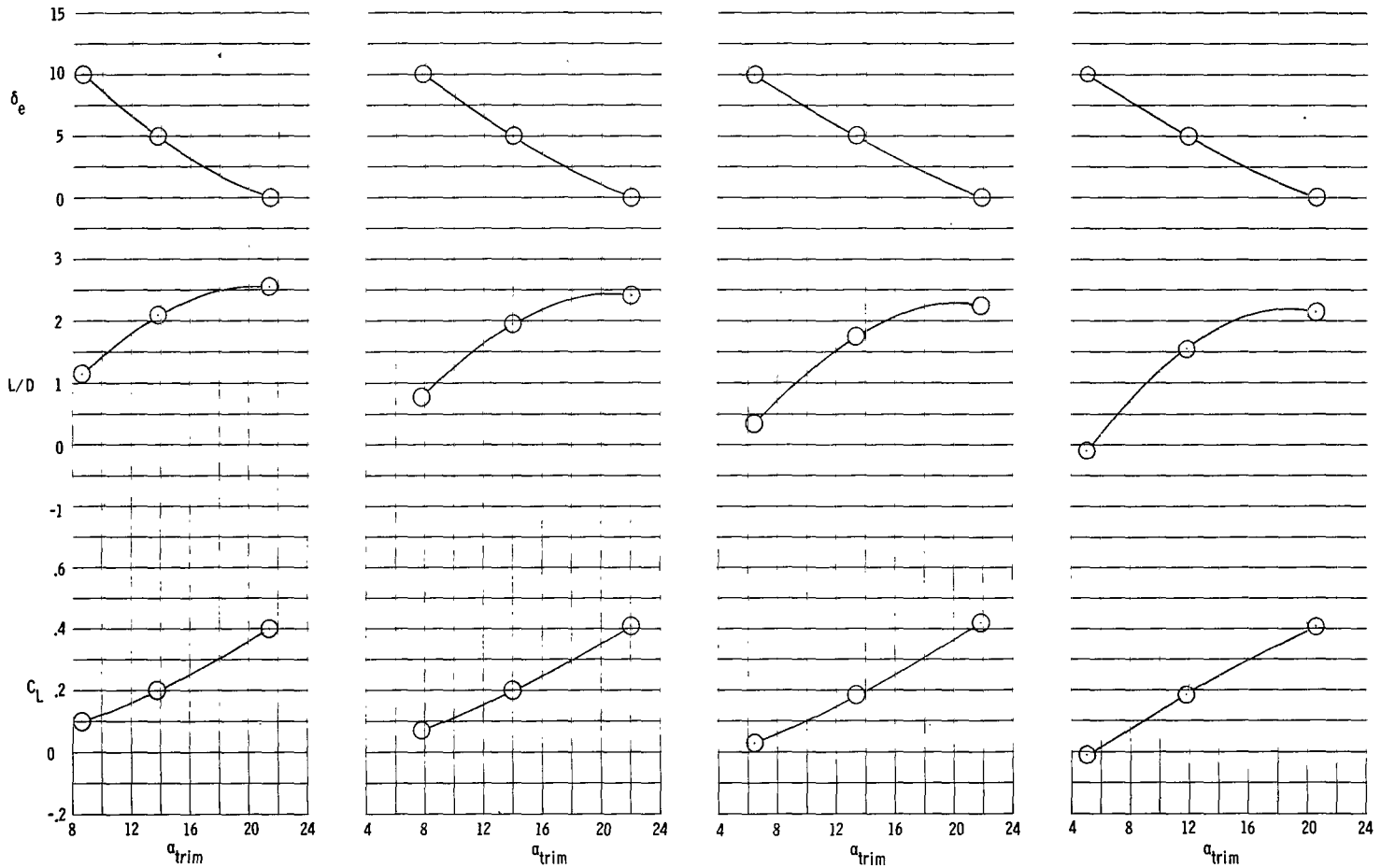

(a) M = 0.60. (b) M = 0.70. (c) M = 0.80. (d) M = 0.90.

Figure 36.- Summary of trimmed longitudinal aerodynamic characteristics of vehicle with modification II tip fins from subsonic to supersonic speeds. Flaps in transonic position.

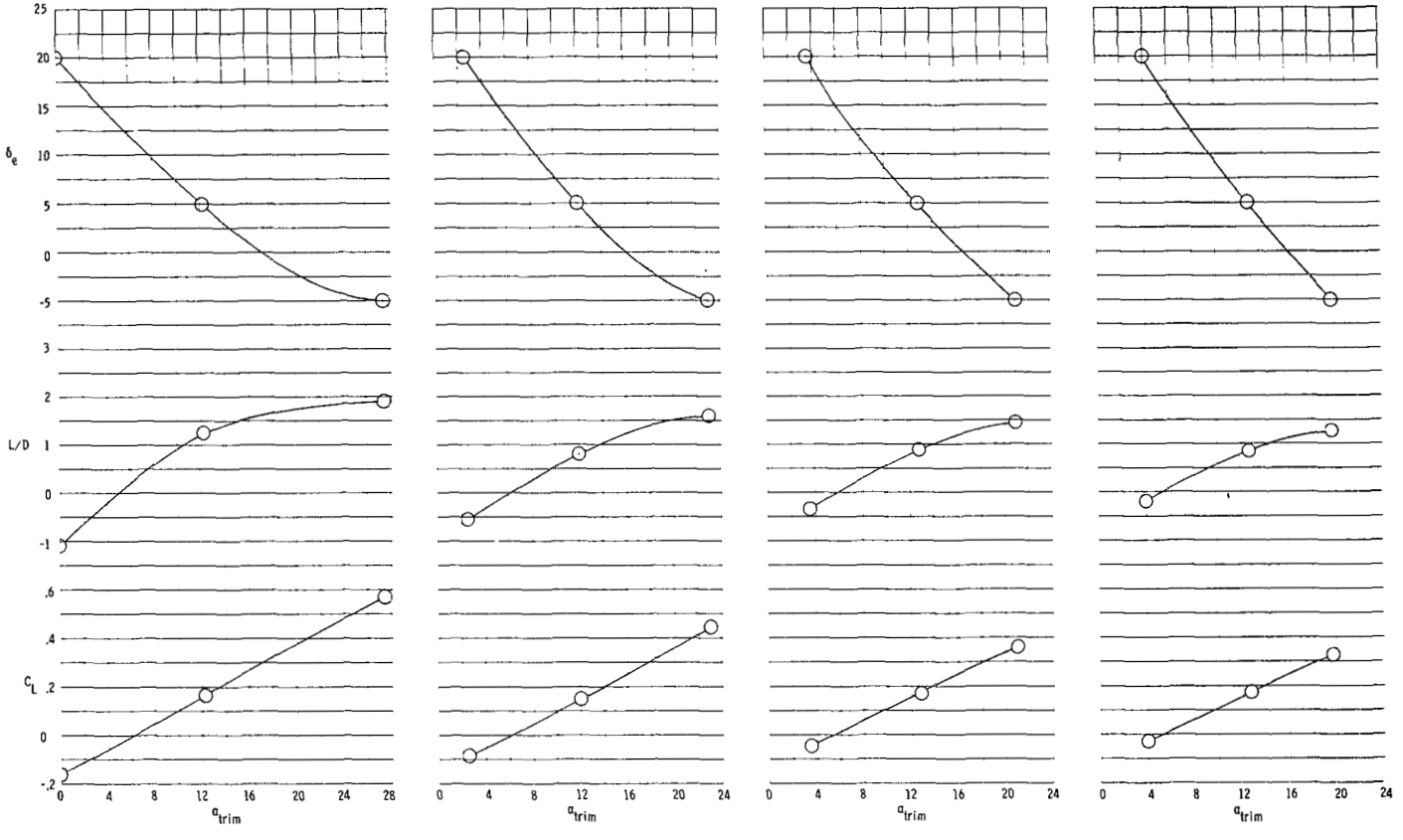

(e) M = 0.95. (f) M = 1.00. (g) M = 1.10. (h) M = 1.20.

Figure 36.- Continued.

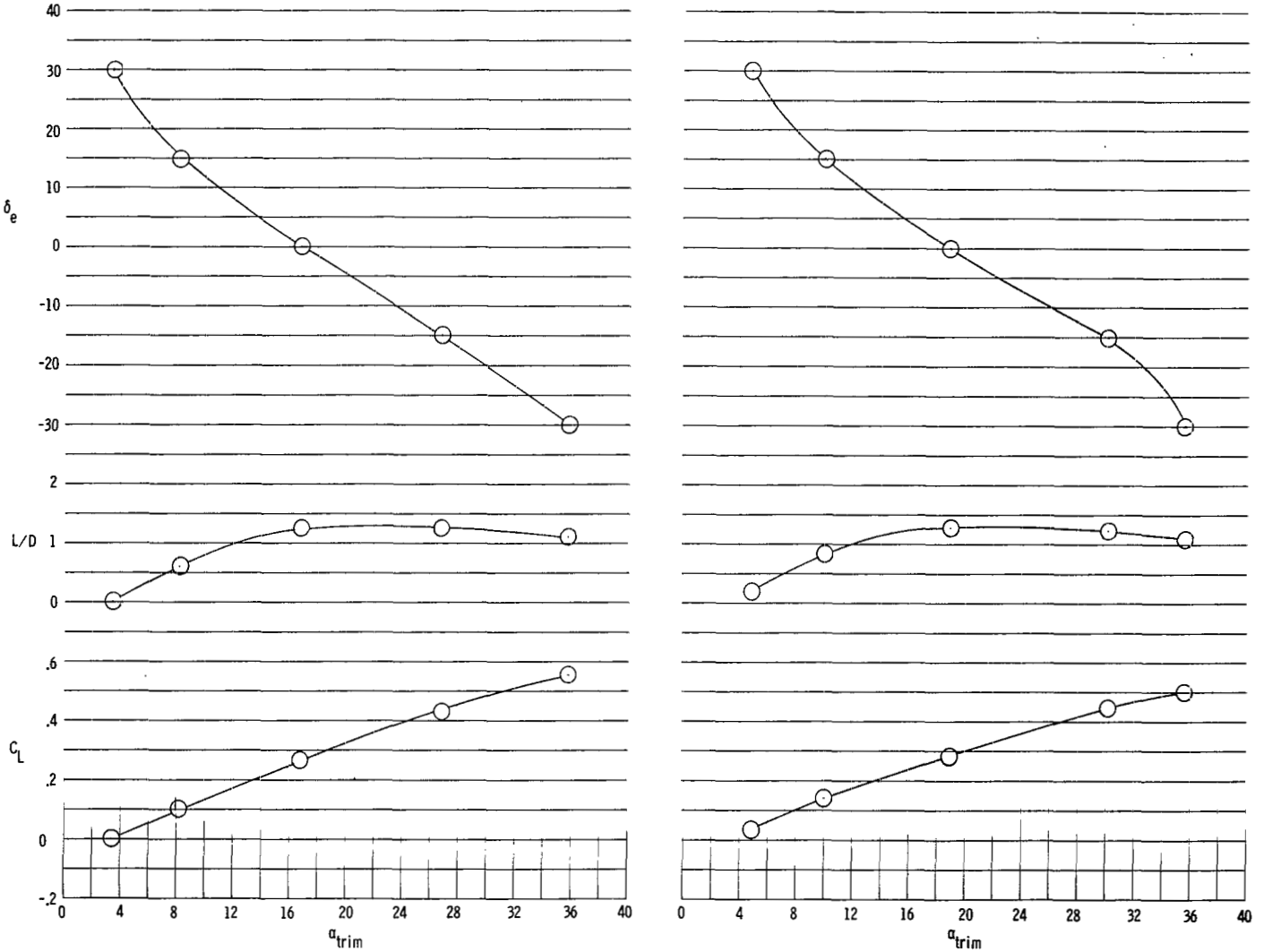

(i) M = 1.50.

(j) M = 1.80.

Figure 36.- Concluded.

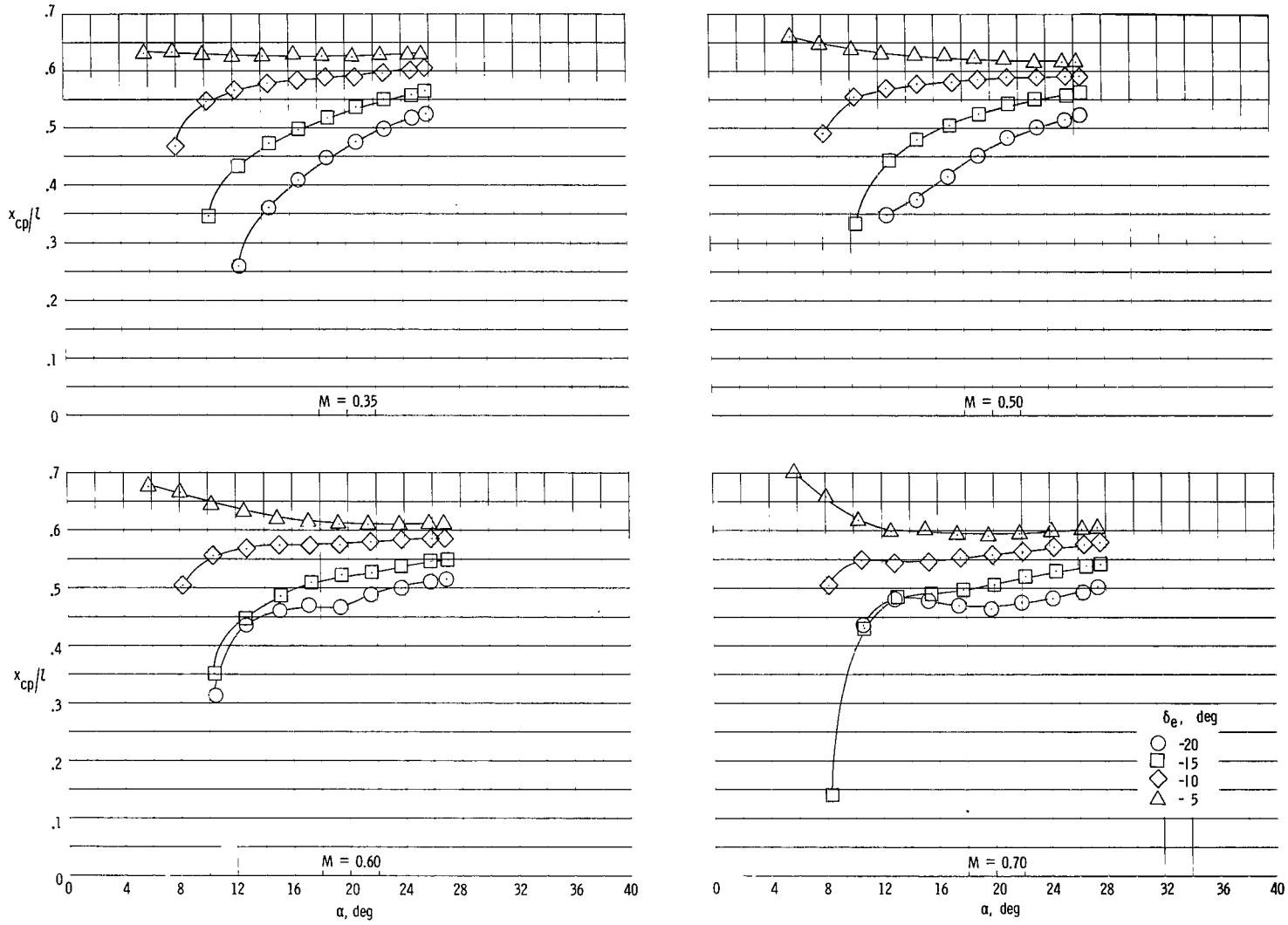

Figure 37.- Summary of longitudinal location of center of pressure of vehicle with modification II tip fins at subsonic speeds. Flaps in subsonic position.

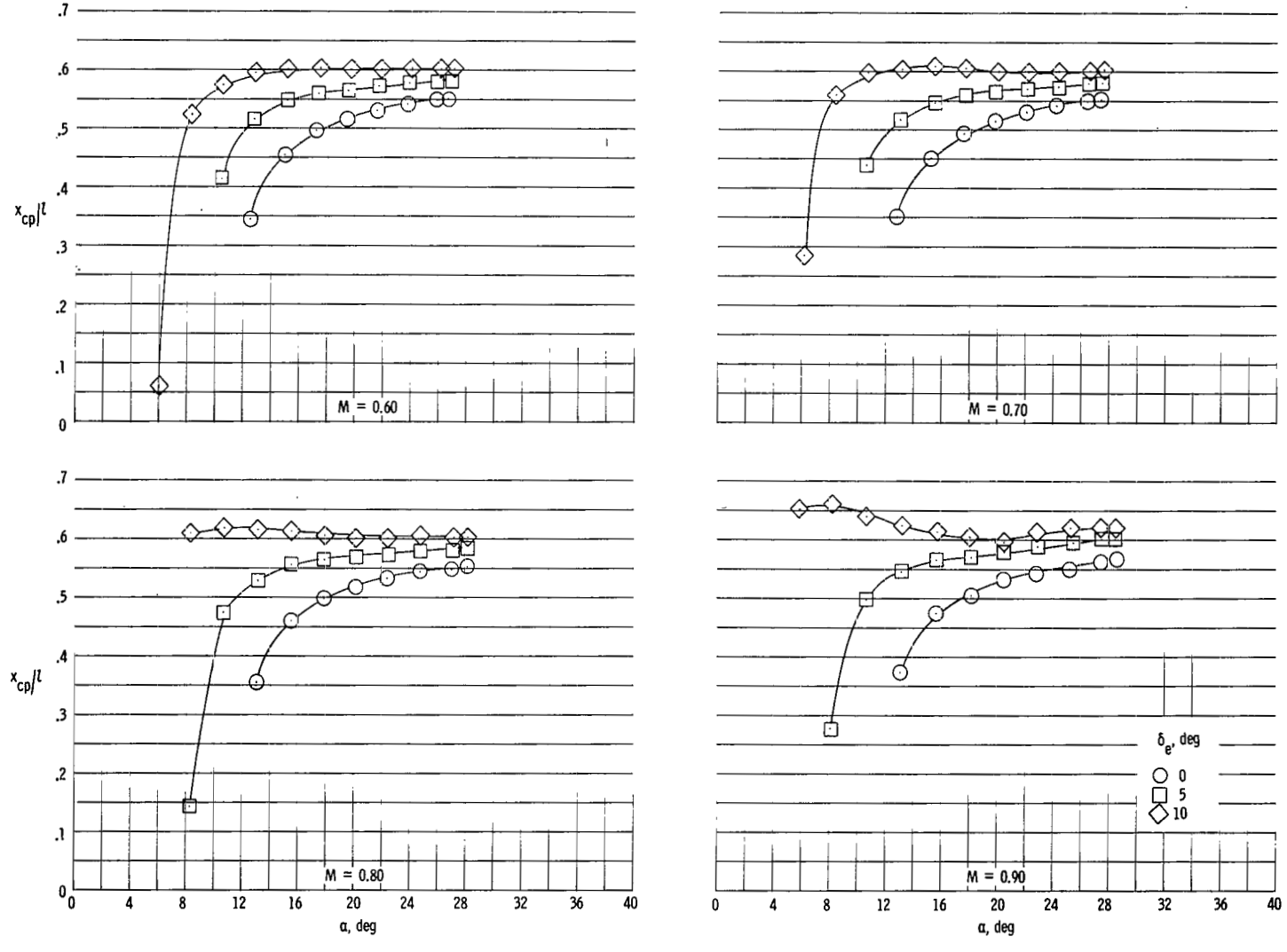

Figure 38.- Summary of longitudinal location of center of pressure of vehicle with modification II tip fins at supersonic speeds. Flaps in transonic position.

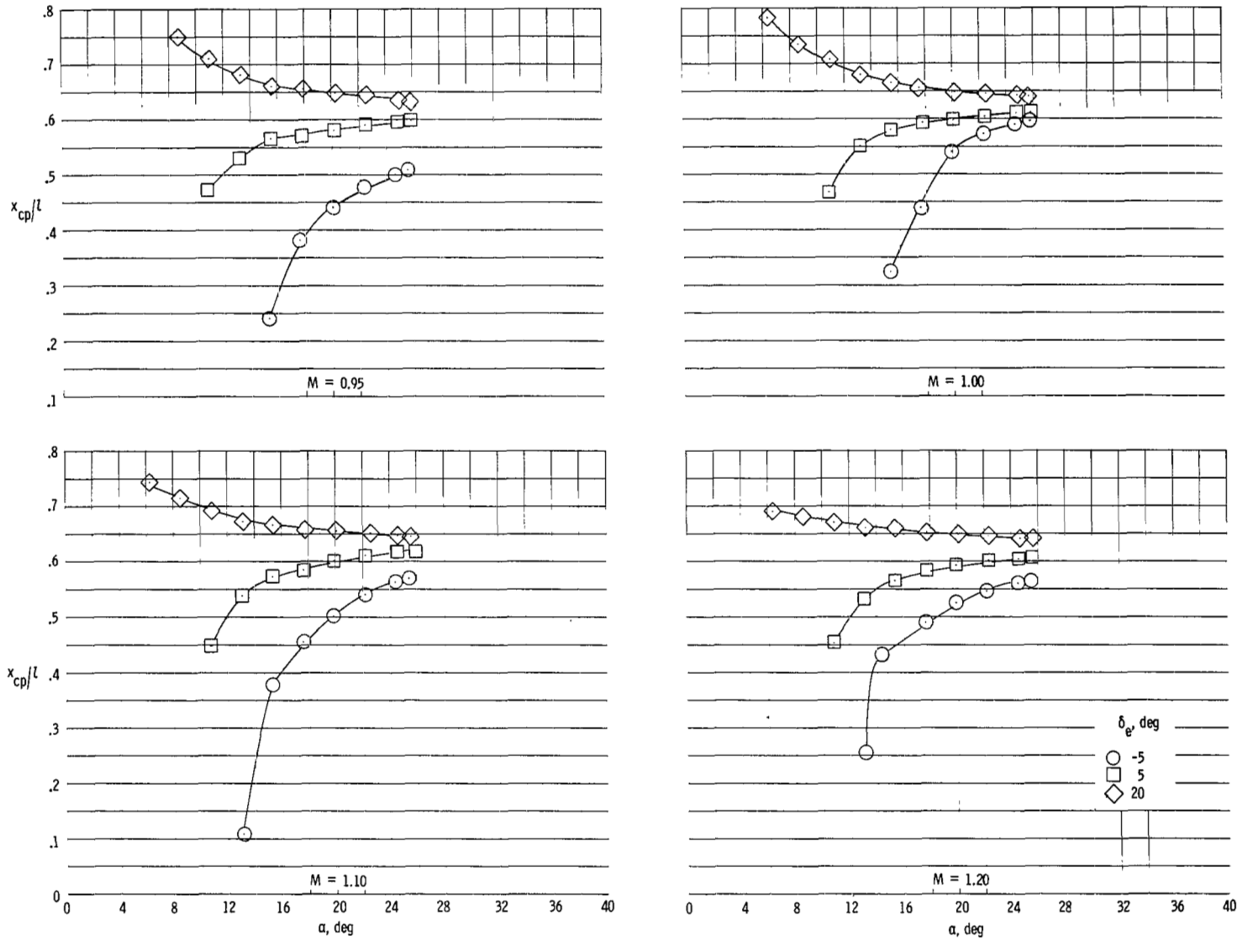

Figure 38.- Continued.

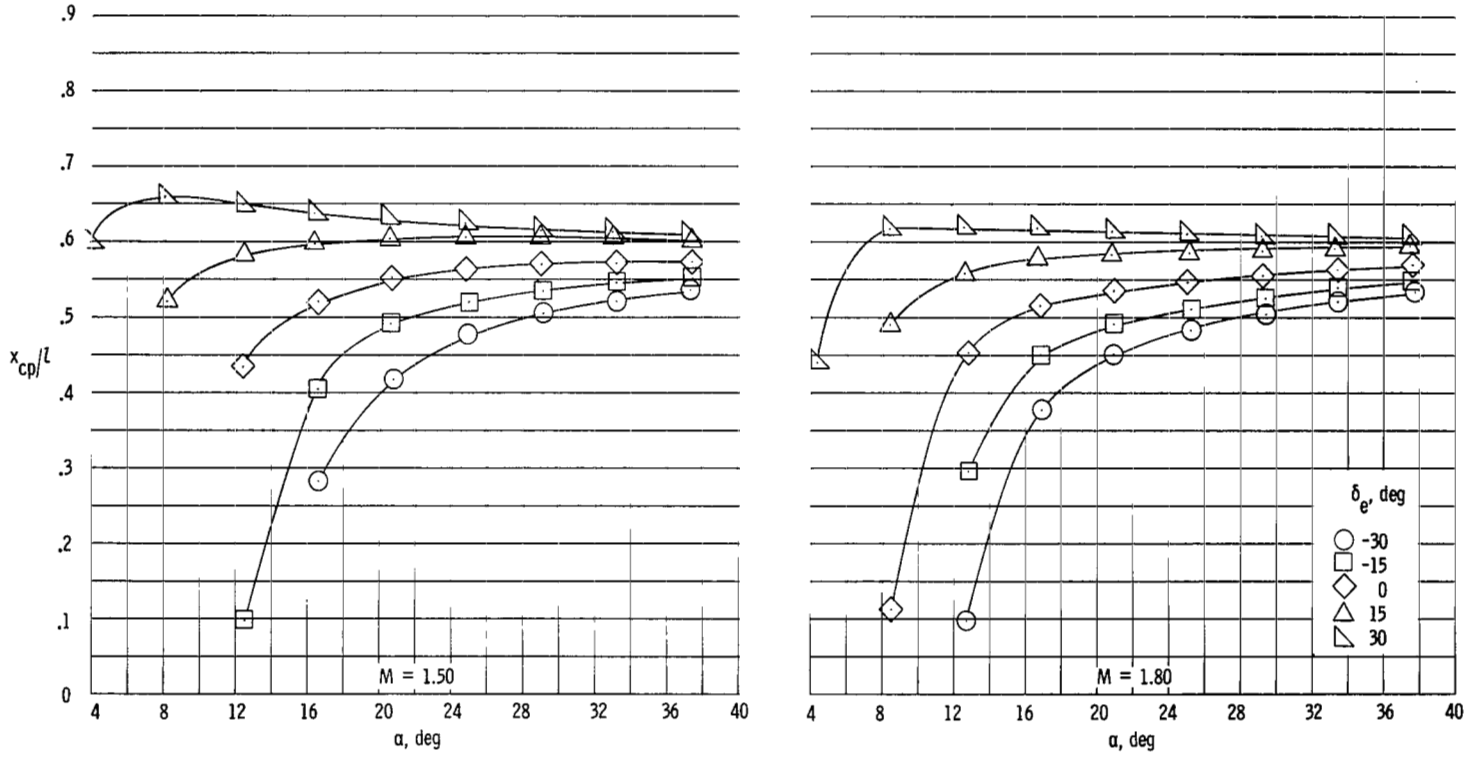

Figure 38.- Concluded.

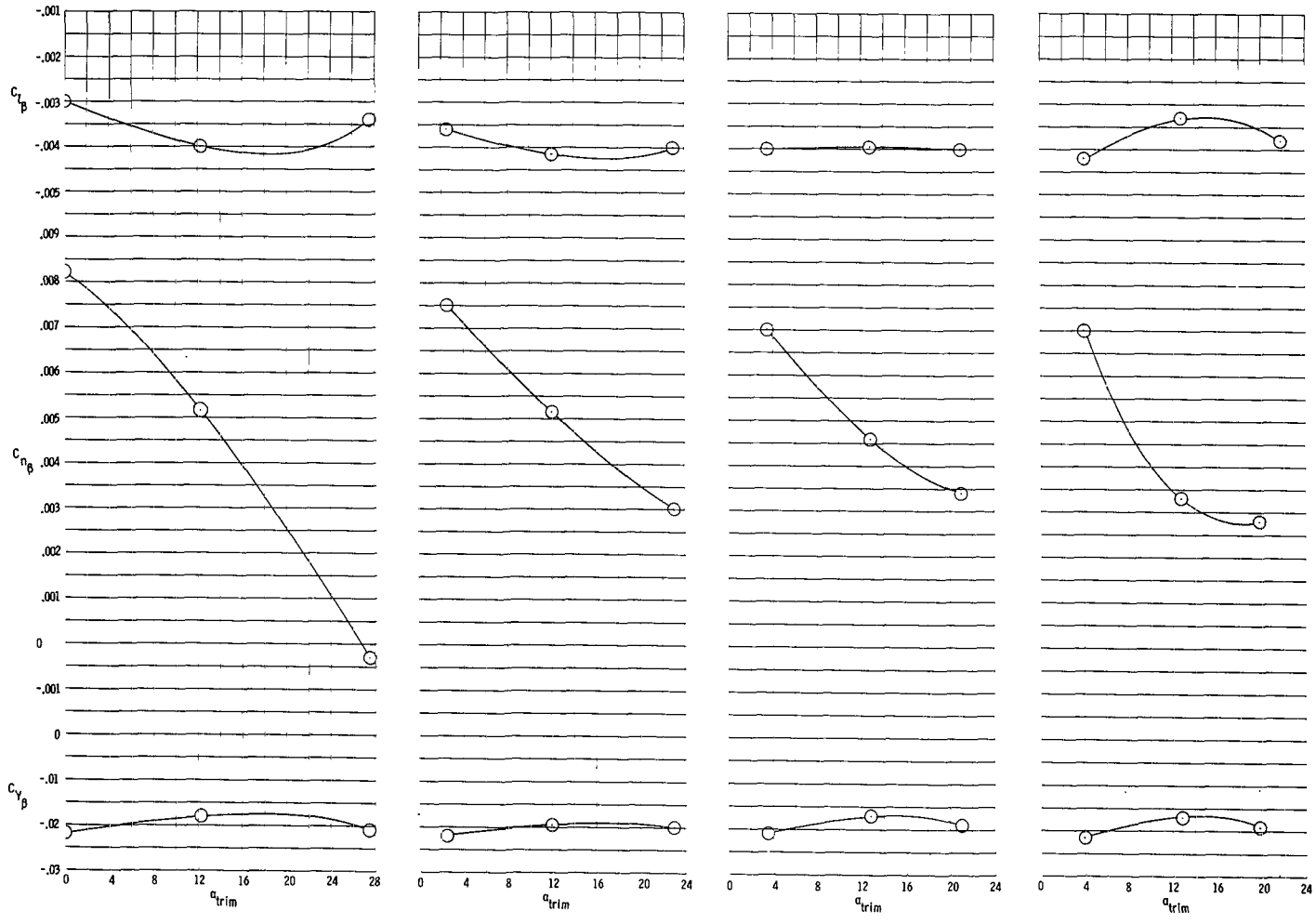

(e) M = 0.95. (f) M = 1.00. (g) M = 1.10. (h) M = 1.20.

Figure 40.- Continued.

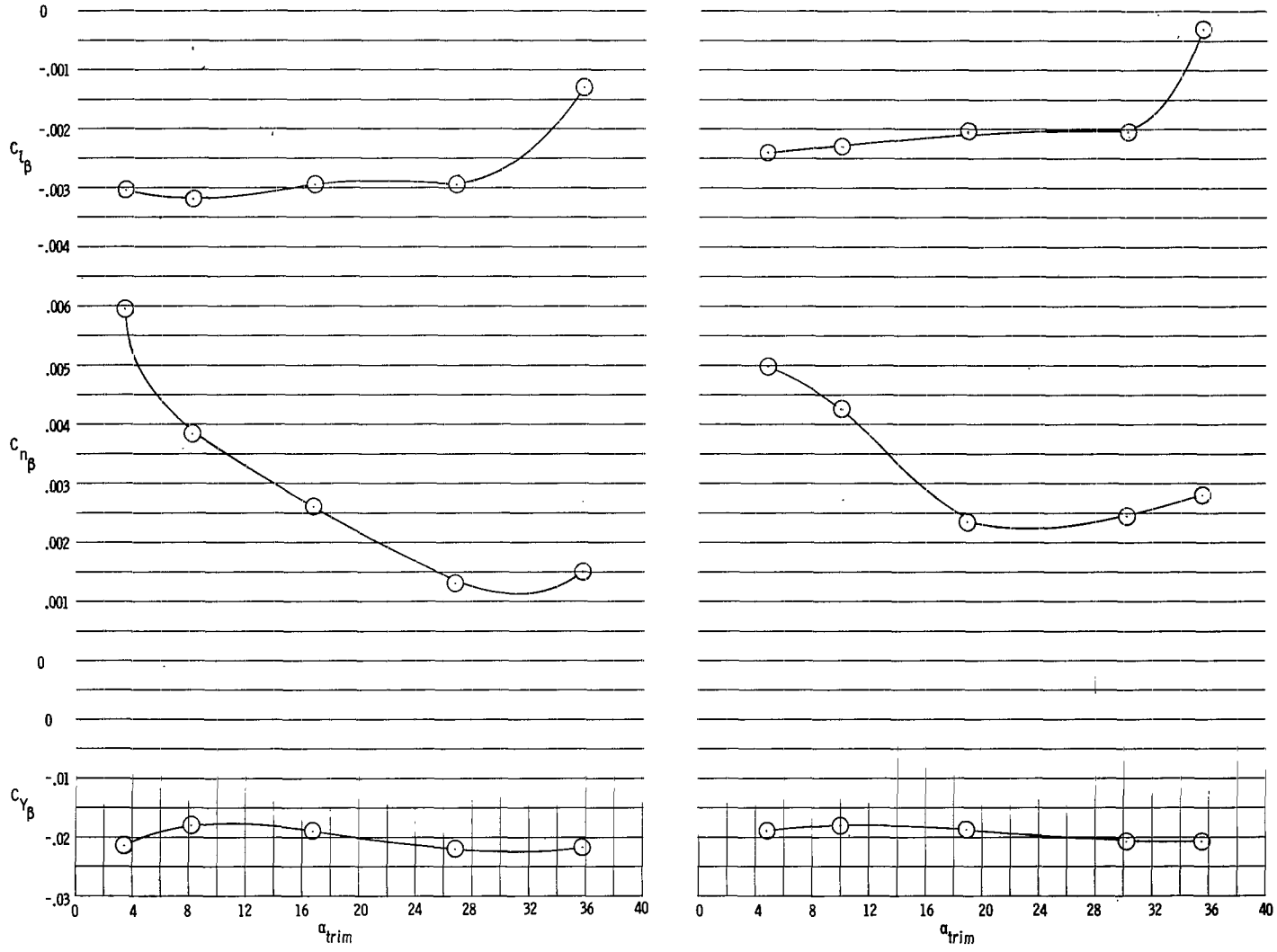

(i) M = 1.50.

(j) M = 1.80.

Figure 40.- Concluded.

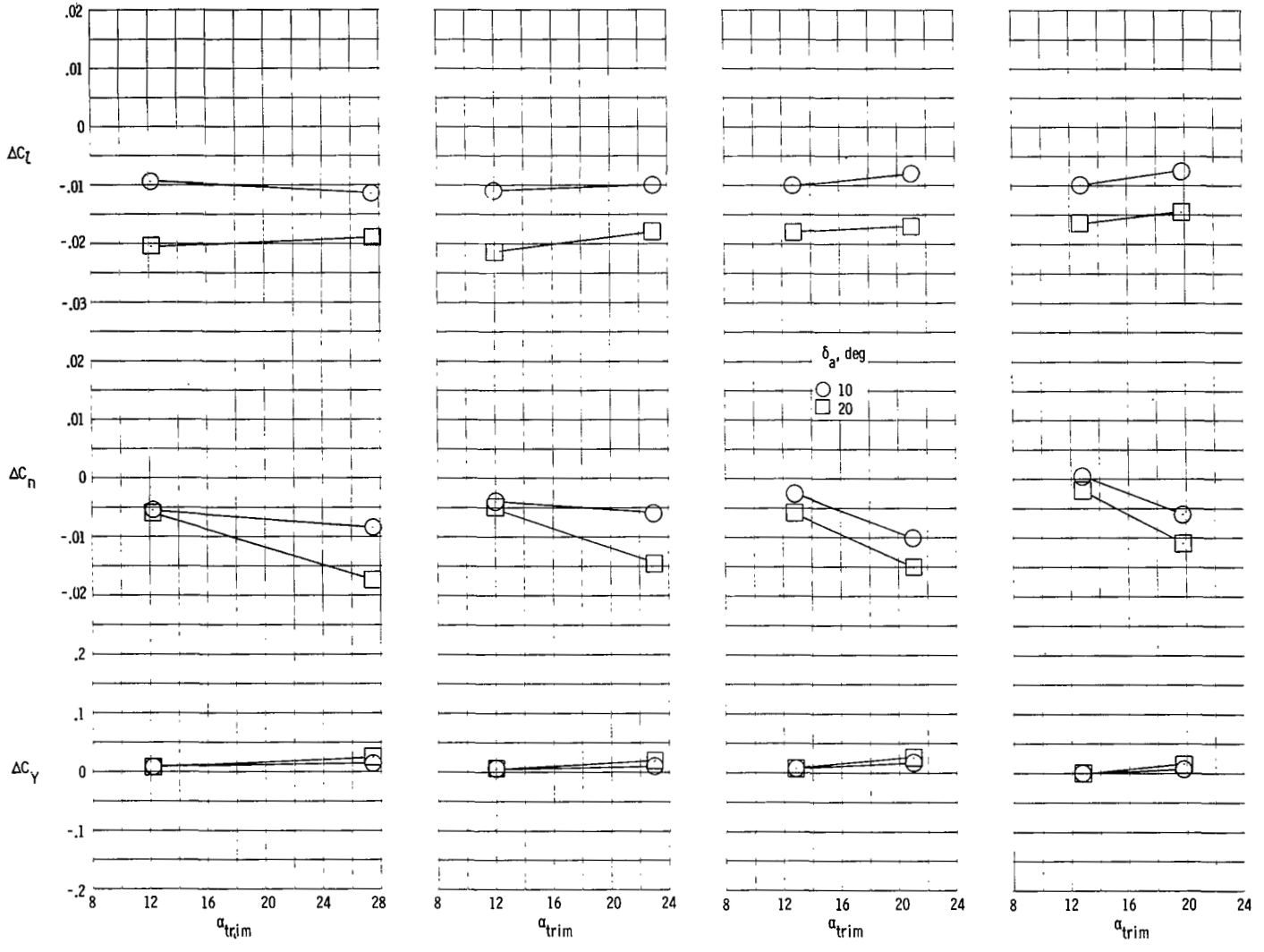

(e) M = 0.95. (f) M = 1.00. (g) M = 1.10. (h) M = 1.20.

Figure 42.- Continued.

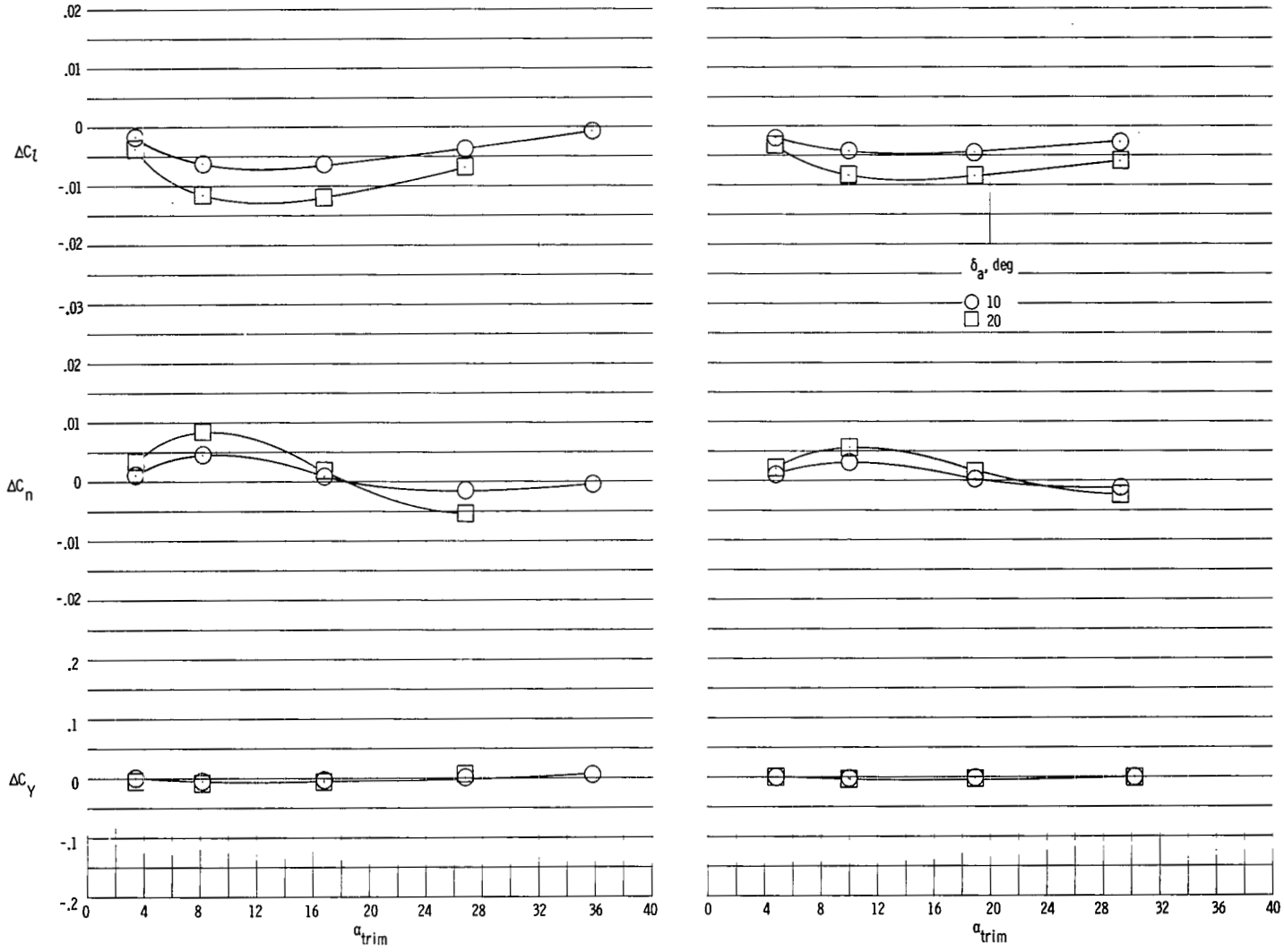

(i) M = 1.50.

(j) M = 1.80.

Figure 42.- Concluded.

"The aeronautical and space activities of the United States shall be conducted so as to contribute . . . to the expansion of human knowledge of phenomena in the atmosphere and space. The Administration shall provide for the widest practicable and appropriate dissemination of information concerning its activities and the results thereof."

—NATIONAL AERONAUTICS AND SPACE ACT OF 1958

NASA SCIENTIFIC AND TECHNICAL PUBLICATIONS

TECHNICAL REPORTS: Scientific and technical information considered important, complete, and a lasting contribution to existing knowledge.

TECHNICAL NOTES: Information less broad in scope but nevertheless of importance as a contribution to existing knowledge.

TECHNICAL MEMORANDUMS: Information receiving limited distribution because of preliminary data, security classification, or other reasons.

CONTRACTOR REPORTS: Scientific and technical information generated under a NASA contract or grant and considered an important contribution to existing knowledge.

TECHNICAL TRANSLATIONS: Information published in a foreign language considered to merit NASA distribution in English.

SPECIAL PUBLICATIONS: Information derived from or of value to NASA activities. Publications include conference proceedings, monographs, data compilations, handbooks, sourcebooks, and special bibliographies.

TECHNOLOGY UTILIZATION PUBLICATIONS: Information on technology used by NASA that may be of particular interest in commercial and other non-aerospace applications. Publications include Tech Briefs, Technology Utilization Reports and Technology Surveys.

Details on the availability of these publications may be obtained from:

SCIENTIFIC AND TECHNICAL INFORMATION OFFICE

NATIONAL AERONAUTICS AND SPACE ADMINISTRATION

Washington, D.C. 20546